1 Introduction

1.1 Background

Earthquake engineering is based on the fact that real structures yield when subjected to design level ground acceleration. The post yield structural response is one of the major parameters that the structural designer is interested in. The level of performance expected from a structure is determined by various factors like its significance, economics, and various social and political issues. This led to the development of Performance Based Earthquake Engineering (PBEE). PBEE ensures that the design meets a set of performance objectives expected from a given building. The prediction of a unique collapse load is not easily available. In dynamic analysis the interaction of the higher mode effects makes the process further involved. The need for an analysis procedure that could trace the structural response from linear elastic to the yielding stage and finally collapse when a system is subjected to earthquake excitation gave rise to Incremental Dynamic Analysis (IDA) (Vamvatsikos and Cornell, 2002). A plot of Intensity Measure (IM) of ground motion versus Damage Measure (DM) of structural response under scaled ground motion is known as an IDA curve. Vamvatsikos and Cornell have demonstrated the utility of this procedure by considering a 9-story steel moment resisting frame. This building was analyzed for different levels of seismic intensity. The output was in the form of demands such as peak roof drift, or maximum base shear for a given hazard level. This data enables the engineer to proceed with the design and the detailing of the structure such that it has enough capacity to sustain the demands imposed by an earthquake corresponding to the pre-determined hazard level.

1.2 Objective and purpose

The purpose of the current study is to study the effect on the IDA curves due to variation of systemic parameters. Only single degree of freedom systems have been used for this purpose. The various systemic parameters of such a system are mass, primary stiffness, secondary stiffness, yield strength, geometric stiffness and damping. A typical five-story office building is considered and each of the systemic parameters is varied one at a time. The weight of the

system was not varied. The model was analyzed with a single ground motion record (also known as Single Record IDA), with a range of variation in parameters. The ground motion was first multiplied with a scale factor. The system's period of vibration and the target pseudo acceleration determined the scale factor. A set of IDA curves was obtained for the corresponding ground motion. This set of curves was compared with another set generated using a different ground motion record. Each system was analyzed using at least five earthquake acceleration records. This study has the following objectives:

1. Effect of rescaling the ground motion each time a parameter is varied.
2. Evaluation of the existing scaling procedures.
3. Identify any trends that might relate the structural response with the variation of the systemic parameters.
4. Determine the most sensitive parameter(s) in dynamic analysis.
5. Study the effect of the different ground motions on a given system using multi-record IDA.

1.3 Application of structural dynamics in earthquake engineering

The importance of dynamic analysis was realized by the structural engineering community following enormous loss of human life and property as a consequence of devastating earthquakes. It was evident that design based on static analysis results did not account for the response that accumulated due to the vibrating or oscillatory motion, generated by the seismic waves. This provided greater motivation to the structural engineer to have a disciplined and organized approach to the subject. Static analysis could account for the nonlinear behavior of real structures. However the effect of repeated cycles of loading and unloading modified the response. An important parameter that affects the dynamic response is the energy dissipation mechanism. This is also known as damping of the system. Nonlinear dynamic analysis is suitable in earthquake engineering because it accounts for the variation in material property, energy dissipation and the cumulative response. The principle of dynamic equilibrium (or D'Alembert's Principle) helped to mathematically model a system for nonlinear dynamic analysis. A set of relations known as equations of motion that

establish a relationship between the external and internal forces similar to force equilibrium in static analysis was formulated. The equation of motion for a multiple degree of freedom system having linear elastic behavior and subjected to base excitation in the form of earthquake ground motion is given by equation 1.1 (Chopra, 2001).

$$m\frac{d^2u}{dt^2} + c\frac{du}{dt} + ku = -m\ell\frac{d^2u_g}{dt^2} \qquad 1.1$$

The letter '*m*' denotes the mass matrix of the system. This is obtained by lumping the mass according to the degree of freedom.

The displacement vector is indicated by '*u*'. Each row of this vector represents the displacement along a degree of freedom.

The letter 'ℓ' denotes the influence vector which consists of a single column containing 1.0 in each row for a shear building. The number of rows is equal to the number of degrees of freedom for the system.

Earthquake ground motion records are incorporated through the function $\frac{d^2u_g}{dt^2}$ which represents the recorded ground acceleration history.

The stiffness matrix and damping matrix are indicated as '*k*' and '*c*' respectively. These properties are obtained by idealizing the real structures so that they can be cast into the mathematical model.

The above differential equation is of second order and nonhomogeneous. The nonlinear property of the stiffness matrix makes the solution further involved. Numerical time stepping methods have been developed to solve such equations. Various computer programs have been written for this purpose. The results presented in this thesis rely heavily on *DRAIN-2DX* (Prakash et al., 1983) and *NONLIN* (Charney, 1997) for arriving at a solution to the equations of motion. Incremental dynamic analysis involves the application of ground motions applied to the structure at monotonically increasing levels of intensity. At each level of intensity the equation of motion is solved using the time stepping technique. *NONLIN* has

a user friendly IDA tool that automatically performs IDA analysis. However, before performing the analysis, *NONLIN* was first verified by comparing its results with those obtained from *DRAIN 2DX*. The results obtained were within 2% of each other, hence *NONLIN* was found suitable for performing IDA. The verification manual for *NONLIN* is presented in Appendix A of the thesis.

1.4 Organization of the thesis

The role of Incremental Dynamic Analysis in the context of Performance Based Earthquake Engineering is discussed in Chapter 2 based on the available literature on the subject. The procedure for performing IDA is elaborated further by the use of an example, and the issue of scaling is discussed. Chapter 3 contains a description of the various hysteretic models and the modeling capabilities of *NONLIN*. This is followed by Chapter 4, which has a detailed description of the IDA tool incorporated in *NONLIN*. All the analysis related to the variation of parameter study was performed using *NONLIN*. The issue of rescaling the earthquake acceleration histories due to variation of the systemic parameters has been examined thoroughly in Chapter 5. The study of variation of parameters on a single degree of freedom system subjected to IDA is given in Chapter 6. The conclusions along with limitations of this study and recommendations for further research are presented in Chapter 7. Appendix A contains the verification manual of *NONLIN* for single and multiple degree of freedom systems.

2 Literature Review

2.1 Overview of Performance Based Earthquake Engineering

For several years experts have been trying to develop a set of guidelines for incorporating the variable nature of seismic forces into building design codes. Performance Based Earthquake Engineering (PBEE) is one of the major steps in that direction. PBEE encompasses design, evaluation and construction engineering. The various components of PBEE are definition of performance objectives, a general design methodology, issues of ground motion modeling, and demand and capacity evaluations (Ghobarah, 2001). A set of performance objectives are laid down that must be satisfied when the structure is subjected to various hazard levels. The stated performance objectives are immediate occupancy, life safety and incipient collapse. The level of expected performance from a building is determined by its importance and the function it is meant to serve. The various limit states that may be used to establish whether the performance objectives are met can be target drift, inelastic rotation of the panel zone, or number of fractured connections in a welded steel frame building. Displacement ductility and energy dissipation can also be used as indices to judge structural performance.

2.1.1 Design and evaluation

Incremental Dynamic Analysis is related to the design and evaluation component of Performance Based Earthquake Engineering. There are basically two approaches to design, force based and displacement based (Ghobarah, 2001). In force based design, the final design is checked to ensure that the drift limits are satisfied. The design forces may be obtained from the static equivalent lateral force method or dynamic equivalent lateral force method (SEAOC. Vision 2000, 1995). In the static equivalent lateral force method, the base shear is computed based on the first mode's period of vibration and under the assumption that the structure will undergo several cycles of inelastic deformation when subjected to seismic forces. The total base shear is distributed over the height of the structure based on the linear mode shape. In the dynamic equivalent lateral force method (SEAOC. Vision 2000, 1995), the distribution of the lateral forces is determined from the natural modes of vibration of the

building. The distribution of the mass and the story stiffness is used for computing the mode shapes. Based on the analysis results for the lateral force distribution, the displacement and the drift are computed, which give an indication of the likely level of damage. If the response remains in the linear elastic range, then internal force or stress criteria can also be used as a damage measure. In displacement based design, the initial member sizing is determined from drift limits and finally the response analysis is conducted. This is an iterative procedure in which a mode shape is first assumed, to calculate the inertial forces and the deflections. The displacements are then compared to the original estimate. The required story stiffness is revised if necessary for the next iteration such that the displacement and drift limits are satisfied. This procedure helps in establishing the section properties of a structure. Finally a response spectrum analysis is performed, which accounts for the individual modal contributions to total structural response.

The various evaluation procedures include elastic analysis, component based elastic analysis, pushover analysis and dynamic nonlinear response history analysis. Pushover Analysis is a simplified nonlinear analysis procedure to determine the capacity and inelastic behavior (e.g. distribution of hinging). IDA comes under the purview of dynamic nonlinear response history analysis. With the help of the above evaluation procedures, it is possible to calculate the response parameters such as stresses, deflections, drifts, ductility demand ratios, and energy dissipation in terms of demand versus capacity at each step. Ghobarah (2001) relates the three performance indices of serviceability, damage control and life safety or collapse prevention with stiffness, strength and ductility respectively. The capacity is determined from the limit states which are a function of the material property and the type of the structural system. The structural evaluation is based on the demand and capacity calculations. There are two different ways of judging the performance. The conventional method is the deterministic approach. This method is based on the assumption of a unique failure mode and collapse capacity. The other approach is the probabilistic approach which accounts for the variability in the properties of the material, collapse capacities and the input forcing function.

The deterministic approach gives a more conservative assessment. The probabilistic approach more realistically simulates the existing structural systems and their properties.

2.1.2 Probabilistic versus deterministic approach for seismic evaluation

A study conducted by Bonowitz and Maison (1998) on welded steel moment resisting frames (WSMFs) using deterministic and probabilistic models gives a good justification for adopting the probabilistic approach. The structural performance of a 9-story pre-Northridge building designed for Los Angeles having fundamental period of 2.4 seconds and 2% of critical damping was evaluated for a ground motion that had a probability of occurrence of 10% over a 50 year period. The ground motion records were selected from those used for the SAC Joint Venture Steel Project. The records were scaled at the fundamental frequency of the structure to UBC standard response spectra at 5% damping. The scale factors are shown in Table 2.1.

Table 2.1 Scaled ground motion records representing 10%/50 year event used in SAC Project.

SAC Name	Record	Distance [km]	Duration [sec]	PGA [g]	Scale Factor
LA03	Imperial Valley, 1979, Array #05	4.1	40	0.39	1.01
LA05	Imperial Valley, 1979, Array #06	1.2	40	0.30	0.84
LA13	Northridge, 1994, Newhall	6.7	60	0.67	1.03
LA15	Northridge, 1994, Rinaldi	7.5	15	0.53	0.79
LA17	Northridge, 1994, Sylmar	6.4	60	0.57	0.99

Two models were used for the deterministic analysis. The “Ductile” model was based on the assumption that all the connections are perfectly ductile so no rotation limits are imposed. The second model “Brittle”, assumed a single conservative capacity for all the connections. The capacity adopted for this was based on tests, and the mean minus one standard deviation value was used. The probabilistic model was called “Variable” and it accounts for the possibility of brittle fracture or failure due to local beam flange buckling. It also accounts for variable capacity obtained from test results. The connections are randomly distributed at

various places and multiple simulations are performed to give the analysis a true probabilistic nature. A36 steel was used for this building model. Two dimensional planar analyses were performed and P-Delta effects were included in the analysis. The beam plastic hinging and weld fracture was modeled using a connection spring. The panel zone spring (PZ) was used to model the panel zone yielding. Connection fracture was also accounted for by plastic rotation. Figure 2.1 illustrates the joint. The plastic rotation capacity was a random variable from the probability distribution based on the tests conducted on pre-Northridge type connections. Some connections fractured before the development of plastic rotation. They were assigned a capacity of 70% of beam yield moment.

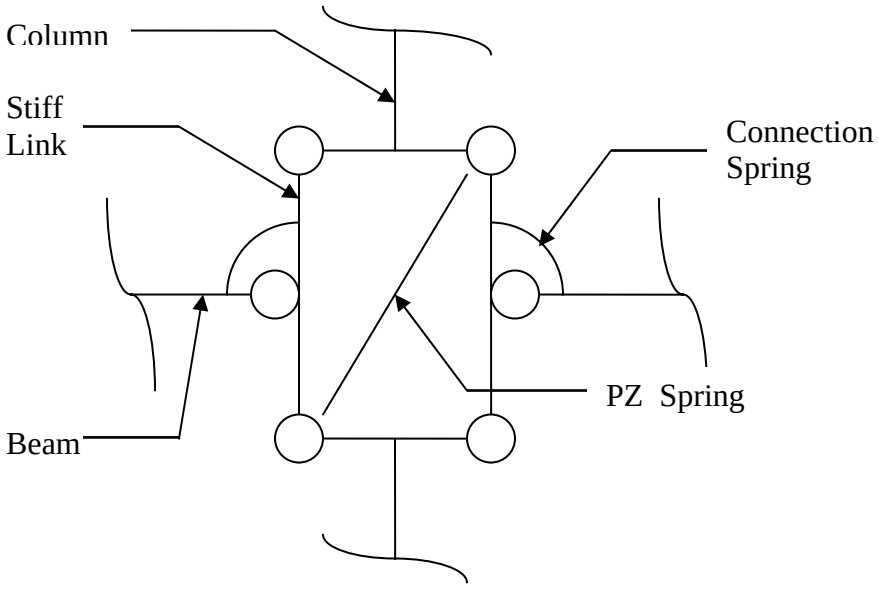

Fig 2.1 Connection model used in Bonowitz and Maison (1998)

Five different ground motion records as per Table 2.1 were applied on the structure. The deterministic models required only one run of each ground motion accelerogram. The probabilistic models were subjected to multiple simulations having different distributions of connections and variable plastic rotation capacities. Five simulations were done for each ground motion accelerogram, resulting in 25 nonlinear runs. The acceptance criteria were

based on FEMA-273 (1996), having allowable inter-story drifts of 2.5% to 5%. The following observations were reported:

(1) The Ductile model had a maximum plastic rotation demand of 0.023 radians in the beam and 0.020 radians in the panel zone.
(2) The Brittle model had more fractures than the Variable model.
(3) Overall frame performance was better in the Variable model than in the brittle model.
(4) In the Variable runs, more difference was observed in the results between the different input ground motion records than between simulations within a given ground motion record.
(5) The choice of the input records is critical and affects the results.

This study adds more credence to the belief that the probabilistic approach is more suitable for assessing frame performance since it simulates actual conditions more closely. However, it is less conservative than the deterministic approach. This can be compensated to a great extent by performing a larger number of simulations. Each simulation has a random distribution of connections having variable capacity distributed across the frame.

2.2 Incremental Dynamic Analysis

Incremental Dynamic Analysis is a useful analysis tool for Performance Based Earthquake Engineering. This procedure was first suggested by Bertero in 1977. A detailed description and step by step methodology suitable for computer programming has been described by Vamvatsikos (2002) in his Ph.D. dissertation.

2.2.1 Procedure and observations

The entire range of structural demands from the linear elastic stage to yielding and finally collapse can be captured by subjecting the structure to increasing levels of ground acceleration. This is graphically represented by the IDA plots. These are obtained by plotting Damage Measures (DMs) versus Intensity Measures (IMs). The common DMs can be roof drift, inter-story drift, residual deformation and ductility demands. Another set of alternatives for DMs may include maximum base shear, spring force, and hysteretic energy. Based on the

amount of energy dissipated during the cycles of loading and unloading, a true damage index can also be formulated. The choice of DM depends on the designer, who may be interested in measuring the demands in terms of either stress or deformation. Spectral acceleration obtained from the standard design response spectra in building codes such as UBC, IBC or NEHRP provisions that corresponds to 5% of critical damping at the system's period of vibration is one of the factors that can be used to scale the target acceleration. The target acceleration is indicated by the Intensity Measure (IM). The scale factor used to multiply the pseudo acceleration must satisfy the condition that the resulting pseudo acceleration at the system's period of vibration must equal the spectral acceleration at the same period. Other examples of IMs can be peak ground acceleration or peak ground velocity. Depending on the IM adopted, scaling factors to be used are decided. Scaling issues are elaborated in the next section. The scaled ground motions are subsequently imposed on the structure and the response is measured.

When a single ground motion is used, the IDA plot obtained is called single-record IDA. This is used extensively in this thesis to illustrate the effect of ground motion on the structural response due to variation in systemic parameters. Multi-record IDA is a plot of the IM versus DM of the system when it is subjected to a suite of ground motion accelerograms. This gives instant information regarding the relative potential of causing damage to the structure by each ground motion accelerogram. Each ground motion is scaled in such a way that the pseudo acceleration at the system's period of vibration is equal to the spectral acceleration at the same period. The following example illustrates a multi-record IDA curve using five different ground motions in Figure 2.2. The model is a typical five story office building having weight per unit volume 8.0 pcf. The dimension of the building is 150ft X 100ft X 65 ft. This gives a total weight of 7800 k. The model is treated as a single degree of freedom system by assuming it has a linear mode shape of vibration and the mass is lumped at the top. The period of vibration of a typical five story building is in the range of 0.5-0.8 second. In this case a period of 0.5 second was assumed. This results in stiffness of 3170 k/in. The strain hardening ratio is assumed to be 0.1. The post-yield strength is 317 k/in. The

yield strength is assumed to be 15% of the weight of the structure. This results in a value of 1170 k. The damping of the system is assumed to be 5% of critical. The building was assumed to be located in a moderately seismic prone area in continental United States. The target spectral acceleration was taken to be 0.25g. The system was subjected to monotonically increasing levels of input ground motion until the spectral acceleration of 0.75g was attained for the input ground motion. The peak displacement response was measured at each intensity level. Nonlinear analysis has been performed. P-delta effects have not been included.

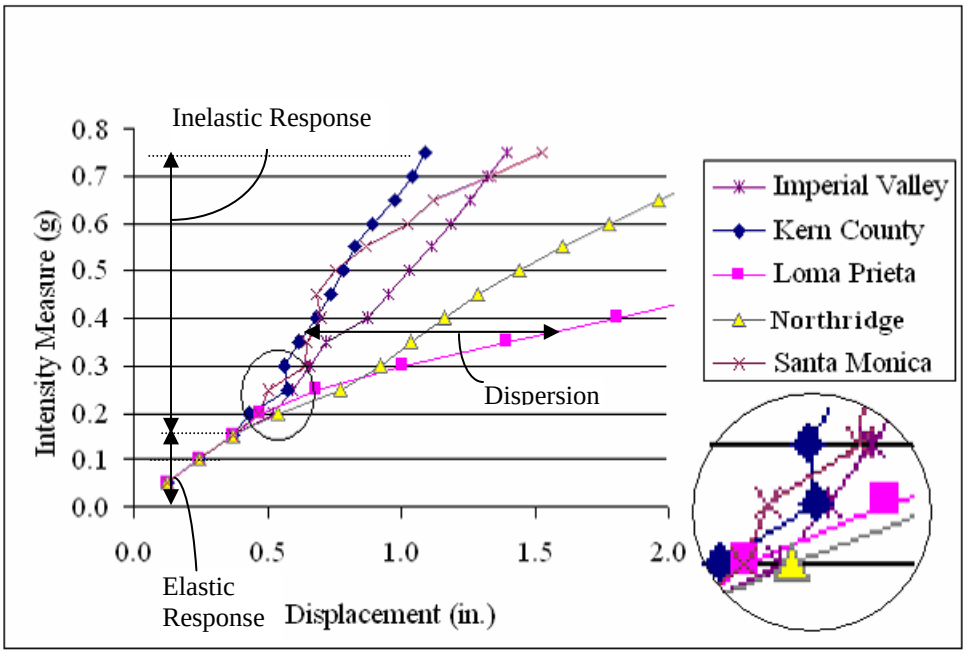

Fig 2.2 Multi-record IDA plot

In Figure 2.2 the region marked as 'Elastic Response' indicates the intensity levels in which the force-deformation relationship is linear for all the ground motions. When the ground motion intensity is increased beyond 0.15g, the system yields for some of the ground motions. The response after yielding is known as 'Inelastic response'. The force deformation relationship is no longer linear. As such the response for each ground motion at a particular intensity level is different. Due to the difference in the response, scatter is observed in the

plot. At a given IM level the difference between the highest peak displacement and the lowest peak displacement is known as ‘Dispersion’.

The following properties can be identified from Figure 2.2:

(1) The curve corresponding to Loma Prieta resembles the familiar elastic-perfectly-plastic behavior. After yielding, the system has a tendency of large drifts for small variation in the level of intensity. Eventually the system reaches a stage of collapse.

(2) For the Northridge ground motion, the system shows some amount of hardening before the system becomes unstable.

(3) The Imperial Valley ground motion has a significant hardening effect on the system that helps in delaying collapse.

(4) The portions of curves corresponding to Santa Monica and Kern ground motions display negative slope at different levels of intensity. As shown in the enlarged detail in Figure 2.2 between intensity levels of 0.25g and 0.30g, the IDA curve for the Kern County ground motion shows negative slope. This non-monotonic behavior has been termed as structural resurrection by Vamvatsikos and Cornell (2002).

The limit states can also be defined and identified from the IDA curves. Based on reaching a certain value of DM (DM-based rule), the lowest point can be termed as the capacity point (e.g. point A in Figure 2.3A). Similarly, on reaching a certain level of IM (when the slope becomes continuously flat) the region can be termed as collapse (IM-based rule, e.g. point B in Figure 2.3B).

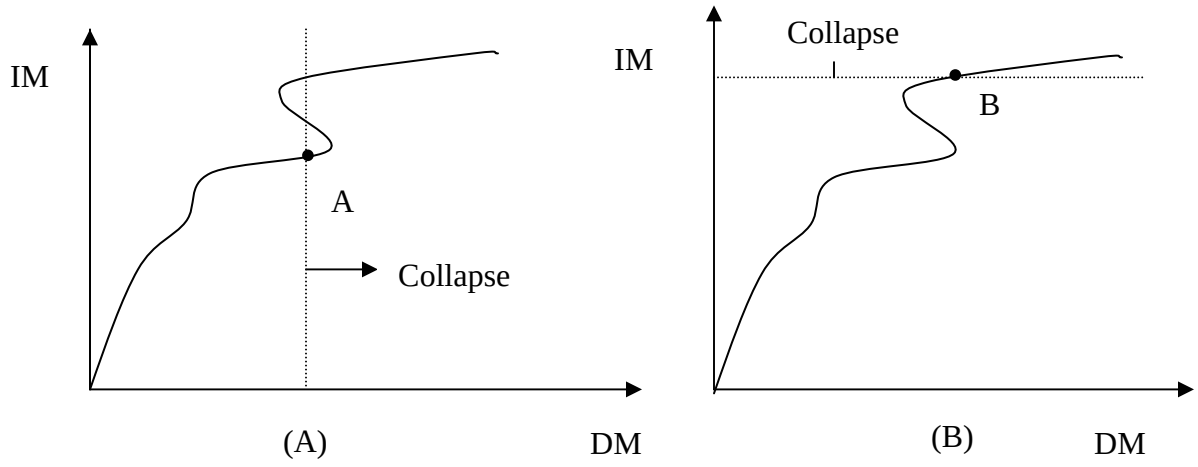

Fig. 2.3 Sample IDA plots

The collapse line can be determined from recommended provisions such as the 20% tangent slope approach given by FEMA-350 (2000). This approach can be applied to IDA curve by assuming that the last point on the curve with a tangent slope of 20 % of the slope in the elastic region is the capacity point. The capacity may also be based on the input from the probabilistic calculations within the framework of performance based earthquake engineering. Vamvatsikos and Cornell (2002) also suggested a hunt and fill algorithm for increasing the efficiency and optimizing the number of nonlinear analysis runs. The purpose of this algorithm is to have a certain number of IDA curves between the bounds. The upper bound is the highest non-collapsing IDA curve and the lowest collapsing curve is the lower bound. The number of curves is decided by the tolerance of the IM gap that the user needs. This gives a better idea of the demand and capacity relationship that is useful for assessing the system at various performance levels.

2.2.2 Scaling issues

Proper scaling of ground motions reduces the number of nonlinear analysis runs by a factor of about four without introducing any bias in the results (Shome et al. 1998). This conclusion was based on a series of nonlinear analysis runs performed on a five degree of freedom model (five story, four bay, steel moment resisting frame). The structure was modeled using a simple stick model. The fundamental frequency of this system was 0.95 Hz and the modal mass participation factor at this frequency was 82%. The ground motion selected could be classified into the following bins:

1. Bin I: M = 5.25-5.75 and R = 5-25 km.
2. Bin II: M = 6.5-7.0 and R = 50-70 km.
3. Bin III: M = 6.7-7.3 and R = 10-30 km.
4. Bin IV: M = 6.5-7.0 and R = 15-35 km.

Each bin contained 20 acceleration histories recorded in California on stiff soil (type S_2 as per UBC, 1994). M stands for the earthquake magnitude and R denotes the closest distance to the fault rupture. The spectral acceleration at the fundamental frequency (0.95 Hz) of the structure and 2% of critical damping was also obtained by using the attenuation law given by

Abrahamson and Silva (1997). The 5% attenuation law results were multiplied with the ratio of the response at 2% and 5% of damped spectra, and the attenuation law result for 1.0 Hz was multiplied with the ratio of response for a frequency of 0.95 Hz and 1.0 Hz at 5% of damping. The results obtained using the attenuation law compared well with the spectral acceleration of the ground motion records. The average spectral acceleration of the 20 ground motion accelerograms from Bin I are close to the average spectral acceleration of Bin II records. However records from Bin II originate at a greater distance so they could help to determine if ground motion characteristics affect the response. Bin III and Bin IV give higher median spectral accelerations, hence they were used to study the effect of scaling the ground motion. The records from Bin I and Bin II were scaled such that they had the same intensity level as that of Bin III and Bin IV. The response obtained was compared with the response from the unscaled ground motion from Bin III and Bin IV. The structural response was computed and classified as local and global damage measures. Local damage measures are parameters that are specific to a particular component of the structure such as panel zone deformation. In nonlinear analysis, the panel zone may or may not yield. Hence a local damage measure is useful for categorizing the response. Global damage measure is an index that is used to quantify the overall frame (or structure) performance. The peak roof drift is an example. The cumulative effect from all the individual components results in the final value of the global response.

The following local damage measures were used in the study by Shome et al. (1998):

(1) Displacement Ductility, μ:

$$\mu = \frac{|u|_{\max}}{u_y}$$

u is the inter-story displacement and u_y is the displacement at incipient yield.

(2) Normalized hysteretic energy, NHE:

$$NHE = \frac{\sum_{1}^{N} (\oint_i R_u du)}{R_y u_y}$$

$R_y u_y$ is defined as the yield strain energy. The numerator denotes the total hysteretic energy dissipated over the N response cycles.

(3) Damage Index, DI:

This is also known as the Park and Ang Index (1985).

$$DI = \frac{|u|_{\max}}{u_{ult}} + \beta \frac{HE}{R_y u_{ult}}$$

HE is the total dissipated hysteretic energy. β is calibration factor, taken as 0.15. u_{ult} is the maximum deformation capacity under monotonically increasing lateral deformation. It is assumed to be $4u_y$.

The following global damage measures were considered:

(1) Global Ductility, μ:

It is the ratio of the maximum roof drift to the yield displacement of the structure.

(2) Global NHE:

It is the ratio of the sum of total hysteretic energies of all the stories to the product of base shear and yield displacement.

(3) Global Damage Index:

It is the weighted sum of the local damage indices defined above for each story. The weighing factor for each story is the ratio of the story's cumulative hysteretic energy to the total hysteretic energy of the stories.

The above damage measures were the parameters used for comparing the results. The following observations were reported:

(1) When non-normalized records (those obtained directly from the bin and used for analysis without any scaling) were used, it was found that the scatter from the median was of the order of 10 in Bin I. For each of the three local and three global damage measures, the median value of results using Bin I accelerograms were within 50% of those obtained using Bin II. Most of the difference could be directly linked to the difference between the median spectral acceleration of the ground motions of the Bins.

(2) A second set of analysis runs was performed using normalized results. All the ground motions of a particular Bin were normalized to the median spectral acceleration of that Bin. It was observed that the median response of each Bin was close to those obtained using non-normalized records. However, it reduced the dispersion by a factor of two. So it can be concluded that normalization does not introduce any bias in the results. Hence a smaller number of analysis runs would be required if the records were normalized.

(3) In order to resolve the question of dependence of the response on M and R, the records of Bin I and Bin II were scaled up to the median spectral acceleration of Bin III. The response was compared to those obtained when non-normalized records of Bin III were used. The differences were within the acceptable range, which proved that the choice of M and R was not a sensitive issue. Differences in median spectral acceleration are the major factor that determines the nature of the results or the dispersion in the median responses.

Based on the above observations, it was conclusively proved by Shome et al. that scaling the ground motion reduces the dispersion between the responses and helps to narrow the number of analysis runs required in order to have a reasonable estimate of the damage measures. Scaling based on median spectral acceleration corresponding to 5% damping at the fundamental frequency was found to give minimum dispersion. It was found that normalization of the records did not introduce any bias in the results, so it can be safely adopted for analysis purpose. Other scaling factors based on peak ground acceleration gave larger values of dispersion.

Hence the target scaling that was adopted in the thesis while performing incremental dynamic analysis was the design spectral acceleration corresponding to 5% of critical damping. For single degree of freedom systems, frequency is one of the factors which affect the scaling. Due to variation in systemic parameters, frequency is also varied. However the median value of frequency of the systems has been used for analysis purpose. The justification for this is provided later in the thesis.

2.2.3 Comparison with Probabilistic Seismic Demand Analysis (PSDA)

The prediction of global demand and collapse capacities is the basic requirement of performance based earthquake engineering. The tools that are available for this purpose are incremental dynamic analysis and probabilistic seismic demand analysis. The former uses stepwise increment of a few records, while the latter is based on a selection of records from different bins. A description of probabilistic seismic demand analysis **(**PSDA) is pertinent because it is an alternative way of approaching the same problem. Mackie and Stojadinovic (2002) studied the performance of California highway overpass reinforced concrete bridges using the above two analysis tools.

The analysis model had the following properties:

(1) It consisted of two equal span overpasses with abutments on either end and no skew.
(2) The ratio of column diameter to superstructure depth (D_c/D_s) was varied to observe if a consistent pattern of results could be obtained for different design parameters.
(3) Simple elastic-plastic elements were used to model the structure.
(4) Analysis included static pushover, modal analysis and dynamic response history.

Some of the demand measures that were used to compare the performance were drift ratio, maximum column curvature and column reinforcing steel stresses.

The IDA method used four ground motions and each was scaled twenty times and used for analysis. In PSDA, four bins having M=6.5 and R=30 km were selected and twenty ground motions having varying levels of intensity were applied on the structure. The following observations were noted:

(1) When the same numbers of nonlinear analysis runs were performed, similar responses was recorded. However for stiffer bridge models the dispersion in the IDA was less and the median value was almost the same with respect to PSDA.
(2) If the same number of nonlinear runs is allowed for PSDA and IDA, then the user has greater flexibility in the Bin approach for using different ground motions. Hence the choice of ground motions is a limiting factor for IDA.
(3) Using IDA, one could go all the way to the collapse stage or dynamic instability. However, when high intensity ground records were used from bins for PSDA, some

of these motions generate regions of numerical instability in the response due to failure in numerical convergence. Hence the region of comparison had to be limited.

From the above study it seems that IDA can capture the demand levels from the linear elastic region through yielding and collapse. If a variety of ground motions are used, the response history analysis results for IDA and PSDA are very close to each other.

3 Description of *NONLIN*

3.1 Introduction

It is pertinent to give a description of the software that has been used to perform the required analysis in this study. As has been mentioned in Chapter 1, *NONLIN* is a useful tool for performing nonlinear dynamic response history analysis. *NONLIN* is a Microsoft Windows based application that has been developed in Visual Basic by Charney and Barngrover (Charney, 1997). The fundamental purpose of *NONLIN* is to provide an aid for understanding the fundamental concepts of structural dynamics and its application to earthquake engineering. Single degree of freedom systems and multiple degree of freedom systems of up to three degrees of freedom can be analyzed with the help of *NONLIN*. For the purpose of this study the single degree of freedom model has been upgraded to perform Incremental Dynamic Analysis. The multiple degree of freedom system has a braced frame incorporating a passive energy device and may be used with or without a base isolator.

3.2 Single Degree of Freedom (SDOF) model

The single degree of freedom model is the simplest model available in *NONLIN*. The input properties for this model consist of its mass, damping, stiffness and forcing function. If weight is entered, then it is converted to mass in appropriate units. The damping can be entered as an absolute value or as a percentage of critical damping. The program is capable of handling material and geometric nonlinearities. Material nonlinearity can be taken into account by specifying yield strength and post yield stiffness. The geometric nonlinearity can be included by activating the P-Delta option and then a value of the geometric stiffness is required. Figure 3.1 illustrates the force-deformation relationship available in the SDOF model in *NONLIN* with the help of the example of the office building described in section 2.2.1. The positive and the negative yield strengths as well as the post-yield stiffness are assumed to be equal in the SDOF model. The system properties input window for the model of the office building as appearing in the *NONLIN* window is depicted in Figure 3.2.

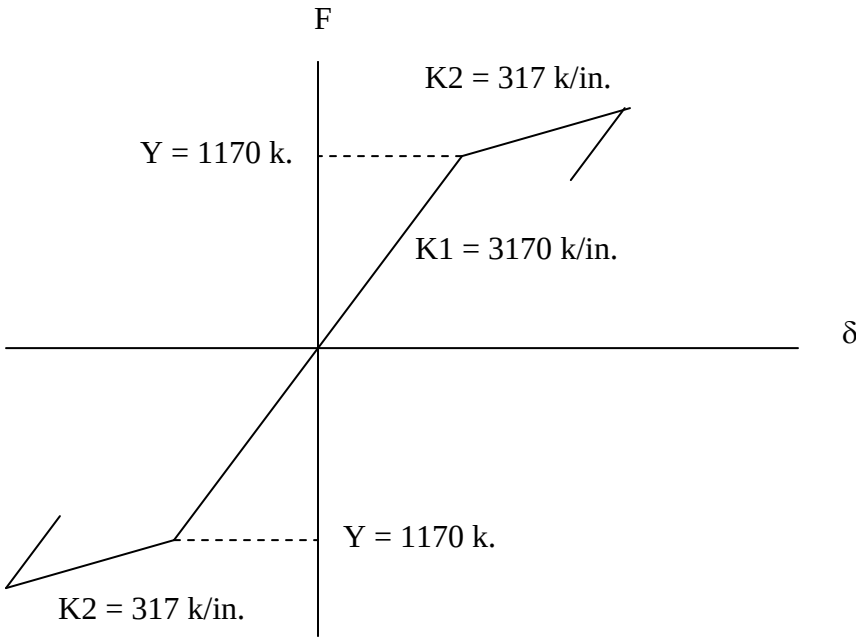

Fig. 3.1 Bilinear hysteretic model used in section 2.2.1

This model is enabled to analyze a problem having material nonlinearity. In this problem the P-Delta option is not enabled. If P-Delta effects are included, the program automatically updates the effective stiffness and the effective yield strength. A detailed description of all the input properties is explained in Chapter 4. Apart from the free vibration problem, various other forcing functions can be applied to the structure. These can be a linear combination of sine wave, square wave or saw shaped functions. *NONLIN* also has a database of about 100 ground acceleration histories which can also be used as a forcing function. The acceleration, velocity and displacement histories for each of these records can be observed. It is also possible to display the response spectra for various values of damping. Tripartite or separate plots can be generated for pseudo velocity, pseudo acceleration and displacement. The design code spectra as per UBC-1994 or FEMA-273 provisions can be overlaid. These can be plotted against the system's period of vibration or frequency. If all the properties and input data are entered correctly, the program is ready to run. Since this program uses time stepping methods for solving the equations of motion, the user has to enter the number of desired time steps per load step. The number of sub-steps has to be increased till a convergence of the analysis results has been achieved. For most problems a time step of 0.0005 second is

sufficient to produce convergence. The equations of motion are solved incrementally in the time domain using the Newmark constant acceleration technique.

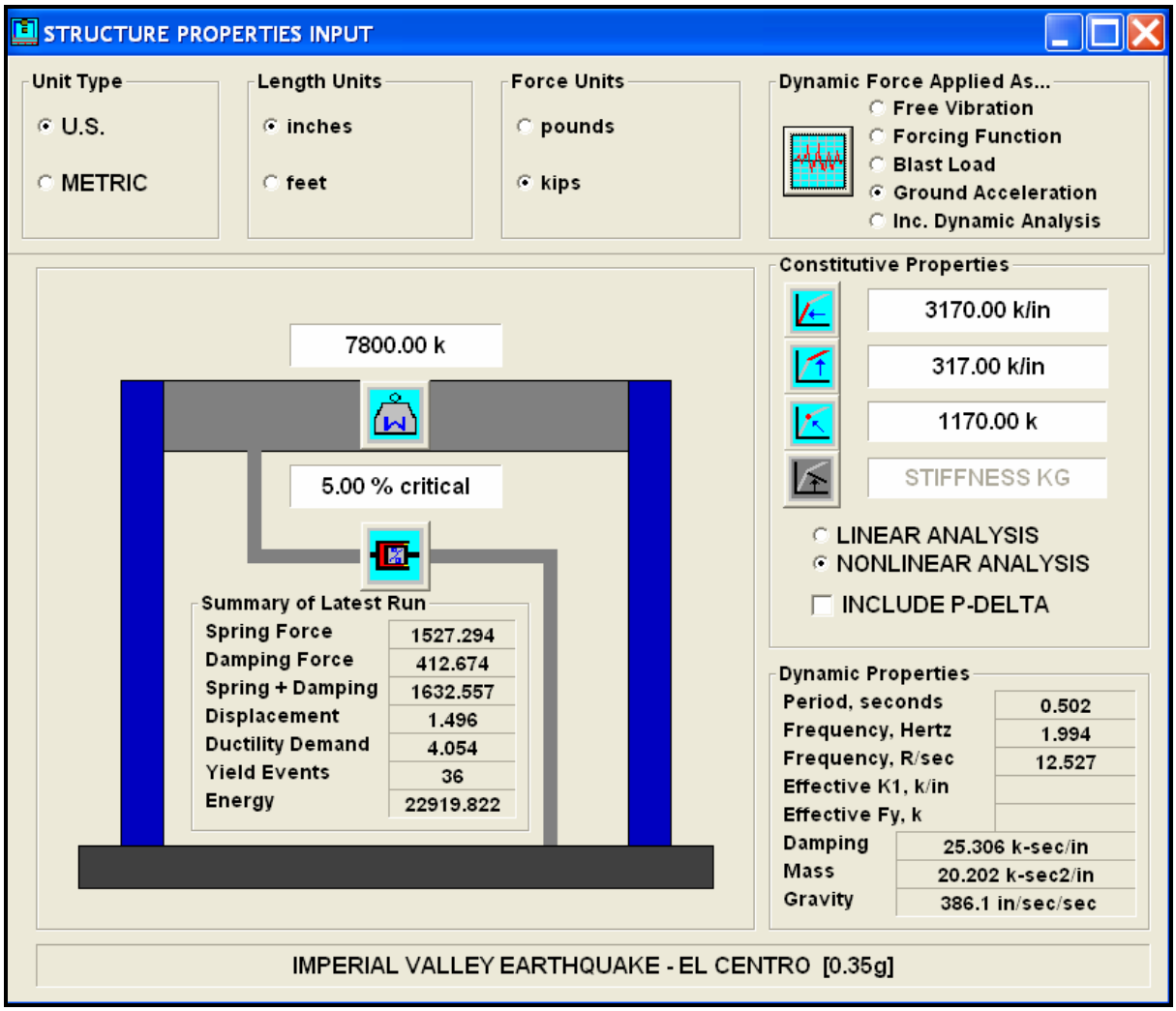

Fig. 3.2 SDOF model of the office building (section 2.2.1) as observed in *NONLIN*

The output can be obtained in a spreadsheet format or as a variety of on-screen plots. As evident from Figure 3.2, the user can verify the system's period of vibration from the "Dynamic Properties" window. A summary of the results is also presented in the same window. A detailed analysis result tabulating the response at each time step is also available. The various response history results that can be plotted are displacement, velocity, total

acceleration, relative acceleration, damping force, spring force, total inertial force and sum of damping and spring force. If nonlinear analysis is performed, then the yield code containing the various instants at which the stiffness changes can be observed. The Fourier Amplitude Spectra can be generated for each response. The Fast Fourier Transform (FFT) tool converts the time function into a frequency function. The transform is normalized to have a maximum value of 1.0. The frequency that has a transform ordinate of 1.0 is the dominant frequency. Using the traveling FFT tool, one can view the frequency content of the response or ground motion for various time intervals. When nonlinear analysis is performed, the hysteretic behavior is an important property. In *NONLIN* the hysteretic loops can be plotted. On the horizontal axis, displacement, velocity, total acceleration or relative acceleration can be selected. The vertical axis may contain any of the forces (spring, damping or inertial) or a combination of these.

The total energy dissipated over the time-span of the earthquake or forcing function can be plotted. The total energy consists of Kinetic + Strain Energy, damping and hysteretic energy. The fraction of each of them to the total is expressed as a percentage and plotted. This is illustrated in Figure 3.3 for the Imperial Valley Earthquake with the help of the model described in section 2.2.1. The blue lines represent the yield events. The percentage of hysteretic energy is an indicator of the damage to the structural system. The energy distribution can be observed graphically at each instant of time.

There is an interactive animation tool in *NONLIN* that allows the user to trace the movement of the structure in real time. With respect to the original undeformed structure, the oscillatory back and forth movement of the structure is displayed. Simultaneously the hysteretic and response history plots are also generated.

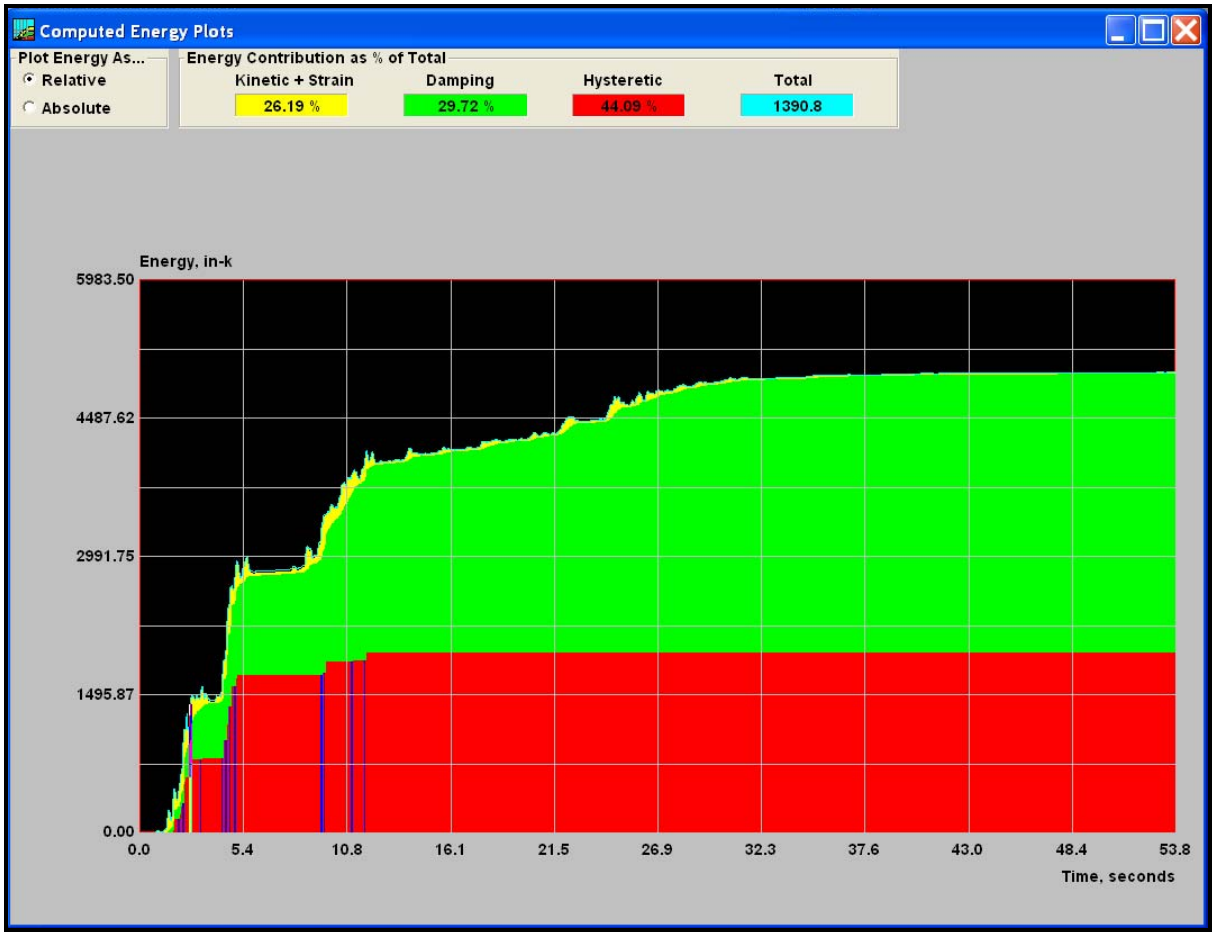

Fig. 3.3 Energy plot in *NONLIN* for the model in section 2.2.1

3.3 Multiple Degree of Freedom (MDOF) model

The multiple degree of freedom models help to analyze more complex structures, including those with passive energy devices and/or base isolators. The most general model in *NONLIN* is a three degree of freedom system as shown in Figure 3.4. This model is termed an isolated braced frame with device. The degree of freedom DOF 1 represents the translational movement of the frame. The device connected between the frame and the base with the help of the brace accounts for passive viscous or non-viscous damping. The degree of freedom of at the top of the brace is indicated by DOF 2. The isolator is represented by DOF 3. In order to solve the equations of motion for dynamic equilibrium, it is required to assemble the mass, stiffness and damping matrices. The mass according to the degrees of freedom is lumped to

produce the mass matrix M given below. The letters m_F, m_D, m_I denote the mass of the frame, device and isolator, respectively.

$$M = \begin{bmatrix} m_F & 0 & 0 \\ 0 & m_D & 0 \\ 0 & 0 & m_I \end{bmatrix}$$

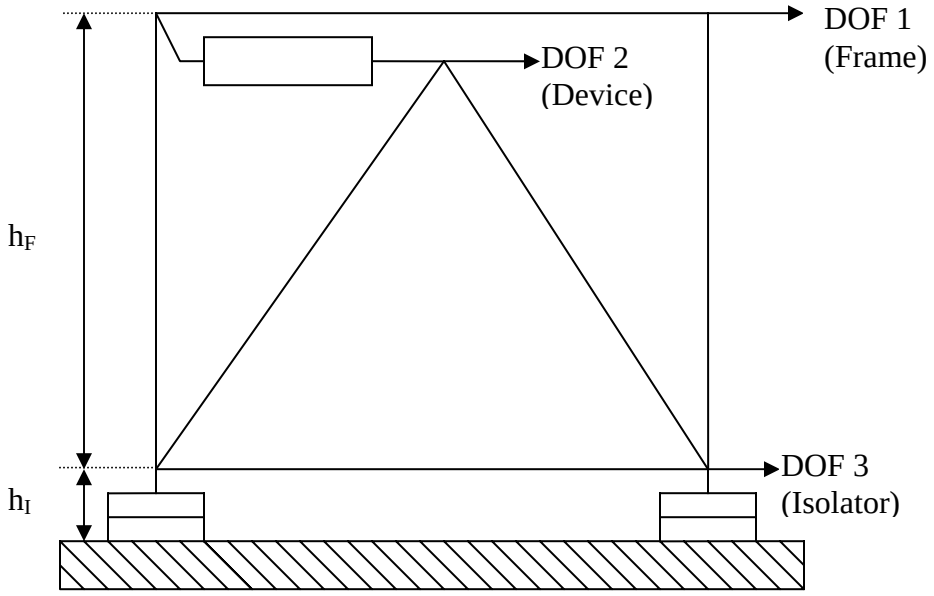

Fig. 3.4 Three degree of freedom model

The stiffness contribution of the frame to the global stiffness (K_F) is derived from the relative displacement between DOF 1 and DOF 3. The stiffness component due to the brace (K_B) is related to the relative movement between DOF 2 and DOF 3. The passive energy device is active when the frame (DOF 1) moves horizontally with respect to bracing (DOF 2). The stiffness of the device is given by K_D. The movement of the isolator is measured with respect to the fixed base. Hence the contribution of the isolator to the global stiffness matrix given by K_I is given by the movement of DOF 3. The height of the frame is h_F, and the height of the isolator, h_I, contributes to the geometric stiffness matrix of the system.

K is the global stiffness matrix and is given by equation 3.1:

$$K = K_F + K_B + K_D + K_I + K_G \qquad 3.1$$

$$K_F(Frame) = \begin{bmatrix} k_F & 0 & -k_F \\ 0 & 0 & 0 \\ -k_F & 0 & k_F \end{bmatrix} \qquad K_B(Brace) = \begin{bmatrix} 0 & 0 & 0 \\ 0 & k_B & -k_B \\ 0 & -k_B & k_B \end{bmatrix}$$

$$K_D(Device) = \begin{bmatrix} k_D & -k_D & 0 \\ -k_D & k_D & 0 \\ 0 & 0 & 0 \end{bmatrix} \qquad K_I(Isolator) = \begin{bmatrix} 0 & 0 & 0 \\ 0 & 0 & 0 \\ 0 & 0 & k_I \end{bmatrix}$$

$$K_G(GeometricStiffness) = \begin{bmatrix} -W_F/h_F & 0 & W_F/h_F \\ 0 & 0 & 0 \\ W_F/h_F & 0 & -W_F/h_F - (W_F + W_I)/h_I \end{bmatrix}$$

In the above expressions, k_F, k_B, k_D, k_I are the tangent stiffness of frame, brace, device and isolator, respectively. W_F and W_I denote the weight of the frame and isolator, respectively. In *NONLIN*, a multiple degree of freedom model allows the use of linear and nonlinear viscous dampers for the device and the isolator. The damping behavior is given by the following relationship:

$$F_D = C|v|^x \, sign(v)$$

F_D represents the damping force. C is the damping coefficient. Deformational velocity is indicated by v, and x is an exponent. The notation *sign* denotes the signum function. The range of values for x lies between 0.4 and 2.0. For a linear viscous dashpot, x is taken as 1.0. When x is taken as 2.0 it represents sudden impact and is known as a kinetic energy damper. Damping in the frame is strictly linear. There is no damping contribution from the chevron brace. The global damping matrix C is formed by assembling the damping contributions from the frame (C_F), device (C_D) and isolator (C_I):

$$C = C_F + C_D + C_I$$

$$C_F(Frame) = \begin{bmatrix} c_F & 0 & -c_F \\ 0 & 0 & 0 \\ -c_F & 0 & c_F \end{bmatrix} \quad C_D(Device) = \begin{bmatrix} c_D & -c_D & 0 \\ -c_D & c_D & 0 \\ 0 & 0 & 0 \end{bmatrix} \quad C_I(Isolator) = \begin{bmatrix} 0 & 0 & 0 \\ 0 & 0 & 0 \\ 0 & 0 & c_I \end{bmatrix}$$

Based on the most general three degree of freedom model, other models having one and two degrees of freedom can be created by deactivating the elements that are not to be considered. This is achieved by assigning the element a very large value of stiffness and/or very low value of mass. The following is a list of built-in models in *NONLIN*:

(1) Simple rigid frame
(2) Braced frame
(3) Braced frame with device
(4) Base isolated frame
(5) Base isolated braced frame
(6) Base isolated frame with device

Table 3.1 illustrates the values that need to be used for reducing the most general three degree problem to a one degree or two degree of freedom problem. These properties are automatically set up by *NONLIN* depending on the model selected.

Table 3.1 Element properties

Model	PROPERTIES			
	Frame	Brace	Device	Isolator
Simple Frame	User Defined	k = 10E10 m = 10E-10 c = 0.0	k = 10E-10 m = 10E-9 c = 0.0	k = 10E10 m = 10E-9 c = 0.0
Braced Frame	User Defined	User Defined	k = 10E10 m = 10E-9 c = 0.0	k = 10E10 m = 10E-9 c = 0.0
Braced Frame with Device	User Defined	User Defined	User Defined	k = 10E10 m = 10E-9 c = 0.0
Base Isolated Frame	User Defined	k = 10E10 m = 10E-10 c = 0.0	k = 10E-10 m = 10E-9 c = 0.0	User Defined
Base Isolated Braced Frame	User Defined	User Defined	k = 10E10 m = 10E-9 c = 0.0	User Defined
Base Isolated Braced Frame with Device	User Defined	User Defined	User Defined	User Defined

Appendix A contains examples of each of the above models. The results obtained from *NONLIN* were compared to those obtained from *DRAIN-2DX* for verification purpose.

3.3.1 Modeling features

NONLIN allows the user to model complex force deformation relationships for all the elements except the bracing. The stiffness of the bracing is strictly linear. The hysteretic behavior of the frame, passive device and isolator can be modeled to display any of the following patterns:

(1) Linearly elastic: This is the simplest behavior where the force is directly proportional to the deformation. The loading and unloading curve is restricted to the same straight line. The backbone curve is illustrated in Figure 3.5. During each cycle the energy is totally conserved and is not dissipated in the form of hysteretic energy.

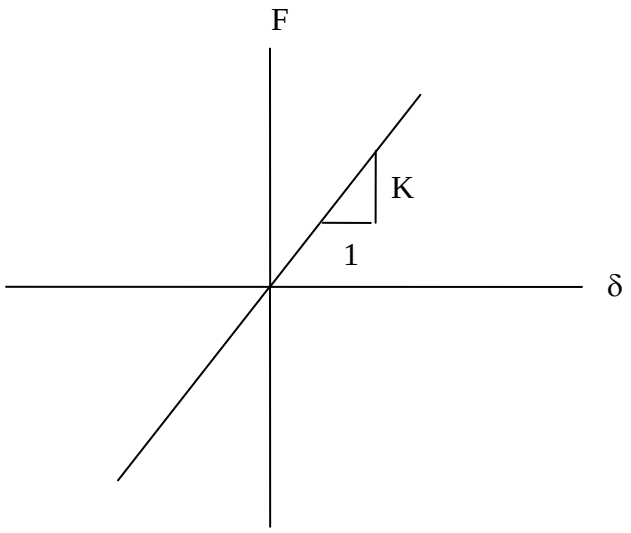

Fig. 3.5 Linearly elastic model

(2) Multi-linear: The backbone curve of the force deformation relationship is as shown below. The positive and negative yield strength values may be different. Similarly the post yield stiffness during the positive and negative excursions may be different. However, the loading and unloading slopes are always parallel to each other. Figure

3.6 shows the backbone of the trilinear model. During each hysteretic cycle, energy is continuously dissipated in this case.

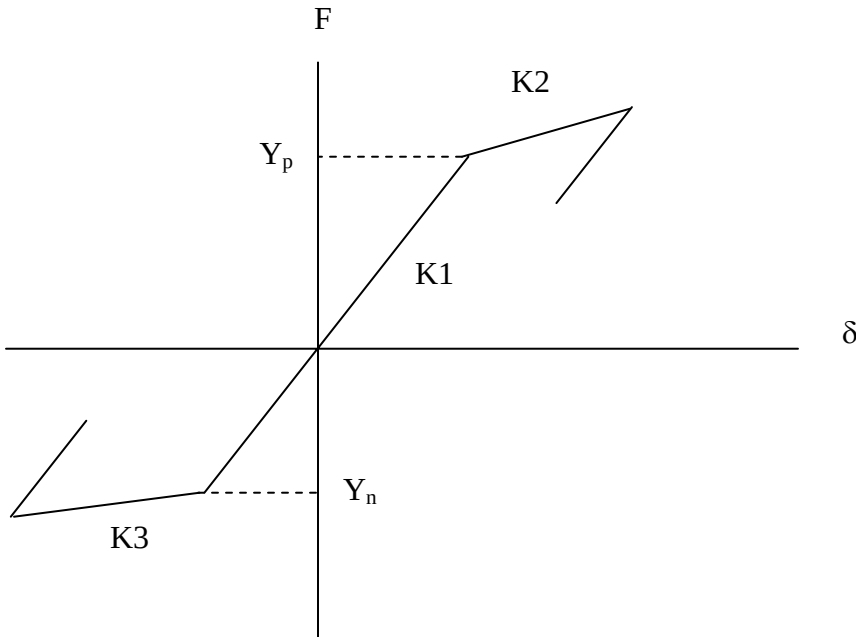

Fig. 3.6 Multi-linear hysteretic model

(3) Trilinear with Bauschinger effect and pinching:

This has the same backbone curve as in the bilinear model. This also includes strength degradation and pinching effects. Strength degradation is based on equation 3.2 (Sivaselvan and Reinhorn, 1999):

$$M_y^{+/-} = M_{yo}^{+/-}[1-(\frac{\phi_{\max}^{+/-}}{\phi_u^{+/-}})^{\frac{1}{\beta_1}}][1-\frac{\beta_2}{1-\beta_2}\frac{H}{H_{ult}}] \qquad 3.2$$

where $M_y^{+/-}$ is the positive or negative yield moment. $M_{yo}^{+/-}$ denotes the initial positive or negative yield moment. $\phi_{max}^{+/-}$ represents the maximum positive and negative curvature. The ultimate positive and negative curvature is indicated by $\phi_u^{+/-}$. H is the hysteretic energy dissipated. H_{ult} is the hysteretic energy dissipated when loaded monotonically to the ultimate curvature without any degradation. The strength degradation parameter that is ductility based is denoted by β_1. The energy based strength degradation parameter is

β_2. The schematic representation of the strength degradation behavior is illustrated in Figure 3.7. The pinching or slip model is often used to represent the cyclic behavior of reinforced concrete.

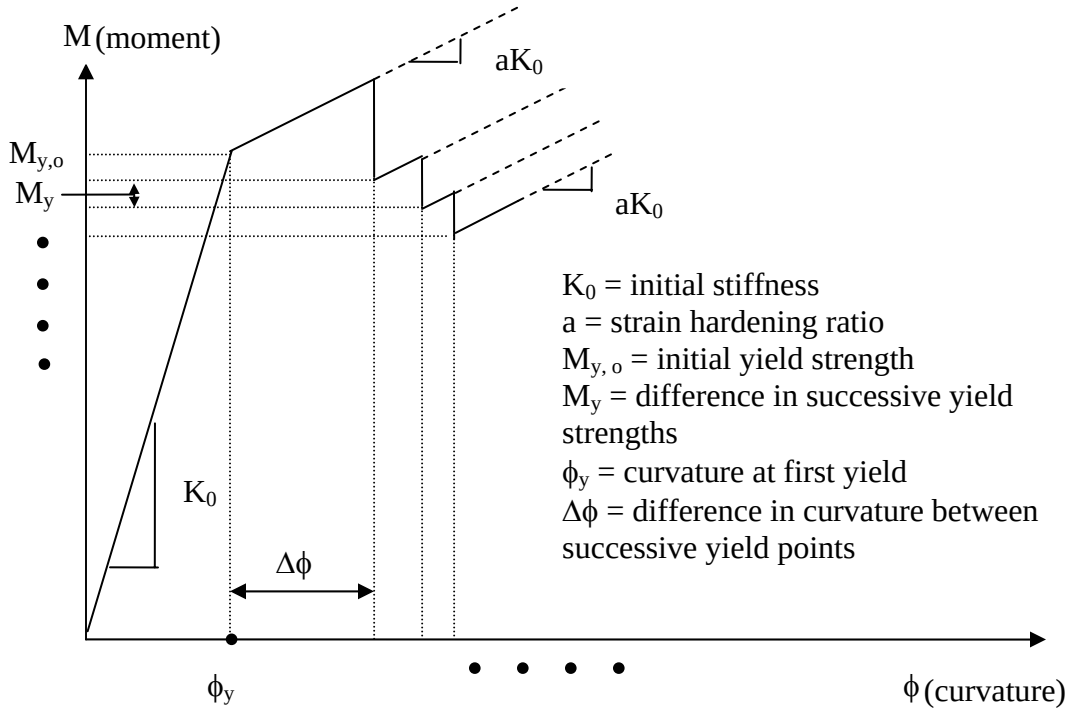

Fig. 3.7 Schematic representation of strength degradation
(Sivaselvan and Reinhorn, 1999)

The main considered behavior is the slope of the post-peak branch and the slope of the unloading branch. For defining pinching, a fictitious intersection point of all hysteretic loops on the initial ascending branch of the load-displacement relationship is determined.

(4) Vertex oriented:

This is related to the modeling of the stiffness degradation characteristics due to geometric stiffness. The geometric stiffness is affected due to increase in ductility in certain materials. The modeling of stiffness degradation has been done according to the pivot rule (Park et al., 1987). As illustrated in Figure 3.8, the stiffness degradation factor (R_K^+) is given by equation 3.3:

$$R_K^{+} = \frac{M_{cur} + \alpha M_y}{K_0 \phi_{cur} + \alpha M_y} \qquad 3.3$$

where M_{cur} is the current moment, ϕ_{cur} is the current curvature, K_0 is the initial elastic stiffness and α is the stiffness degradation parameter. M_y may be positive or negative yield moment.

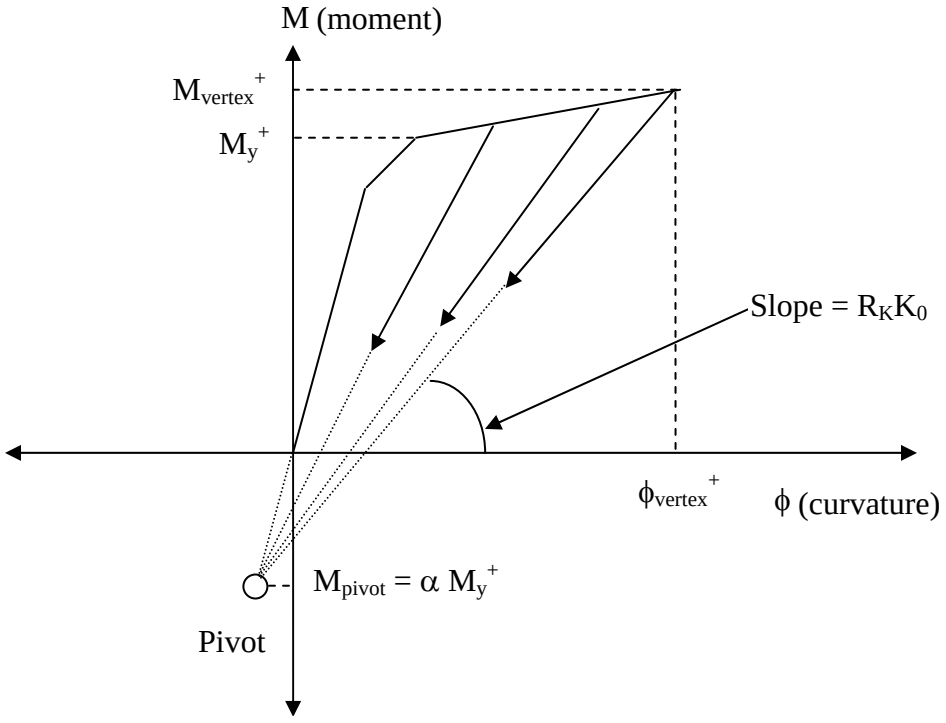

Fig. 3.8 Modeling of stiffness degradation for positive excursion
(for negative excursion the "+" sign changes accordingly)
(Sivaselvan and Reinhorn, 1999)

(5) Smooth model:

This provides for a smooth transition into yielding. Hence this model is suitable for describing various types of energy dissipating devices in structural systems. The positive and negative strain hardening slopes must be equal in this case. The basic model consists of two springs (Sivaselvan and Reinhorn, 1999). The post yield spring is a linear spring with post yield stiffness and a hysteretic spring, which controls the smooth transition from elastic to inelastic range. The smoothness and the shape of the curve can be controlled by suitably varying the parameters in the hysteretic spring. In order to account

for pinching, an additional spring can be added in series with the hysteretic spring. The additional stiffness observed in some of the elements at higher deformations can also be incorporated using a gap-closing spring. This spring can be set up in parallel with the post-yielding spring and the hysteretic spring.

The trilinear, vertex-oriented and smooth models have not been included in the verification manual in Appendix A. The IDA tool in *NONLIN* is capable of modeling only bilinear models that have symmetric properties in the loading and unloading cycles.

4 Incremental dynamic analysis using *NONLIN*

4.1 Introduction

Incremental dynamic analysis (IDA) (Vamvatsikos and Cornell, 2002) requires a series of nonlinear dynamic analysis runs until a given level of specified intensity measure (IM) is attained. The damage measure (DM) at each level of intensity is recorded and then plotted against IM. *NONLIN* is capable of performing IDA very efficiently for single degree of freedom systems. The output is available in the form of a spreadsheet or graphical display of the IDA curves. This chapter contains a detailed description of all the available features in the IDA tool in *NONLIN* that have been developed exclusively for research purposes.

4.2 System properties input

The various parameters of a single degree of freedom system include weight, damping, primary stiffness, yield strength, post-yield stiffness, and geometric stiffness. These values must be given by the user prior to analysis. Figure 4.1 depicts the IDA property entry window as existing in *NONLIN*. Once the values are entered at appropriate places, the program automatically writes the system's period of vibration.

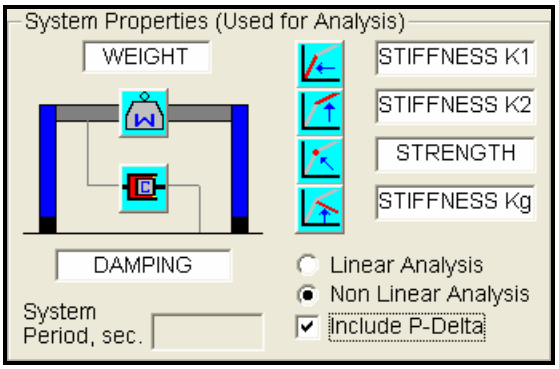

Fig. 4.1 System Properties input window in *NONLIN*

4.2.1 Weight

The mass of a system is required for computing the system's period, which is necessary for performing further analysis. Weight has to be entered in force units; this is subsequently converted to appropriate mass units. However in the main SDOF model in *NONLIN* the user has the option of entering mass directly.

4.2.2 Damping

Damping is an important parameter that not only affects the system but also affects the scaling of the ground motion. The scaling can be set according to the damping of the system or according to requirements of a building code. The value of damping has to be entered in terms of percent of critical damping.

4.2.3 Primary stiffness (K_1)

Primary stiffness, also known as initial stiffness, is an intrinsic property of the system. K_1 can be determined through a force-displacement relationship, Figure 4.2. In linear analysis this is the sole stiffness that holds for the system.

4.2.4 Secondary Stiffness (K_2)

This is also known as post-yield stiffness. This defines the nonlinear response and the behavior of the system in the hysteretic cycles under loading and unloading. K_2 is always less than the initial stiffness (K_1). The program does not allow the user to enter a negative value for K_2. If the post-yield stiffness is less than zero due to geometric stiffness, it can be included by incorporating P-Delta effects.

4.2.5 Yield Strength (F_y)

The yield point in the force displacement curve is where the stiffness of the system changes. At each time-step the program calculates the spring force. If the spring force exceeds the specified value (F_y) then it indicates yielding takes place and the stiffness is accordingly

updated. The yield strength and secondary stiffness can be enabled only if the nonlinear analysis option is selected in the *NONLIN* window.

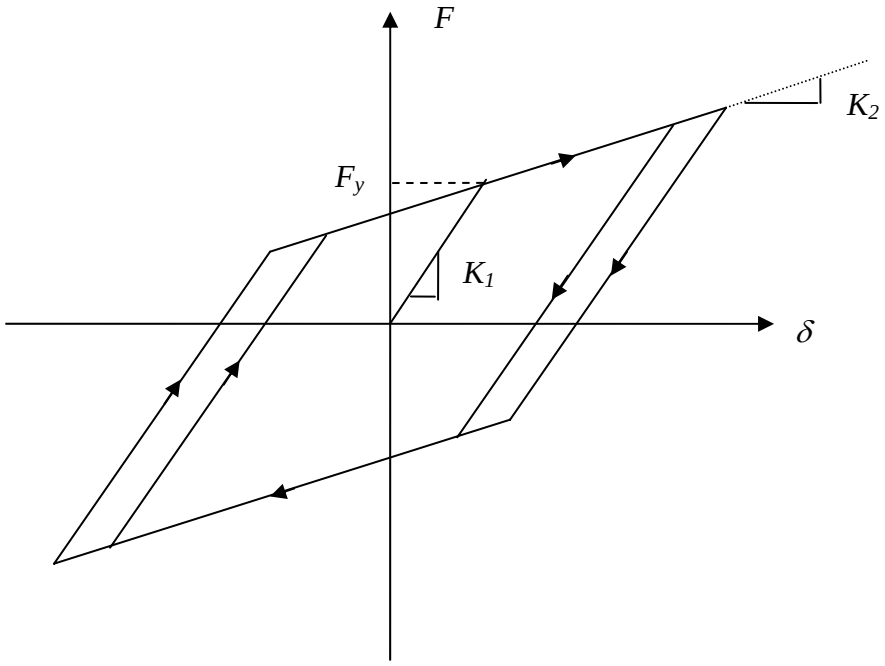

K_1 = Initial Stiffness
K_2 = Secondary Stiffness
F_y = Yield Strength

Fig. 4.2 Force displacement relationship

4.2.6 P-Delta option (K_G)

Nonlinearity that results due to the interaction of the axial load with the transverse deflection in an element is known as P-Delta effects. If P-Delta effects are incorporated, there is a reduction of the stiffness of the structure. In *NONLIN* the geometric stiffness has to be specified (K_G). The effect of incorporating geometric stiffness is illustrated in Figure 4.3 with the help of an example of elastic-perfectly-plastic material. Initial stiffness is K_1 and if K_G is specified, *NONLIN* automatically updates it to K_1^R**.** Since the material is perfectly plastic, post-yield stiffness is 0 k/in. Due to the inclusion of geometric stiffness, K_2^R equal to K_G is

used for analysis purposes. The program also automatically updates the yield strength to $F_{y,o}$ which is calculated using Equation 4.1.

$$F_{y,o} = F_y(1 - \frac{P}{K_1 h}) \qquad 4.1$$

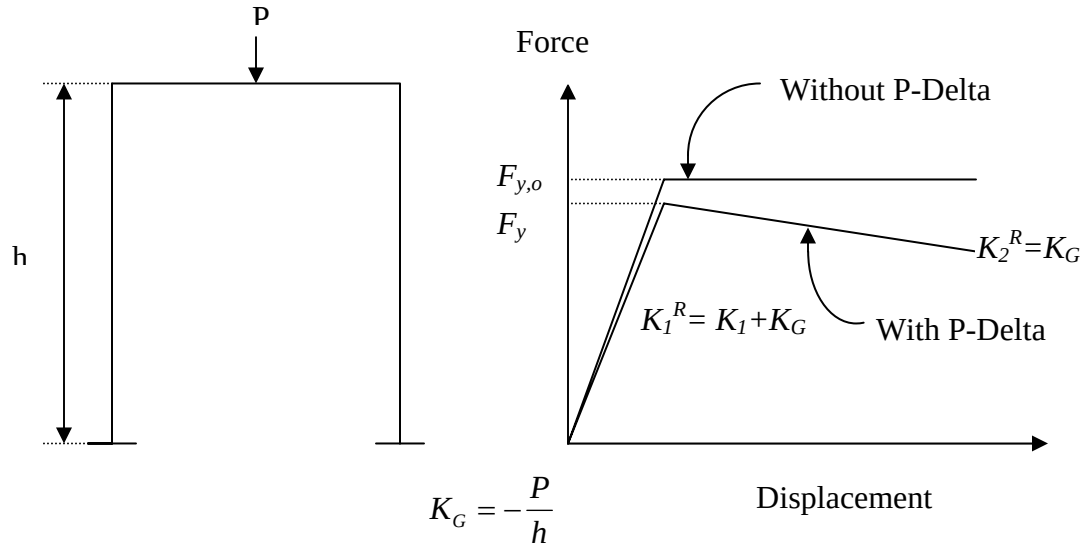

Fig. 4.3 P-Delta Effects occurring in a system having elastic-perfectly-plastic behavior

4.3 Scaling parameters

As has been mentioned earlier in Chapter 2, normalization of the accelerograms is a very effective method for reducing the number of nonlinear runs in order to close in on the median structural response. According to Shome et al. (1998), if normalized accelerograms are used, the number of required nonlinear analyses is reduced by a factor of 4 and the same median damage response is obtained. Available alternatives for scaling include peak ground acceleration and spectral acceleration at the structure's fundamental frequency at 5% damping. In *NONLIN* the user has the option of selecting the frequency and damping value for deciding the scale factor.

The window as shown in Figure 4.4 contains the following two option buttons, out of which only one can be enabled:

- Use System Parameters

- Use Target Scaling Parameters

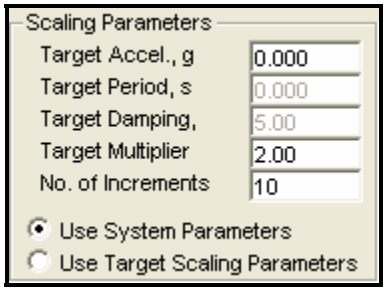

Fig. 4.4 Scaling parameters window

If the first option is selected, then the scaling is done according to the system's period of vibration. The second option can be used if the user wants to use some other value of time period for scaling the ground motions. This will be further elaborated in section 4.3.1.

The following values are also user defined:

(1) Target acceleration (P_A)

(2) Target period (T_1)

(3) Target damping

(4) Target multiplier

(5) Number of increments

Figure 4.5 represents a typical design spectrum as described in various building codes. A design spectrum is a specification of the level of design force or deformation and is a function of the natural period of vibration and damping. In Figure 4.5, T_1 is the period of vibration of the structure. Corresponding to T_1, the level of prescribed pseudo-acceleration is P_A. This is known as the target acceleration in *NONLIN*. A target multiplier is required for incremental dynamic analysis. P_B is obtained by multiplying the target acceleration with the target multiplier. P_B is the maximum intensity that the system will be subjected to during IDA. The user may specify the number of increments of the intensity measure between zero and P_B. This determines the number of different nonlinear runs to be performed on the structure. The scaling factor for each of these runs also depends on the intensity level.

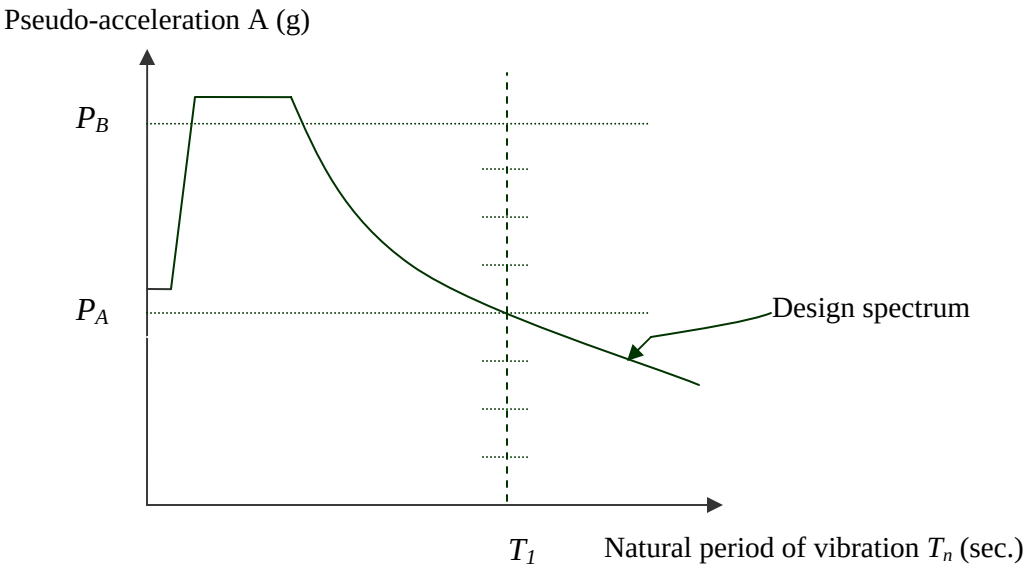

Fig 4.5 Typical design spectrum

In the above case (Figure 4.5), the system would be analyzed for eight different intensity levels for a single ground motion.

Run 1: Original Ground Motion x Scale Factor x Target Multiplier x (1/8)

Run 2: Original Ground Motion x Scale Factor x Target Multiplier x (2/8)

Run 3: Original Ground Motion x Scale Factor x Target Multiplier x (3/8)

Run 4: Original Ground Motion x Scale Factor x Target Multiplier x (4/8)

Run 5: Original Ground Motion x Scale Factor x Target Multiplier x (5/8)

Run 6: Original Ground Motion x Scale Factor x Target Multiplier x (6/8)

Run 7: Original Ground Motion x Scale Factor x Target Multiplier x (7/8)

Run 8: Original Ground Motion x Scale Factor x Target Multiplier x (8/8)

The scale factor for all the above eight runs is decided based on the target acceleration T_A. The determination of the scale factors is illustrated in Figure 4.6. A, B, C correspond to the different ground motions that are applied to a structure. A constant damping value is used for creating the Response Spectrum for all three ground motions. Pseudo-acceleration $A = \omega^2 D = \omega^2 u_o$. ω is the frequency corresponding to the natural period of vibration T_1 and u_o is the peak deformation of the system. The values of T_A are obtained from Figure 4.6.

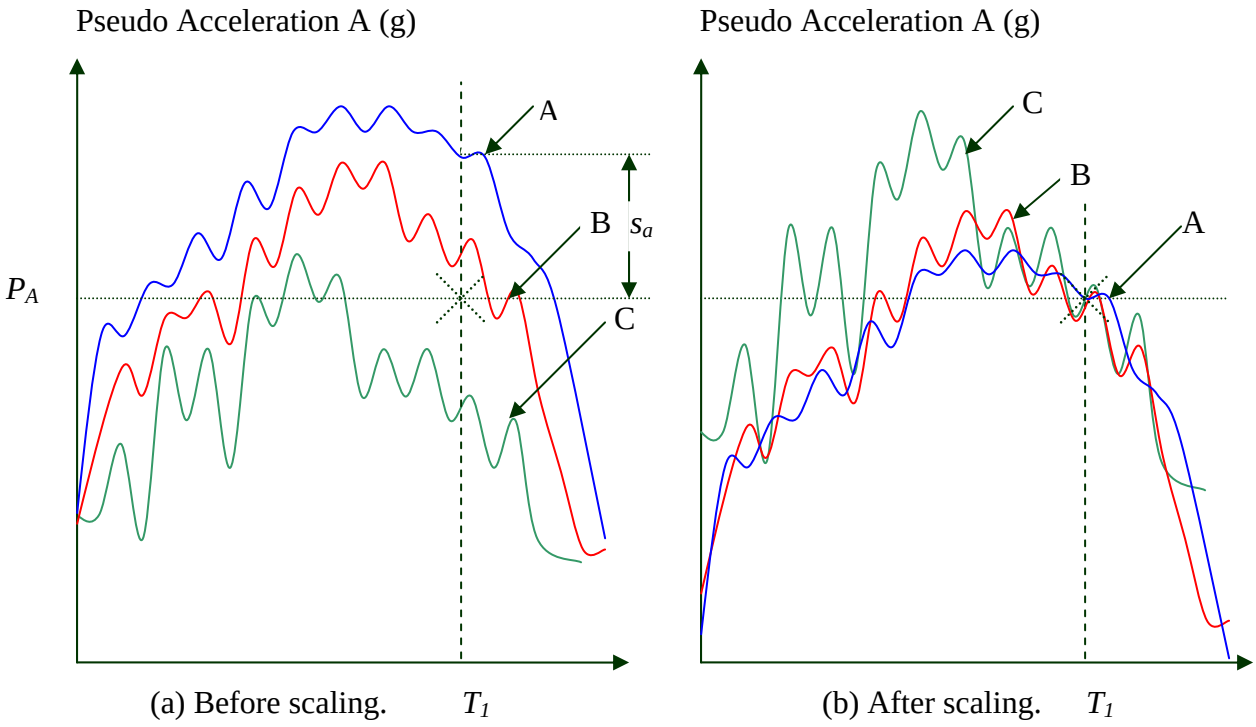

Fig 4.6 Determination of scale factor

The original ground motions in Figure 4.6(a) are scaled in such a way that at the natural period of vibration of the system all the three ground motions pass through the same point marked with X in Figures 4.6 (a) and (b). This determines the scale factor to be applied to each of the original ground motions. For the response of A, the scale factor should be such that the curve is scaled down by s_a. Similarly the curve corresponding to B has to be scaled down, but C has to be scaled up. The scale factor can also be user defined by assigning a time period that is not the natural period of vibration of the system. However, as recommended by Shome et al. (1998), the natural period of vibration is set as default. *NONLIN* has a database of various ground motion records. Using the IDA tool, a maximum of 12 ground motions can be selected. The procedure for selecting the ground motions is illustrated in Figure 4.7. Selecting one earthquake at a time and clicking the right arrow, the selected ground motions are placed in the box of 'Selected Earthquakes'. If any record is not required for analysis, it can be removed using the left arrow. By clicking on the 'Plot?' option, one can view the IDA plot of the response after the analysis run has been performed for the corresponding ground motion. It is color coded in order to distinguish one ground motion from another. The

‘Update Plot’ option is enabled if a particular ground motion is checked or unchecked from the ‘Plot’ option. This gives the user greater flexibility to select and view the IDA for any particular ground motion or any combination from the suite of ‘Selected Earthquakes’. When ‘RS Plot’ is selected, then a new window is created showing the response spectrum plot of the earthquakes for which plots were requested. The response spectrum can be observed for original and scaled ground motions. Individual plots can be created for each response such as displacement, spectral velocity or spectral acceleration. A tripartite graph can also be generated containing all the three response values in one plot. If the system parameters or scaling parameters are changed, the ‘Auto Scale’ is activated. If system parameters are changed, the user may skip the scaling update option and use the original scale factor for analyzing the system. However if the scaling parameters are changed, the user must update the scaling to activate the analysis run. After ensuring that all the input is entered correctly, the ‘Run’ command is used to perform the IDA. When the IDA is complete, a window containing the various plots is automatically obtained. If it is required to replace the original set of ground motions with another set of ground motions, the user has to click on ‘Clear List’ and then a new suite of earthquake records can be selected as described above. After the IDA is completed, one can exit the IDA tool by choosing the ‘Close’ button.

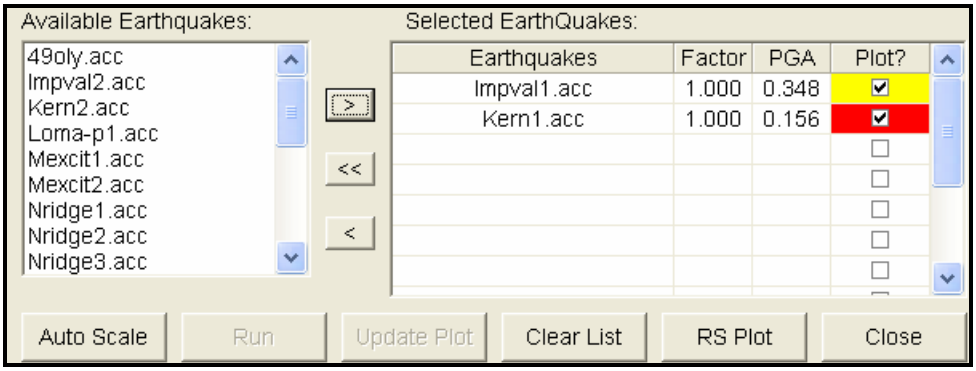

Fig 4.7 Ground motion selection

4.3.1 Use of target scaling parameters

The use of target scaling parameters in computing the scale factor is discussed here. The effect of scaling is illustrated in Table 4.1 and Table 4.2. The single degree of freedom system described in section 2.2.1 and having W = 7800 k, K_1 = 3170 k/in, K_2 = 317 k/in, F_y = 1170 k and ζ = 5% of critical was selected. The period of vibration of the above system is 0.502 seconds and this was used for scaling purpose. Target acceleration P_A = 0.25g, target multiplier = 3, hence P_B = 0.75g. The number of increments was 15. Table 4.1 (a) contains the original peak ground accelerations of the respective motions. When these were scaled, the factors that were obtained are shown in Table 4.1 (b). The final peak ground acceleration (PGA) is obtained by multiplying the original PGA by the scale factor. These correspond to a P_A of 0.25g. At each intensity level, the ground motions are scaled in a similar fashion to obtain the scaling factors which are subsequently used for performing the rest of the analyses.

Table 4.1 Scaling of ground motions using system's period of vibration

(a)

Earthquake	Factor	PGA (g)
Imperial Valley	1.0	0.348
Kern County	1.0	0.156
Loma Prieta	1.0	0.276
Northridge	1.0	0.604
Santa Monica	1.0	0.883

(b)

Earthquake	Factor	PGA (g)
Imperial Valley	0.303	0.106
Kern County	0.664	0.103
Loma Prieta	0.465	0.128
Northridge	0.186	0.112
Santa Monica	0.360	0.318

In Table 4.2 (a) the scaling is based on peak ground acceleration. A target period of 0.0 second was assigned in *NONLIN* to obtain the required scale factor. The resulting PGA is equal for all the five ground motions and is equal to the target acceleration of 0.25g. To study the effect of scaling at a target period (T_1) greater than the system's period of vibration, the target period was set to 3.0 seconds. The scale factors and the resulting peak ground acceleration are shown in Table 4.2 (b). The target damping may be equal to the percentage

critical damping of the system. If a different value is assigned, the response spectrum is first generated for the corresponding value of damping and then the scale factors are computed. This feature offers greater flexibility to the user for scaling the ground motions for any set of parameters.

Table 4.2 Scaling of ground motions using PGA scaling and for T = 3.0 seconds

Earthquakes	Factor	PGA (g)
Imperial Valley	0.718	0.250
Kern County	1.606	0.250
Loma-Prieta	0.907	0.250
Northridge	0.414	0.250
Santa Monica	0.283	0.250

Earthquakes	Factor	PGA (g)
Imperial Valley	2.188	0.762
Kern County	5.621	0.875
Loma-Prieta	4.021	1.109
Northridge	0.951	0.575
Santa Monica	1.988	1.755

The response spectra for the original ground motion having peak ground acceleration as shown in Table 4.1 (a) are shown in Figure 4.8. This corresponds to a damping of 5% of critical.

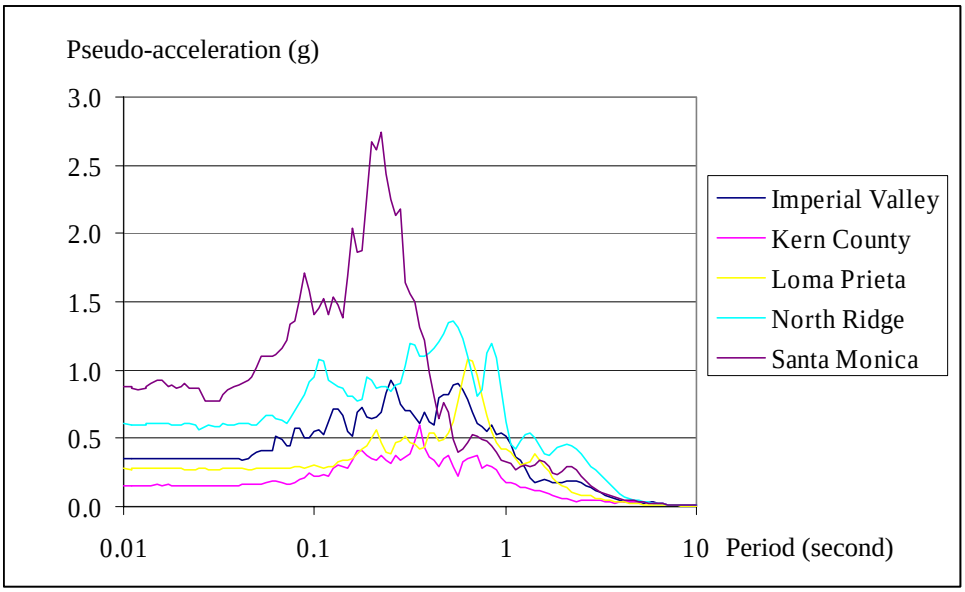

Fig. 4.8 Response spectra of the original ground motions

The response spectra when the ground motions are scaled according to the factors given in Table 4.1 (b), which is based on the system's period of vibration, i.e. 0.502 seconds, and 5% of critical damping are shown in Figure 4.9. When the target period is set as zero, the scaling is done with respect to the PGA as shown in Figure 4.10. The corresponding scale factors can be found in Table 4.2 (a).

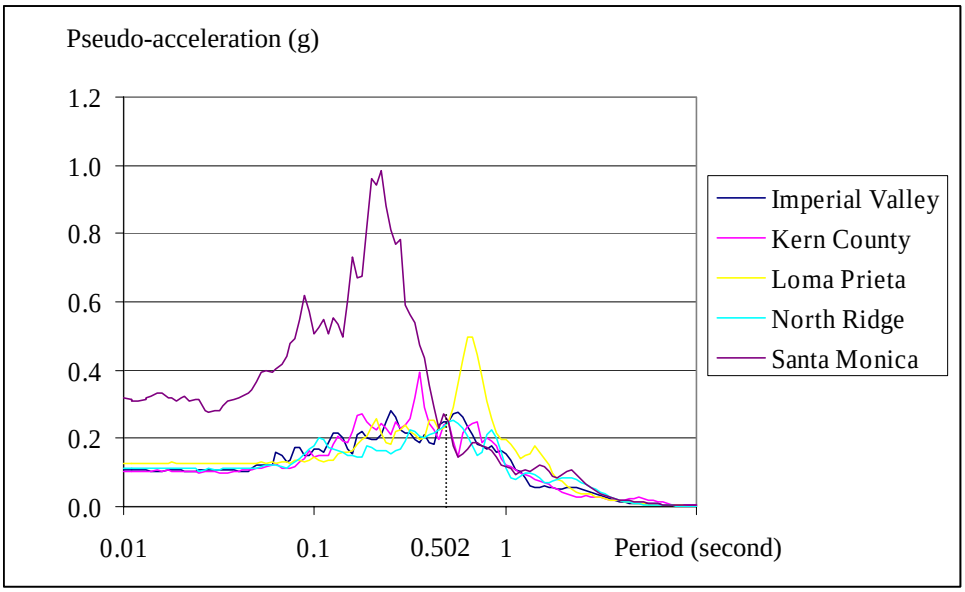

Fig. 4.9 Response spectra of the ground motions based on system's period of vibration

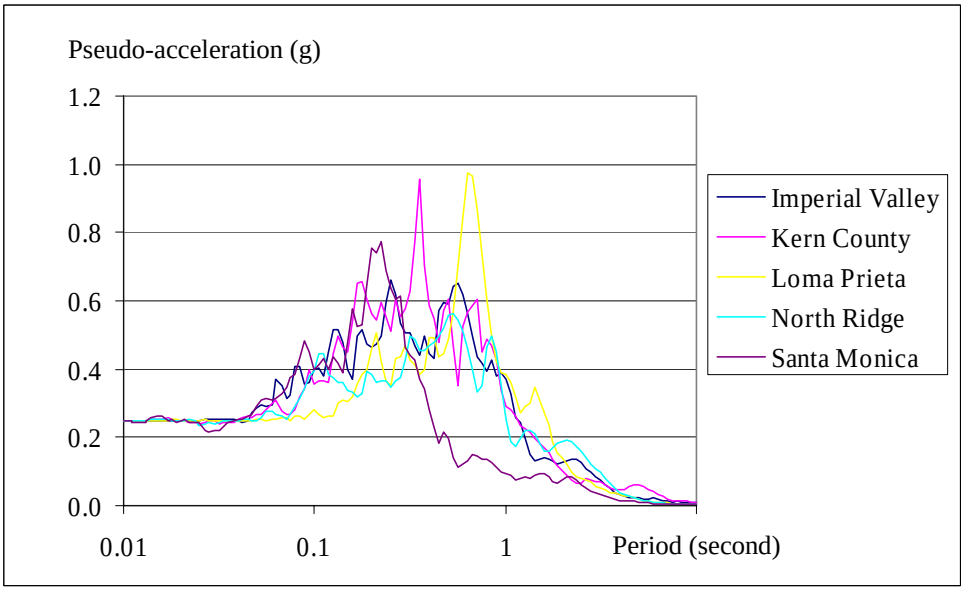

Fig. 4.10 Response spectra of the ground motions based on PGA scaling

The effect of using a high value for the target period is illustrated in Figure 4.11. The scale factors as shown in Table 4.2 (b) were obtained by using a period of 3.0 seconds. The scale factors for all the ground motions are greatest in this case. This indicates that the target acceleration of 0.25g was higher than the spectral acceleration level (at 3.0 seconds) of the original ground motion except for the Northridge earthquake having a scale factor of 0.951 second. Hence the response spectra of Figure 4.11 have the highest values for the pseudo acceleration.

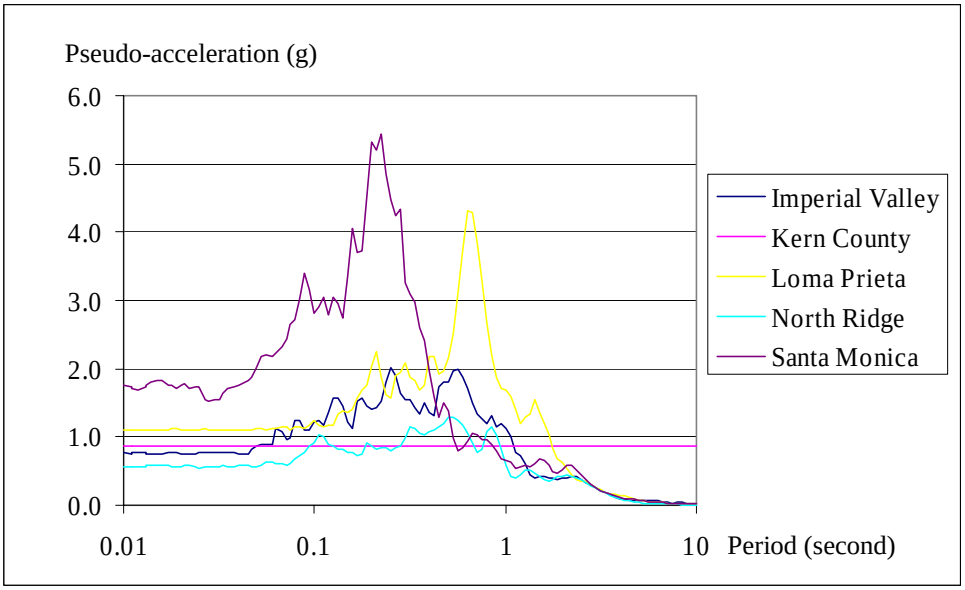

Fig. 4.11 Response spectra of the ground motions based on target period of 3.0 seconds

After the scaling is completed, all the required data is available for performing the analyses. For each earthquake, analysis is performed for all the intensity levels. The response is plotted in a graph. The vertical axis always represents the intensity level. The horizontal axis denotes the response.

The horizontal axis contains the following responses:

(1) Peak Displacement: The absolute maximum deformation of the structure is known as the peak displacement.

(2) Peak Ductility Demand: Ratio of peak dynamic displacement to displacement at which yielding takes place.

(3) Peak Base Shear: The maximum value of the total inertial force (mass times the total acceleration) when the system is analyzed for a given intensity of ground motion. This can also be obtained by taking the sum of the elastic force and the damping force.

(4) Peak Residual Deformation: It is the deformation of the system measured at the end of the response history analysis.

(5) Total Yield Events: This records the number of instants the structure yields and also the time at which each yielding event takes place.

(6) Positive Yield Events: This corresponds to the number of times yielding takes place when the force and displacement both act in the positive direction.

(7) Negative Yield Events: This corresponds to yielding when force and displacement act in the negative direction.

(8) Hysteretic Energy: It is the total energy dissipated over the various cycles of loading and unloading.

(9) Damage Index: This is the damage index developed by Park and Ang (1985):

$$DI_{PA} = \frac{u_{\max}}{u_{mon}} + \frac{\beta E_H}{F_y u_{mon}}.$$

u_{max} is the maximum deformation. u_{mon} is the maximum deformation capacity under monotonically increasing lateral deformation. E_H is the irrecoverable hysteretic energy. F_y is the yield strength and β is a constant.

Figure 4.12 (a) and (b) depicts the multi-record IDA curves as observed in *NONLIN* and *MS-Excel* respectively for the system described above. For scaling the ground motion according to the system's period of vibration (0.502 second), the option 'Use System Parameter' is enabled. In this case the displacement is measured along the horizontal axis and the intensity level is indicated along the vertical axis. The cross hairs on the plot are indicators of various intensity levels. Using the arrows, one can view individual response histories at each level of

intensity. The color code of the IDA curves is the same that was used for scaling the ground motion. So the user is able to distinguish the response due to a particular ground motion. At each level the displacement and spring force history plots are available on the right. This plot can also be magnified. The box at the right hand bottom corner of the window displays the response history for a single earthquake. By clicking on the right hand dropdown box, one can select the earthquake. The left hand dropdown box enables the user to choose the type of response desired. The various responses that are available in this option are Ductility Demand, Spring Force, Displacement, Yield Code and Input time history.

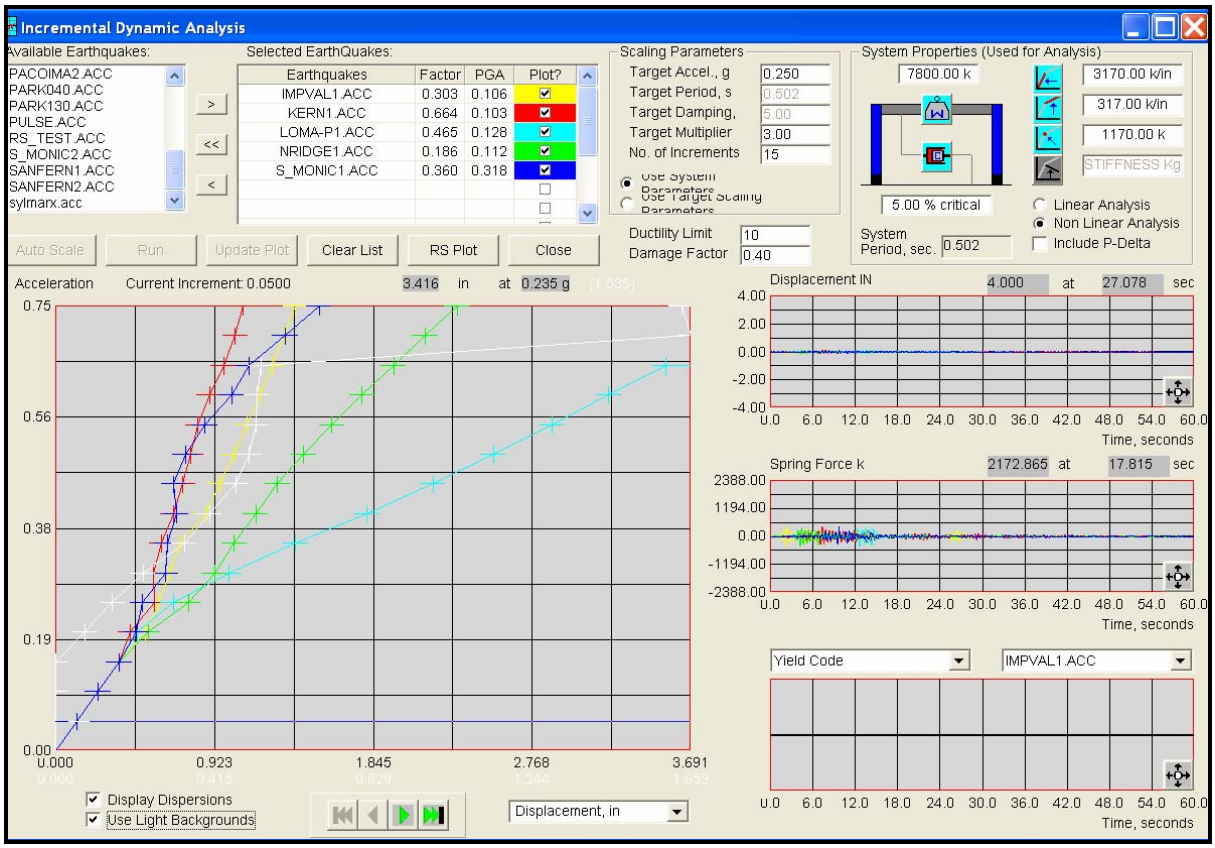

Fig 4.12 (a) Multi-record IDA curves for five ground motions using system's period of vibration as observed in *NONLIN*

In order to highlight the IDA curves according to the contrast desired, one may check the option 'Use Light Background'. If it is unchecked, the background color of the plot area is dark. At each intensity level the coefficient of variation can be observed by checking the

option ‘Display Dispersion’. Coefficient of variation is the ratio of the standard deviation to the mean of all the recorded responses at a given intensity level. This is elaborated in greater detail in Chapter 5.

Due to the various user-friendly graphical options, *NONLIN’s* IDA tool was considered appropriate for generating the required IDA curves necessary in this study. In order to compare the results for single record IDA study, only one ground motion was used at a time. The results were then exported to *MS-Excel* and the curves for a given range of variation of parameters were plotted on the same graph. This procedure was necessary because the present version of the IDA tool in *NONLIN* is capable of generating only multi-record IDA. Figure 4.13 and Figure 4.14 present the multi-record IDA plots obtained using a scale factor corresponding to a target period of 0.0 second (PGA scaling) and 3.0 seconds, respectively. These plots have been included to show the effect of the scale factor on the response of the system. These plots were generated in *MS-Excel* and show that the data obtained from *NONLIN* is compatible with *MS-Excel*.

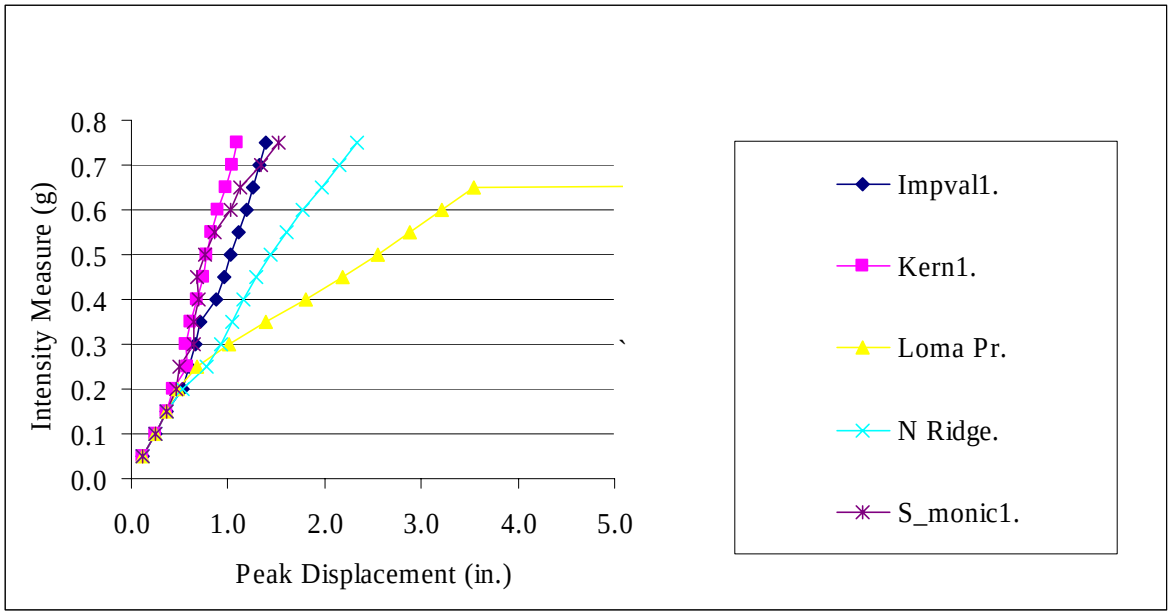

Fig 4.12 (b) Multi-record IDA curves for five ground motions using system’s period of vibration as plotted in *MS-Excel*

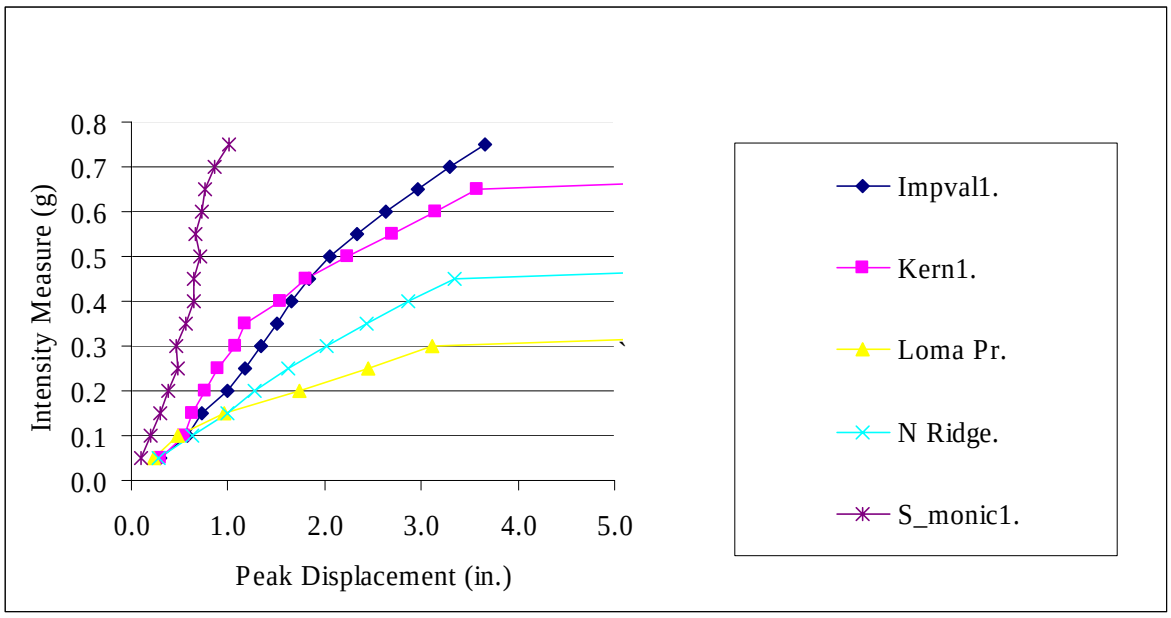

Fig 4.13 Multi-record IDA curves for five ground motions using PGA scaling

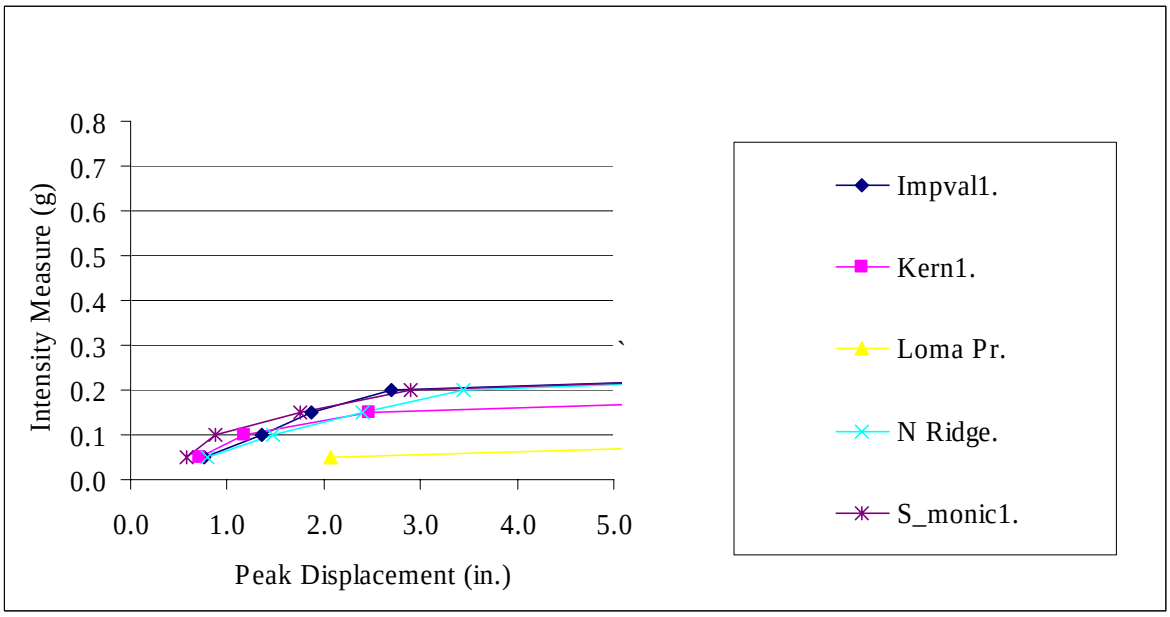

Fig 4.14 Multi-record IDA curves for five ground motions using target scaling of 3.0 seconds

The effects of the target period on the response can be observed from the IDA plots of Figures 4.12-4.14. In Figure 4.12 the system collapses when subjected to Loma Prieta ground motion at an intensity measure of 0.65g. For all other ground motions the system is stable. When PGA scaling is used as in Figure 4.13, higher values of response are obtained at each intensity level and the system collapses for Loma Prieta, Northridge and Kern County ground motions. If the scale factor is based on target scaling of 3.0 seconds, the response obtained is as shown in Figure 4.14. The system cannot sustain an earthquake of intensity measure greater than 0.2g. This study indicates the sensitivity of the scaling parameter used on the response. The lowest response was obtained when the system's period of vibration is used as the target period. Hence one must be very careful in selecting the scale factor. If a system is designed based on any arbitrary scale factor, then it may lead to overconservative designs. Another aspect of scaling is discussed in Chapter 5 with the help of a single-record IDA study on a given system.

5. Effect of rescaling in variation of parameter study

5.1 Concept of rescaling

Incremental Dynamic Analysis (IDA) (Vamvatsikos and Cornell, 2002) involves the use of scaled ground motion records applied as a forcing function on the structure. As has been described in Chapter 4 the scaling is done such that for a particular ground motion the pseudo-acceleration equals the design spectral acceleration as given by the building codes. The variation of parameter study involves varying the stiffness, damping and the yield strength. If P-delta effects are included or the geometric stiffness is changed, it affects the stiffness and hence the scaling. Since the scaling factor is a function of the time-period and damping, it is directly affected if either stiffness or damping is changed. There are two ways of approaching this problem. The first method is to rescale the ground motion each time a parameter is varied. The rescaled ground motion is then applied on the structure having the corresponding set of parameters (stiffness or damping). This method is termed as the Updated Scaling Method. The second approach is to identify the median value from the given range of the parameters used. Based on this median value, the scale factor is computed. This scale factor is multiplied with the original ground motion and applied to all the cases involving the variation of a particular parameter. This method has been named as Median Scaling Method. The only way of determining the suitability of updated scaling with respect to the median scaling method is to run IDA on different systems using the two procedures. Then the response obtained from the two sets can be compared. The dispersion in the results for both the cases can be measured using the coefficient of variation. The coefficient of variation (C.O.V) is a statistical measure and is calculated from the standard deviation. At each intensity level, a set of responses is recorded. The elements of this set comprise the results obtained from a nonlinear response history analysis for different variations of a given parameter. Standard deviation is the root-mean-square (rms) deviation and is always positive. The expression for standard deviation is given by Equation 5.1:

$$\sigma = \sqrt{\frac{\sum_{i=1}^{n}(x_i - \mu)^2}{n}} \qquad 5.1$$

where σ is the standard deviation, x_i is the response obtained from each analysis, μ is the average value of a set of responses and n is the number of responses. The coefficient of variation is the ratio of the standard deviation (σ) of a specific set to its mean (μ).

5.2 Procedure

Five different ground motions were used in this study to generate the IDA curves. They were Imperial Valley, Kern County, Loma Prieta, Northridge and Santa Monica ground motions. These records were selected because they provided a range of peak ground accelerations (PGA). As shown in Table 5.1, of the given records the lowest PGA of 0.156g was for Kern County and the highest of 0.883g was for Santa Monica ground motion. The duration of the earthquake for all of these records except the Loma Prieta earthquake was over 50 seconds. Each of these was scaled for both Median Scaling and Updated Scaling Method. For median scaling, each ground motion was scaled only once for a given intensity level. However, for updated scaling, each ground motion was rescaled each time a parameter was varied. Table 5.1 shows the scale factor used for each ground motion corresponding to a target acceleration (T_A) of 0.25g at the target period equal to the period of vibration of the system described in section 2.2.1 and also given below.

Weight = 7800 k.

Damping = 5% of critical.

Initial stiffness = 3170 k/in.

Post yield stiffness = 317 k/in.

Yield strength = 1170 k.

The scale factors shown in Table 5.1 were multiplied with the original ground motion to arrive at the scaled acceleration histories shown in Figure 5.1 (a-e).

Table 5.1 Scaled accelerations histories obtained for target acceleration of 0.25g and used for the Median Scaling Method

Ground Motion	Original PGA (g)	Scale Factor	Scaled PGA (g)
Imperial Valley	0.348	0.303	0.105
Kern County	0.156	0.664	0.104
Loma Prieta	0.276	0.465	0.128
Northridge	0.604	0.186	0.112
Santa Monica	0.883	0.362	0.320

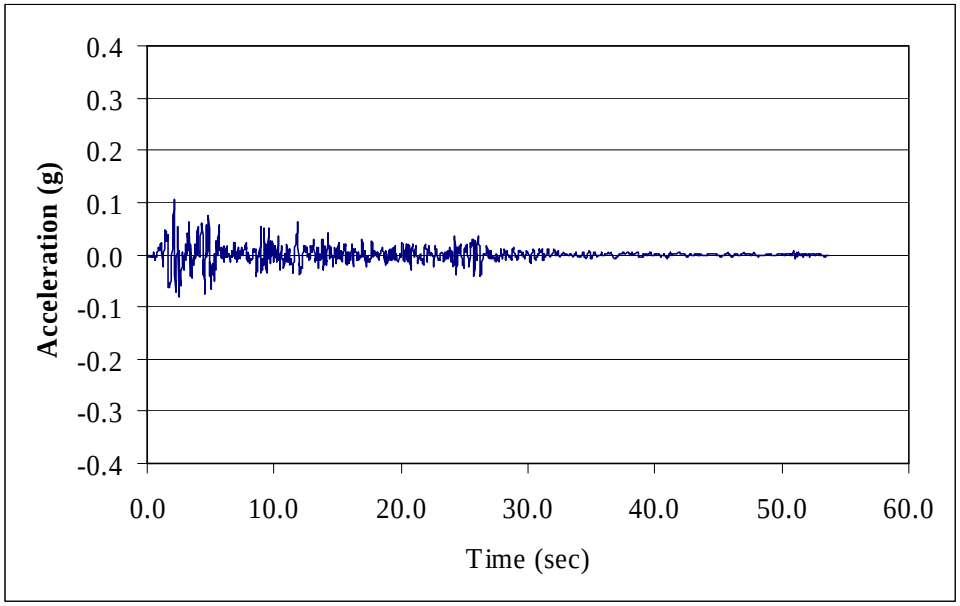

Fig. 5.1(a) Scaled acceleration time history of Imperial Valley Ground Motion

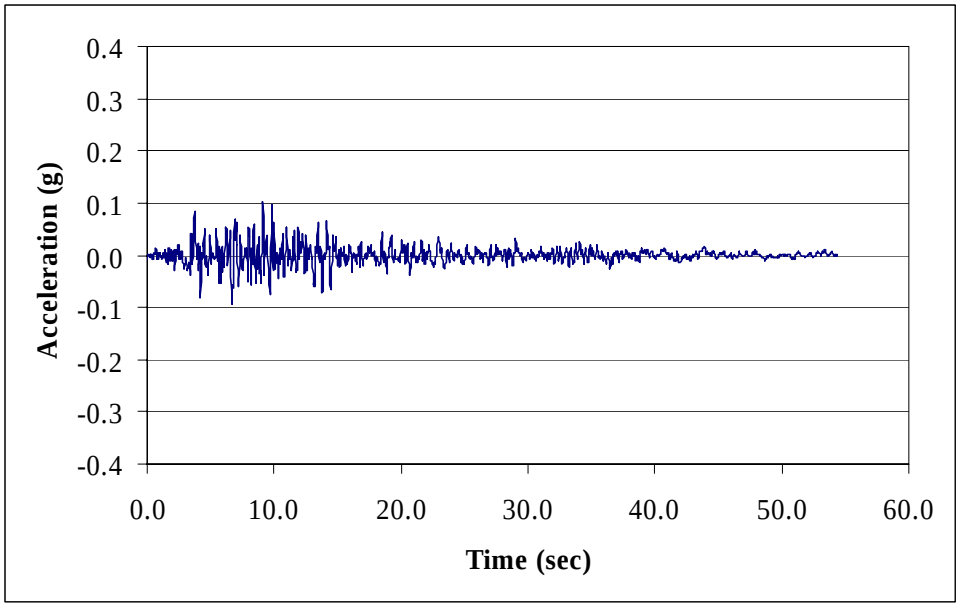

Fig. 5.1(b) Scaled acceleration time history of Kern County Ground Motion

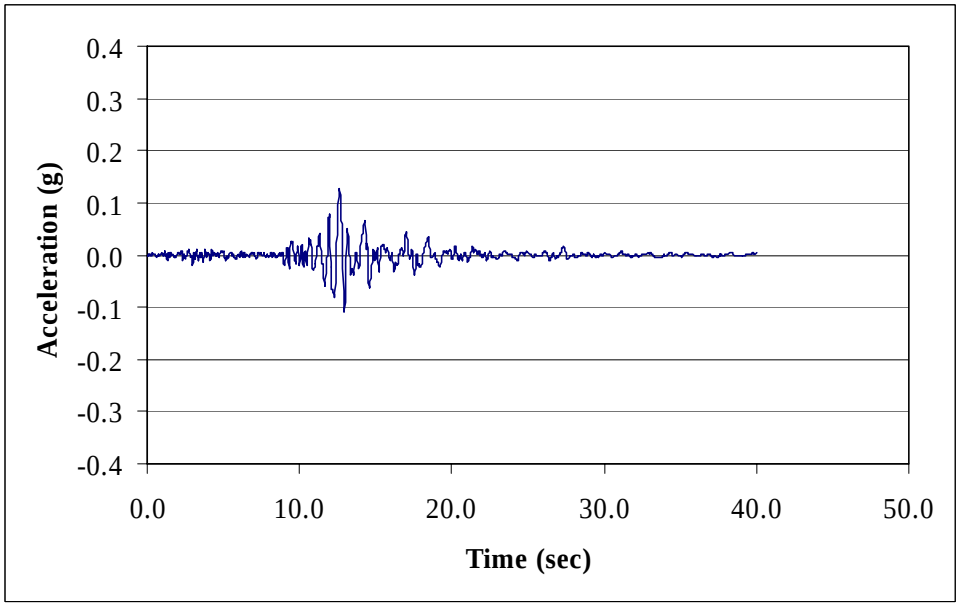

Fig. 5.1(c) Scaled acceleration time history of Loma Prieta Ground Motion

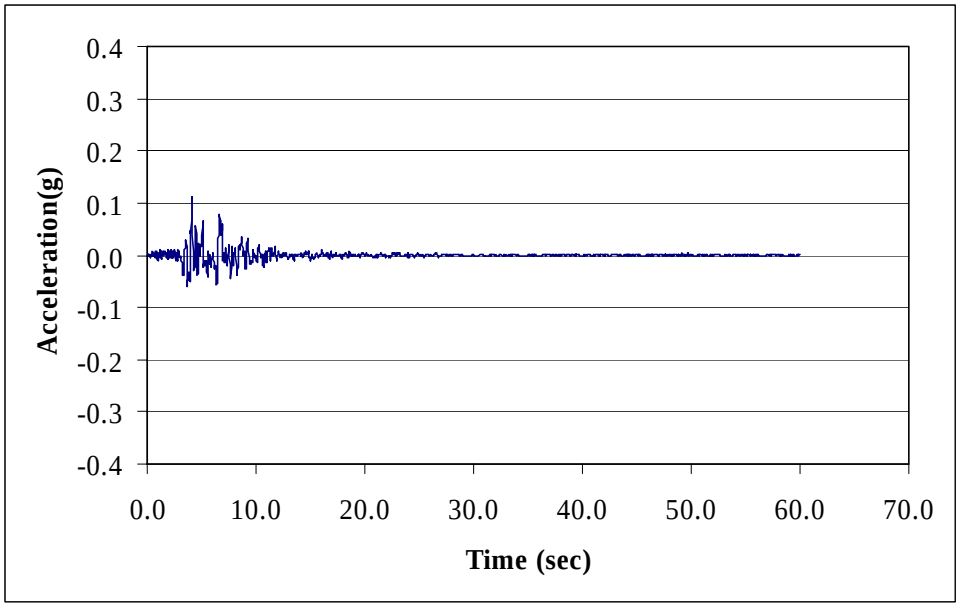

Fig. 5.1(d) Scaled acceleration time history of Northridge Ground Motion

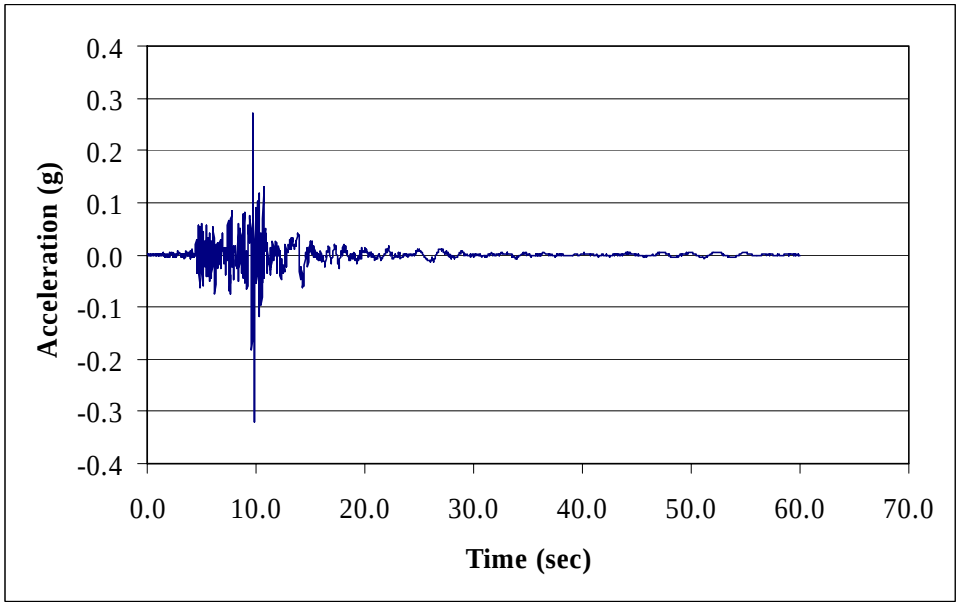

Fig. 5.1(e) Scaled acceleration time history of Santa Monica Ground Motion

The value of the initial stiffness was varied and the corresponding scale factor was used in the case of Updated Scaling Method. The values of stiffness used were 2770 k/in., 2970 k/in., 3170 k/in., 3370 k/in. and 3570 k/in. The scaling was based on 5% of critical damping and the period of vibration is shown in Table 5.2 for the updated scaling procedure. In the case of median scaling, all the IDA curves were generated based on a single scale factor arrived at by using a time period of 0.502 second. This corresponds to the median value of the parameter which is derived from the system having stiffness of 3170 k/in. For the case of updated scaling, the scale factors corresponding to the stiffness are shown in Table 5.3. The scale factors that were obtained using a stiffness of 3170 k/in. were used in the Median Scaling Method as shown in Table 5.1.

The damage measures that were used to compare the analysis results were peak displacement and ductility demand.

Table 5.2 Period of vibration of the different systems used in the Updated Scaling Method of analysis

Initial Stiffness (k/in.)	Mass (k-sec^2/in.)	$T = 2\pi\sqrt{\frac{m}{k}}$ (sec)
2770	20.21	0.537
2970	20.21	0.518
3170	20.21	0.502
3370	20.21	0.487
3570	20.21	0.473

Table 5.3 Scale factors used in the Updated Scaling Method of analysis for target acceleration of 0.25g

Ground Motion	K = 2770 k/in.	K = 2970 k/in.	K = 3170 k/in.	K = 3370 k/in.	K = 3570 k/in.
Imperial Valley	0.277	0.287	0.303	0.309	0.302
Kern County	0.917	0.740	0.664	0.660	0.702
Loma Prieta	0.385	0.433	0.465	0.489	0.512
Northridge	0.185	0.184	0.186	0.191	0.199
Santa Monica	0.529	0.429	0.362	0.330	0.331

5.3 Results

5.3.1 Results for the Imperial Valley ground motion

The analysis was performed using the IDA tool available in *NONLIN*. The results were exported to an *MS Excel* spreadsheet and the graphs were plotted. The response for Imperial Valley ground motion using median scaling has been plotted in Figure 5.2 (a). The curves are distinct at each level of intensity. There is no overlap at any of the levels of intensity. A converging trend is observed. The inverse relationship between stiffness and drift is evident. When updated scaling was used to obtain the IDA curves for Figure 5.2 (b), there is overlap at various stages. There is lack of uniformity between the response and the stiffness of the system used for analysis. For the plot of peak ductility demand generated for median scaling as in Figure 5.3 (a) and with updated scaling as in Figure 5.3 (b), there is not much of a difference between the relative shapes of the curves in either cases. The dispersion is measured using the coefficient of variation. To enable easy comparison between the coefficients of variation for any two plots, the values of the coefficient of variation were magnified five times. In Table 5.4, column 1 represents the various intensity levels. Column

2 and column 3 have the values for the coefficient of variation of peak displacement and ductility demand, respectively, for systems analyzed without rescaling. Column 4 and column 5 contain the values for the coefficient of variation of peak displacement and ductility demand, respectively, for the system analyzed with updated scaling. Column 6 is the ratio of the value in Column 2 to the corresponding value in Column 4. If this ratio is greater than 1.0, it indicates that the coefficient of variation for peak displacement is greater for systems analyzed without rescaling. Column 7 is the ratio of the value in Column 3 to the corresponding value in Column 5. If the ratio is greater than 1.0 it indicates that the coefficient of variation for ductility demand is greater for systems with median scaling. It is seen that the entire column 6 and half of the entries in Column 7 are greater than 1.0. Hence from the results of peak displacement response it can be observed that dispersion is greater when the Median Scaling Method is adopted than for the Updated Scaling Method. However, if peak ductility demand is used as the damage result, the coefficient of variation is less in the Median Scaling Method at higher levels of intensity when the system shows inelastic response.

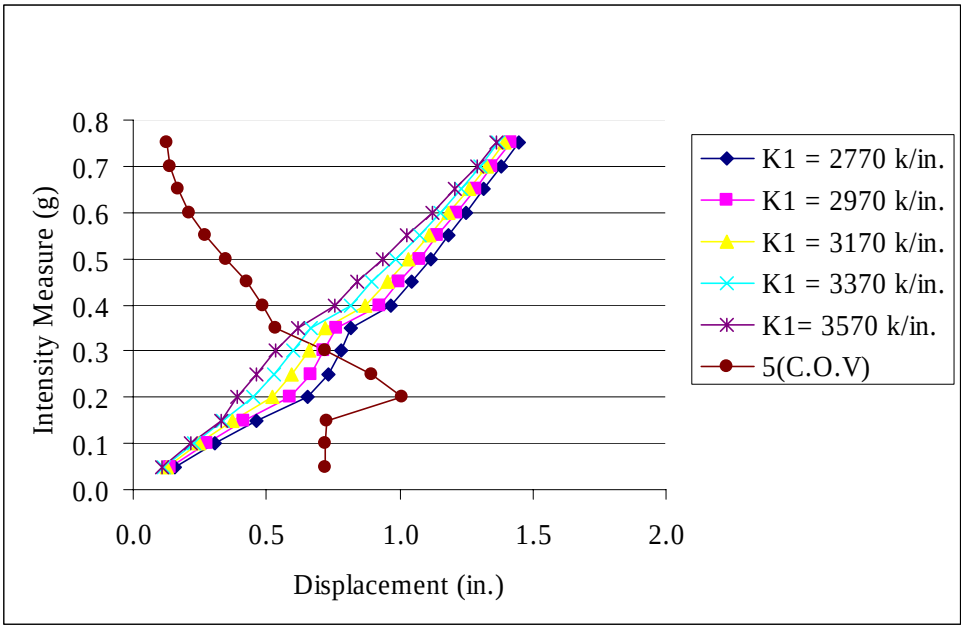

(a) IDA plots without rescaling (scaling done with K1 = 3170 k/in.)

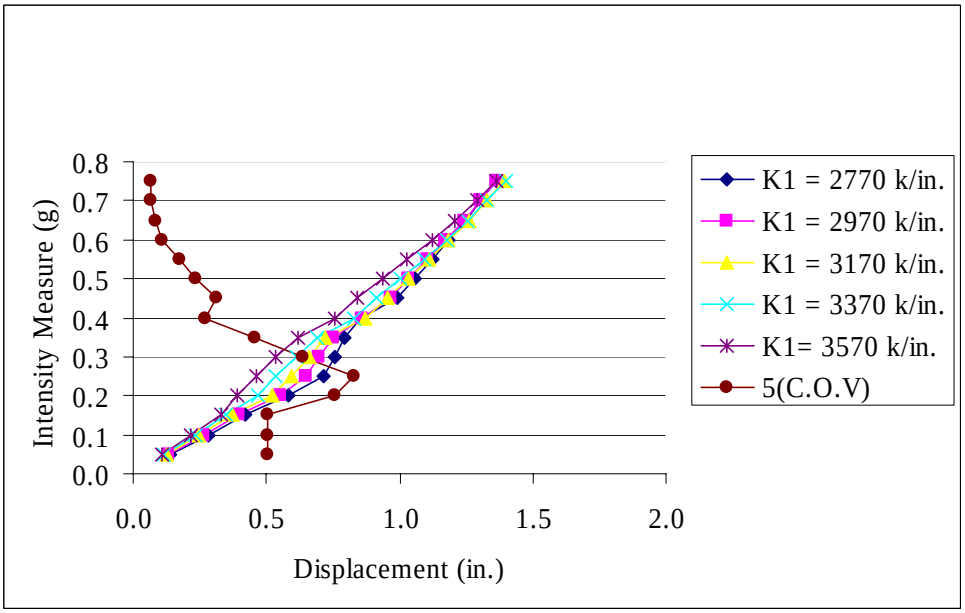

(b) IDA plots with updated scaling

Fig. 5.2(a-b) IDA plots of peak displacement response for the Imperial Valley ground motion

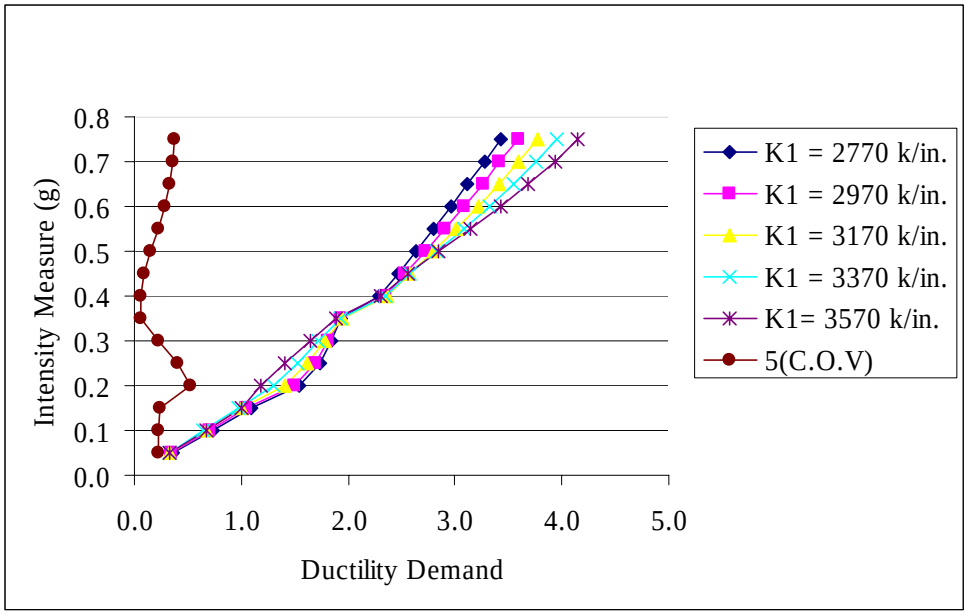

(a) IDA plots without rescaling (scaling done with K1 = 3170 k/in.)

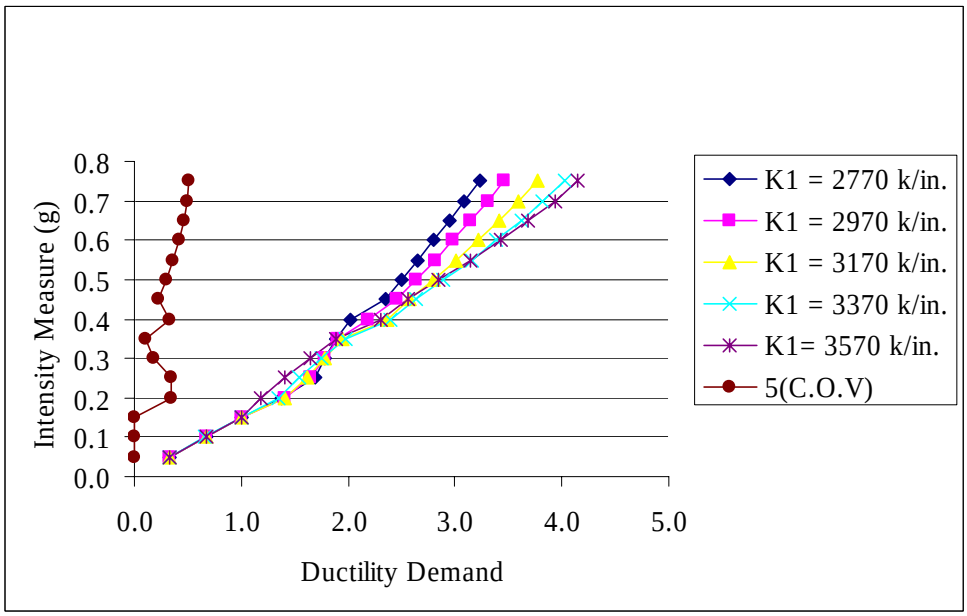

(b) IDA plots with updated scaling

Fig. 5.3(a-b) IDA plots of ductility demand for the Imperial Valley ground motion

Table 5.4 Coefficients of variation for the response analysis results for the Imperial Valley Ground Motion

	Median Scaling		Updated Scaling			
	Peak Displ.	Ductility Demand	Peak Displ.	Ductility Demand		
Column 1	Column 2	Column 3	Column 4	Column 5	Column 6	Column 7
Intensity Level	Coefficient of variation Figure 5.2 (a)	Coefficient of variation Figure 5.2 (b)	Coefficient of variation Figure 5.3 (a)	Coefficient of variation Figure 5.3 (b)	Ratio of Column 2 to Column 4	Ratio of Column 3 to Column 5
0.050	0.144	0.045	0.101	0.001	1.434	*
0.100	0.144	0.045	0.101	0.001	1.434	*
0.150	0.146	0.047	0.101	0.001	1.449	*
0.200	0.202	0.105	0.152	0.068	1.330	1.543
0.250	0.179	0.081	0.165	0.070	1.081	1.166
0.300	0.144	0.046	0.128	0.036	1.125	1.291
0.350	0.107	0.011	0.092	0.022	1.169	0.489
0.400	0.097	0.012	0.055	0.067	1.781	0.176
0.450	0.086	0.017	0.062	0.046	1.373	0.373
0.500	0.070	0.031	0.047	0.059	1.470	0.526
0.550	0.055	0.046	0.034	0.073	1.590	0.624
0.600	0.042	0.058	0.021	0.085	1.970	0.683
0.650	0.033	0.067	0.017	0.092	1.965	0.725
0.700	0.027	0.073	0.013	0.099	2.161	0.738
0.750	0.025	0.076	0.013	0.103	1.911	0.738

* Large due to zero C.O.V for linear systems

5.3.2 Results for the Kern County ground motion

The above system was analyzed for the Kern County ground motion. Figure 5.4 (a) shows the peak displacement response with the median scaling method and Figure 5.4 (b) is obtained using the updated scaling procedure. There is significantly greater dispersion in Figure 5.4 (b). It is also observed from Figure 5.4 (b) that the dispersion increases with a decrease in stiffness and one may conclude that it leads to instability. However, this is not the case as observed from Figure 5.4 (a). The same trend is observed in the ductility plots of Figure 5.5 (a) and Figure 5.5 (b). The dispersion is less for median scaling. The ratios between the coefficients of variation are listed in Table 5.5. All the values in column 6 and most of them in column 7 are less than 1.0 (in the region of inelastic response). Hence the

coefficient of variation of the response is less for median scaling than it is for updated scaling.

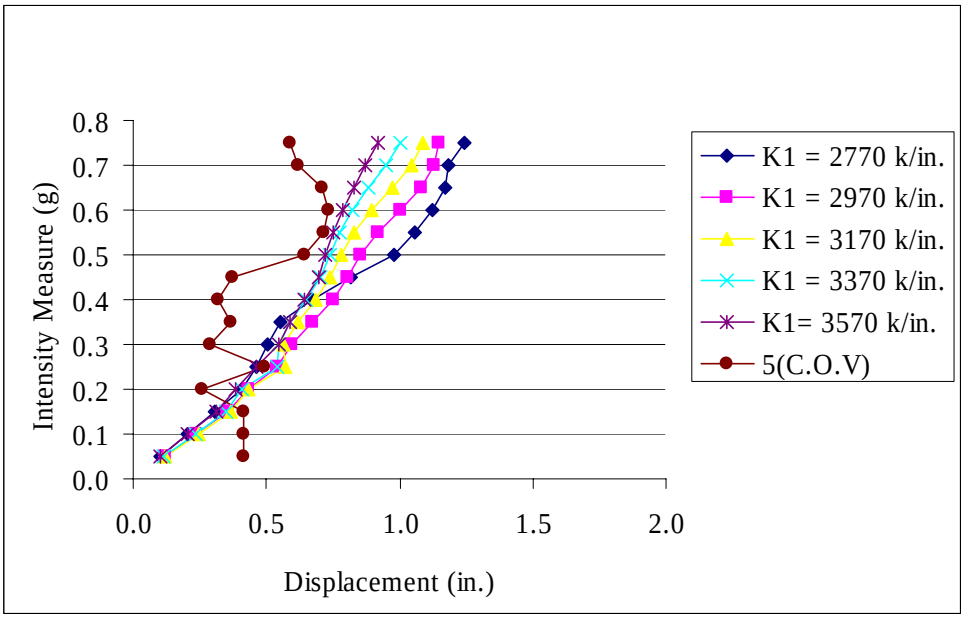

(a) IDA plots without rescaling (scaling done with K1 = 3170 k/in.)

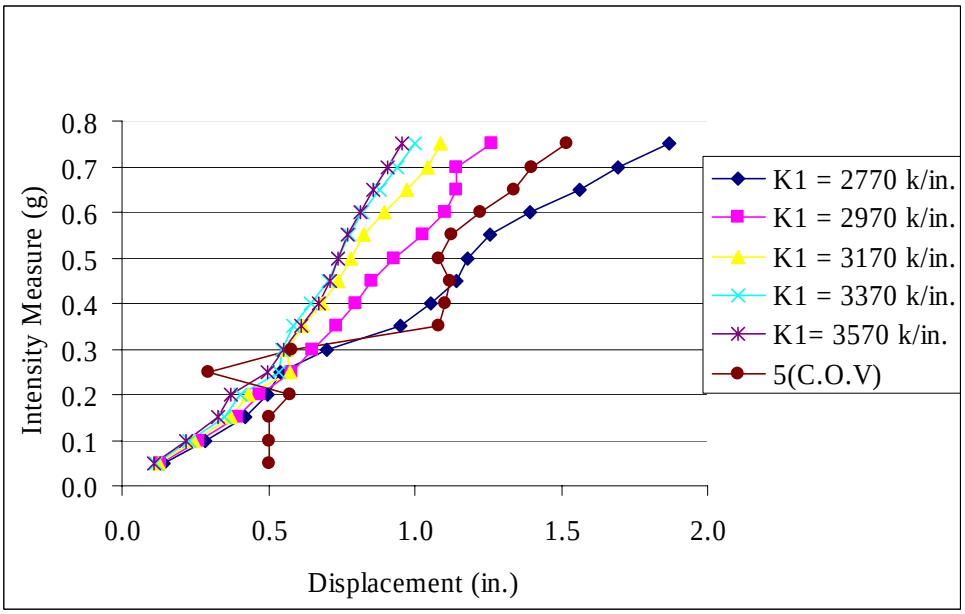

(b) IDA plots with updated scaling

Fig. 5.4(a-b) IDA plots of peak displacement response for the Kern County ground motion

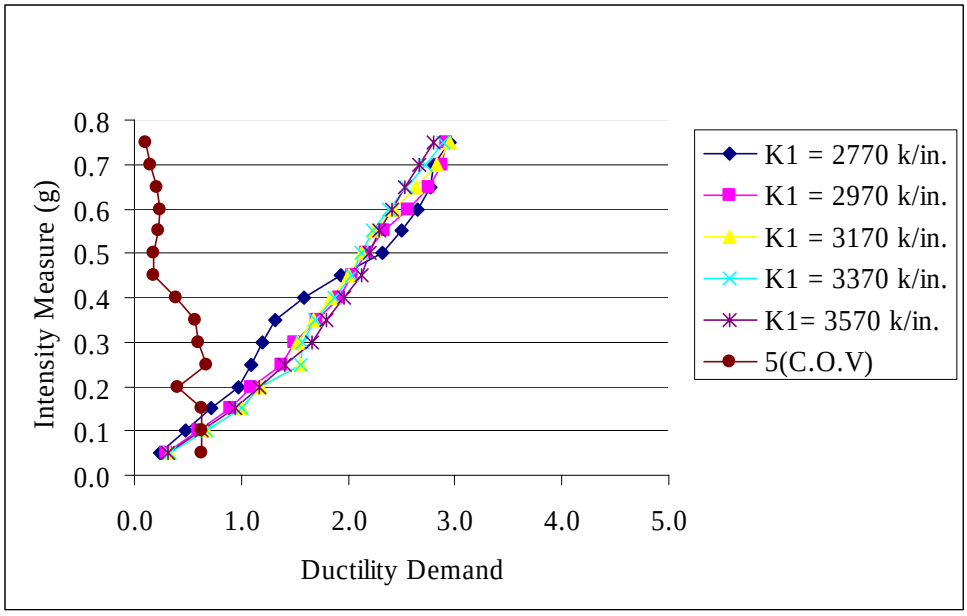

(a) IDA plots without rescaling (scaling done with K1 = 3170 k/in.)

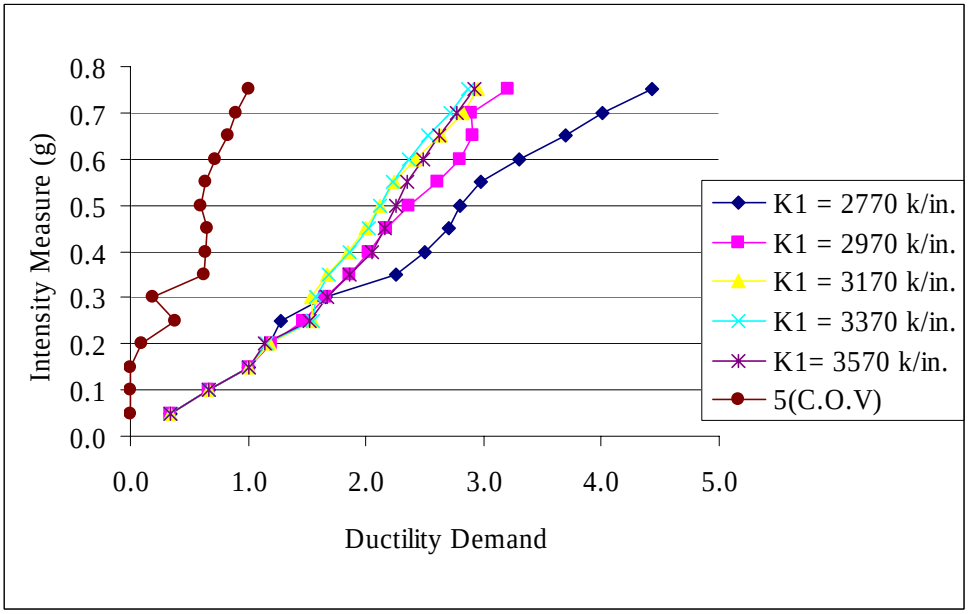

(b) IDA plots with updated scaling

Fig. 5.5(a-b) IDA plots of ductility demand for the Kern County ground motion

Table 5.5 Coefficients of variation for the response analysis results for the Kern County Ground Motion

	Median Scaling		Updated Scaling			
	Peak Displ.	Ductility Demand	Peak Displ.	Ductility Demand		
Column 1	Column 2	Column 3	Column 4	Column 5	Column 6	Column 7
Intensity Level	Coefficient of variation Figure 5.4 (a)	Coefficient of variation Figure 5.4 (b)	Coefficient of variation Figure 5.5 (a)	Coefficient of variation Figure 5.5 (b)	Ratio of Column 2 to Column 4	Ratio of Column 3 to Column 5
0.050	0.083	0.126	0.101	0.001	0.826	*
0.100	0.083	0.126	0.101	0.001	0.826	*
0.150	0.083	0.126	0.101	0.001	0.826	*
0.200	0.051	0.080	0.115	0.019	0.446	4.204
0.250	0.098	0.135	0.059	0.076	1.665	1.776
0.300	0.058	0.118	0.116	0.039	0.498	3.072
0.350	0.074	0.115	0.216	0.125	0.342	0.922
0.400	0.063	0.078	0.221	0.129	0.285	0.606
0.450	0.074	0.034	0.224	0.130	0.331	0.266
0.500	0.128	0.036	0.216	0.119	0.593	0.298
0.550	0.143	0.046	0.226	0.127	0.635	0.363
0.600	0.147	0.047	0.245	0.145	0.599	0.324
0.650	0.142	0.042	0.268	0.166	0.529	0.253
0.700	0.123	0.030	0.279	0.179	0.442	0.170
0.750	0.117	0.021	0.303	0.201	0.386	0.104

* Large due to zero C.O.V for linear systems

5.3.3 Results for the Loma Prieta ground motion

When the single degree of freedom system was analyzed for the Loma Prieta earthquake, it was observed that after a certain level of intensity of scaled ground motion (0.6g) the system became unstable. Figure 5.6 (a) displays uniform relative response between the systems, similar to the case of Imperial Valley ground motion. The response with the updated scaling method as shown in Figure 5.6 (b) is not uniform. There is a reversal of the trend after the yield point. Figures 5.7 (a) and (b) displaying the ductility demands are almost identical but the reversal in trend occurs earlier for Figure 5.7 (b). Table 5.6 displays the ratios between the coefficients of variation for displacement response. It is observed that at lower intensities the coefficient of variation for median scaling is more than that observed for updated scaling.

Again, for ductility the trend reverses at higher intensities where the coefficient of variation for median scaling is less. Since the area of interest is the response after yielding, it can be concluded the Median Scaling Method gives consistent results.

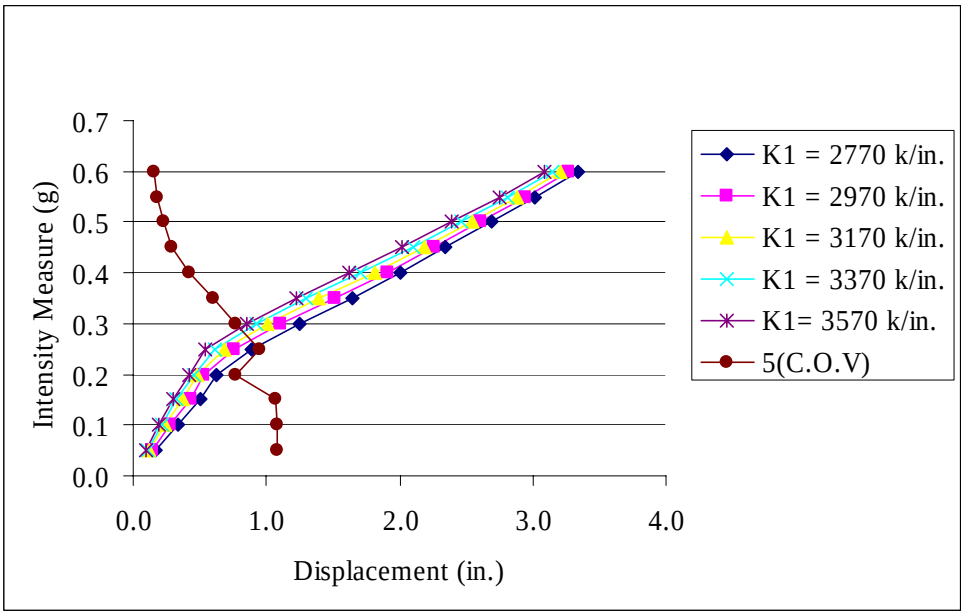

(a) IDA plots without rescaling (scaling done with K1 = 3170 k/in.)

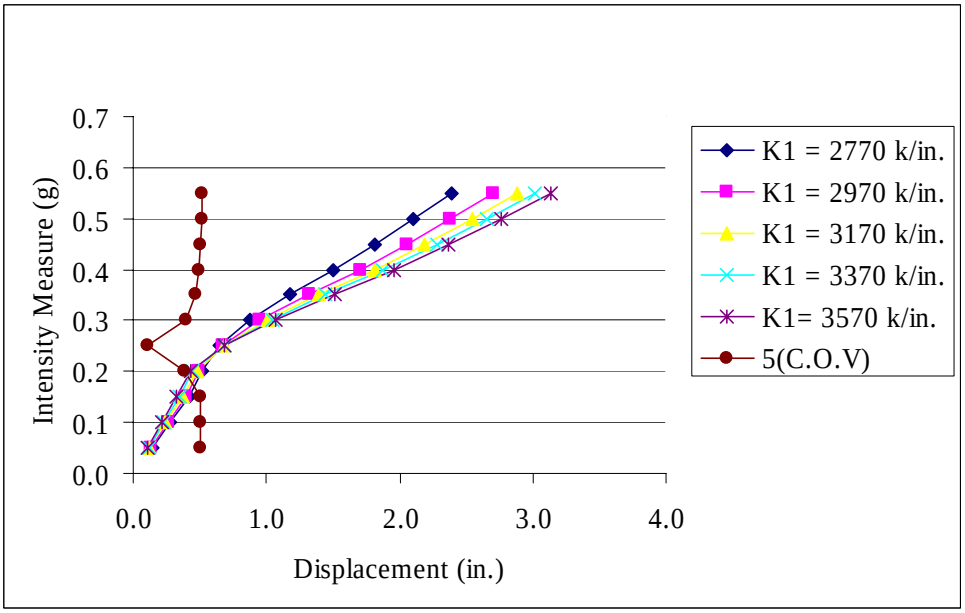

(b) IDA plots with updated scaling

Fig. 5.6(a-b) IDA plots of peak displacement response for the Loma Prieta ground motion

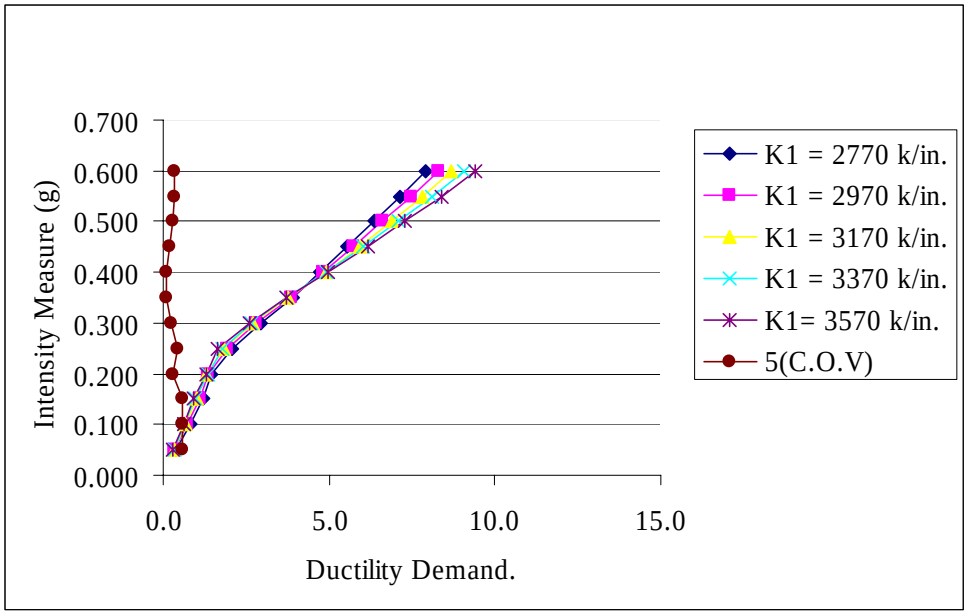

(a) IDA plots without rescaling (scaling done with K1 = 3170 k/in.)

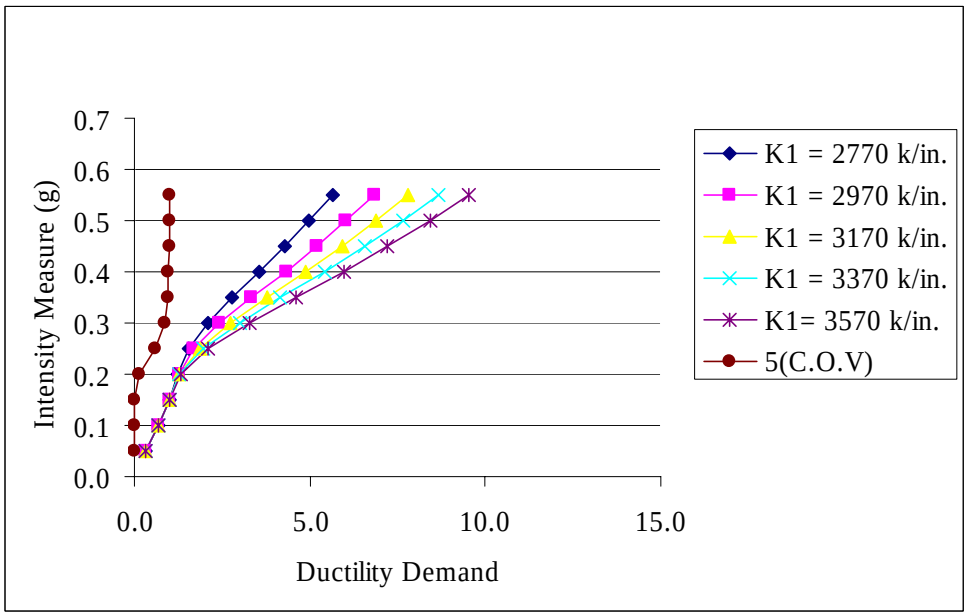

(b) IDA plots with updated scaling

Fig. 5.7(a-b) IDA plots of ductility demand for the Loma Prieta ground motion

Table 5.6 Coefficients of variation for the response analysis results for the Loma Prieta Ground Motion

	Median Scaling		Updated Scaling			
	Peak Displ.	Ductility Demand	Peak Displ.	Ductilty Demand		
Column 1	Column 2	Column 3	Column 4	Column 5	Column 6	Column 7
Intensity Level	Coefficient of variation Figure 5.6 (a)	Coefficient of variation Figure 5.6 (b)	Coefficient of variation Figure 5.7 (a)	Coefficient of variation Figure 5.7 (b)	Ratio of Column 2 to Column 4	Ratio of Column 3 to Column 5
0.050	0.217	0.114	0.101	0.001	2.154	*
0.100	0.217	0.114	0.101	0.001	2.154	*
0.150	0.214	0.112	0.101	0.001	2.124	*
0.200	0.153	0.055	0.077	0.019	2.004	2.915
0.250	0.190	0.090	0.022	0.076	8.769	1.179
0.300	0.153	0.052	0.078	0.039	1.956	1.343
0.350	0.119	0.019	0.094	0.125	1.268	0.151
0.400	0.084	0.017	0.099	0.129	0.845	0.129
0.450	0.058	0.042	0.102	0.130	0.572	0.324
0.500	0.046	0.054	0.103	0.119	0.447	0.453
0.550	0.036	0.064	0.103	0.127	0.354	0.499

* Large due to zero C.O.V for linear systems

5.3.4 Results for the Northridge ground motion

For the Northridge ground motion the IDA curves have similar shapes for the cases of median and updated scaling. The only difference between Figure 5.8 (a) and Figure 5.8 (b) is observed at higher levels of intensity. The curves in the latter case show a more converging trend. The plots for ductility demand in Figure 5.9 (a) and Figure 5.9 (b) also display similar behavior, but when updated scaling is adopted the dispersion tends to increase at higher intensities. The coefficient of variation for each of these curves is shown in Table 5.7. For peak displacement, the coefficient of variation is always greater for median scaling than it is for updated scaling. For ductility demand, at lower intensities this pattern is followed, but at higher intensities the coefficient of variation for median scaling is less than that for updated scaling. These observations are similar to those reported for the response of the structure when the Imperial Valley ground motion was used. For the Imperial Valley ground motion, the coefficient of variation was less for the median scaling method for ductility demand.

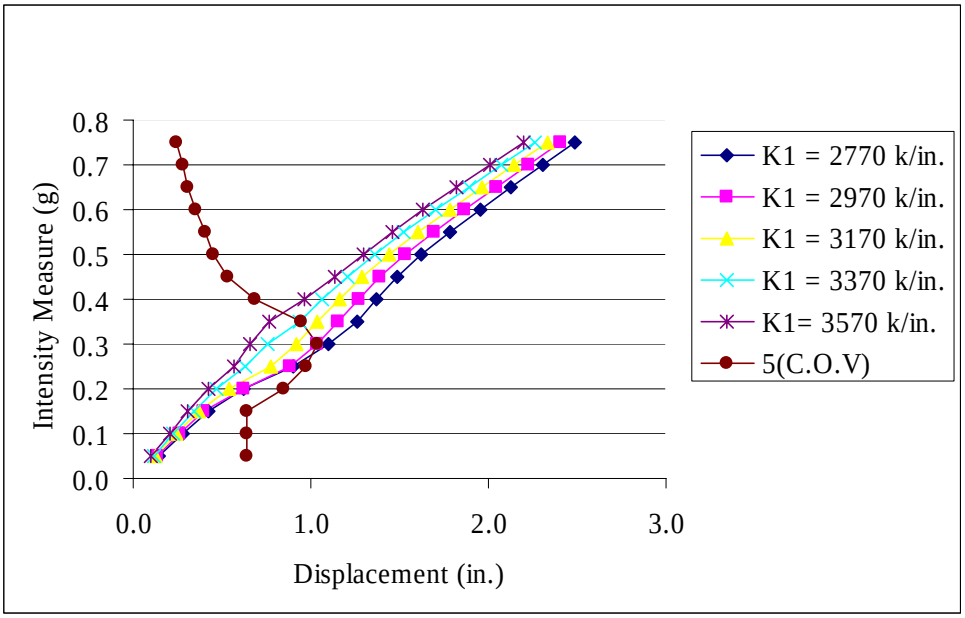

(a) IDA plots without rescaling (scaling done with K1 = 3170 k/in.)

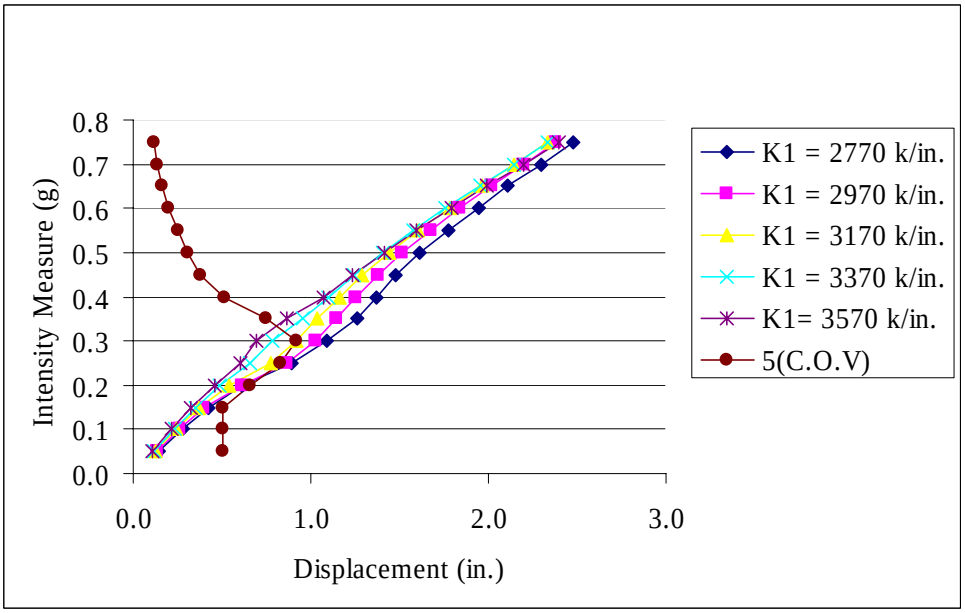

(b) IDA plots with updated scaling

Fig. 5.8(a-b) IDA plots of peak displacement for the Northridge ground motion

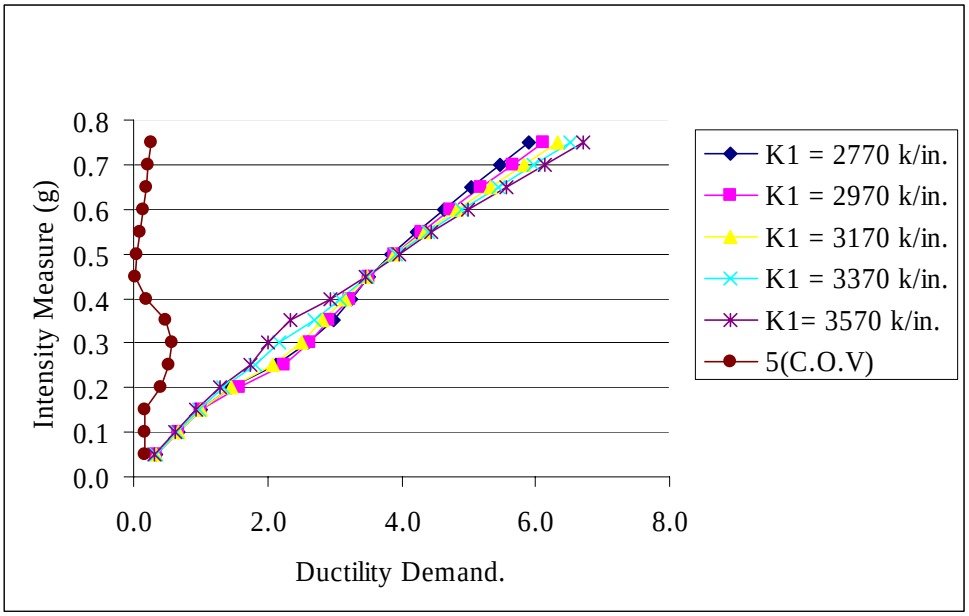

(a) IDA plots without rescaling (scaling done with K1 = 3170 k/in.)

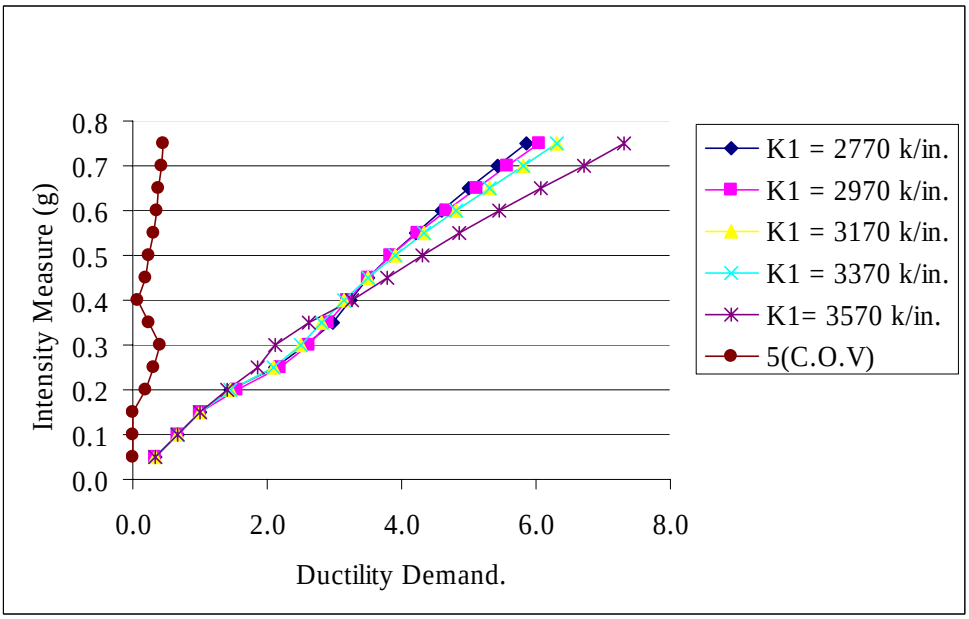

(b) IDA plots with updated scaling

Fig. 5.9(a-b) IDA plots of ductility demand for the Northridge ground motion

Table 5.7 Coefficients of variation for the response analysis results for Northridge Ground Motion

	Median Scaling		Updated Scaling			
	Peak Displ.	Ductility Demand	Peak Displ.	Ductility Demand		
Column 1	Column 2	Column 3	Column 4	Column 5	Column 6	Column 7
Intensity Level	Coefficient of variation Figure 5.8 (a)	Coefficient of variation Figure 5.8 (b)	Coefficient of variation Figure 5.9 (a)	Coefficient of variation Figure 5.9 (b)	Ratio of Column 2 to Column 4	Ratio of Column 3 to Column 5
0.050	0.128	0.032	0.101	0.001	1.270	*
0.100	0.128	0.032	0.101	0.001	1.270	*
0.150	0.128	0.032	0.101	0.001	1.270	*
0.200	0.169	0.081	0.132	0.040	1.277	2.040
0.250	0.194	0.105	0.165	0.062	1.174	1.687
0.300	0.207	0.115	0.184	0.082	1.124	1.409
0.350	0.188	0.095	0.149	0.047	1.266	2.013
0.400	0.136	0.038	0.102	0.015	1.334	2.482
0.450	0.106	0.006	0.076	0.036	1.399	0.180
0.500	0.090	0.011	0.061	0.050	1.480	0.217
0.550	0.081	0.020	0.050	0.060	1.609	0.330
0.600	0.071	0.029	0.040	0.070	1.761	0.418
0.650	0.061	0.039	0.032	0.078	1.929	0.498
0.700	0.055	0.045	0.027	0.084	2.006	0.535
0.750	0.049	0.052	0.024	0.088	2.022	0.584

* Large due to zero C.O.V for linear systems

5.3.5 Results for the Santa Monica ground motion

The peak displacement with median scaling is plotted in Figure 5.10 (a) and for updated scaling in Figure 5.10 (b). In Figure 5.10 (b) systems having less stiffness show greater displacement, which is not the case in Figure 5.10 (a). The ductility demand curves also show similar behavior. In Figure 5.11 (a) the ductility demand curves have been plotted and they show significantly less dispersion than in Figure 5.11 (b). The ratio of the coefficients of variations has been listed in Table 5.8. The coefficient of variation for median scaling is less than that for updated scaling. These observations are similar to those that were obtained when Kern County ground motion was used. For Kern County ground motion the coefficient

of variation was less in the median scaling method for peak displacement response and also for ductility demands.

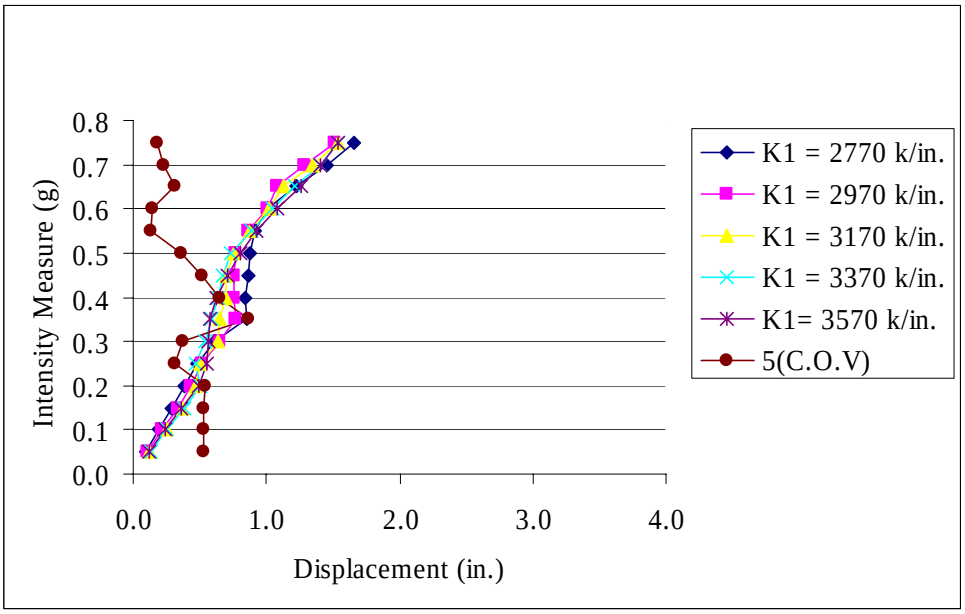

(a) IDA plots without rescaling (scaling done with K1 = 3170 k/in.)

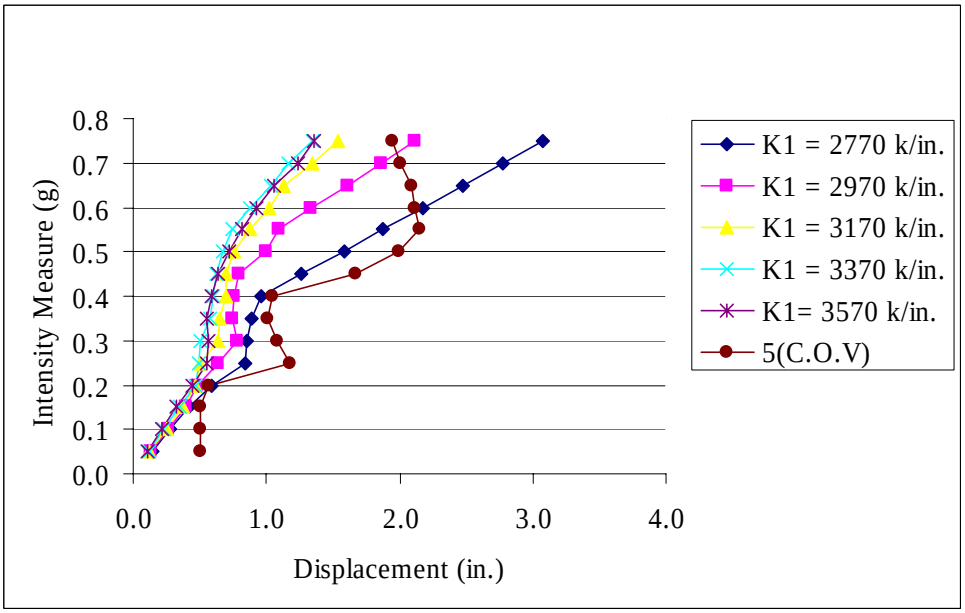

(b) IDA plots with updated scaling

Fig. 5.10(a-b) IDA plots of peak displacement for the Santa Monica ground motion

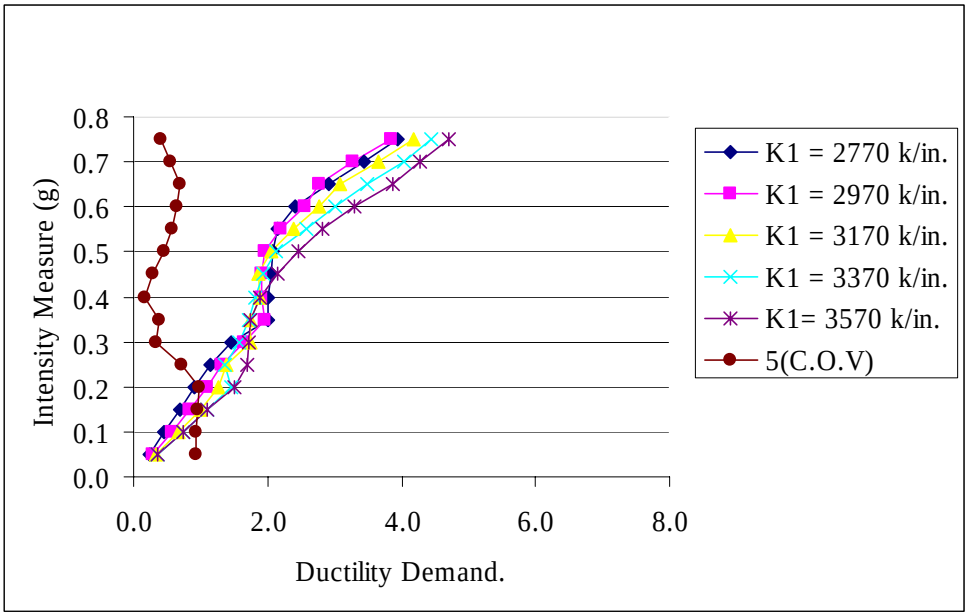

(a) **IDA plots without rescaling (scaling done with K1 = 3170k/in.)**

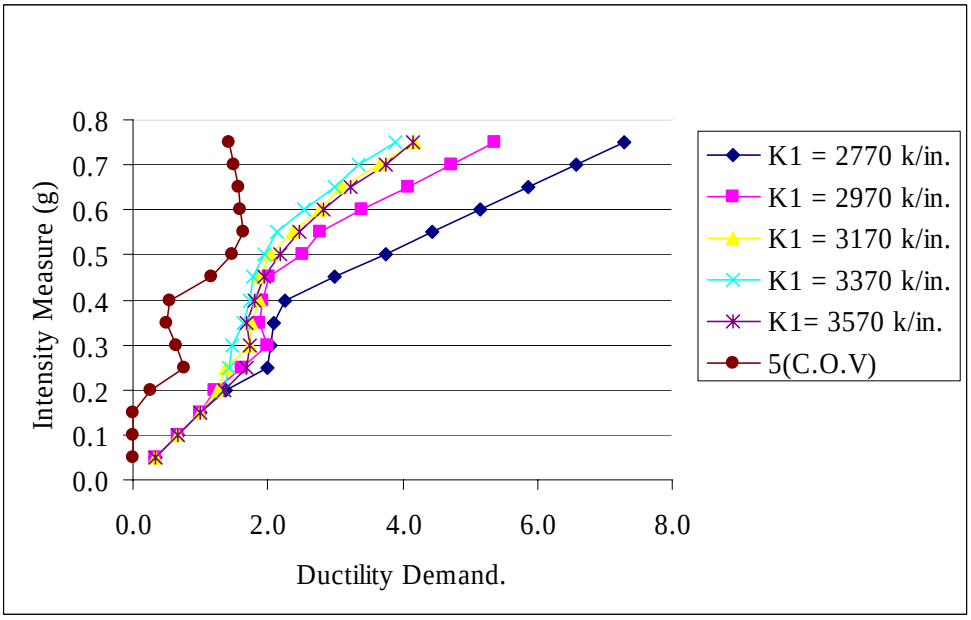

(b) IDA plots with updated scaling

Fig. 5.11(a-b) IDA plots of ductility demand for the Santa Monica ground motion

Table 5.8 Coefficients of variation for the response analysis results for the Santa Monica Ground Motion

	Median Scaling		Updated Scaling			
	Peak Displ.	Ductility Demand	Peak Displ.	Ductility Demand		
Column 1	Column 2	Column 3	Column 4	Column 5	Column 6	Column 7
Intensity Level	Coefficient of variation Figure 5.10 (a)	Coefficient of variation Figure 5.10 (b)	Coefficient of variation Figure 5.11 (a)	Coefficient of variation Figure 5.11 (b)	Ratio of Column 2 to Column 4	Ratio of Column 3 to Column 5
0.050	0.106	0.188	0.101	0.002	1.055	*
0.100	0.106	0.188	0.101	0.002	1.055	*
0.150	0.106	0.189	0.101	0.002	1.059	*
0.200	0.107	0.198	0.113	0.052	0.948	3.794
0.250	0.063	0.145	0.236	0.153	0.267	0.951
0.300	0.075	0.069	0.217	0.127	0.345	0.541
0.350	0.173	0.075	0.202	0.101	0.858	0.745
0.400	0.131	0.034	0.209	0.109	0.626	0.315
0.450	0.104	0.057	0.334	0.233	0.312	0.245
0.500	0.072	0.090	0.399	0.295	0.179	0.304
0.550	0.026	0.115	0.430	0.326	0.061	0.355
0.600	0.028	0.127	0.423	0.318	0.067	0.399
0.650	0.062	0.140	0.417	0.313	0.148	0.448
0.700	0.045	0.112	0.402	0.298	0.113	0.375
0.750	0.037	0.083	0.388	0.284	0.095	0.291

* Large due to zero C.O.V for linear systems

5.4 Effect on rescaling due to variation in damping

The two factors that affect the scaling are stiffness and damping. The effect of changing the stiffness was investigated in the previous section. In this section five values of damping, 2% of critical, 4% of critical, 5% of critical, 6% of critical and 8% of critical were adopted for scaling purpose. When median scaling was used, the scale factor was computed based on a stiffness of 3170 k/in. and damping of 5% of critical. For updated scaling the stiffness was maintained at 3170 k/in. but the damping was varied and the corresponding value was used for determining the scale factor. Two ground motions, namely Kern County having PGA of 0.156g and Santa Monica ground motion having PGA of 0.883g, were used. An extensive series of tests was not carried out since it was seen for the previous section that a distinct

trend is not evident. The input ground motions are as shown in Figure 5.1 (b) and Figure 5.1 (e). The response for the Kern County ground motion is shown in Figure 5.12 (a-b).

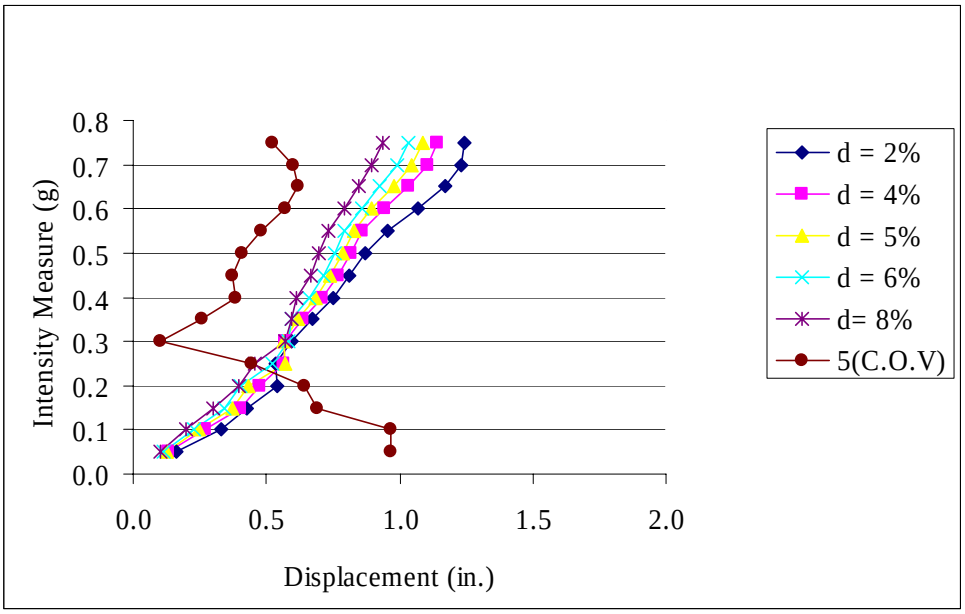

(a) IDA plots without rescaling (scaling done based on 5% of critical damping)

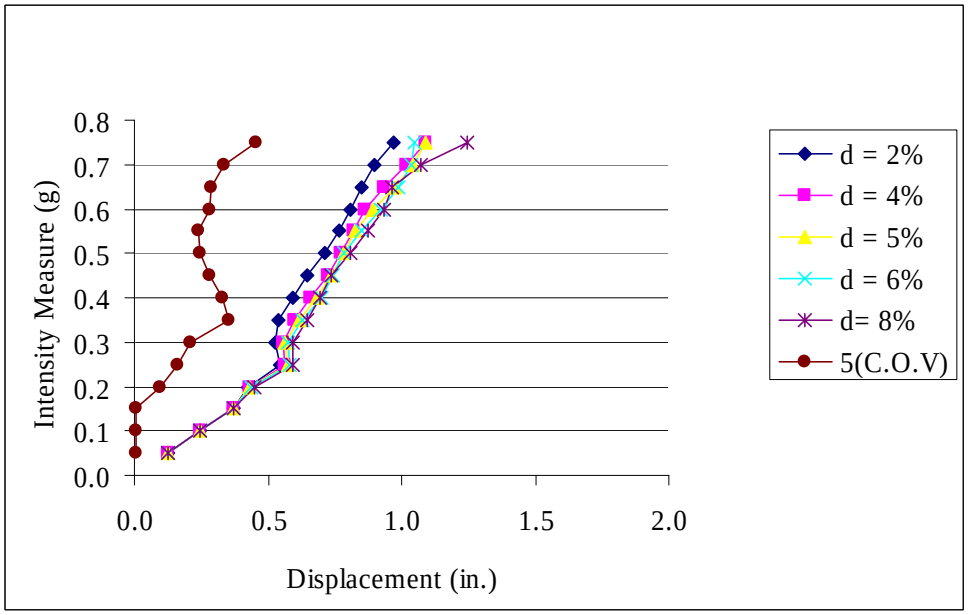

(b) IDA plots with updated scaling

Fig. 5.12(a-b) IDA plots of peak displacement with damping variation for the Kern County ground motion

It is observed from Figure 5.12 (a) that the response decreases in the elastic as well as in the inelastic region with increase in damping. But when the updated scaling procedure was used, this trend is not observed as evident from Figure 5.12 (b). The ratios of the coefficients of variation for the response have been shown in Table 5.9. It is seen that the C.O.V for median scaling is greater than for updated scaling.

Table 5.9 Coefficients of variation for the response analysis results for the Kern County Ground Motion due to damping

	Median Scaling	Updated Scaling	
	Peak Displ.	Peak Displ.	
Column 1	Column 2	Column 3	Column 4
Intensity Level	Coefficient of variation Figure 5.12 (a)	Coefficient of variation Figure 5.12 (b)	Ratio of Column 2 to Column 3
0.050	0.969	0.004	262.765
0.100	0.969	0.004	262.765
0.150	0.689	0.004	186.732
0.200	0.644	0.099	6.529
0.250	0.442	0.161	2.751
0.300	0.100	0.208	0.481
0.350	0.260	0.354	0.735
0.400	0.382	0.332	1.151
0.450	0.372	0.282	1.318
0.500	0.409	0.243	1.685
0.550	0.483	0.242	2.000
0.600	0.573	0.283	2.024
0.650	0.618	0.290	2.132
0.700	0.599	0.334	1.792
0.750	0.522	0.455	1.148

Figure 5.13 (a) gives the peak displacement response for median scaling using a scale factor based on 5% of critical damping for the Santa Monica ground motion. It is observed that in the elastic and inelastic regions the response decreases with damping. Figure 5.13 (b) gives the peak displacement response for updated scaling. It is observed that in the inelastic region, response increases with increase in damping. The dispersion values are shown in Table 5.10.

The coefficient of variation for median scaling was more than in updated scaling at higher intensities.

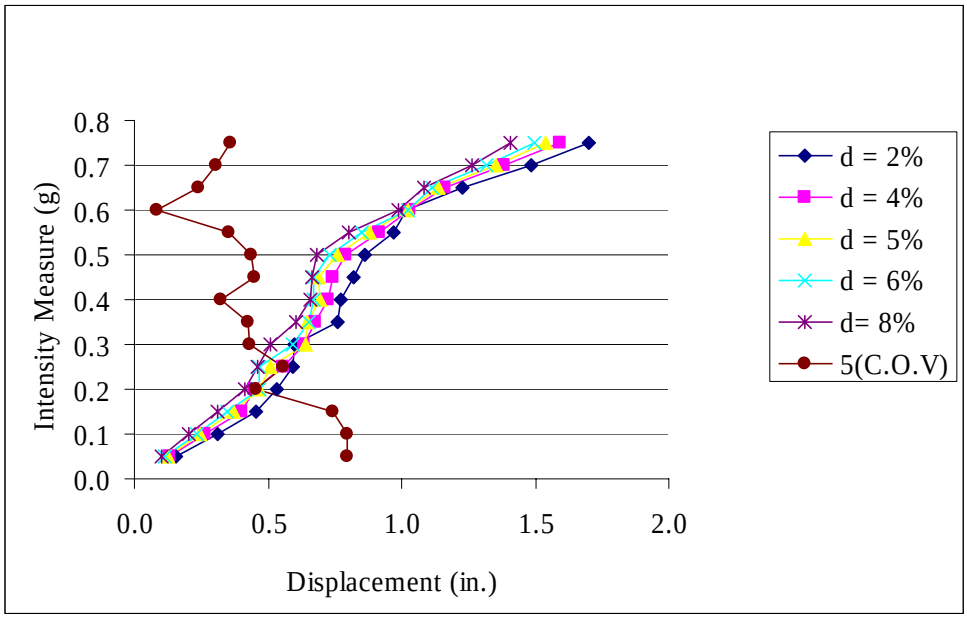

(a) IDA plots without rescaling (scaling done based on 5% of critical damping)

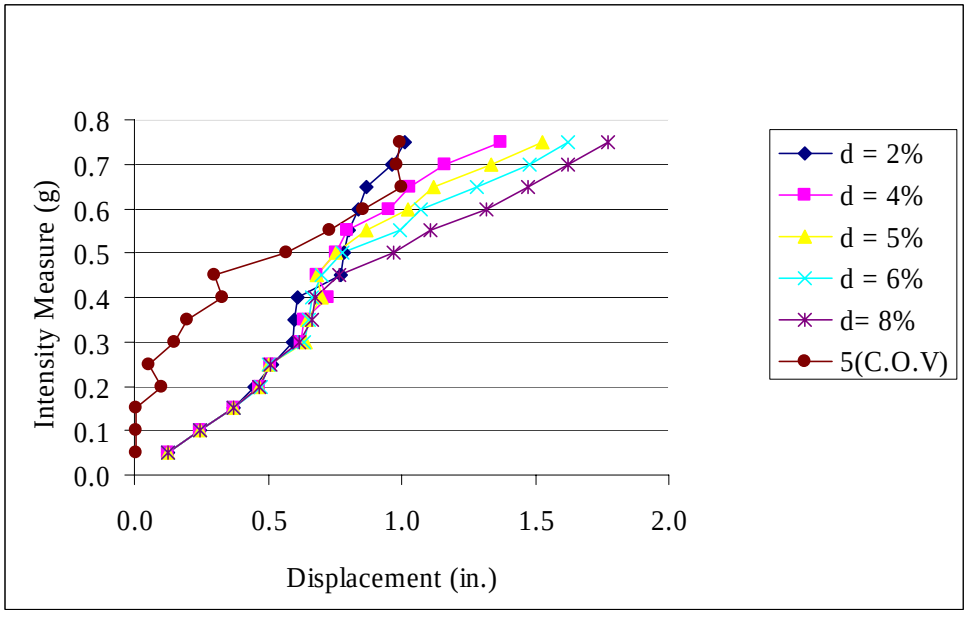

(b) IDA plots with updated scaling

Fig. 5.13(a-b) IDA plots of peak displacement with damping variation for the Santa Monica ground motion

Table 5.10 Coefficients of variation for the response analysis results for the Santa Monica Ground Motion due to damping

	Median Scaling	Updated Scaling	
Column 1	Column 2	Column 3	Column 4
Intensity Level	Coefficient of variation Figure 5.13 (a)	Coefficient of variation Figure 5.13 (b)	Ratio of Column 2 to Column 3
0.050	0.797	0.006	*
0.100	0.797	0.006	*
0.150	0.742	0.006	*
0.200	0.453	0.102	4.464
0.250	0.556	0.054	10.302
0.300	0.433	0.150	2.877
0.350	0.428	0.195	2.189
0.400	0.326	0.328	0.994
0.450	0.446	0.298	1.499
0.500	0.438	0.570	0.767
0.550	0.354	0.729	0.486
0.600	0.086	0.854	0.101
0.650	0.238	0.999	0.238
0.700	0.304	0.985	0.309
0.750	0.358	0.993	0.361

* Large due to zero C.O.V for linear systems

5.5 Conclusions

Two methods have been suggested for scaling the ground motion records. They are Median Scaling Method and Updated Scaling Method. The procedure for implementing these has been described. In order to ascertain the efficacy of these two methods, a given structure was subjected to five different ground motions using both methods of scaling. A plot of the response and the values of the coefficient of variation have been obtained for each individual case. The data used to compare the scaling methods are the relationship between stiffness and response, and the ratios of the coefficients of variation. The above test results support the following conclusions:

(1) The nature of the IDA curves for the Imperial Valley ground motion and the Northridge ground motion display similar trends. The response is uniform; that is, systems with greater stiffness display less peak displacement for the median scaling case. However the coefficient of variation is greater for median scaling than it is for updated scaling for the case of peak displacement. For the case of ductility demand at higher intensity levels (in the inelastic region), the coefficient of variation is less when the Median Scaling approach is adopted. Since the area of interest is the response obtained after yielding, this observation supports the adoption of the Median Scaling approach.

(2) The nature of the IDA curves for Kern County and Santa Monica are identical. When median scaling was adopted, there was lack of uniformity between individual response curves. They are not distinct; however the coefficient of variation was less in the Median Scaling Method.

(3) For Loma Prieta ground motion there is a distinct pattern in the response with respect to the stiffness. But the coefficient of variation for the median scaling method was higher than for updated scaling at lower intensities. At higher intensities this trend is reversed. Hence the Median Scaling Method gives more consistent results in the inelastic region.

(4) For studying the effect of damping on the scale factor, Kern County and Santa Monica ground motions were used. In both cases it was observed that when the scaling was based on the median damping value, the response was less at higher values of damping. No clear trend could be identified when updated scaling was used.

Due to the highly variable nature of the ground motion, a firm judgment cannot be reached. The nature of the response cannot be easily predicted in the nonlinear region. The coefficient of variation, the measure adopted to measure dispersion, does not always show a definite trend. However it is observed that the results for median scaling are more agreeable from a stiffness-response perspective. After yielding occurs, the dispersion in the results is less when the Median Scaling Method is adopted than with the Updated Scaling Method. The Median

Scaling Method serves as a suitable datum for comparing the responses obtained. To compare different structural systems, it is more reasonable to use the same scaled ground motions. Hence median scaling is used to scale the ground motions for the problems that will be presented in the following chapters.

6 Study of variation of parameters

6.1 Objective

The variation of parameter study is based on single record IDA. Only one systemic parameter is varied at a time. Scaling corresponding to the median value from the range of parameters is used for scaling all the ground motions. For each value of the parameter, the IDA is plotted. At the end of the process, a set of different IDA curves for the variation of a single parameter was obtained. These were then investigated to identify any trends. In some cases a distinct trend was observed, while in others no definite relationship could be identified. The damage measures that were used were peak displacement response and base shear. For each variation of a parameter, a few multi-record IDAs were also used. The purpose of using multi-record IDAs was to provide a comparison with single-record IDA and to illustrate the difference between the two. Three multi-record IDAs were generated for each variation of parameter. They corresponded to the highest value, median value and lowest value of a particular parameter. The scaling was done corresponding to the median value of the parameter.

6.2 Variation of stiffness

For studying the effect of varying the stiffness on the IDA curves, the system described in section 2.2.1 having the following properties was used:

Weight = 7800 k

Damping = 5% of critical

Yield Strength = 1170 k

α (Ratio of post-yield stiffness to primary stiffness) = 0.1

The above characteristics are obtained from a typical five-story office building having weight per unit volume of 8.0 pcf. The dimensions of the building are 150ft X 100 ft X 65 ft. The period of vibration is assumed as 0.5 second.

The different sets of stiffness used were

(1) K1 = 2770 k/in. and K2 = 277 k/in.

(2) K1 = 2970 k/in. and K2 = 297 k/in.

(3) K1 = 3170 k/in. and K2 = 317 k/in.

(4) K1 = 3370 k/in. and K2 = 337 k/in.

(5) K1 = 3570 k/in. and K2 = 357 k/in.

The scaling was done corresponding to K1 = 3170 k/in. The coefficient of variation, magnified by a factor of five, was also plotted for each curve.

Figure 6.1 shows the peak displacement response for different systems subjected to the same scaled ground motion of the Imperial Valley. Systems having higher stiffness have less displacement in the elastic and inelastic regions. The coefficient of variation is greatest at the yield point. At higher levels of intensity, the curves show a converging trend as evident from the C.O.V curve. The effect of the Kern County ground motion is shown in Figure 6.2. At lower levels of intensity, no distinct trend can be observed. At higher levels of intensity, systems having lower stiffness show greater displacement. For the Loma Prieta ground motion in Figure 6.3, a uniform pattern of systems with greater stiffness displaying lower response is observed. Beyond a certain level of intensity the ductility limit was exceeded, indicating dynamic instability. The response for the Northridge ground motion in Figure 6.4 is similar to the Imperial Valley ground motion. However no distinct trend can be identified from Figure 6.5 with the IDA plot for the Santa Monica ground motion.

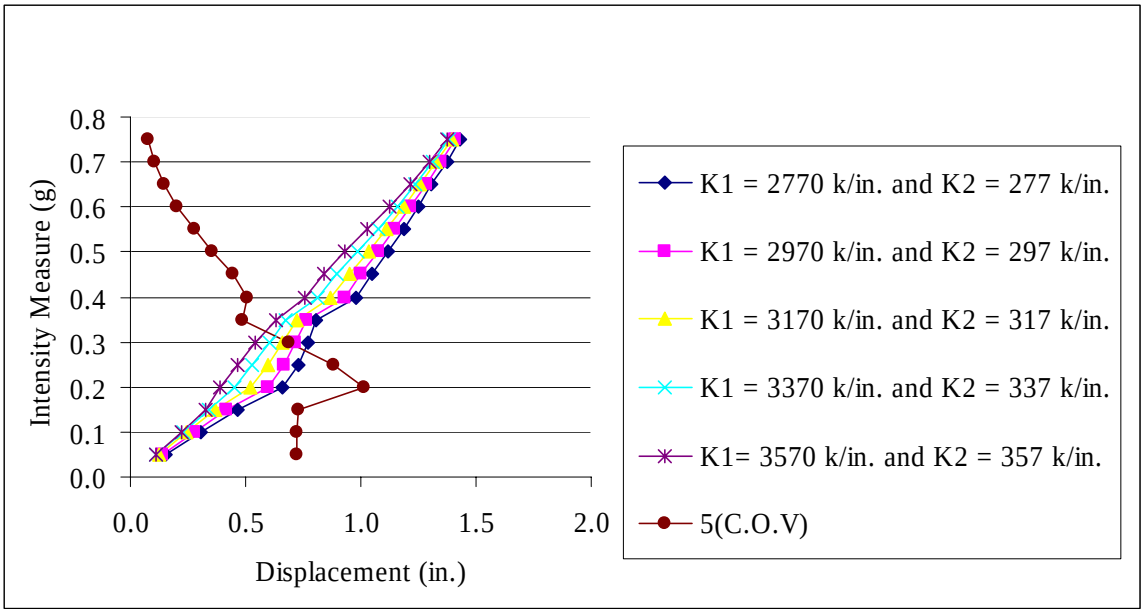

Fig. 6.1 IDA plots of peak displacement response for the Imperial Valley ground motion for variable stiffness

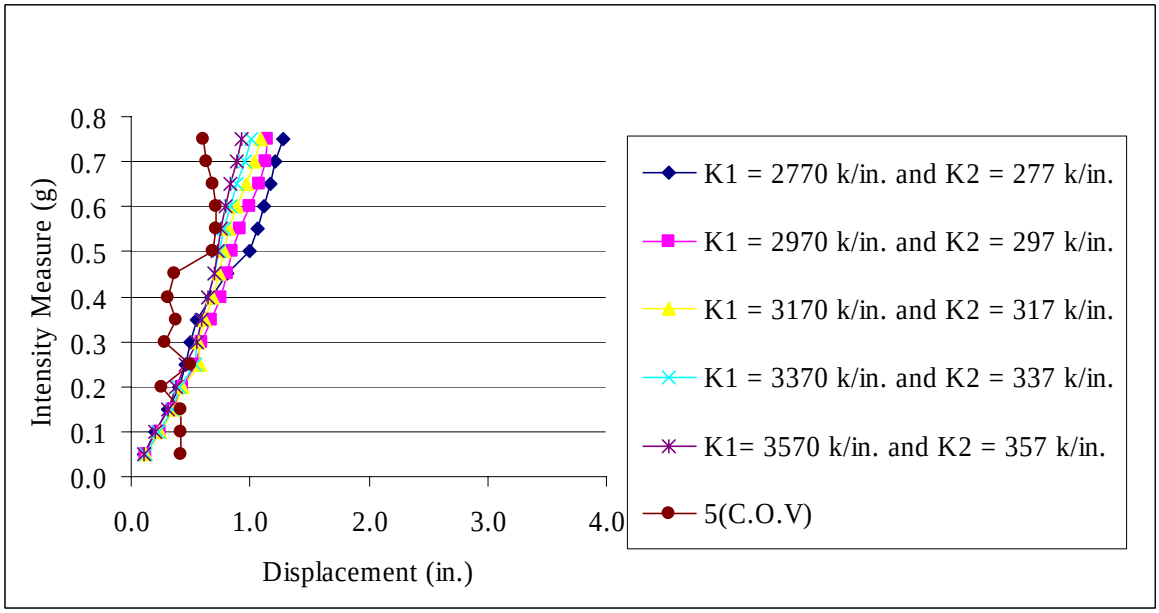

Fig. 6.2 IDA plots of peak displacement response for the Kern County ground motion for variable stiffness

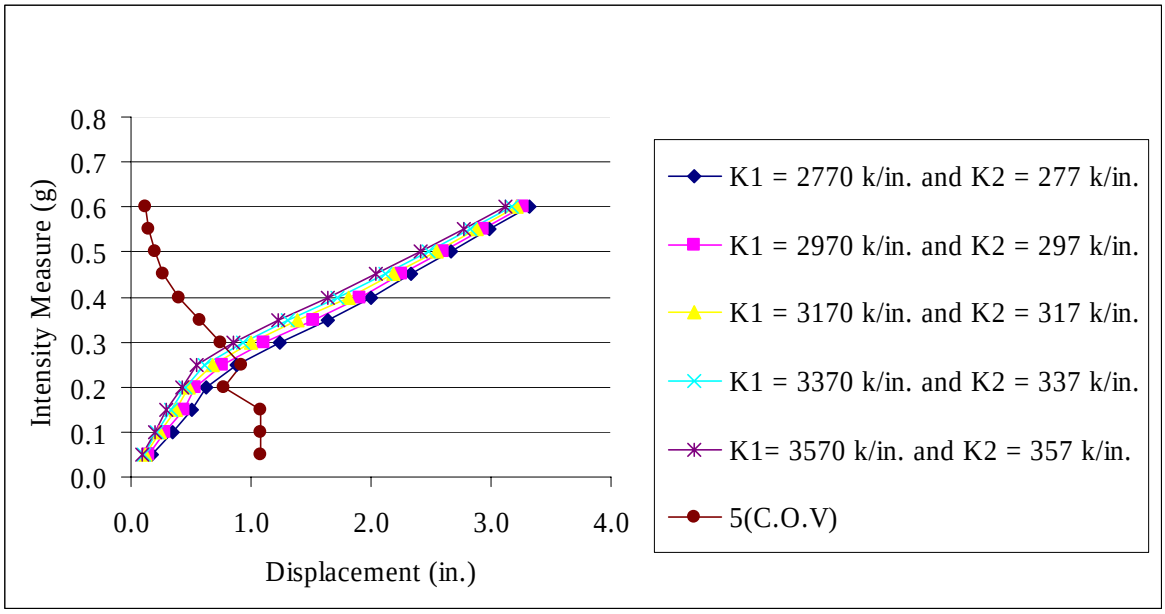

Fig. 6.3 IDA plots of peak displacement response for the Loma Prieta ground motion for variable stiffness

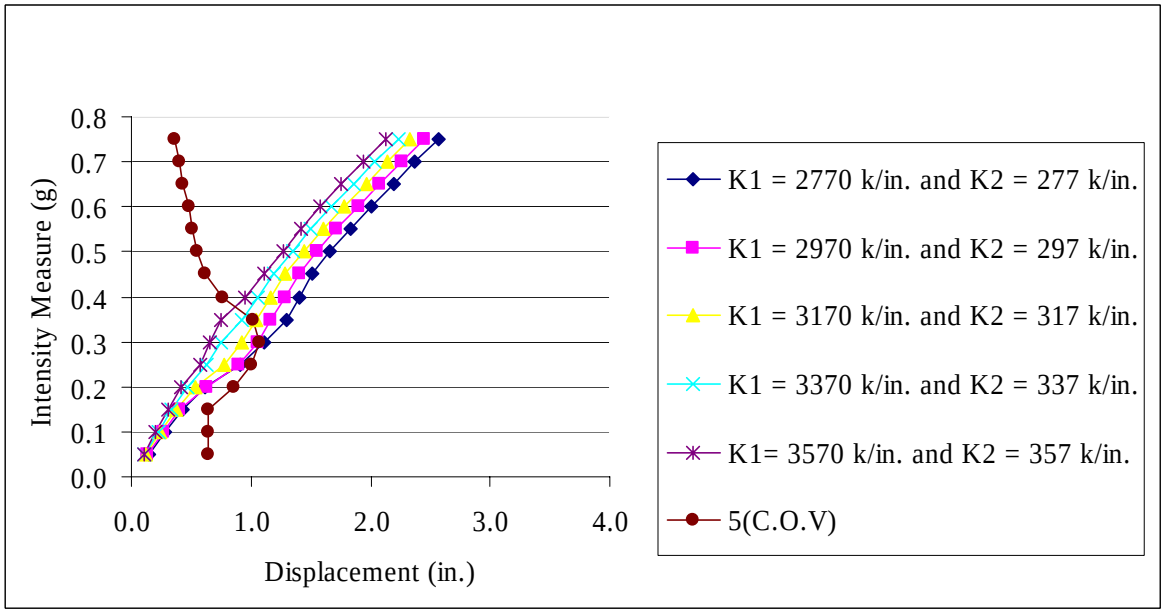

Fig. 6.4 IDA plots of peak displacement response for the Northridge ground motion for variable stiffness

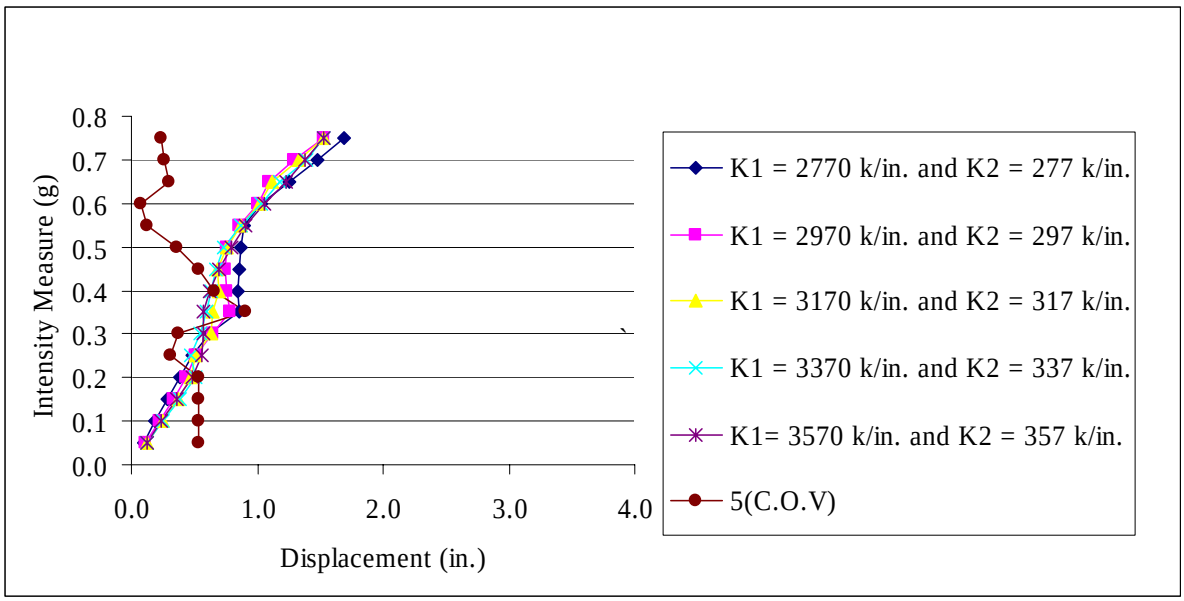

Fig. 6.5 IDA plots of peak displacement response for the Santa Monica ground motion for variable stiffness

Multi-record IDA curves are shown in Figure 6.6 through Figure 6.8. The lowest, median and highest values were selected from the ranges of the parameters. Figure 6.6 shows the multi-record IDA corresponding to K1 of 2770 k/in. and K2 of 277 k/in. The scale factor used was derived using K1 of 3170 k/in. Figure 6.7 is obtained for a system having K1 of 3170 k/in. and K2 of 317 k/in. The same scale factor as used in the previous case was used. Figure 6.8 shows the multi-record IDA corresponding to K1 of 3570 k/in. and K2 of 357 k/in. The scale factor used was derived using K1 of 3170 k/in. It can be observed that the basic shape of the curves is similar. The coefficient of variation before yielding is zero in Figure 6.7; however it is not equal to zero in Figure 6.6 and Figure 6.8. The reason is that these IDA plots were created for scaling corresponding to K1 of 3170 k/in. so that the same ground motion can be used for all the cases.

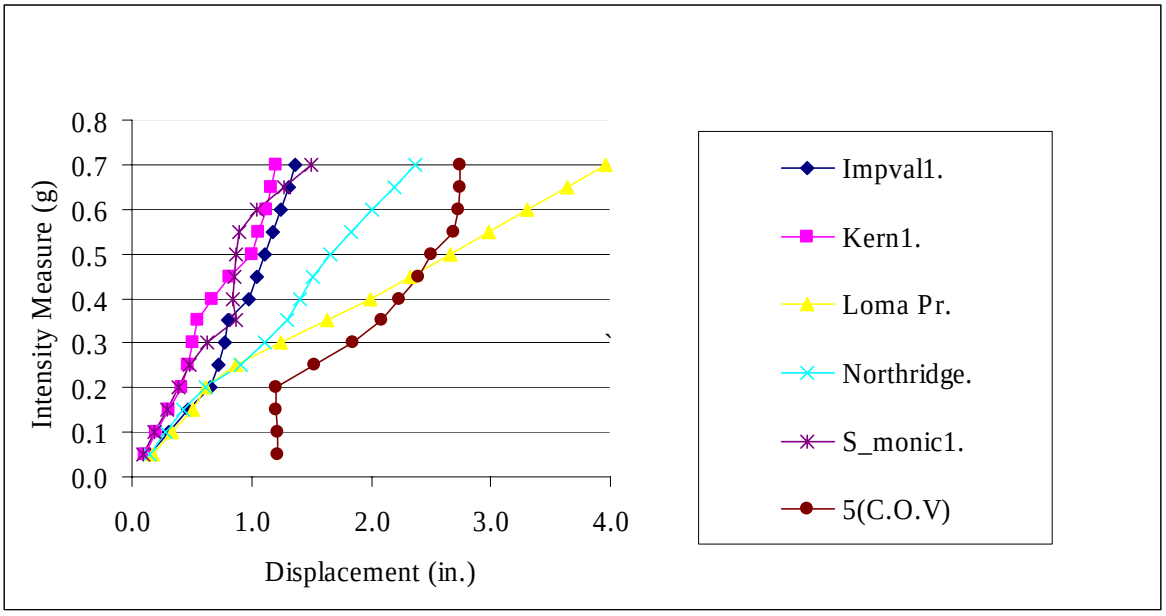

Fig. 6.6 Multi-record IDA plot of peak displacement response for different ground motion for the system having K1 = 2770 k/in. and K2 = 277 k/in.

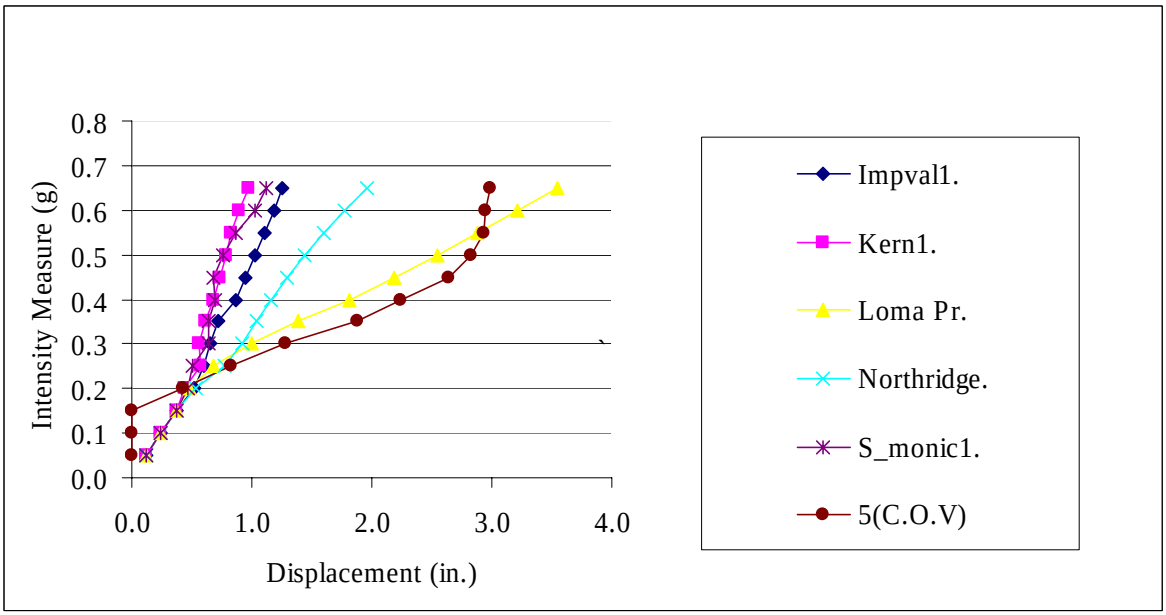

Fig. 6.7 Multi-record IDA plot of peak displacement response for different ground motion for the system having K1 = 3170 k/in. and K2 = 317 k/in.

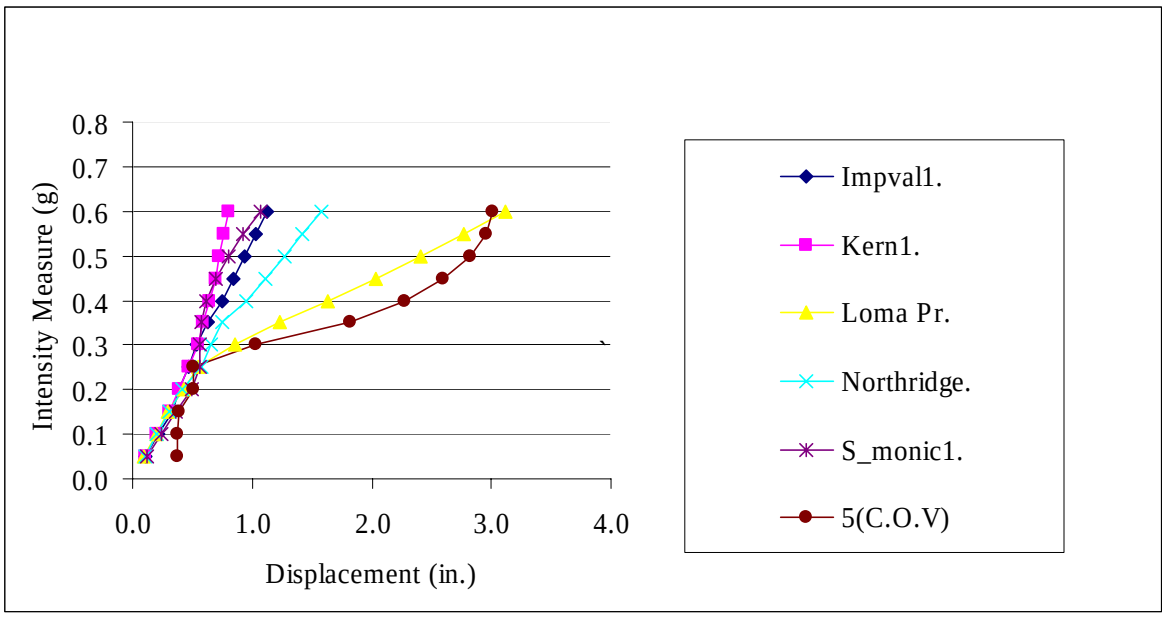

Fig. 6.8 Multi-IDA plot of peak displacement response for different ground motion for the system having K1 = 3570 k/in. and K2 = 357 k/in.

Figures 6.9-6.13 display the single record IDA plots for the base shear for the same system used above and using the same ground motions. The base shear was taken approximately equal to the spring force since it was not possible to recover the damping force in *NONLIN* when this analysis was performed. Since the system has 5% critical damping, the major contribution to base shear occurs from the spring force. Base shears for all the systems are almost equal at all the stages in Figure 6.9 in which the Imperial Valley ground motion was used. Figure 6.10 was obtained using the Kern County ground motion, and the base shears are almost equal in the elastic and inelastic regions. For the case of the Loma Prieta ground motion in Figure 6.11, the base shear is greater for systems having less stiffness, but this trend is reversed at higher intensities in the inelastic region. Figure 6.12 shows the multi-record IDA plot for the Northridge ground motion, and the values for base shear are almost equal at all levels of intensity. In Figure 6.13 the multi-record IDA for the Santa Monica ground motion is plotted. No clear trend can be identified from these curves. Since dispersion was negligible for base shear, the coefficient of variation has not been plotted.

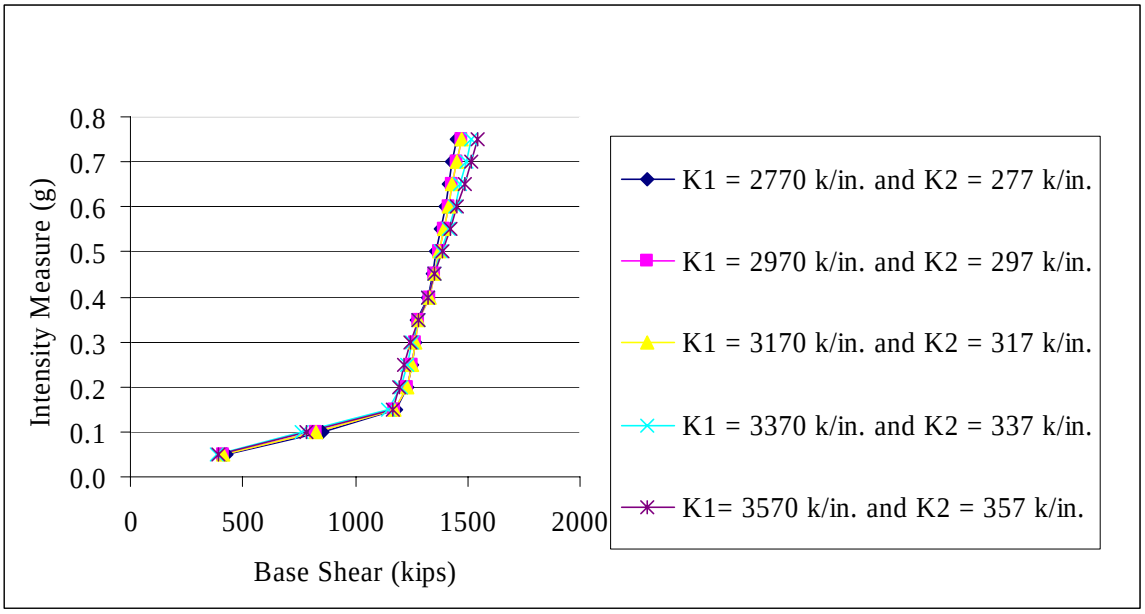

Fig. 6.9 IDA plots of base shear for the Imperial Valley ground motion for variable stiffness

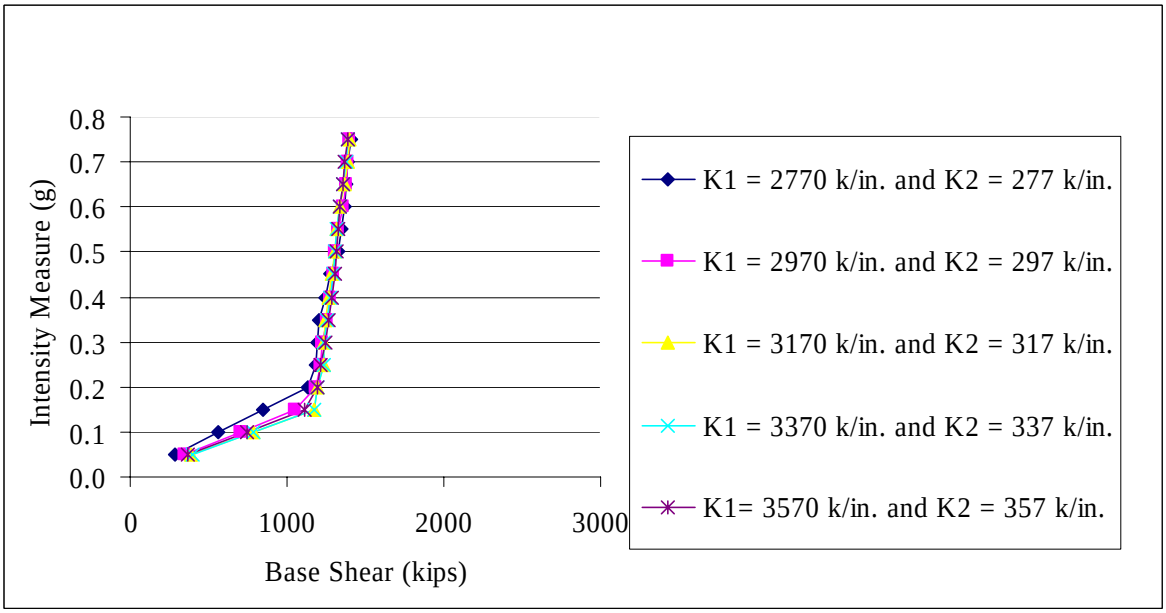

Fig. 6.10 IDA plots of base shear for the Kern County ground motion for variable stiffness

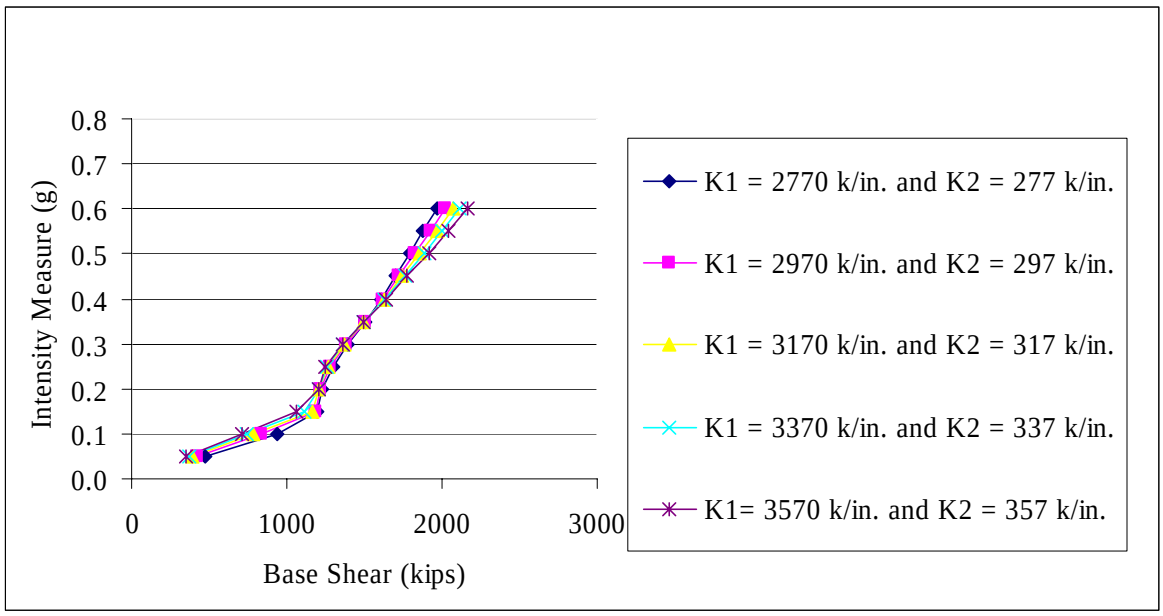

Fig. 6.11 IDA plots of base shear for the Loma Prieta ground motion for variable stiffness

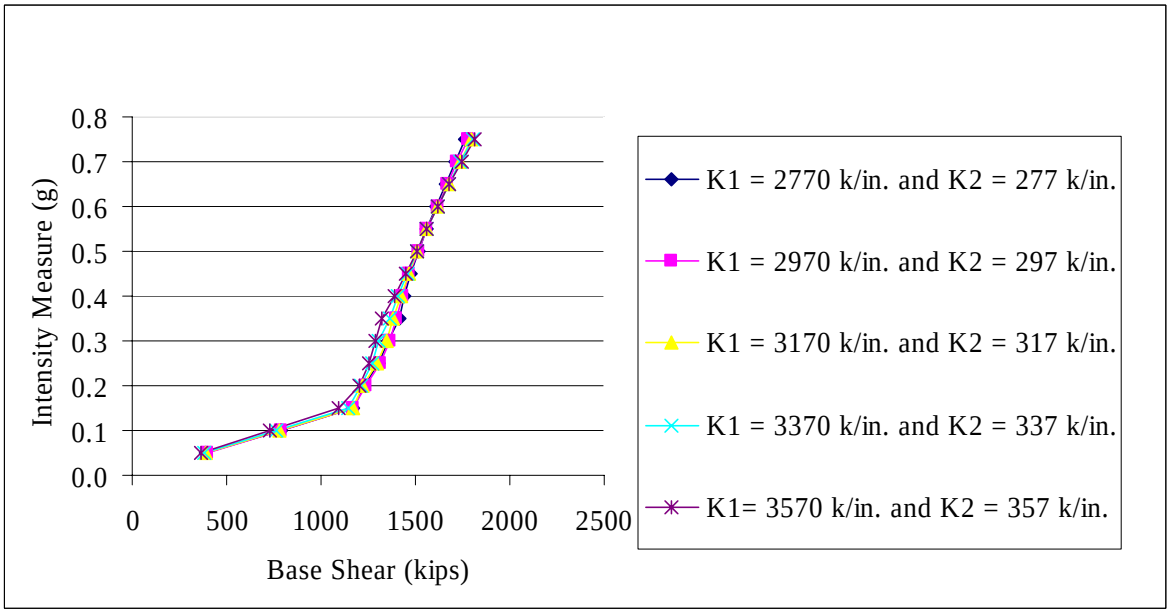

Fig. 6.12 IDA plots of base shear for the Northridge ground motion for variable stiffness

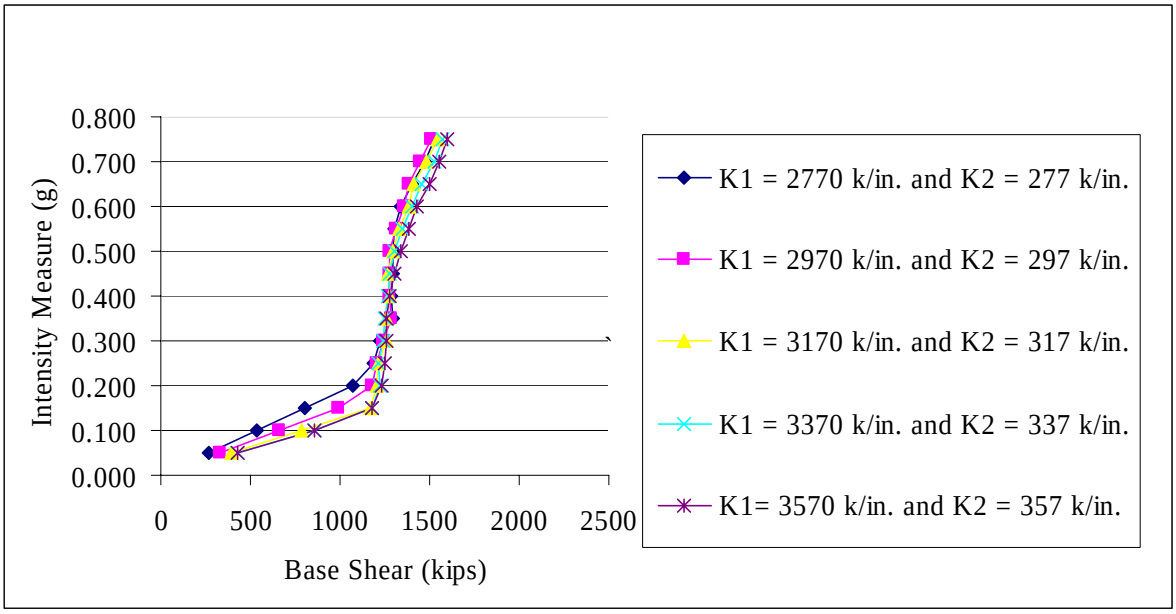

Fig. 6.13 IDA plots of base shear for the Santa Monica ground motion for variable stiffness

Figures 6.14-6.16 display the multi-record IDAs for which base shear was used as the damage measure. The results of the same analysis used for plotting peak displacement were used. Figure 6.14 contains the IDA for the system having K1 = 2770 k/in. and K2 = 277 k/in. In Figure 6.15 the median stiffnesses of the range, that is, K1 of 3170 k/in. and K2 of 317 k/in., were used. For Figure 6.16, K1 of 3570 k/in. and K2 of 357 k/in. were used. It is evident that after yielding the basic shapes of the curves remain similar. If the scaling factor is consistent with the stiffness used, the IDA curves for various ground motions coincide in the elastic region as in Fig 6.15. Otherwise distinct curves are obtained in the elastic region as in Fig 6.14 and Fig 6.16.

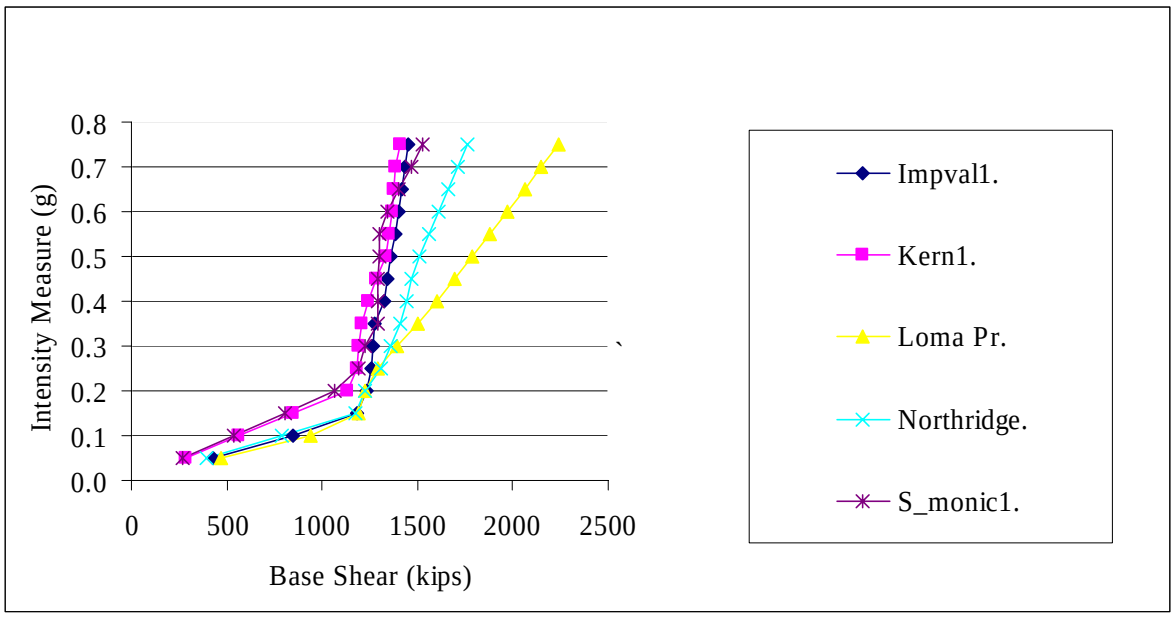

Fig. 6.14 Multi-record IDA plot of base shear for different ground motion for the system having K1 = 2770 k/in. and K2 = 277 k/in.

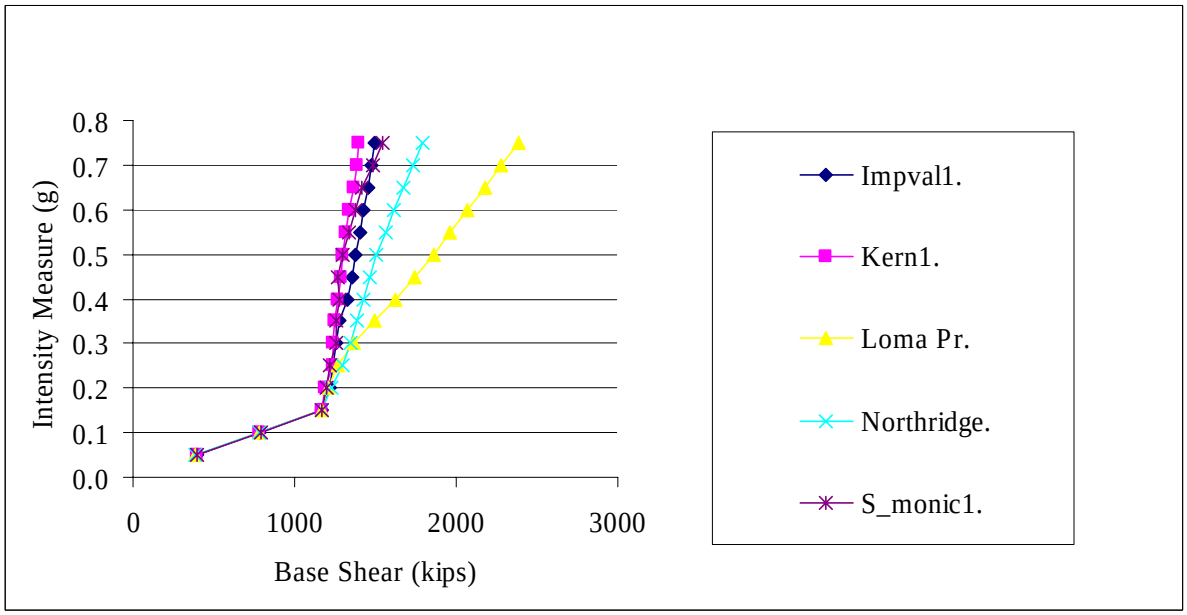

Fig. 6.15 Multi-record IDA plot of base shear for different ground motion for the system having K1 = 3170 k/in. and K2 = 317 k/in.

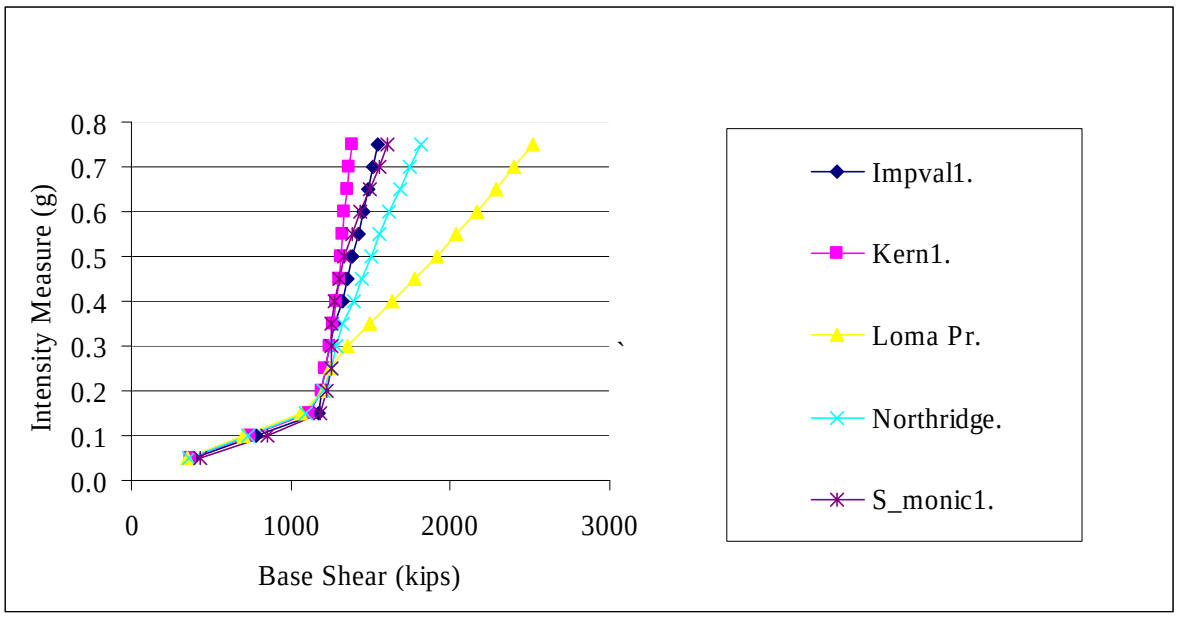

Fig. 6.16 Multi-IDA plot of base shear for different ground motion for the system having K1 = 3570 k/in. and K2 = 357 k/in.

6.3 Variation of damping

To study the effect of variation of damping on a given system subjected to IDA, a range of damping values was used, keeping the other systemic parameters constant. The system used to study the effect of damping has the following parameters:

Weight = 7800 k

Initial Stiffness = 3170 k/in.

Post-yield Stiffness = 317 k/in.

Yield Strength = 1170 k

The various values of damping used were 1%, 3%, 5%, 7% and 9% of critical damping. However the scaling for each ground motion was based on 5% of critical damping to ensure that the same scaled ground motion was used for each case. In Figure 6.17, the Imperial Valley ground motion was used for this purpose. A distinct trend is evident: systems having lower damping show greater displacement. This trend is valid in the elastic and the inelastic regions. Similarly for the Kern County ground motion in Figure 6.18, the damping-displacement inverse relationship is valid at all levels of intensity. Figure 6.19 displays the

Loma Prieta ground motion in which at all levels of intensity the response becomes less if damping is increased. However the dispersion tends to increase at higher levels of intensity. Finally after an intensity level of 0.55 g the system becomes unstable. In the case of the Northridge ground motion record as in Figure 6.20, the response decreases uniformly in the elastic and the inelastic regions. The nature of the IDA curve is similar to those obtained for the Imperial Valley ground motion. Figure 6.21 shows the IDA curve for the Santa Monica ground motion. The damping-response inverse relationship holds for this case also.

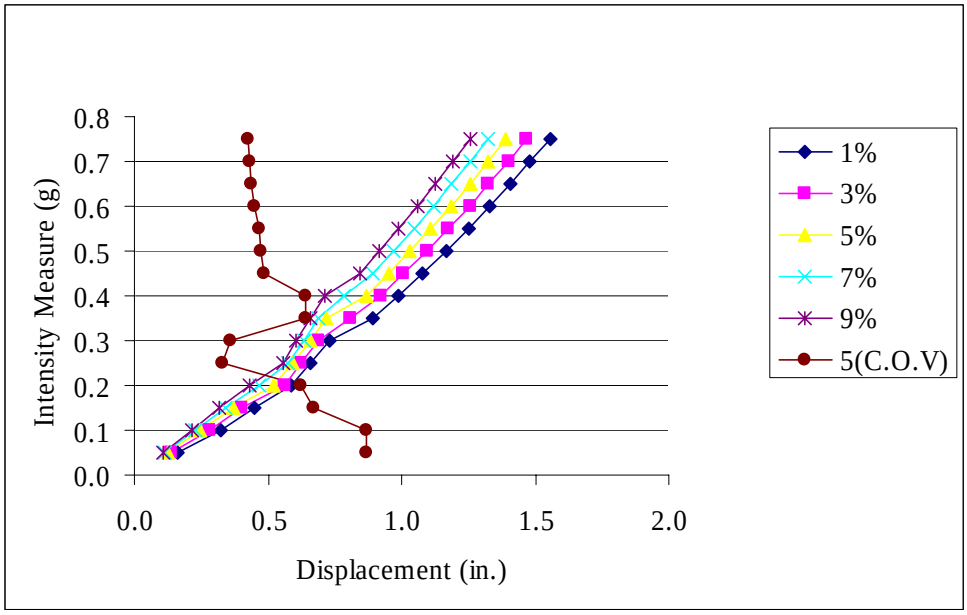

Fig. 6.17 IDA plots of peak displacement response for the Imperial Valley ground motion for variable damping

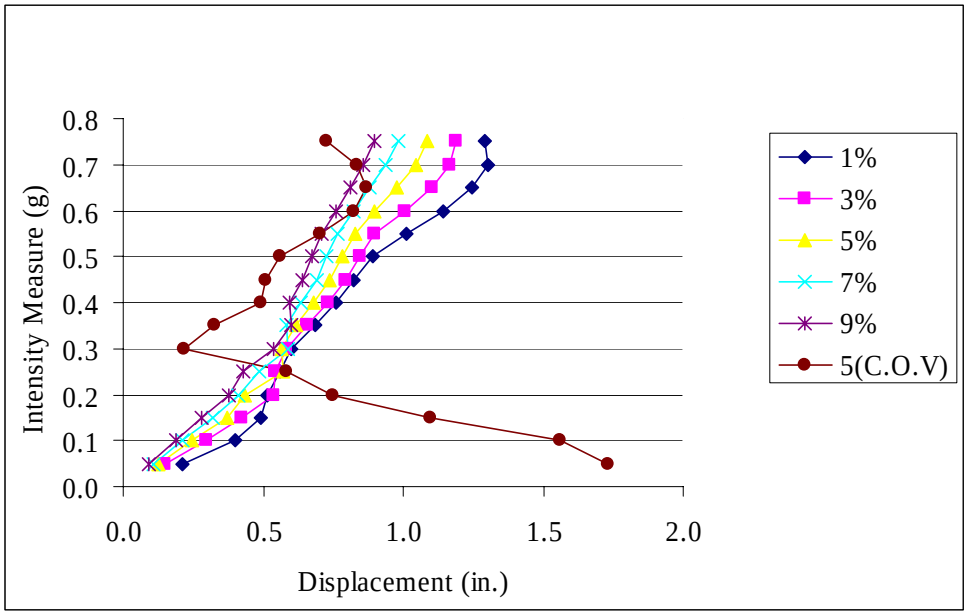

Fig. 6.18 IDA plots of peak displacement response for the Kern County ground motion for variable damping

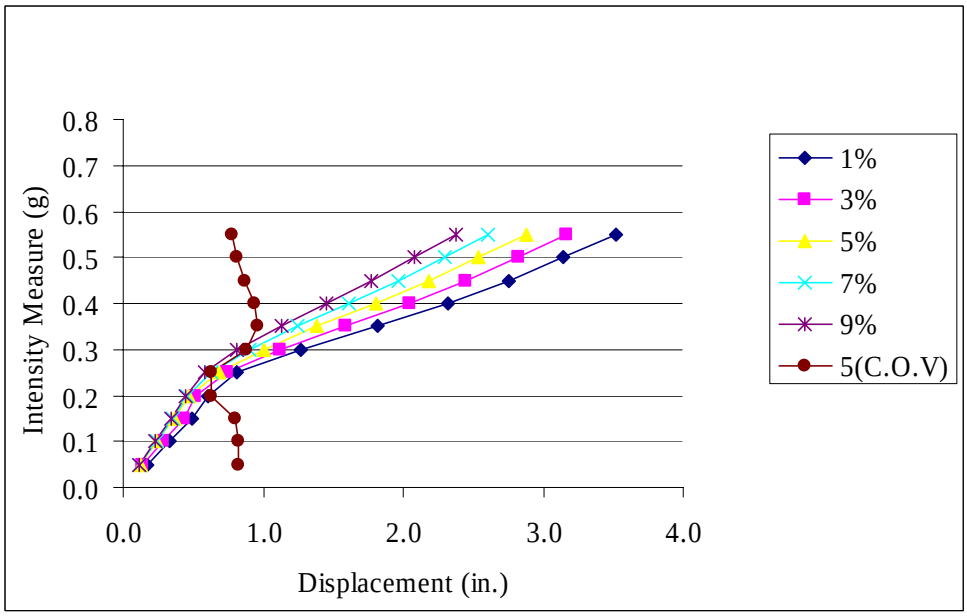

Fig. 6.19 IDA plots of peak displacement response for the Loma Prieta ground motion for variable damping

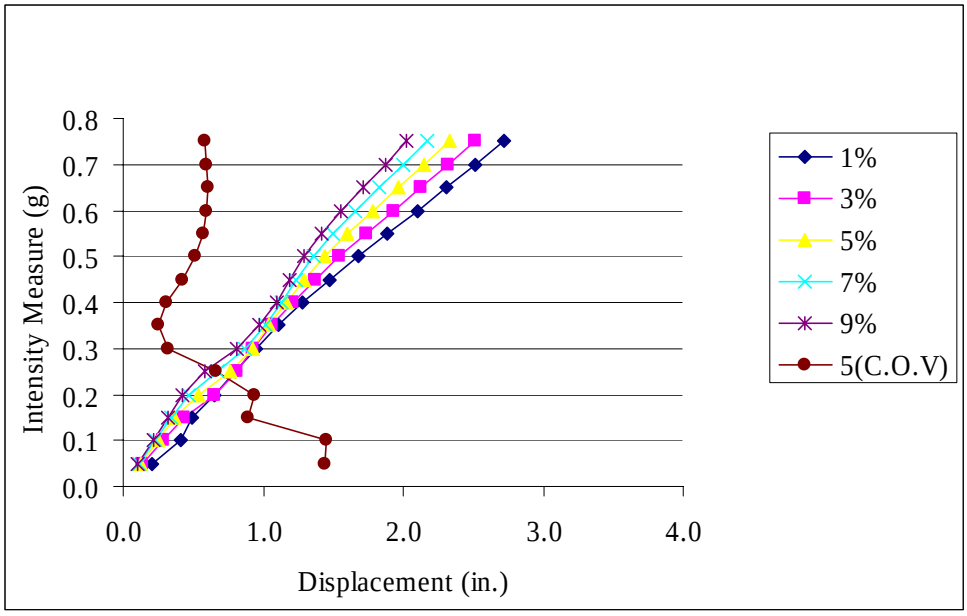

Fig. 6.20 IDA plots of peak displacement response for the Northridge ground motion for variable damping

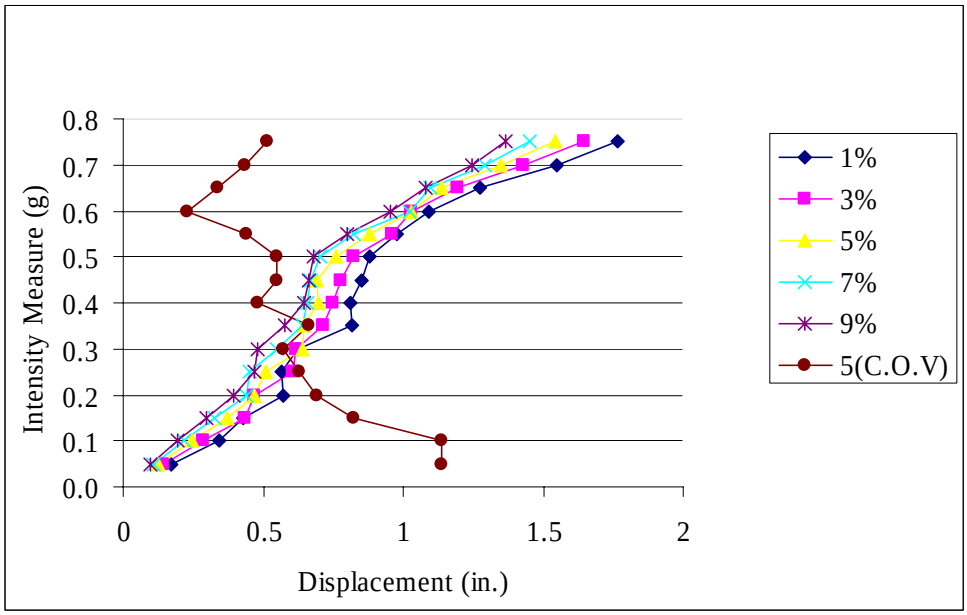

Fig. 6.21 IDA plots of peak displacement response for the Santa Monica ground motion for variable damping

The multi-record IDA plots for systems having 1%, 5% and 9% damping are shown in Figure 6.22, Figure 6.23 and Figure 6.24 respectively. The ground motion that was used was scaled for 5% damping which is the median value from the given range. It is observed that relative shapes of the curves are similar. But with higher values of damping the magnitude of the response decreases. In Figure 6.22, the linear part of the curve is not coincident because the damping of the system is 1% of critical damping, but the ground motion that was used was scaled for 5% of critical. In Figure 6.23, since the damping of the system is consistent, the elastic part is convergent. The response from all three systems is the least in the case of Figure 6.24 since it has the highest value of damping.

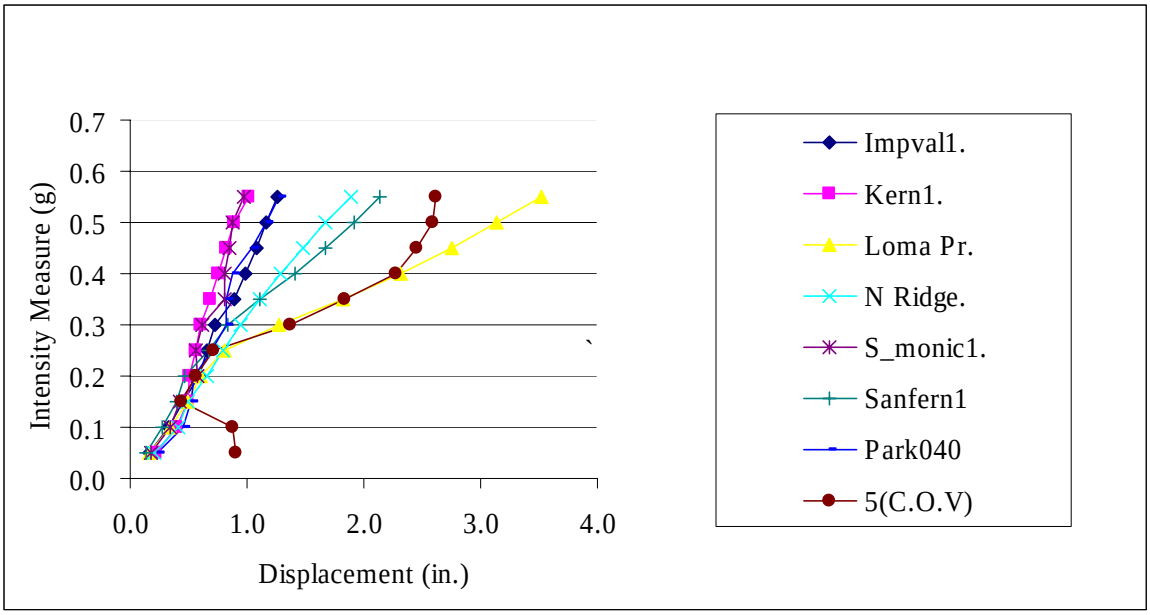

6.22 Multi-record IDA plots of peak displacement response for different ground motion on the system subjected to 1% of critical damping

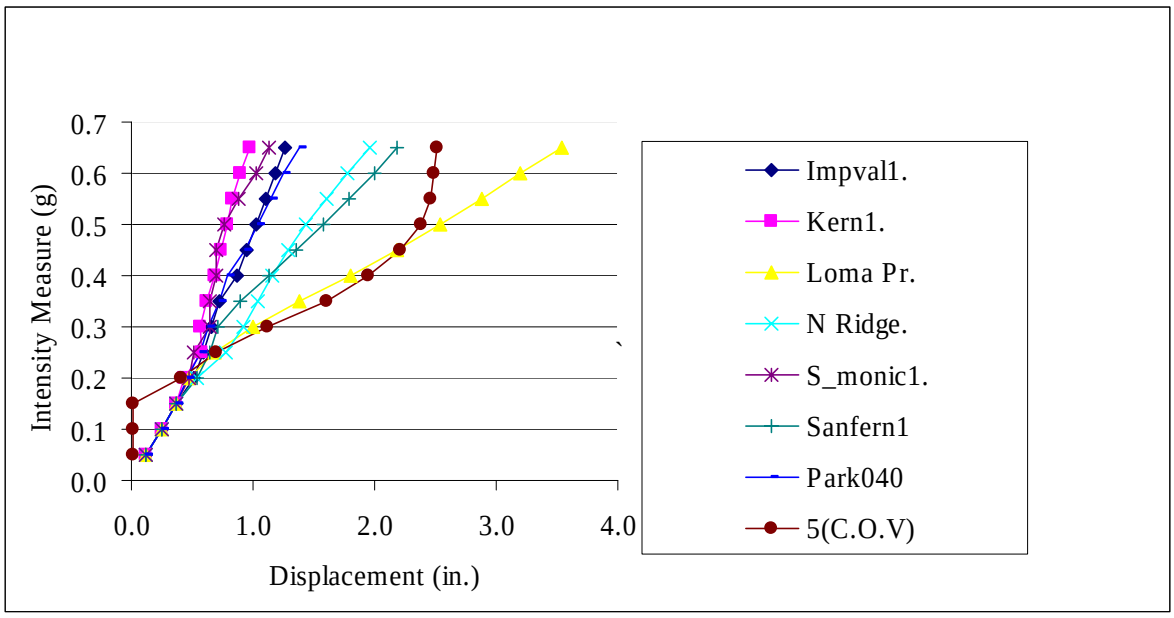

6.23 Multi-record IDA plots of peak displacement response for different ground motion on the system subjected to 5% of critical damping

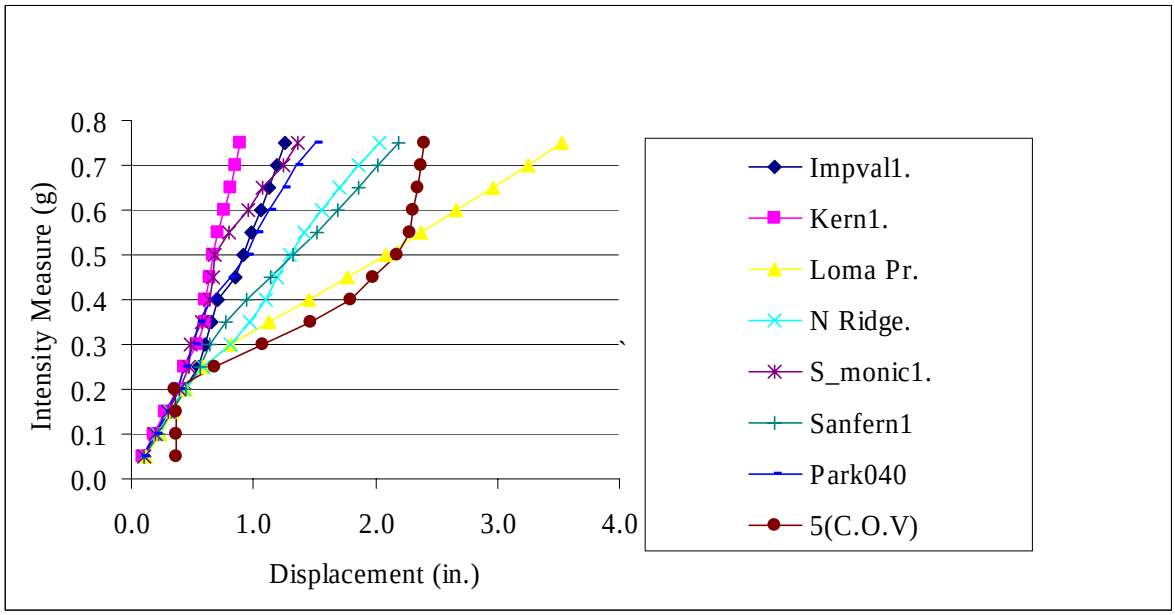

6.24 Multi-record IDA plots of peak displacement response for different ground motion on the system subjected to 9% of critical damping

The base shear for the study was assumed to be approximately equal to the elastic force because it was difficult to obtain the exact base shear in *NONLIN*. Since the damping was taken as 5% of critical damping, this assumption was justified. The base shear has been plotted using the values of elastic force for the study of variation of stiffness, yield strength and geometric stiffness. However, when the effect of variation of damping on the system was performed, the total base shear was recovered from the total inertial force. The plot of spring force as well as total base shear has been included when the variation of damping study was conducted to illustrate the effects due to them.

Figure 6.25 shows the spring force for the Imperial Valley ground motion for different values of damping. It is clear that for low values of damping, the spring force is greater at a given intensity level. The base shear when the Imperial ground motion was applied to the structure is shown in Figure 6.26. In the inelastic region the base shear increases with an increase in damping. For the Kern County ground motion the spring force decreases with increase in damping in the elastic and the inelastic regions as observed in Figure 6.27. However, when the damping force was recovered and added to the spring force in order to plot the base shear in Figure 6.28, it was observed that the base shear increases with increase in damping. For the Loma Prieta ground motion in Figure 6.29, the spring force is less if damping is increased at all levels of intensity. No definite trend can be identified in the base shear for the Loma Prieta ground motion in Figure 6.30. For the Northridge ground motion in Figure 6.31, the damping versus spring force inverse relationship holds. When the base shear was plotted for the Northridge ground motion in Figure 6.32 due to variation in damping, no definite trend could be identified. The plot of spring force for the Santa Monica ground motion in Figure 6.33 shows that the spring force decreases for increase in damping in the elastic and the inelastic regions. The base shear for the Santa Monica ground motion has been plotted in Figure 6.34. The base shear increases with increase in damping in the inelastic region. So it can be concluded that the increase in damping reduces the base shear in the elastic region, but increases the base shear in the inelastic region.

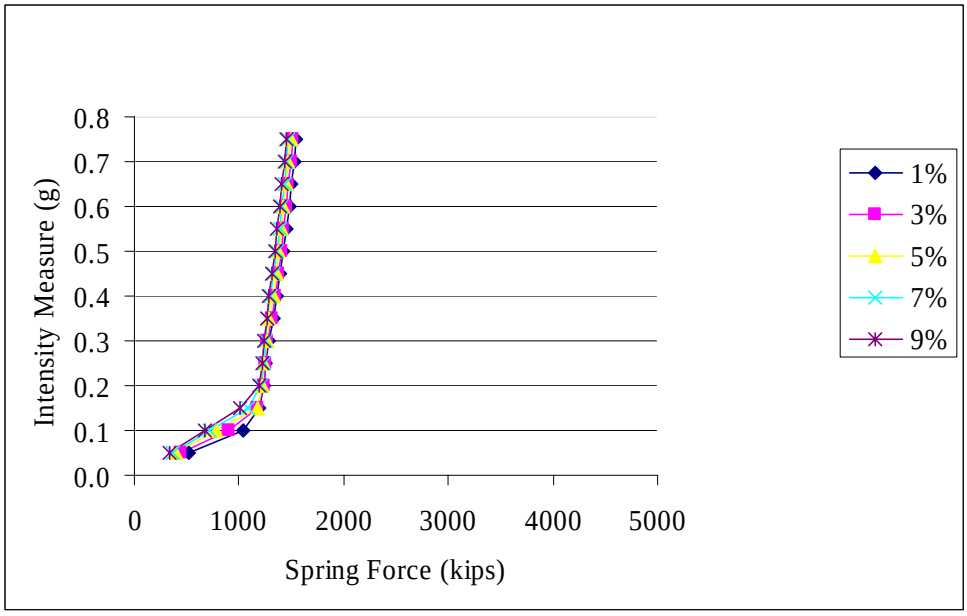

Fig. 6.25 IDA plots of spring force for the Imperial Valley ground motion for variable damping

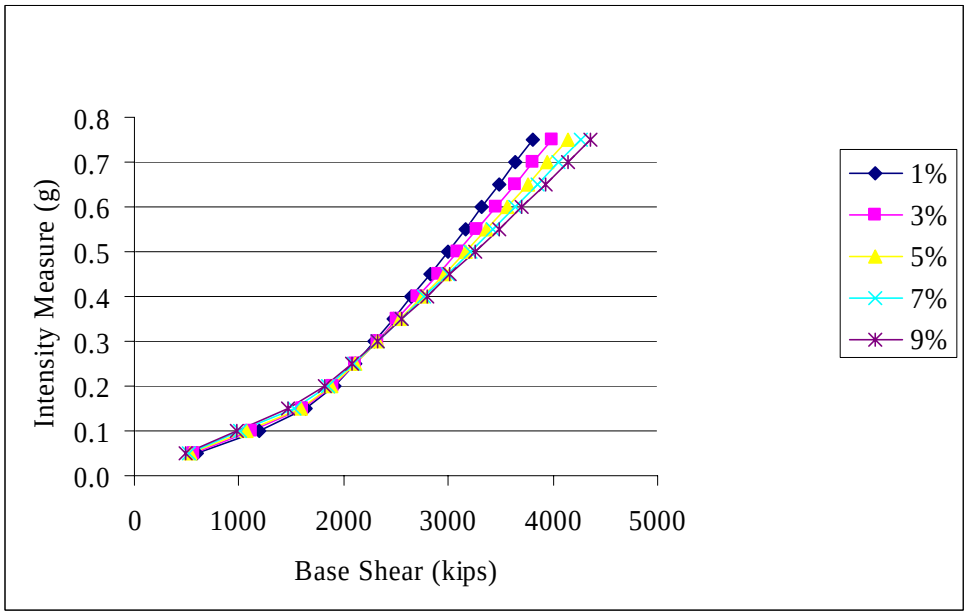

Fig. 6.26 IDA plots of base shear for the Imperial Valley ground motion for variable damping

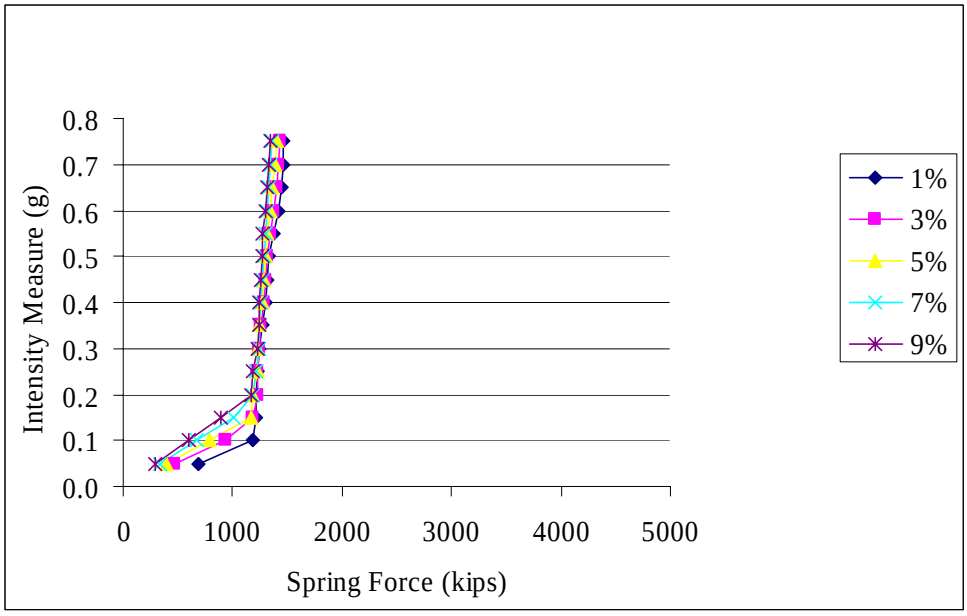

Fig. 6.27 IDA plots of spring force for the Kern County ground motion for variable damping

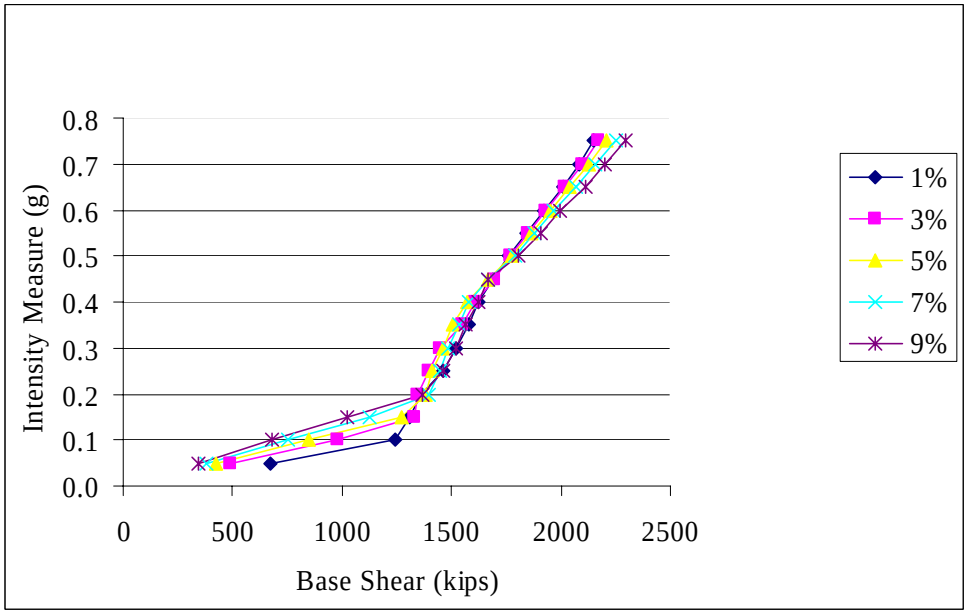

Fig. 6.28 IDA plots of base shear for the Kern County ground motion for variable damping

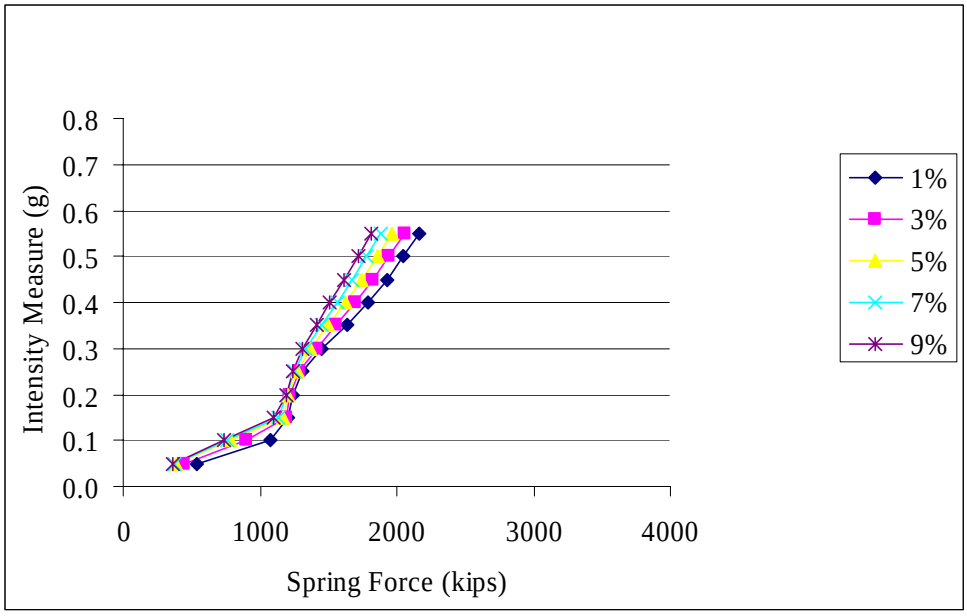

Fig. 6.29 IDA plots of spring force for the Loma Prieta ground motion for variable damping

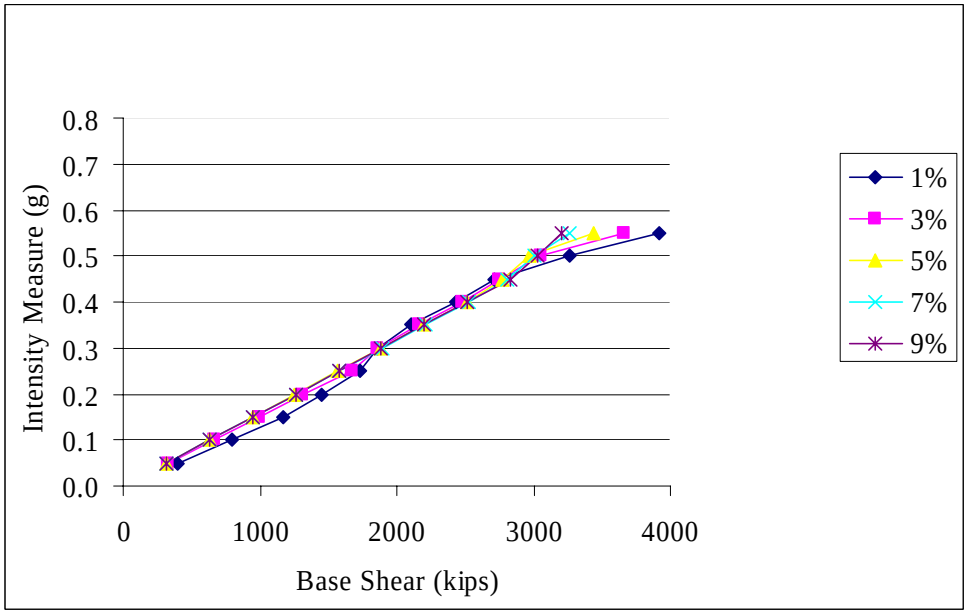

Fig. 6.30 IDA plots of base shear for the Loma Prieta ground motion for variable damping

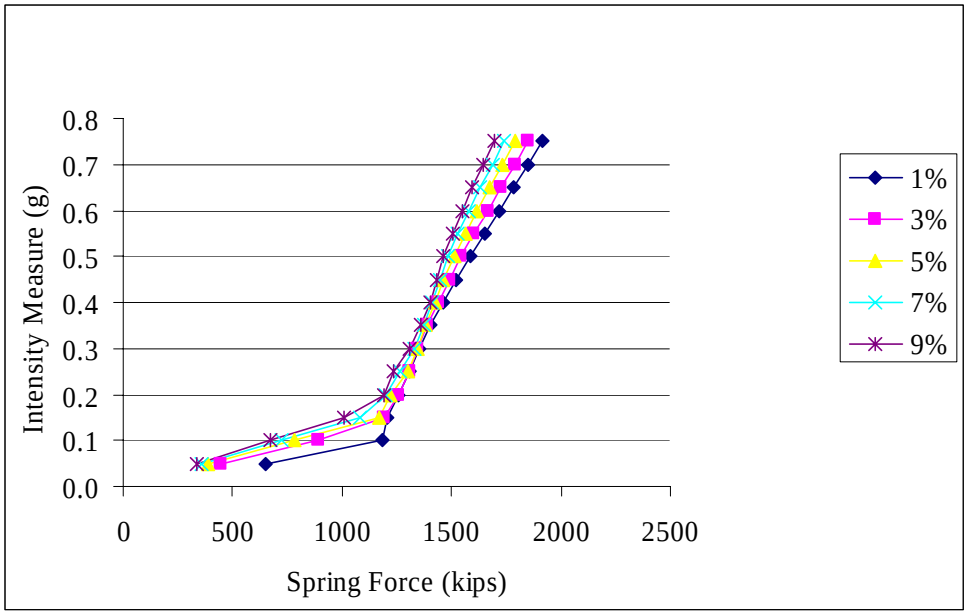

Fig. 6.31 IDA plots of spring force for the Northridge ground motion for variable damping

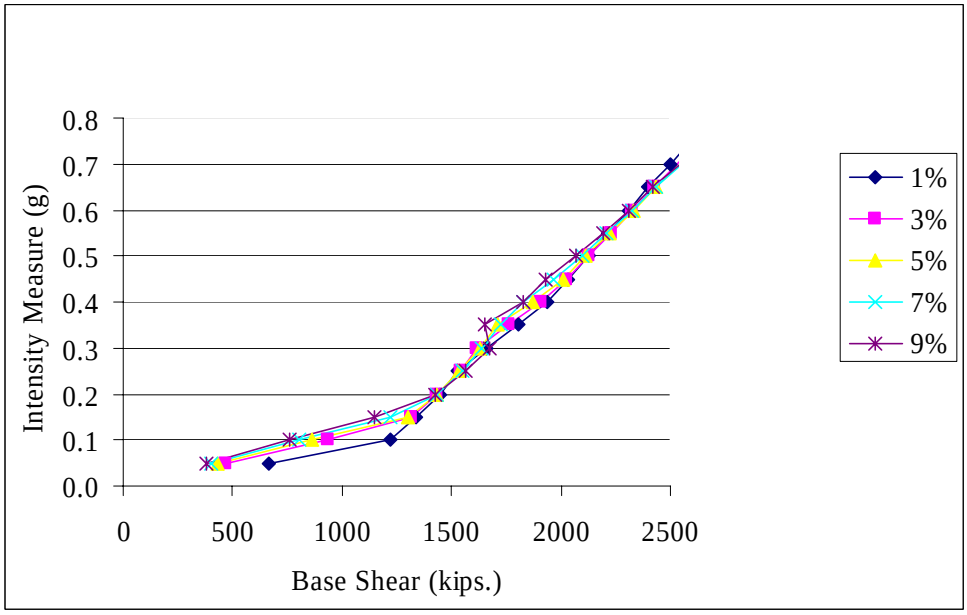

Fig. 6.32 IDA plots of base shear for the Northridge ground motion for variable damping

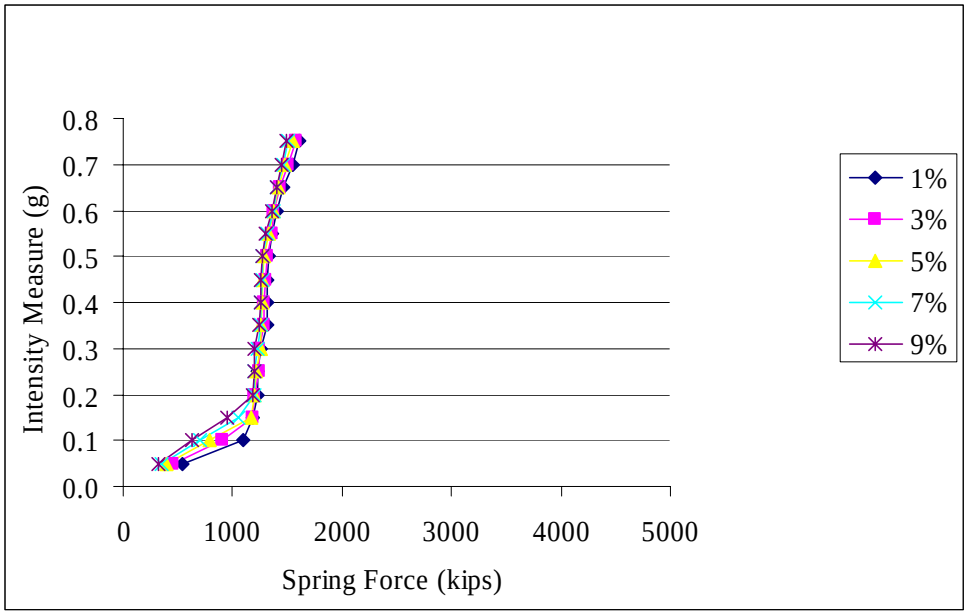

Fig. 6.33 IDA plots of spring force for the Santa Monica ground motion for variable damping

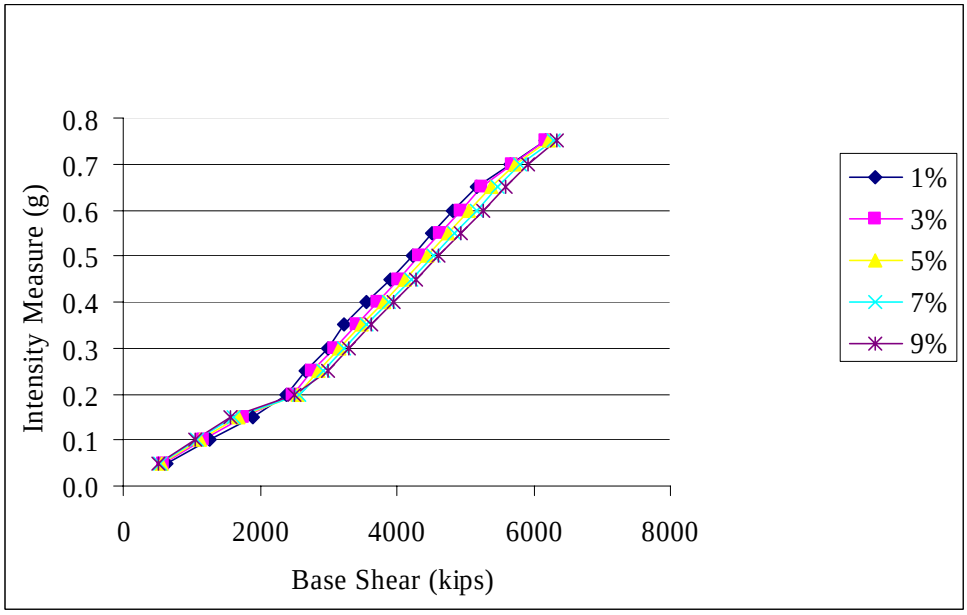

Fig. 6.34 IDA plots of base shear for the Santa Monica ground motion for variable damping

Multi-record IDA curves were plotted for base shear for 1%, 5% and 9% damping. The scale factor used in all the cases was the same and derived from 5% of critical damping. In Figure 6.35 the multi-record IDA is plotted for 1% of critical damping. The base shear for 5% damping is shown in Figure 6.36. The base shear is greater than it was for 1% of critical damping, however the basic shape of the curves remains similar. When the damping value used is 9% of critical damping, the base shear increases as observed in Figure 6.37.

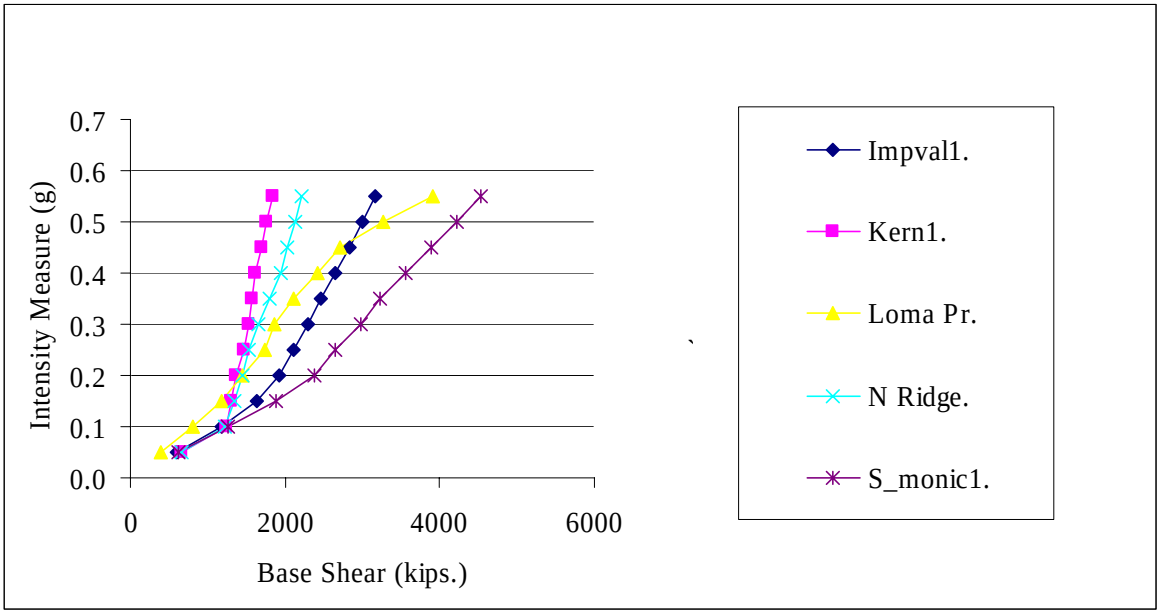

Fig. 6.35 Multi-record IDA plots of base shear for different ground motion on the system subjected to 1% of critical damping

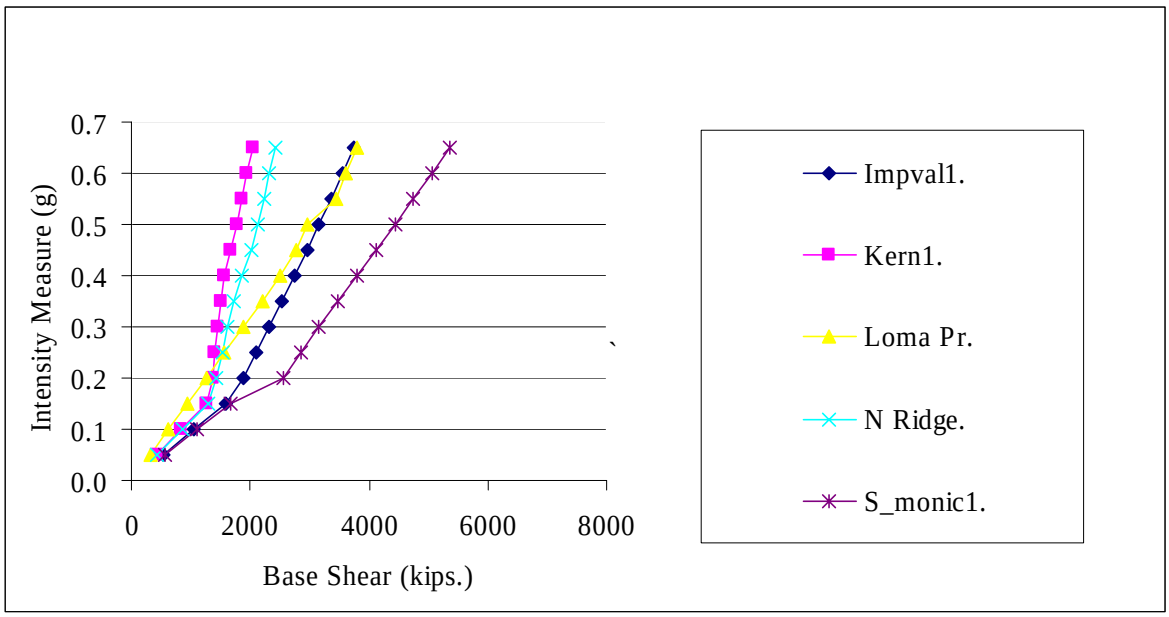

Fig. 6.36 Multi-record IDA plots of base shear for different ground motion on the system subjected to 5% of critical damping

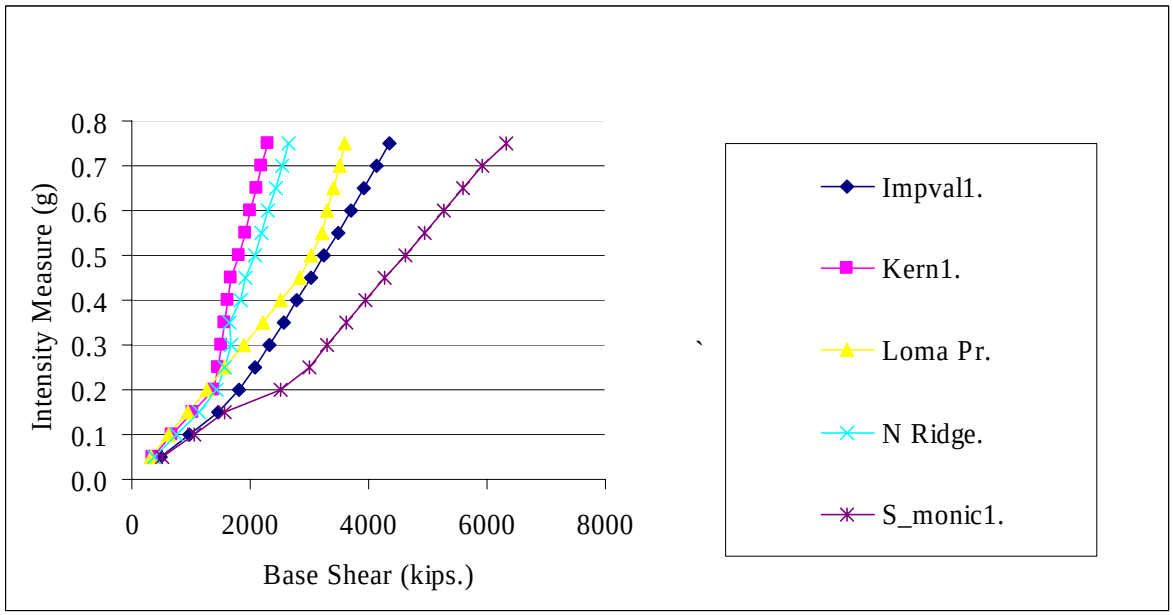

Fig. 6.37 Multi-record IDA plots of base shear for different ground motion on the system subjected to 9% of critical damping

6.4 Variation in yield strength

The yield strength is an important factor that determines the response. The cycles of loading and unloading will be affected if the yield point is varied. In this study the system used was the same one as in previous cases; the yield strength is the only variable factor.

Weight = 7800 k

Initial Stiffness = 3170 k/in

Post-yield Stiffness = 317 k/in

Damping = 5% of critical

The ground motions are scaled according to the above parameters.

The values of yield strength used were 870 k, 970 k, 1070 k, 1170 k, 1270 k, 1370 k and 1470 k. The curves obtained were compared to one obtained from linear analysis in which the system did not yield. According to the "equal displacement" concept, an empirical observation states that for moderate period structures, inelastic global displacements are generally approximately equal to the displacements of the corresponding elastic model. This was achieved by using F_y = 1,000,000 k.

Figure 6.38 shows the IDA plot for the Imperial Valley ground motion record. The system with the lowest yield strength yields first. It is also observed in the inelastic region that systems having lower yield strength display less response at the same intensity level. For a given value of response, the system with the lowest yield strength can sustain the greatest intensity of the ground motion. The response for the Kern County ground motion is displayed in Figure 6.39. No clear trend can be identified from the IDA plot. Figure 6.40 shows the results for the Loma Prieta ground motion. As in the Imperial Valley case, also the system having lower yield strength yields first. For a given intensity of earthquake, the system having lowest yield strength displays the greatest response in the inelastic region. At a given value of response, the system having highest yield strength can sustain the greatest earthquake. The IDA for the Northridge ground motion is depicted in Figure 6.41. It can be observed that systems with lower yield strength yield first. However there is no specific trend in the post-yield response. Hence no comment can be made about the dependence of the response on the yield strength. For the Santa Monica ground motion in Figure 6.42, no

definite trend can be identified regarding the response or the yielding. In Figures 6.38-6.42 the response for linear elastic response is indicated by the line corresponding to F_y = 1,000,000 k. It can be observed that all the curves are either to the left or the right of this line. For the Imperial Valley, Kern County and Santa Monica ground motions, the IDA curves are to the left of this line. For the Loma Prieta and Northridge ground motions, the IDA curves are on the right side of the elastic line, which indicates that the responses are less predictable and can cause more damage.

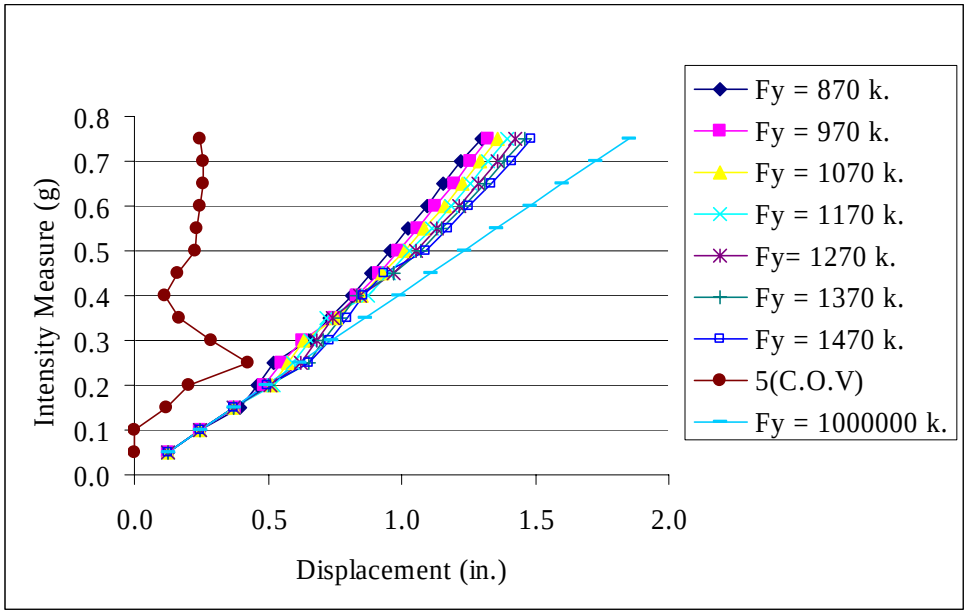

Fig. 6.38 IDA plots of peak displacement response for the Imperial Valley ground motion for variable yield strength

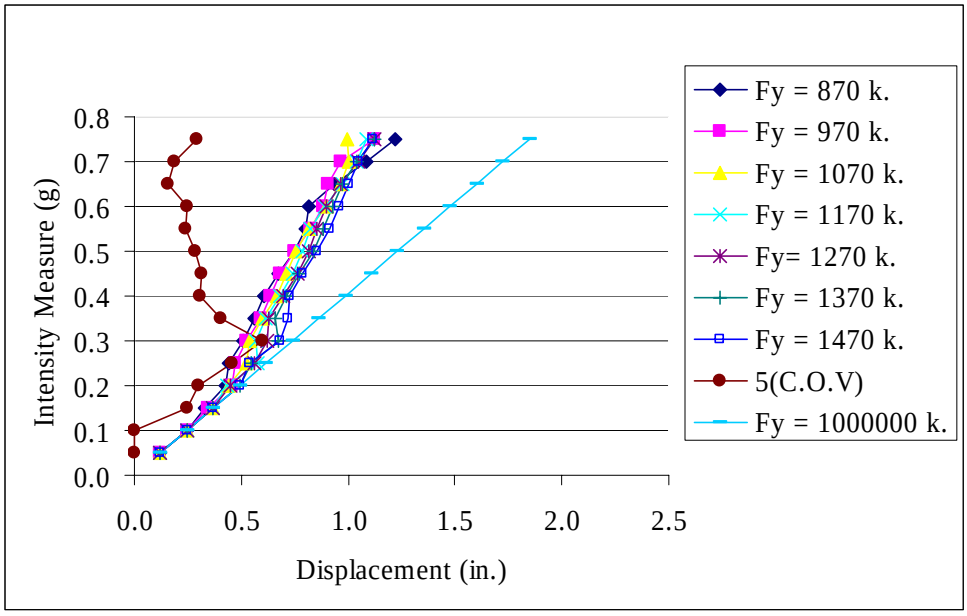

Fig. 6.39 IDA plots of peak displacement response for the Kern County ground motion for variable yield strength

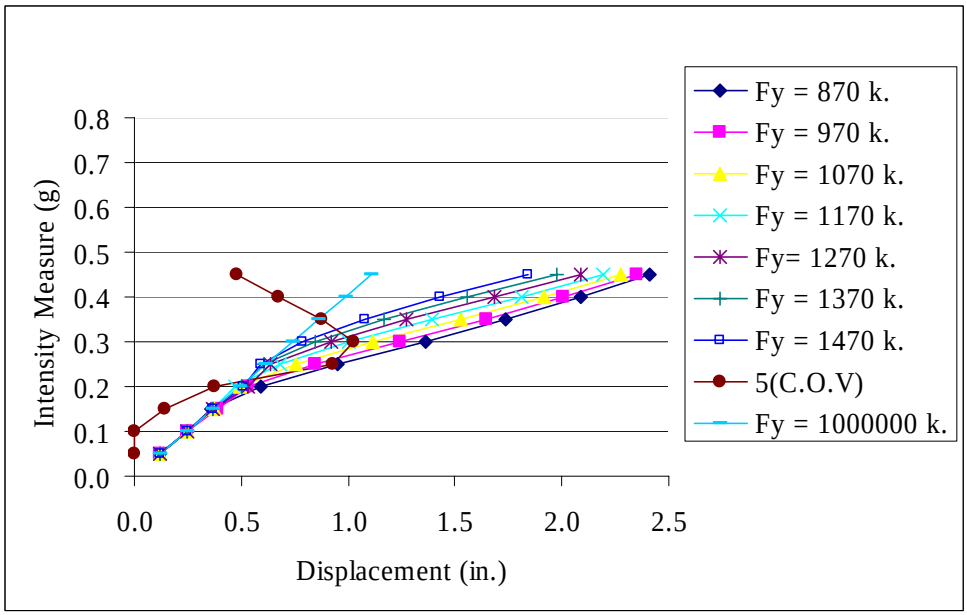

Fig. 6.40 IDA plots of peak displacement response for the Loma Prieta ground motion for variable yield strength

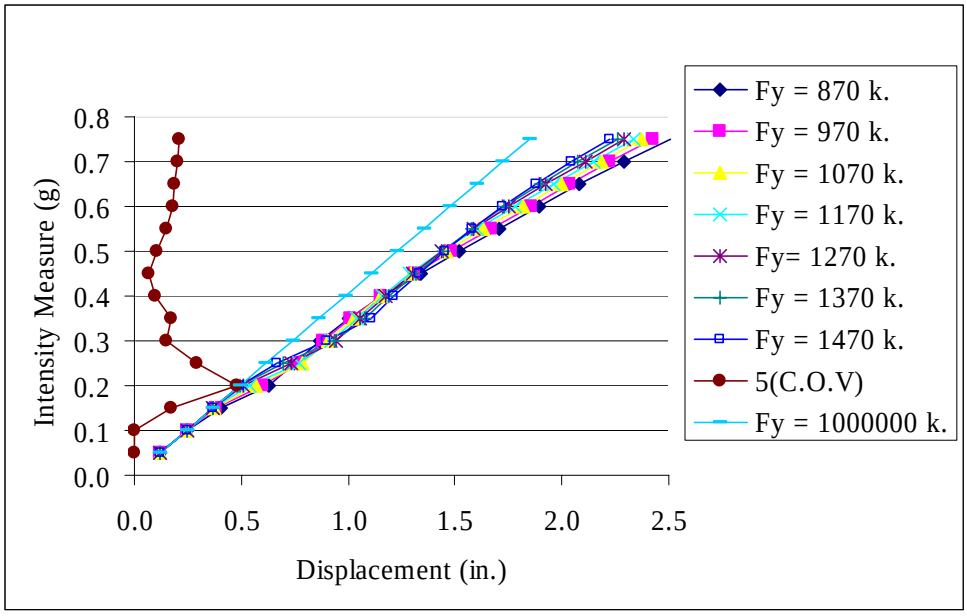

Fig. 6.41 IDA plots of peak displacement response for the Northridge ground motion for variable yield strength

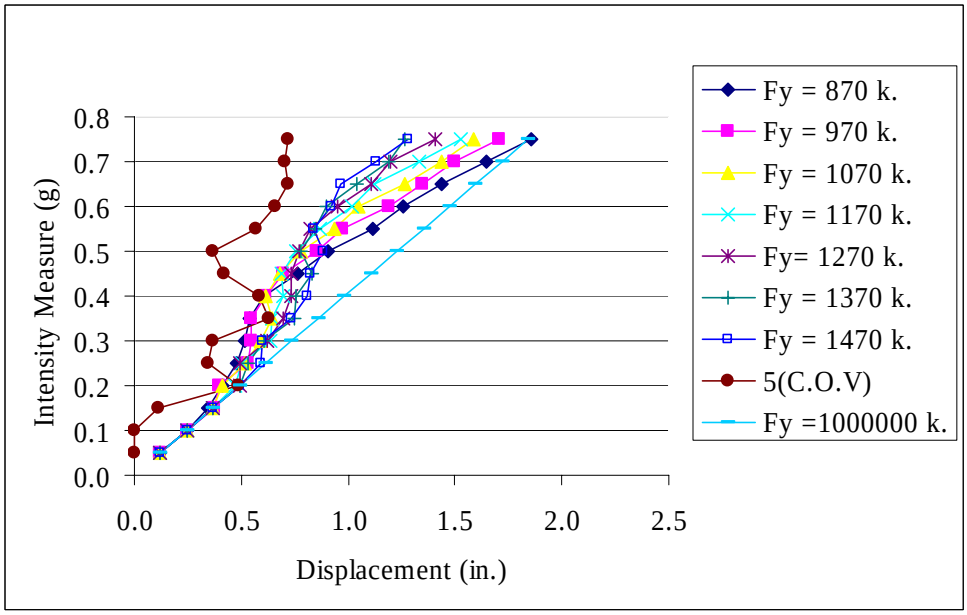

Fig. 6.42 IDA plots of peak displacement response for the Santa Monica ground motion for variable yield strength

The multi-record IDA plots corresponding to systems having yield strengths of 870 k, 1170 k and 1470 k are illustrated in Figures 6.43, 6.44 and 6.45, respectively. It can be observed that the basic shapes of the curves are similar for all the cases. Since the value of the yield strength does not affect the scaling, hence in the linearly elastic region the curves are convergent in all three cases.

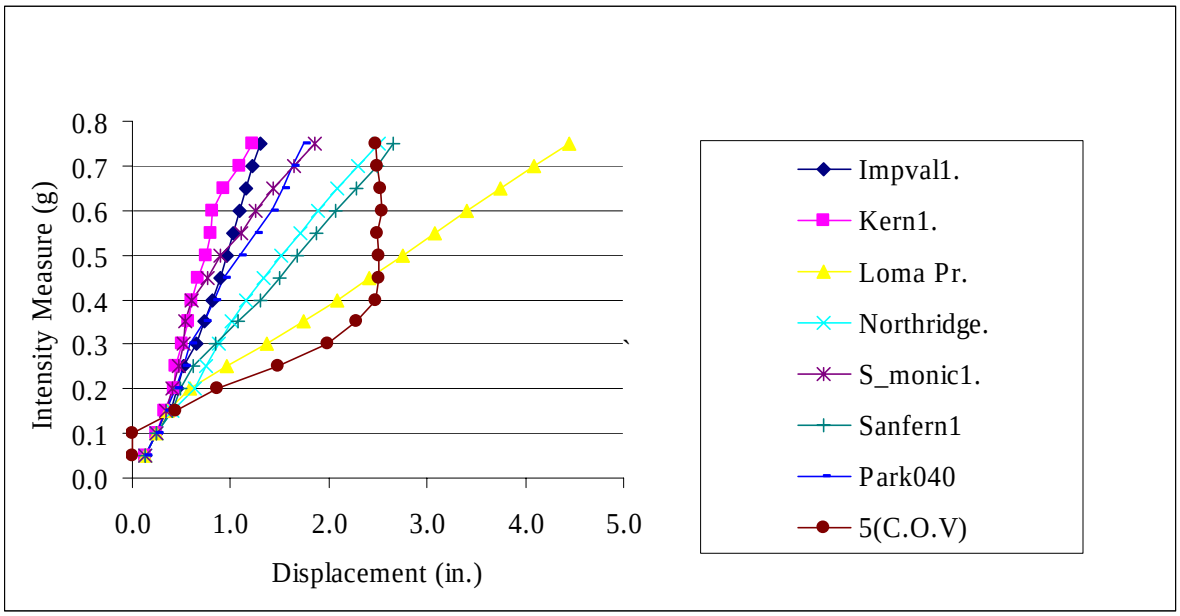

Fig. 6.43 Multi-record IDA plots of peak displacement response for different ground motion on the system having yield strength of 870 k

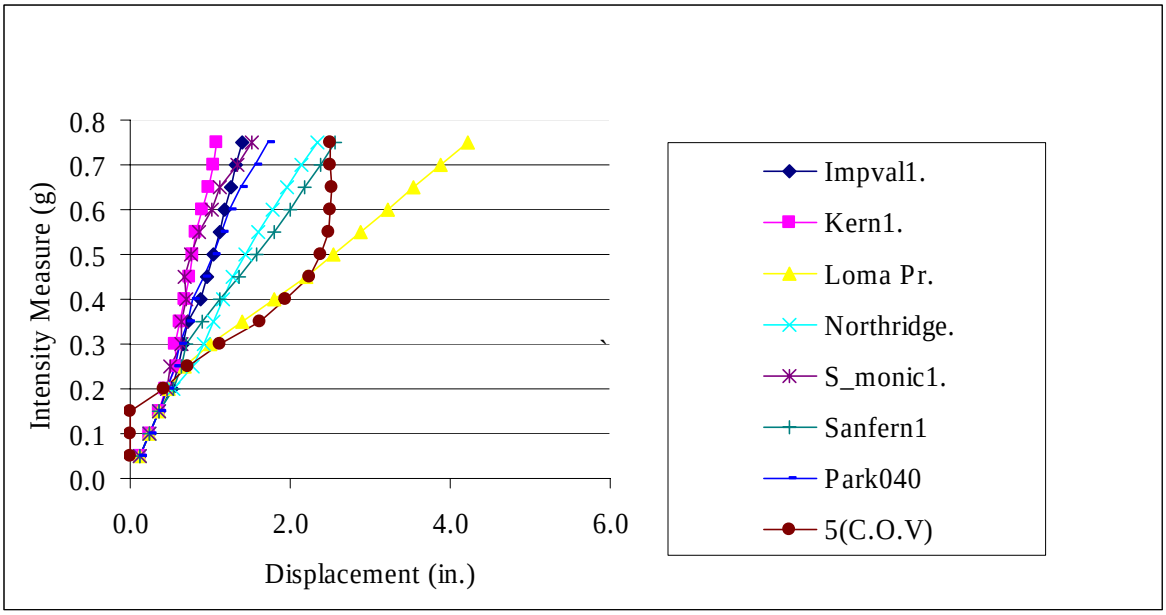

Fig. 6.44 Multi-record IDA plots of peak displacement response for different ground motion on the system having yield strength of 1170 k

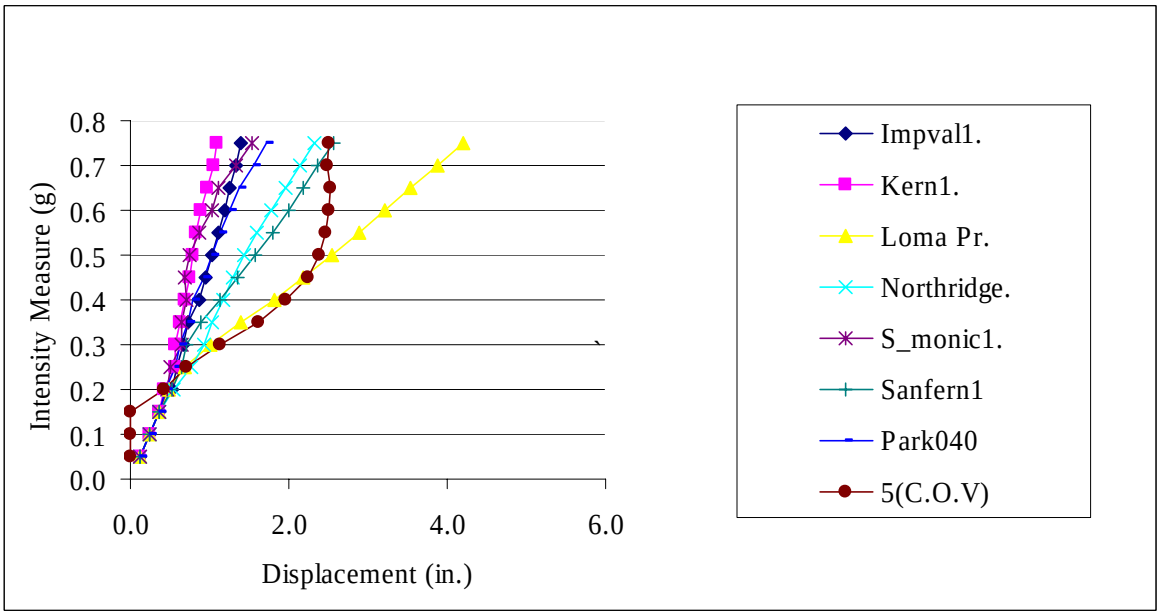

Fig. 6.45 Multi-record IDA plots of peak displacement response for different ground motion on the system having yield strength of 1470 k

Figure 6.46 is a plot of the base shear for systems having variable yield strength and subjected to the Imperial Valley ground motion. It can be observed that base shear is lower for systems having less yield strength, and yielding also occurs first for systems having lower yield strength. Similar behavior was also exhibited when the Kern County ground motion was applied to the same system as shown in Figure 6.47. The results for the Loma Prieta ground motion are presented in Figure 6.48. The behavior is consistent with the other ground motions. In Figure 6.49 the effect of using the Northridge ground motion is demonstrated. The yielding takes place as per the yield strength of the system. A uniform pattern is observed in the post-yield response. When the Santa Monica ground motion was used, as shown in Figure 6.50, the yielding occurs in the same sequence. This clearly justifies the claim that the value of the yield strength governs the onset of the inelastic behavior.

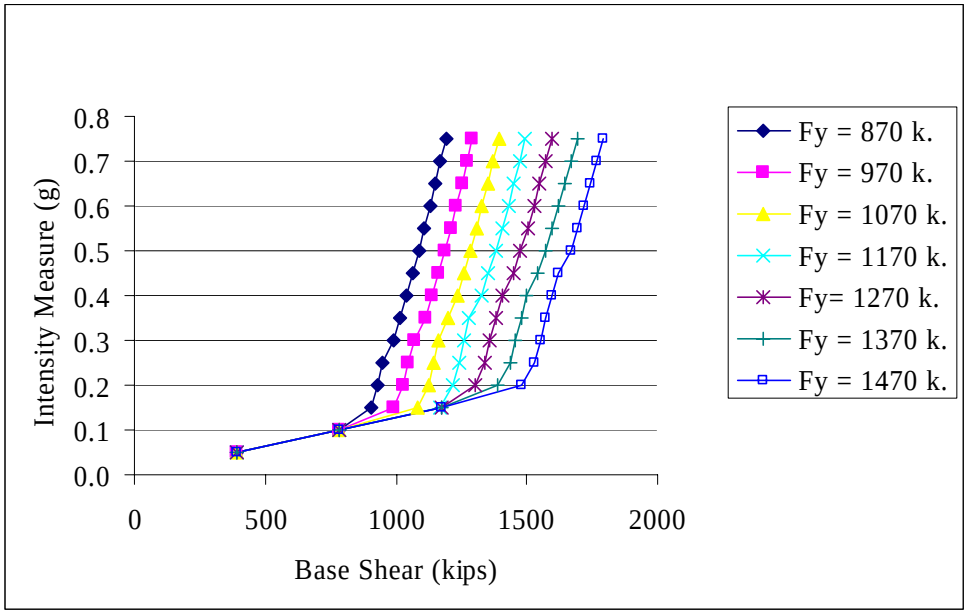

Fig. 6.46 IDA plots of base shear for the Imperial Valley ground motion for variable yield strength

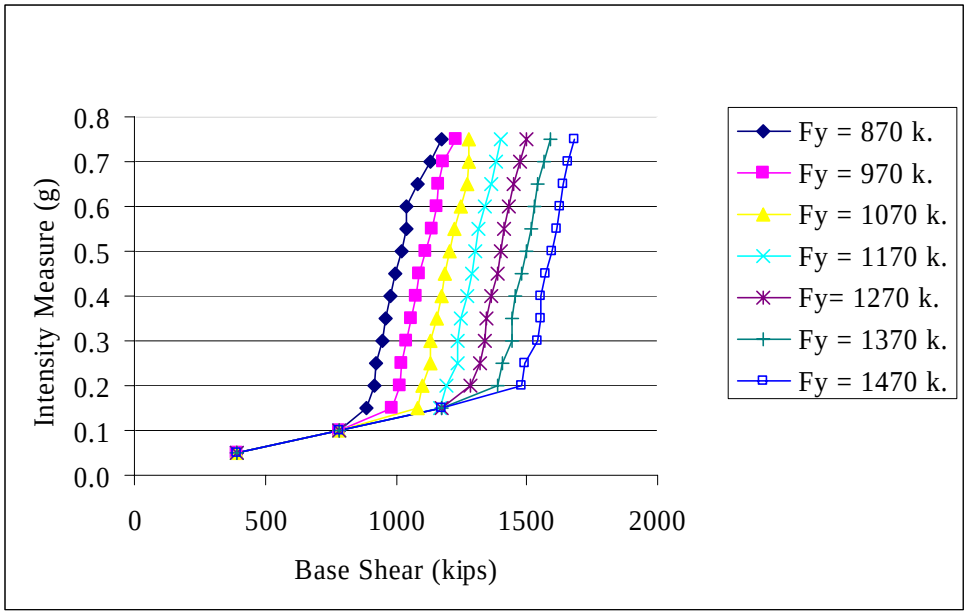

Fig. 6.47 IDA plots of base shear for the Kern County ground motion for variable yield strength

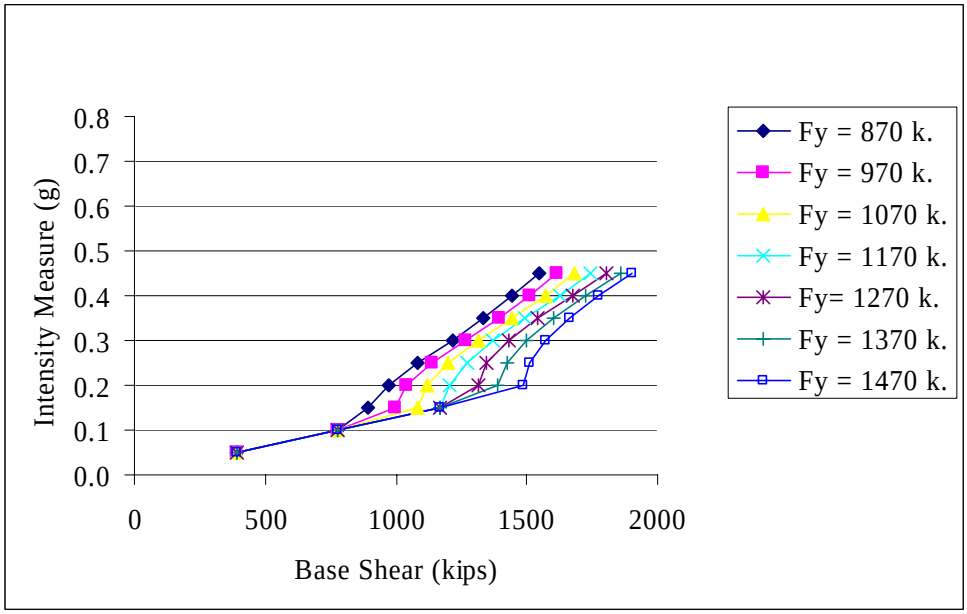

Fig. 6.48 IDA plots of base shear for the Loma Prieta ground motion for variable yield strength

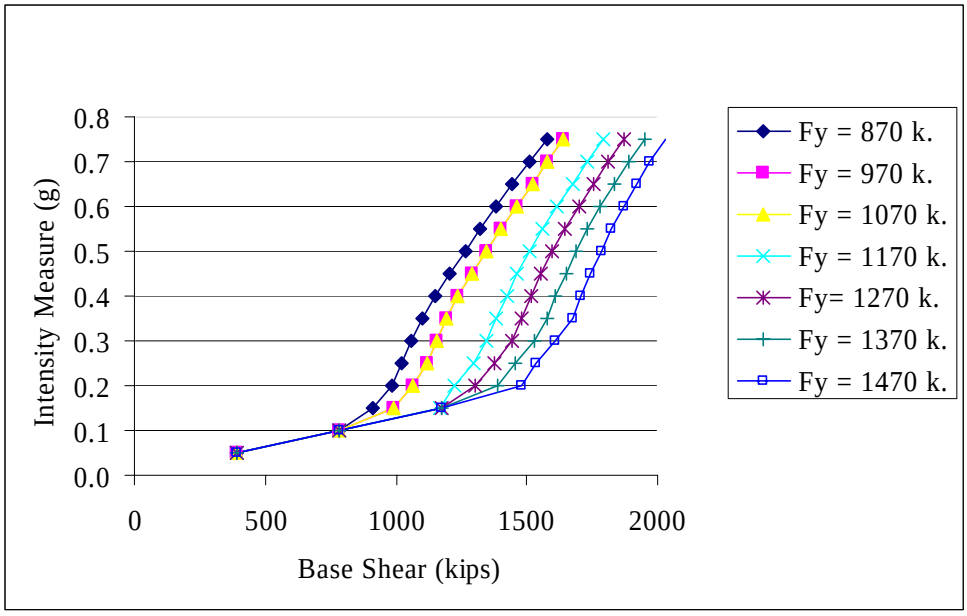

Fig. 6.49 IDA plots of base shear for the Northridge ground motion for variable yield strength

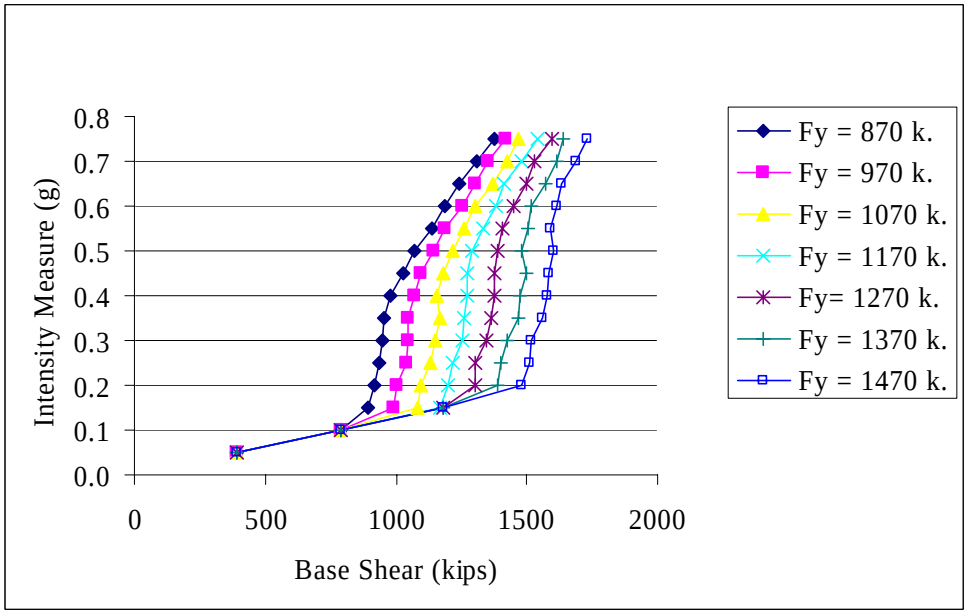

Fig. 6.50 IDA plots of base shear for the Santa Monica ground motion for variable yield strength

The multi-record IDA plots are generated using different systems having yield strengths of 870 k, 1170 k and 1470 k as shown in Figures 6.51, 6.52 and 6.53, respectively. The span of the linearly elastic portion is the least when the yield strength is the least, as in Figure 6.51. In Figure 6.52 the span of the linearly elastic portion is greater than in the previous case. When the yield strength is greatest, the system yields if it is subjected to a high intensity earthquake as in Figure 6.53.

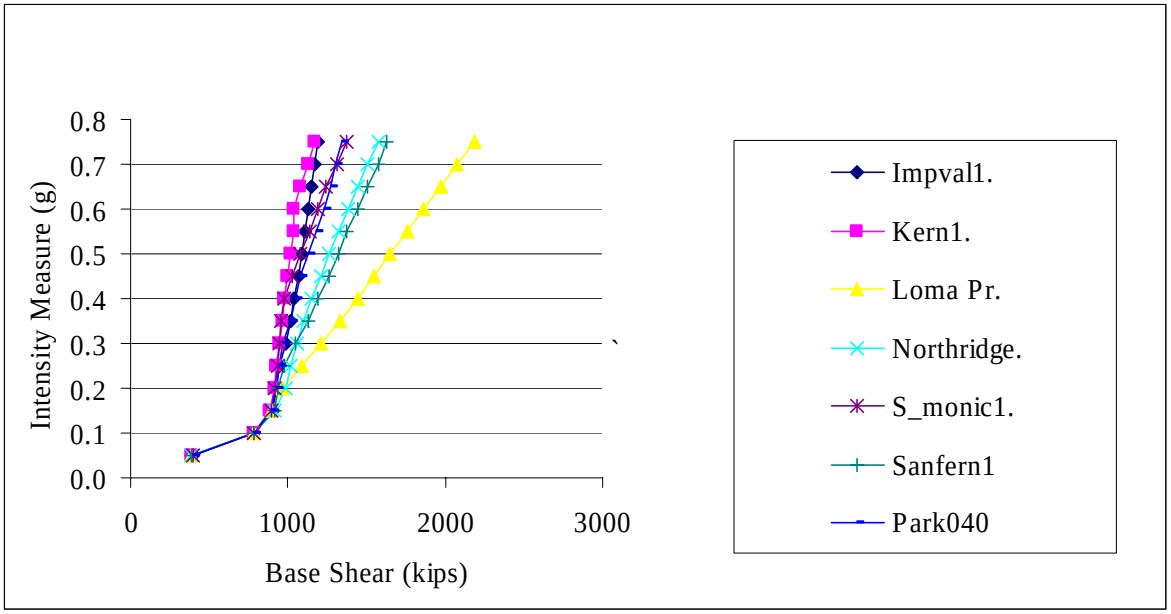

Fig. 6.51 Multi-record IDA plot of base shear for different ground motion on the system having yield strength of 870 k

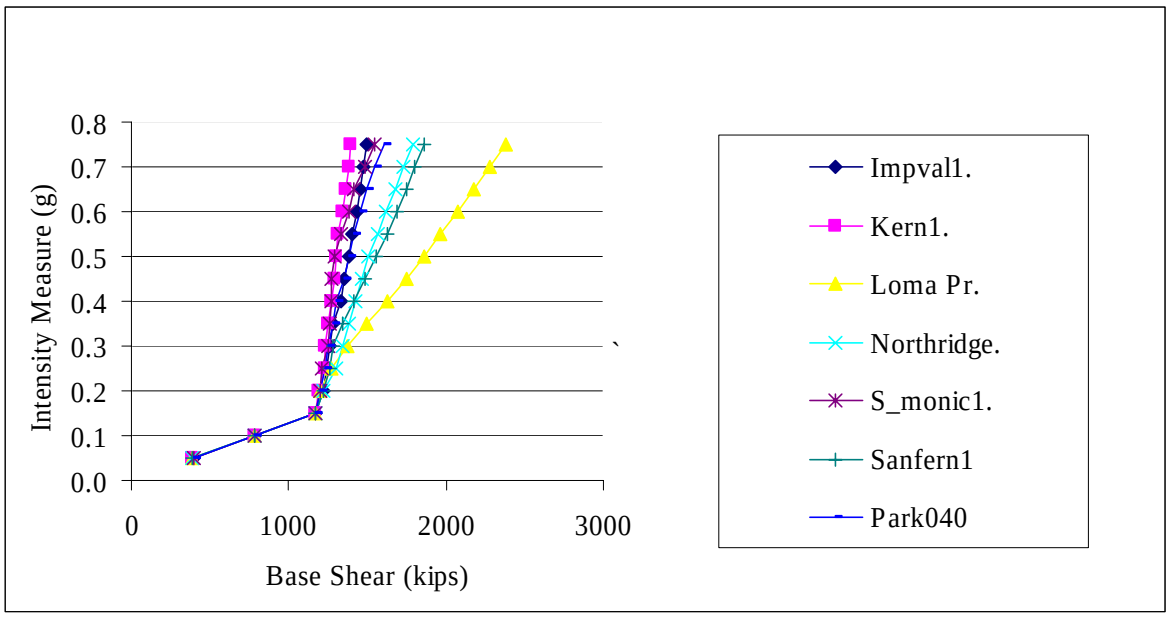

Fig. 6.52 Multi-record IDA plot of base shear for different ground motion on the system having yield strength of 1170 k

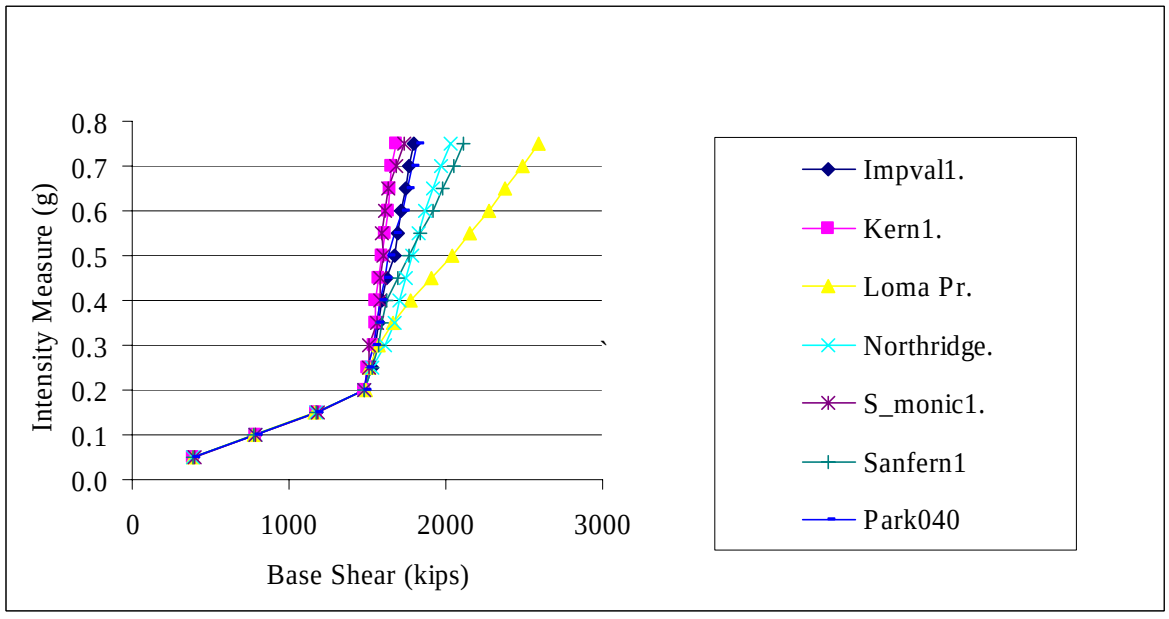

Fig. 6.53 Multi-record IDA plot of base shear for different ground motion on the system having yield strength of 1470 k

6.5 Variation in geometric stiffness

Geometric stiffness is a factor that takes into account the decrease in stiffness due to P-Delta effects. It has been observed that large geometric stiffness causes instability in static analysis. Applying P-Delta effects in incremental dynamic analysis provides a means to study its effect on dynamic analysis. Figures 6.54-6.58 show IDA curves incorporating P-Delta effects.

The system as described in section 2.2.1 had the following basic characteristics:

Weight = 7800 k

Initial Stiffness = 3170 k/in.

Post-yield Stiffness = 317 k/in.

Yield Strength = 1170 k

Damping = 5% of critical

The scaling was based on the above parameters.

The structure was analyzed without P-Delta effects and using geometric stiffnesses of 100 k/in., 150 k/in., 250k/in., 317 k/in., 350 k/in., 400 k/in., and 450 k/in. When the geometric stiffness is set equal to 317 k/in., it indicates elastic-perfectly-plastic behavior. For geometric stiffness greater than 317 k/in., negative secondary stiffness occurs in the system.

For the Imperial Valley ground motion, when the IDAs are plotted as in Figure 6.54, it can be observed that dispersion starts occurring when negative stiffness occurs. If the geometric stiffness is small, it does not significantly affect the IDA curves. The results for the Kern County ground motion are plotted in Figure 6.55. When the geometric stiffness exceeds 150 k/in., dispersion begins to occur, which increases significantly for a small increase in the geometric stiffness. At a geometric stiffness of 350 k/in., “structural resurrection” is observed. In Figure 6.56 P-Delta effects are introduced to the system subjected to the Loma Prieta ground motion. At lower intensities there is a marginal increase in the response when geometric stiffness is increased. For high values of geometric stiffness, the response decreases with P-Delta effects. In Figure 6.57, the results for the Northridge ground motion are presented. The response increases monotonically with the increase in geometric stiffness. But after the system attains elastic-perfectly-plastic state corresponding to a geometric

stiffness of 317 k/in., the system becomes unstable. For the Santa Monica ground motion in Figure 6.58, the system becomes unstable at a geometric stiffness of 350 k/in.

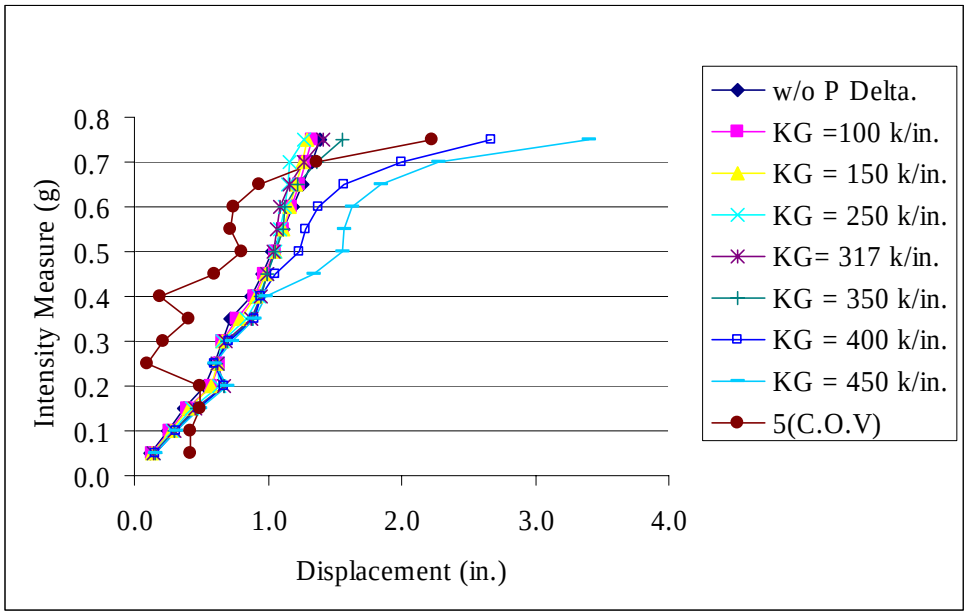

Fig. 6.54 IDA plots of peak displacement response for the Imperial Valley ground motion for variable geometric stiffness

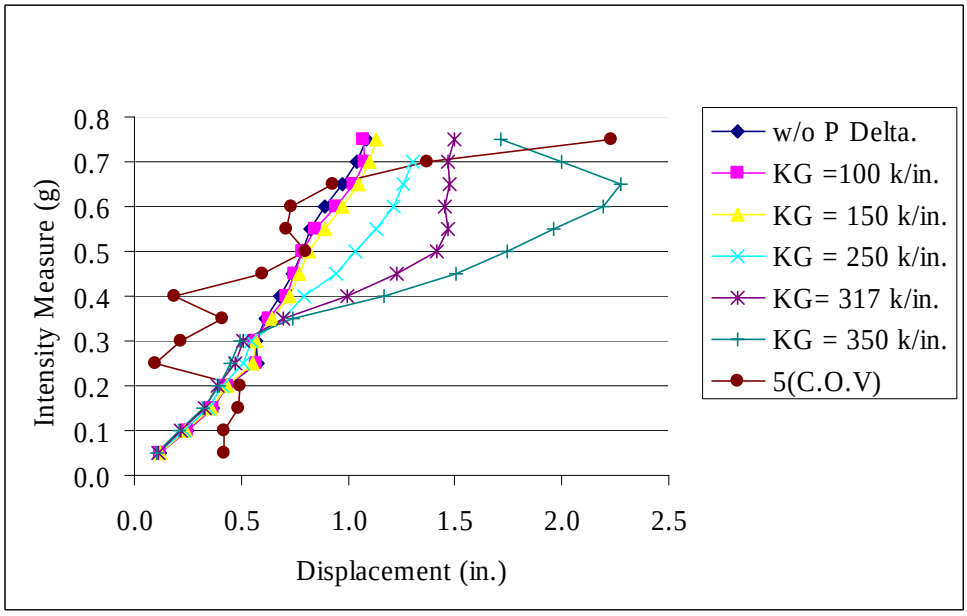

Fig. 6.55 IDA plots of peak displacement response for the Kern County ground motion for variable geometric stiffness

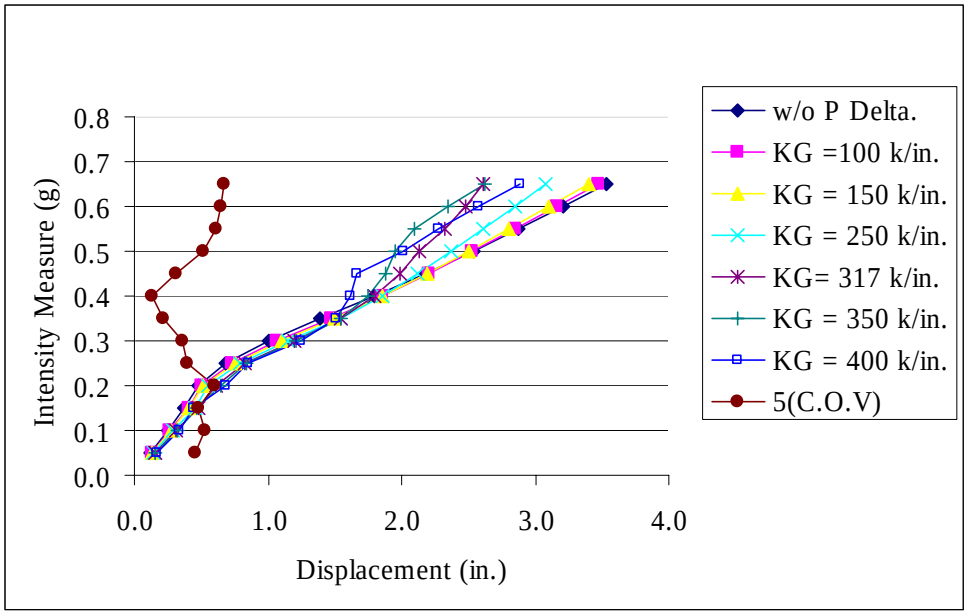

Fig. 6.56 IDA plots of peak displacement response for the Loma Prieta ground motion for variable geometric stiffness

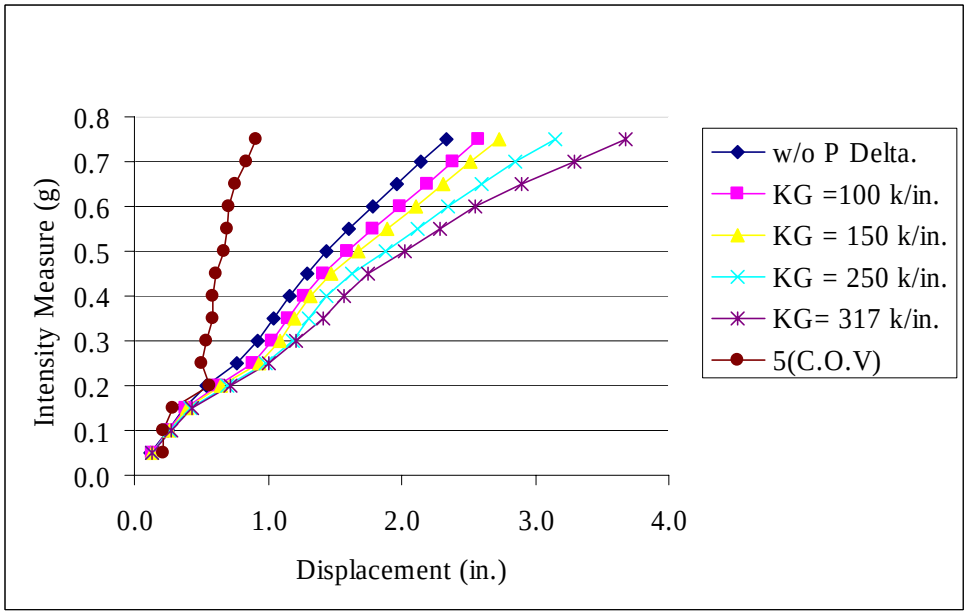

Fig. 6.57 IDA plots of peak displacement response for the Northridge ground motion for variable geometric stiffness

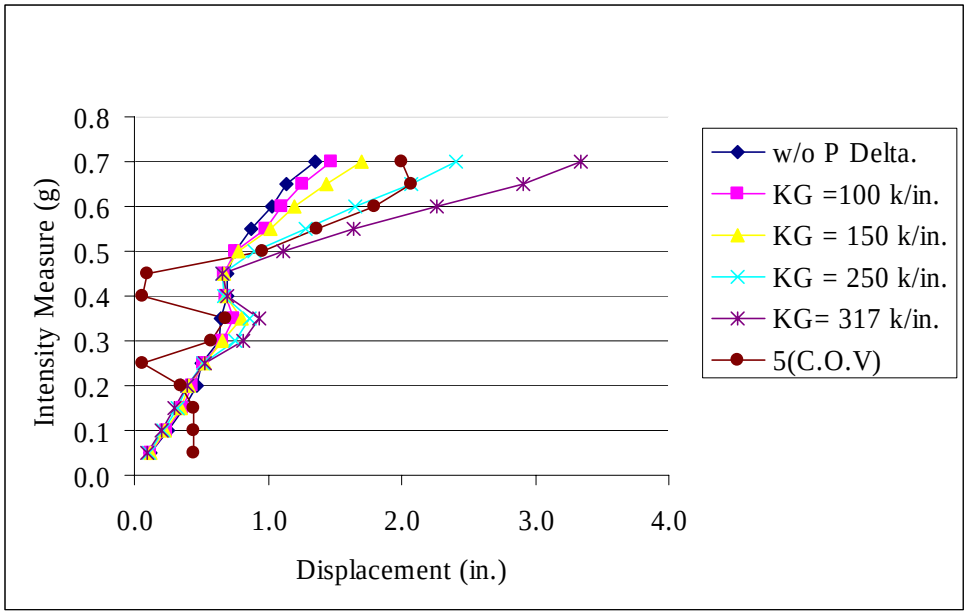

Fig. 6.58 IDA plots of peak displacement response for the Santa Monica ground motion for variable geometric stiffness

The multi-record IDA plots incorporating P-Delta effects are presented in Figures 6.59-6.61. In Figure 6.59 the curves correspond to a geometric stiffness of 250 k/in. The system remains stable for all the ground motions at higher levels of intensity. When the geometric stiffness is increased to 317 k/in. as in Figure 6.60, resulting in elastic-perfectly-plastic behavior, the response for all the ground motions increase at all levels of intensity. After an intensity level of 0.7 g is reached, the system becomes unstable for all the ground motions. Figure 6.61 contains the response when a geometric stiffness of 350 k/in. is applied to the system. The system becomes unstable at an intensity level of 0.65 g.

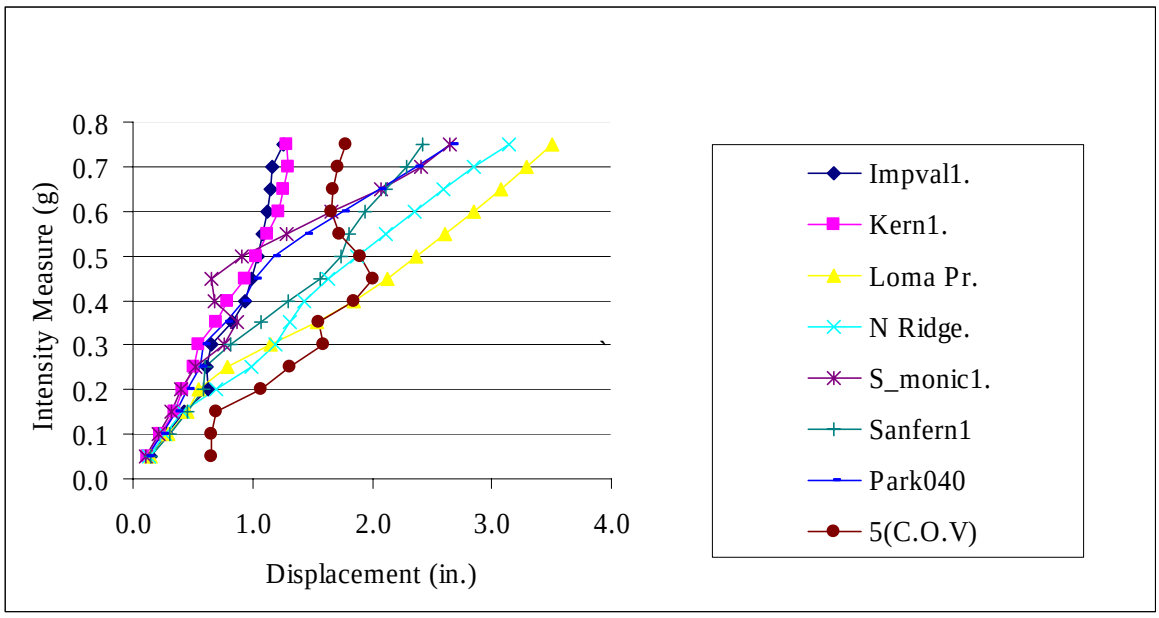

Fig. 6.59 Multi-record IDA plots of peak displacement response for different ground motion on the system subjected to geometric stiffness of 250 k/in.

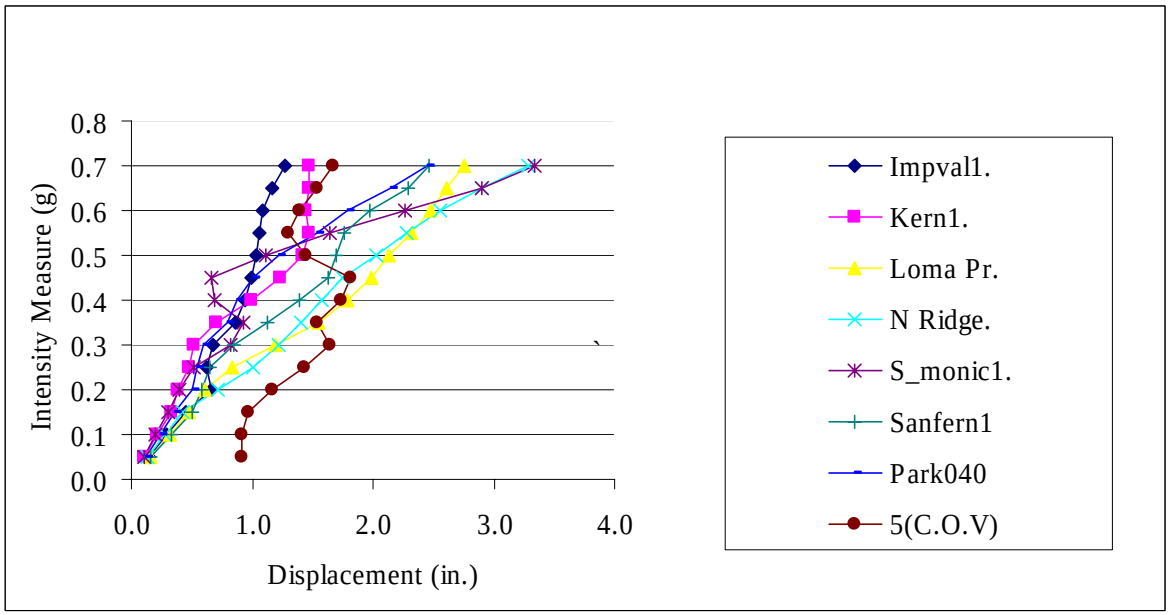

Fig. 6.60 Multi-record IDA plots of peak displacement response for different ground motion on the system subjected to geometric stiffness of 317 k/in.

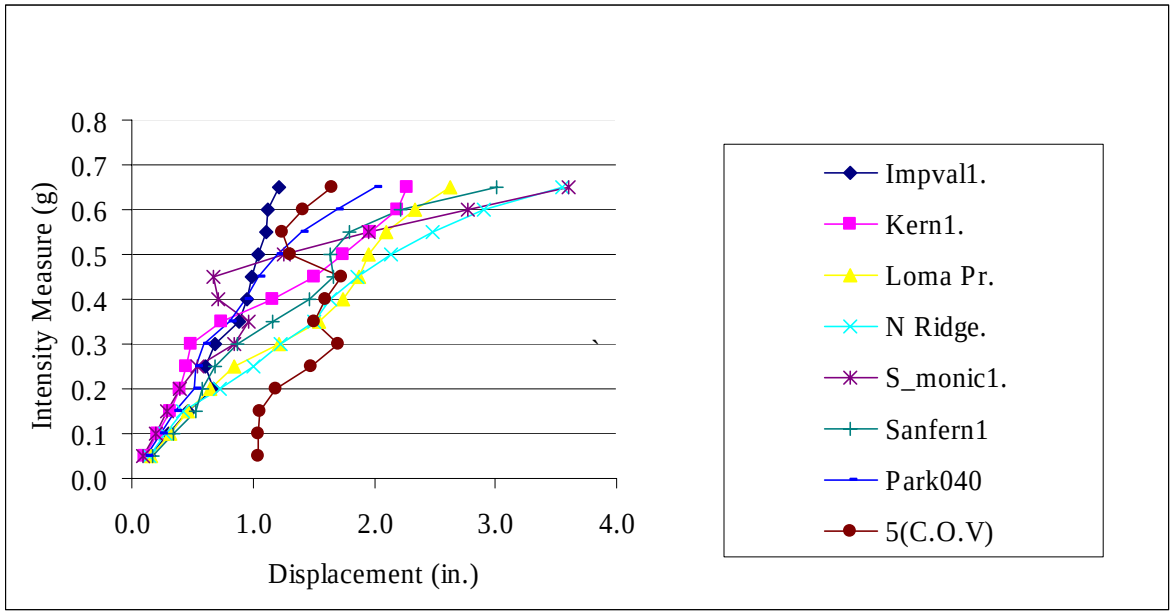

Fig. 6.61 Multi-record IDA plots of peak displacement response for different ground motion on the system subjected to geometric stiffness of 350 k/in.

The influence of P-Delta effects on the base shear is illustrated in Figures 6.62-6.66. The results for the Imperial Valley ground motion are shown in Figure 6.62. It is observed that an increase in the geometric stiffness decreases the base shear. There is a decrease till the system is elastic-perfectly-plastic. On further increasing the geometric stiffness, the base shear increases, but eventually the system becomes dynamically unstable. For the Kern County ground motion, in Figure 6.63 similar behavior is observed, but beyond a geometric stiffness of 350 k/in. the system becomes unstable. Figure 6.64 displays the IDA plots for the Loma Prieta ground motion. The base shear decreases with increase in the geometric stiffness till it reaches a value of 317 k/in. On further increasing the geometric stiffness, the base shear increases. The base shear for the Northridge ground motion is plotted in Figure 6.65. As in the previous cases, a similar behavior is observed. After the geometric stiffness reaches 350 k/in. the system becomes unstable. Figure 6.66 contains the IDA plot of the base shear for the same system subjected to the Santa Monica ground motion. The system becomes unstable after a geometric stiffness of 317 k/in. is attained, which corresponds to elastic-perfectly-plastic behavior.

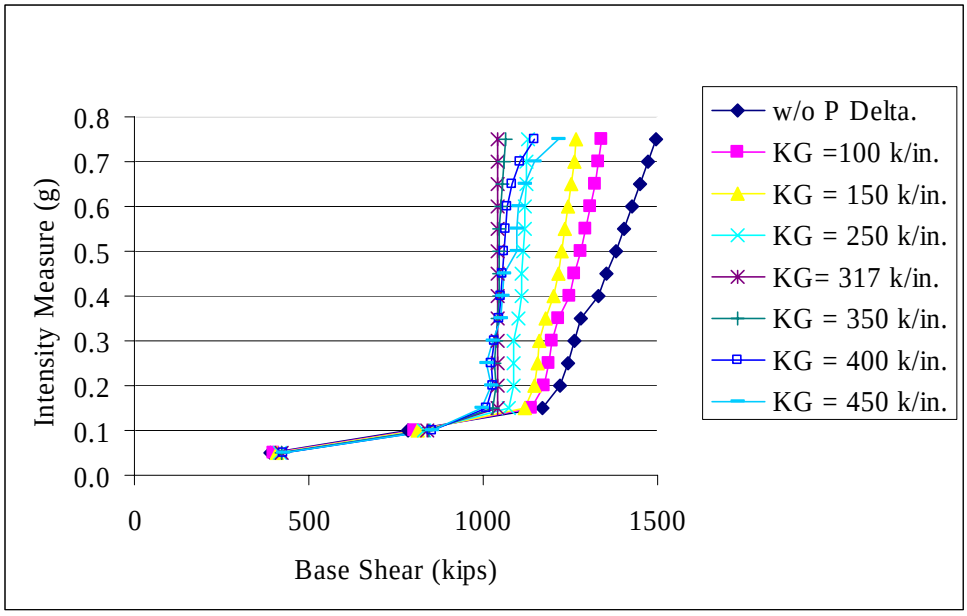

Fig. 6.62 IDA plots of base shear for the Imperial Valley ground motion for variable geometric stiffness

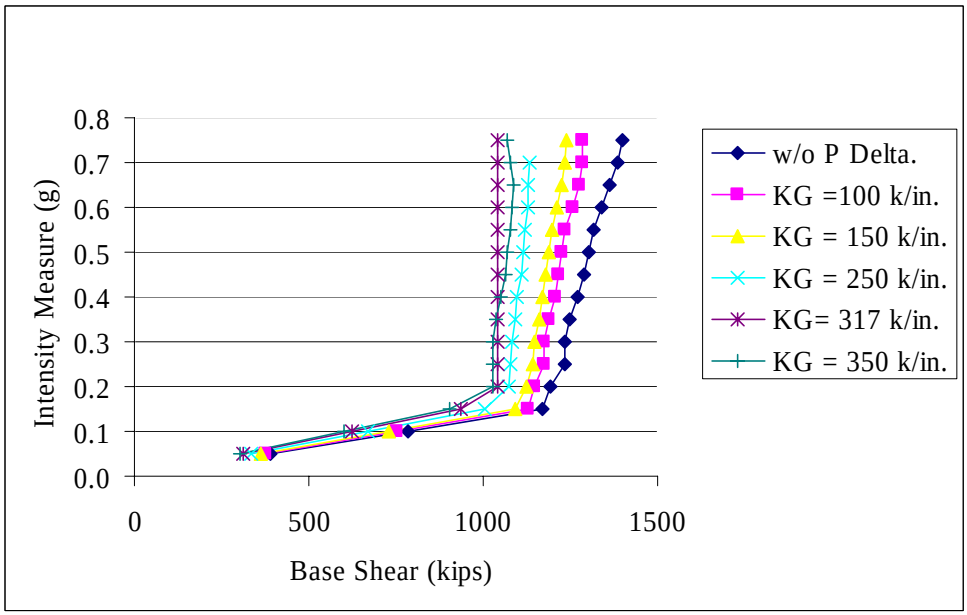

Fig. 6.63 IDA plots of base shear for the Kern County ground motion for variable geometric stiffness

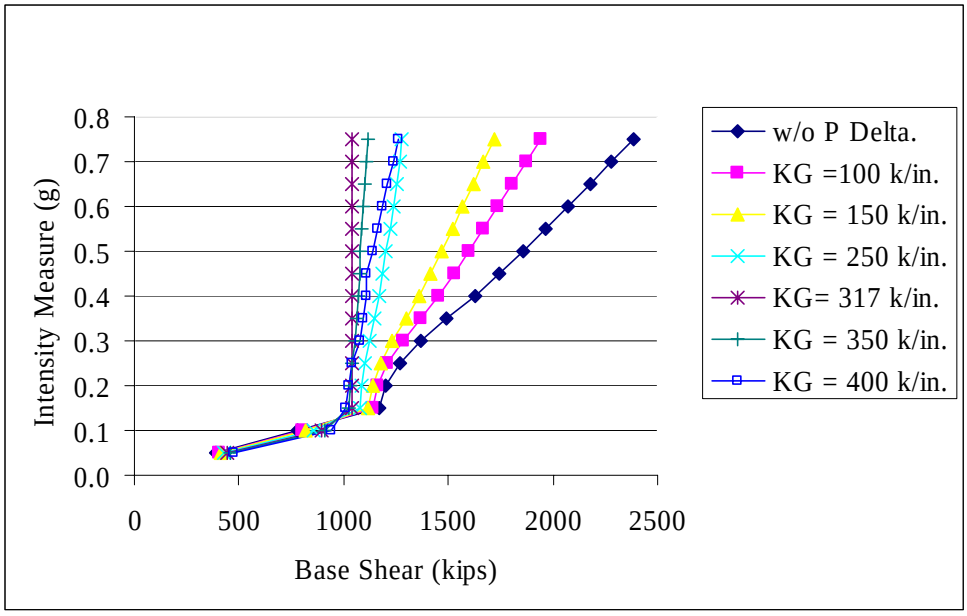

Fig. 6.64 IDA plots of base shear for the Loma Prieta ground motion for variable geometric stiffness

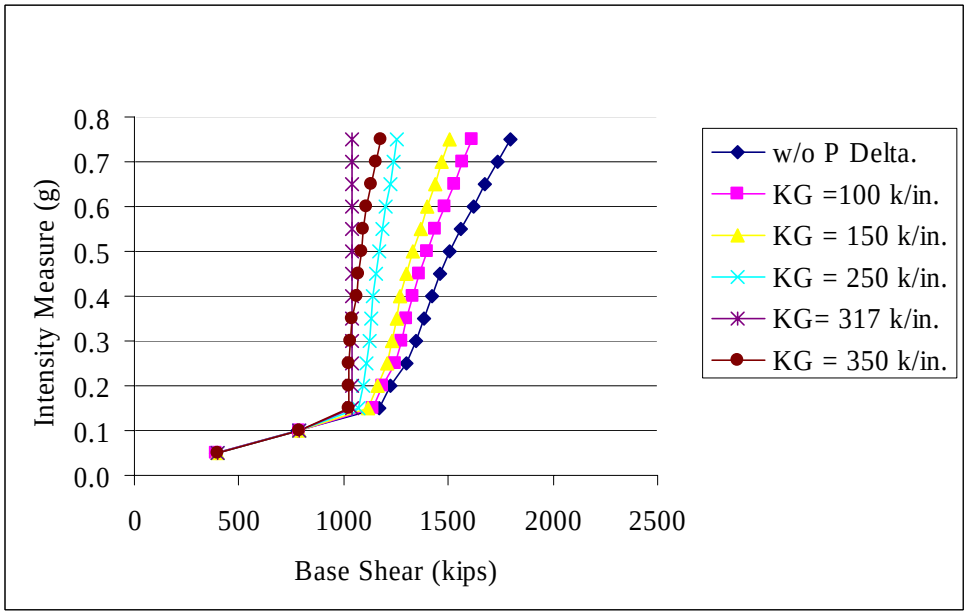

Fig. 6.65 IDA plots of base shear for the Northridge ground motion for variable geometric stiffness

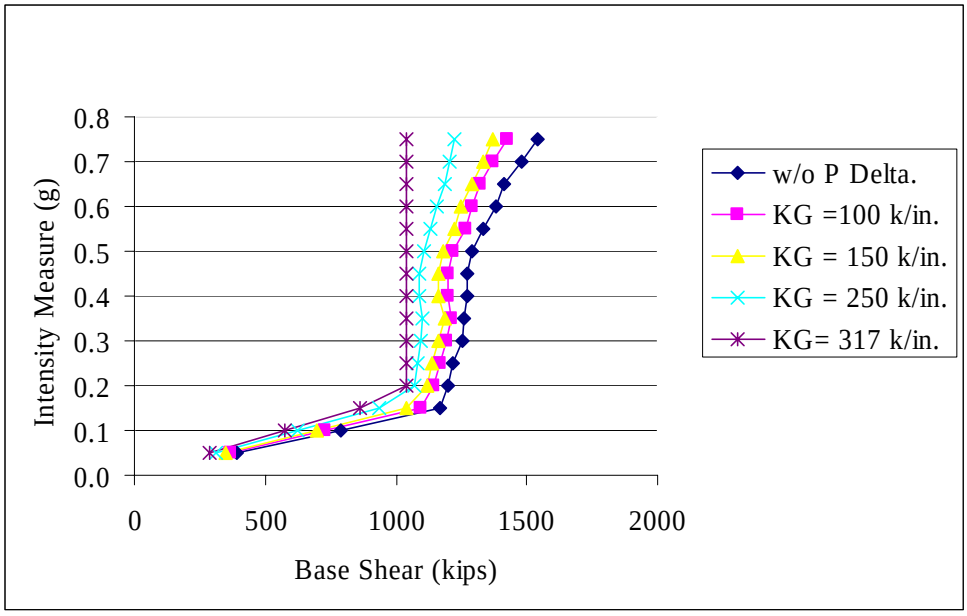

Fig. 6.66 IDA plots of base shear for the Santa Monica ground motion for variable geometric stiffness

The multi-record IDA curves corresponding to geometric stiffnesses of 250 k/in. and 350 k/in. are presented in Figure 6.67 and 6.68, respectively. When the geometric stiffness is equal to 250 k/in. the system does not become dynamically unstable at higher intensities. When it is increased to 350 k/in. and then analyzed, it is observed that the system becomes unstable at an intensity of 0.65g.

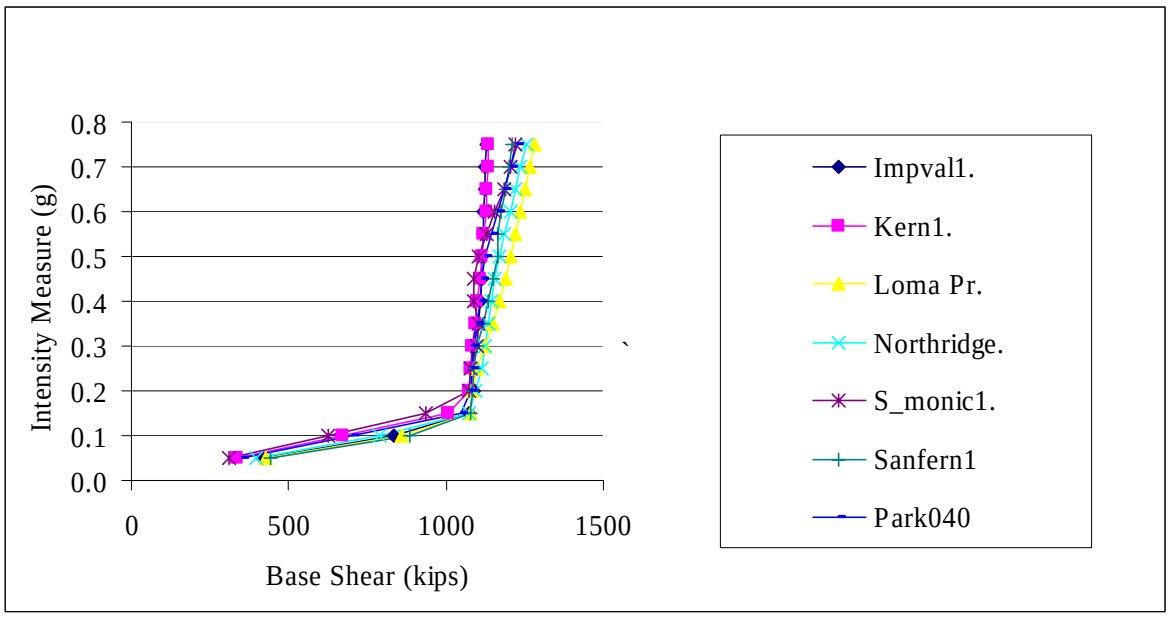

Fig. 6.67 Multi-record IDA plots of base shear for different ground motion on the system having geometric stiffness of 250 k/in.

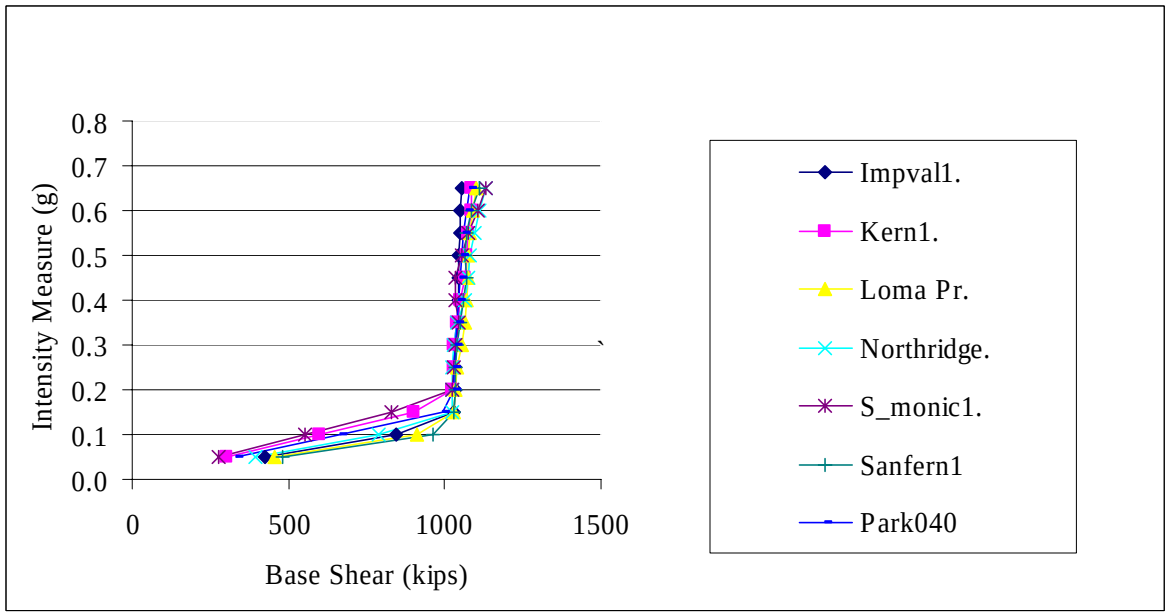

Fig. 6.68 Multi-record IDA plots of base shear for different ground motion on the system having geometric stiffness of 350 k/in.

7. Conclusions

7.1 Description of the procedure

This study was set up to determine the effect of ground motion and the systemic parameters on the structural response of a given single degree of freedom system. Incremental dynamic analysis was chosen for this purpose because it provides a disciplined approach for evaluating the structural response against monotonically scaled ground motions. The software used for performing the analysis was *NONLIN* version 7.03. The user friendly graphical interface of this software that enables the visualization of input and output was one of the reasons that this software was selected. All the results were obtained in spreadsheet format and they could be plotted as observed in the various graphs that have been presented in the previous chapters. The system that was used was a typical five-story office building modeled as a single degree of freedom system. The weight was 7800 k, damping was 5% of critical, primary stiffness was 3170 k/in, secondary stiffness was 317 k/in, and yield strength was 1170 k. Each of these parameters, with the exception of weight, was varied through a range of values. Each such system was subjected to a selected number of ground motions using the IDA procedure. An important issue that was resolved was whether it was required to update the scaling each time a parameter was varied. Based on a number of tests, it was decided to adopt scaling based on the median value of the parameter. The Median Scaling Method provided a suitable datum for comparing the results. The scaling was based on the condition that the pseudo-acceleration of the system must equal the spectral acceleration at the system's period of vibration and corresponding to 5% of critical damping. Single record IDA curves were plotted for various ground motions. The measure of dispersion that was used in this study was the coefficient of variation. For a particular parameter variation, if the coefficient of variation remains low most of the time, then it is an indication that the particular parameter is less sensitive.

7.2 Results

7.2.1 Rescaling

The primary stiffness is an important factor that affects the scaling. The values of primary stiffness used were 2770 k/in., 2970 k/in., 3170 k/in., 3370 k/in. and 3570 k/in. The first set of analysis was performed based on scaling corresponding to 3170 k/in. (median scaling), and the second set was based on scaling corresponding to the stiffness used (updated scaling). The shape of the IDA curves for most of the ground motions was consistent with respect to the stiffness-response relationship. Greater values of stiffness resulted in less displacement. The coefficient of variation was used as an index for measuring the dispersion. For some ground motions the coefficient of variation was greater for the updated scaling method than for the median scaling method, while in other cases the latter was greater than the former. In most cases the coefficient of variation was lower in the inelastic region if the Median Scaling Method was adopted. The response after yielding is considered more significant in this study. For some ground motions, however, the basic shape was not consistent from the stiffness-response perspective due to more dispersion when rescaling was done. Generally a trend towards convergence was recorded for most ground motions at higher intensities when the median scaling was adopted. Based on these observations, median scaling method was preferred for this study. A suitable datum was required for comparing the response due to variation of parameters. Scaling based on the median value of the parameter provided a means for comparing the response due to the variation of a particular parameter.

7.2.2 Variation in stiffness

The primary stiffness values used for this study were 2770 k/in., 2970 k/in., 3170 k/in., 3370 k/in. and 3570 k/in. The secondary stiffness used in combination with these was 10% of the original stiffness. Single-record IDA curves were obtained for five different ground motions. Multi-record IDA curves were also obtained using 2770 k/in., 3170 k/in. and 3570 k/in. for the stiffness. With the help of these analysis, results the following conclusions were reached:

(1) At a given intensity level, systems with greater stiffness do not always show lesser response. In the linearly elastic region, a stiffness-response inverse relationship holds. But in the inelastic region there is often a reversal of the trend.

(2) The yielding in the system can be identified at the first point where the slope changes. This marks the beginning of the hysteretic loops, and the coefficient of variation is greatest in the region where the first yielding of the system takes place. At higher levels of intensity, the coefficient of variation decreases, indicating a converging trend for the different systems.

(3) The scaling has a definite influence on the multi-record IDA curves. If the scaling is updated each time a parameter is varied and used for performing the analysis, the curves for different ground motions coincide in the linearly elastic region. However if the scaling is not consistent with the system's properties, then distinct curves are obtained in the linearly elastic region. To compare the response of various systems, the same scaling was retained in this study. It was observed that there was not a significant difference in the relative shape of the IDA curves in different cases. The response was magnified by some factor when the stiffness was decreased.

7.2.3 Variation in damping

Single record IDA curves were generated using 1%, 3%, 5%, 7% and 9% of critical damping. However the ground motion records were scaled based on 5% of critical damping. For multi-record IDA, seven ground motions were applied to systems having 1%, 5% and 9% of critical damping. The following conclusions could be drawn from the tests.

(1) With increase in damping, the response is reduced both in the elastic as well as the inelastic region. This is evident from the distinct nature of the IDA curves for various ground motions. The curves do not cross each other. An important observation was that the spring force decreases with increase in damping. However in some cases the base shear, comprising the sum of elastic and damping forces, increases with increase in damping in the inelastic region.

(2) On inspecting the multi-record IDA curves it is seen that at 1% of critical damping the ductility limit of a few systems has been exceeded. Hence the nature of the curves is different than at 5% of critical damping. At 9% of critical damping, the relative performance of the system remains the same between the ground motions as in 5% of critical damping, but there is an increase in the dispersion. Hence the system is sensitive to an increase in damping.

7.2.4 Variation in yield strength

The effect of variation of yield strength was observed by varying the yield strength of the system. The values used were 870 k, 970 k, 1070 k, 1170 k, 1270 k, 1370 k and 1470 k. From the graphs, the following observations can be noted:

(1) The coefficient of variation is the least among all the parameters. Hence this is the least sensitive parameter. In spite of the inherent variability in the nature of ground motion the systems with the least stiffness yield first. The systems that yielded first also showed lower post-yield response than other systems. However with respect to the 'elastic line' (IDA curve for linear analysis) all the curves were either to the left or the right of this line. The curves that are to the right of the elastic line have more potential for causing damage to the system since their response is less predictable.

(2) Using the "equal displacement concept", for the same level of response it was observed that in some cases systems having a lower value of the yield strength were able to resist a higher intensity of earthquake. The opposite trend was also recorded in some of the cases. Hence no definite conclusion can be drawn.

(3) From the multi-record IDA curves it can be observed that the basic shape of the curve is almost similar for the cases of F_y = 870k, F_y = 1170k and F_y = 1470k. The dispersion values decrease with increase in the yield strength. This is due to the fact that systems with higher values yield later. However the basic nature of the response is not affected.

7.2.5 Variation in geometric stiffness

The P-Delta effect also influences the response because it adds geometric nonlinearity to the system. Hence various values of the geometric stiffness were added to the system and tested with the ground motion records. The following observations were noted.

(1) For low values of geometric stiffness the response is not affected. But as the value is increased, dispersion increases at a greater rate till the system becomes dynamically unstable. Most systems become unstable when negative stiffness occurs due to the introduction of geometric nonlinearity. For some ground motions the system became unstable after the elastic-perfectly-plastic stage was attained. In other instances the system was able to sustain a certain degree of negative secondary stiffness.

(2) The base shear decreased as the geometric stiffness was increased till the system became elastic-perfectly-plastic. Then it started to increase for negative stiffness till the system became unstable.

7.3 Summary

Based on the analysis results, the following conclusions can be drawn for single degree of freedom systems subjected to incremental dynamic analysis:

(1) The response history of a system subjected to a particular ground motion is unique. Some trends may occur for most of the cases, but not always.

(2) Increasing the stiffness often results in lower peak displacement. But in the inelastic region this trend may be reversed. Maximum dispersion occurs at the yield point.

(3) Greater damping results in lower response. This occurs monotonically all along the intensity scale.

(4) Strength degradation does not affect the basic nature of the IDA curves. It is the least sensitive factor in the variation of the parameter study. Systems with lower yield strength always yield first.

(5) The response is affected by the value of the geometric stiffness. At lower values the response is not greatly affected. But increasing the geometric stiffness increases the peak response. This occurs until the system becomes dynamically unstable.

7.4 Limitations

The limitations of this study include:

(1) A limited number of ground motion records were used; in most cases 5 or 6 records were applied to the system.

(2) The range of variability of a particular parameter was limited.

(3) Peak response and base shear were the only factors that were used for the purpose of comparison.

(4) Coefficient of variation was the only measure used for determining the dispersion.

(5) Only a single model was tested.

(6) The base shear was taken approximately equal to the spring force for the study involving variation of stiffness, yield strength and geometric stiffness. Since the damping was taken equal to 5% of critical damping, this assumption can be justified. However when the variation of damping was studied, the total base force was recovered.

7.5 Recommendations for further research

The validity of these results can be verified by using different single degree of freedom systems subjected to incremental dynamic analysis. Many real world structures can be modeled as single degree of freedom systems, and single record and multi-record IDA curves for various ground motions can be generated. A wide variation of parameters can be used. In this study only one parameter was varied at a time. A combination of parameters can be varied at a time. This may help to optimize a structural system subjected to a particular ground motion. However such a combination might not work for a different ground motion. So only after subjecting a structure to an array of ground motion records, one might arrive at an acceptable combination of parameters. Such a system has to be economically feasible and also satisfy the serviceability requirements.

The scaling adopted in this study was based on the spectral acceleration at the system's period of vibration at 5% of critical damping. This is as suggested by Shome et al. (1998).

For the variation of parameter study, scaling corresponding to the median value of the parameter was adopted. This was based on lower dispersion in this case, hence it was concluded that median scaling serves as a suitable datum for comparing the results. This might not always be the case. The entire basis for comparison rests on the scale factor used for multiplying the ground motion records. Scaling is a very sensitive issue, and the results obtained and their interpretation must be correlated with the scaling procedure. Other ways of scaling need to be adopted for the variation of parameter study, and the results may provide us some insight. The shapes of the IDA curves for a few ground motions were similar, but for some of them they were very different. If the response could be correlated with the ground motion, then it would help to better predict of the response.

In this study the variation of hysteretic behavior on the response has not been included. This is a complex phenomenon involving degrading strength and degrading stiffness during each hysteretic loop. As discussed in section 3.3.1, the MDOF model in *NONLIN* is capable of modeling this behavior. This model needs to be first verified before using it for research purpose.

This study has been limited to only single degree of freedom systems. A variation of parameter study for multi-degree of freedom systems would be more useful for real structures. Although in most cases the first mode may dominate, interaction due to higher mode effects has a very important role in determining the response. For such a system there are lot of parameters that can be varied, e.g., as story stiffness, modal damping and their effects can be studied. The result of such a study might show some trends that may or may not be similar to those obtained for single degree of freedom systems. *NONLIN* has a three degree of freedom system that has a braced frame with a damper and an isolator. For a given frame, the damper and the isolator properties can be varied to produce an efficient system capable of resisting seismic effects. Variation of parameter studies making use of incremental dynamic analysis give an analytical technique that provides a method of measuring the system's demands at various levels of intensity. This tool can be used for designing a system. However the scope of its application to model real structures would be limited. Hence a

computer program capable of performing incremental dynamic analysis on multi-degree of freedom systems would be a very useful tool for evaluating existing structures for seismic effects. This would provide an alternative approach to the traditional Bin approach.

References

Abrahamson, N. A. and Silva, W. J. (1997), "Empirical response spectral attenuation relations for shallow crustal earthquakes", *Seismological Research Letters*, 68, 1, pp. 94-127.

Bonowitz, D., and Maison, B.F. (1998), "Are Steel Frames Safe? Probabilistic Seismic Evaluation of Existing WSMF Buildings", *Proceedings of the 6th U.S. National Conference on Earthquake Engineering*, Seattle, WA.

Bertero, V.V. (1977), "Strength and deformation capacities of buildings under extreme environments." *Structural Engineering and Structural Mechanics.* Pister, K.S. (ed.), Prentice Hall: Englewood Cliffs, NJ, pp. 211-215.

Chopra, A.K. (2001), *Dynamics of Structures: Theory and Applications to Earthquake Engineering.* Prentice Hall: Englewood Cliffs, NJ.

Charney, F.A. (1997), "NONLIN: A Computer Program for Earthquake Engineering Education." The EERC-CUREe Symposium in Honor of Vitelmo V. Bertero, Berkeley, California, Berkeley: Earthquake Engineering Research Center, University of California, pp. 251-254.

FEMA-273 (1996), NEHRP guidelines for the seismic rehabilitation of buildings. *Report No. FEMA-273*, SAC Joint Venture, Federal Emergency Management Agency, Washington, DC.

FEMA-350 (2000), Recommended seismic design criteria for new steel moment-frame buildings. *Report No. FEMA-350*, SAC Joint Venture, Federal Emergency Management Agency, Washington, DC.

Ghobarah, A. (2001), “Performance-based design in earthquake engineering: state of development”, *Engineering Structures* 23, pp. 878-884.

Mackie, K., and Stojadinovic, B. (2002), “Relation between Probabilistic Seismic Demand Analysis and Incremental Dynamic Analysis”, *Proceedings of the 7th U.S. National Conference on Earthquake Engineering*, Boston, MA.

Park, Y.J., Ang, A.H.S., and Wen, Y.K. (1985), “Seismic damage analysis of reinforced concrete buildings.” *Journal of Structural Engineering*, ASCE, 111, 4, pp. 740-757.

Park, Y.J., Reinhorn, A.M., and Kunnath, S.K. (1987), “IDARC: Inelastic Damage Analysis of Reinforced Concrete Frame – Shear-wall Structures ” *Technical report MCEER-87-008*, State University of New York at Buffalo.

Prakash, V., Powell, G.H., and Campbell, S. (1993), *DRAIN-2DX Base Program Description and User Guide: Version 1.10*. Department of Civil Engineering, University of California, Berkeley, CA.

SEAOC. Vision 2000 (1995) *Performance Based Seismic Engineering of Buildings - Volume I*, Vision 2000 Committee, Structural Engineers Association of California, Sacramento, CA.

Shome, N., Cornell, C.A., Bazzurro, P., and Carballo, J.E. (1998), “Earthquakes, Records and Nonlinear Responses”, *Earthquake Spectra*, 14, 3, pp. 469-498.

Sivaselvan, M.V. and Reinhorn, A.M. (1999), “Hysteretic models for cyclic behavior of deteriorating inelastic structures”, *Technical report MCEER-99-0018*, State University of New York at Buffalo.

UBC (1994) *Uniform Building Code*, International Conference on Building Officials, Whittier, CA.

Vamvatsikos, D. and Cornell, C.A. (2002), "Incremental Dynamic Analysis." *Earthquake Engineering and Structural Dynamics*, 31, 3, pp. 491-514.

Vamvatsikos, D. (2002), *Seismic Performance, Capacity, and Reliability of Structures as Seen Through Incremental Dynamic Analysis*, Ph.D. Dissertation, Department of Civil and Environmental Engineering, Stanford University, CA.

Appendix A. Verification of *NONLIN*

A.1 Introduction

The study was performed using *NONLIN* 7.03 (Charney, 1997). The reason for using *NONLIN* is that it has a user friendly graphical interface that allows the user to enter the input properties and perform the analysis. The results can be presented in an *MS-Excel* worksheet or as a variety of onscreen plots. The two basic models in *NONLIN* are single degree of freedom system and multiple degree of freedom system. The multiple degree freedom models can analyze a system having one, two or three degrees of freedom. The verification of the multiple degree of freedom system has been presented here. The results obtained from the single degree of freedom system were compared to those obtained using the multiple degree of freedom model having a single degree of freedom. The same single degree of freedom system was then used for performing IDA. The results of the nonlinear response history analysis from *NONLIN* were compared with those obtained using *DRAIN-2DX* (Prakash et al., 1993). *NONLIN* has six inbuilt models. Each model was analyzed for two sets of problems: one did not include geometric stiffness and the second one included the geometric stiffness. The in-built models in *NONLIN* save the user a significant amount of time by eliminating the need to build each model using various elements such as springs or rigid bars. In *DRAIN-2DX* one has to simulate each model correctly before proceeding ahead with the analysis.

A.2 Verification of one degree of freedom systems

The two single degree of freedom models are “simple frame” and “braced frame”. The “simple frame” consists of a rigid frame having only one degree of freedom along the horizontal direction parallel to the plane of the frame. Figure A.1 represents the “simple frame” as modeled in *DRAIN-2DX*. This model does not include the P-Delta effects. A description of the model and its various features is followed by a *DRAIN* input file containing the various commands that are required in order to replicate the model in *NONLIN*.

Model 1. Simple Frame (Single degree of freedom problem)

Problem parameters

Weight = 15.0 k

Initial Stiffness = 50.0 k/in.

Secondary Stiffness = 25.0 k/in.

Yield Strength = 15.0 k

Damping = 3.59 % of critical.

Ground Motion = Imperial Valley Earthquake (El Centro).

The model is replicated in *DRAIN* using a combination of truss and frame elements and rotational spring as in Figure A.1.

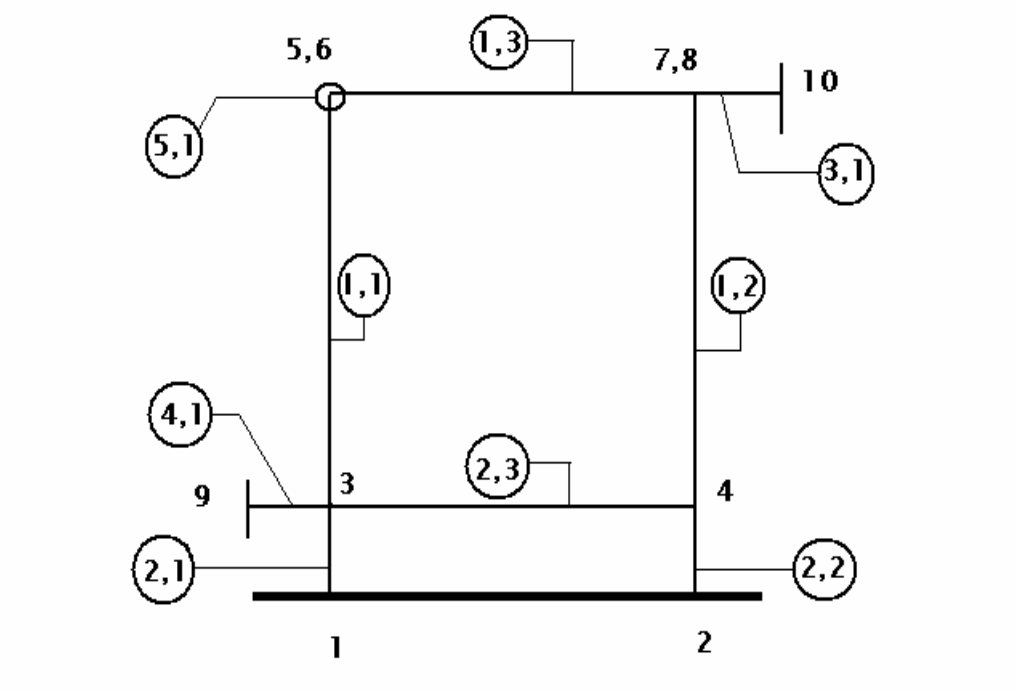

Fig A.1 "Simple Frame" created in *DRAIN 2-DX*

Description of the above model:

Joints 1, 2, 9, 10 have been restrained against vertical and horizontal movement and rotation.

Joints 3, 4, 5, 6, 7, 8 have their vertical degree of freedom restrained.

The horizontal degrees of freedom of joints 5 and 6 have been slaved. Similarly joints 7 and 8 are also required to have equal displacement in the horizontal direction.

The mass distributed to each of the two nodes 5 and 6 is given by Equation A.1:

$$\frac{15}{2(386.4)} = 0.0194 \text{ k.sec}^2/\text{in.} \qquad \text{A.1}$$

Members marked 1,1 1,2 1,3 are frame elements that are supposed to act only as rigid links; as such, the modulus of elasticity has been set to a high value of 1.0.E+10 ksi. For similar reasons, these members have been assigned a moment of inertia of 10000 in^4 and cross sectional area of 10000 in^2.

Members marked 2,1 2,2 and 2,3 are rigid truss bar elements having modulus of elasticity 1.0.E+10ksi and an area of 10.00 in^2.

The member marked 3,1 connected between 7 and 10 accounts for the damping of the frame.

The damping of the system is calculated as follows.

'm' is the mass of the system, 'k' is the stiffness, 'ω' is the circular frequency and 'c' is the damping constant.

$$m = \frac{15}{386.4} = 0.0388 \text{ k.sec}^2/\text{in.} \qquad \text{A.2}$$

$$\omega = \sqrt{\frac{k}{m}} = 35.898 \text{ rad/sec.} \qquad \text{A.3}$$

$$c = 2\omega m(0.0359) = 0.1 \qquad \text{A.4}$$

Member 3,1 is modeled in such a way that it does not contribute to the stiffness of the frame, but accounts for the damping. The stiffness of member 3,1 is given by

$$\frac{A.E}{L} = \frac{10(0.001)}{10} = 0.001 \text{ k/in.} \qquad \text{A.5}$$

The above expression is multiplied by 'β' to obtain the damping constant 'c' given by

$$c = \frac{\beta.A.E}{L} = 100(0.001) = 0.1 \qquad \text{A.6}$$

The member marked 4,1 between joints 9 and 3 takes into account the stiffness of the isolator. However in this example it is just another rigid link. This member is activated for problems involving a base isolator.

Member 5,1 between joints 5 and 6 is a plastic hinge that controls the stiffness properties of the frame.

Initial stiffness of frame = K = 50 k/in. (given)

Yield strength = F_y = 15 k (given)

Height of frame = H = 100 in.

Initial rotational stiffness of spring = $K_\theta = K(H^2)$= 50E+04 k.in/rad

Yield Strength = $F_y(H)$ = 1500 k.in.

The ratio of post yield stiffness to initial stiffness is specified to be 0.5.

The corresponding *DRAIN* file is shown below.

```
!UNITS L in F k   [Inserted by NonlinPro]
*STARTXX
  sm_fr1          0 1 0 1
!                      ^      Change to one to include P-Delta Effects
!============================================================
*NODECOORDS
C       1        0.0   -10.0
C       2      200.0   -10.0
C       3        0.0     0.0
C       4      200.0     0.0
C       5        0.0   100.0
C       6        0.0   100.0
C       7      200.0   100.0
C       8      200.0   100.0
C       9      -10.0     0.0
C      10      210.0   100.0
!============================================================
*RESTRAINTS
S 111         1
S 111         2
S 010         3
S 010         4
S 010         5
S 010         6
S 010         7
S 010         8
S 111         9
S 111        10
!============================================================
*SLAVING
S 100         5         6
S 100         7         8
!============================================================
```

```
*MASSES
S 100   0.01941        5                                    0.0000
S 100   0.01941        8
!================================================================
*ELEMENTGROUP
   2    0    0          0.00         Upper Columns and Beam (assumed rigid)
   1    0    1
   1 1.000E+10     0.010     10000     10000  4.0  4.0  2.0
   1    1  1.00E+10  1.00E+10
   1         3         5           1    0    1    1
   2         4         8           1    0    1    1
   3         6         7           1    0    1    1
!================================================================
*ELEMENTGROUP
   1    0    0          0.00         Isolator posts and base beam (assumed rigid)
   1
   1 1.000E+10       .50     10.00  1.00E+10  1.00E+10    0
   1         1         3           1
   2         2         4           1
   3         3         4           1
!================================================================
*ELEMENTGROUP
   1    0    0        100.000          Upper Skyhook damper
   1
   1      .001       .50     10.00  1.00E+10  1.00E+10    0
   1         7        10           1
!================================================================
*ELEMENTGROUP
   1    1    0          0.00         Isolator Device
   1
   1  100000.0       .30     10.00  1.00E+10  1.00E+10    0
   1         9         3           1
!================================================================
*ELEMENTGROUP
   4    1    0          0.00         Plastic hinge (stiff = h^^2 times lateral K)
   1
   1    50E+04       .50  1500.000  1500.000      0.10    3    0
   1         5         6           1
!================================================================
*RESULTS
NSD    010
NSV    010
NSA    010
E      010
```

```
!============================================================
*ACCNREC
 imp1    impval1.acn          (8F10.0)IMPERIAL VALLEY EARTHQUAKE - EL CENTRO
 2688    8    0    0      1.00   0.03937       .02      0.00
!============================================================
*MODE                          Modal Analysis
   2                0    0
!============================================================
*PARAMETERS
OD       0        0    2
DC  1    0    0    2
!============================================================
*ACCN                          Resp Hist
      20.050000    1    0.0005
1     imp1      1.00     1.000
!============================================================
*STOP
```

The same problem can be solved in *NONLIN* using the "Simple Frame" model. The excitation force is the Imperial Valley Earthquake. Table A.1 shows the results for the problem using *DRAIN-2DX* and by using *NONLIN* single degree of freedom model (SDOF) as well as multiple degree of freedom model (MDOF).

Table A.1 Comparison of the results for the "Simple Frame" model

Software	Timestep (sec)	Period of Vibration (sec)	Damping (% critical)
DRAIN-2DX	0.0005	0.175	3.59
NONLIN SDOF	0.0005	0.175	3.59
NONLIN MDOF	0.0005	0.175	3.59

		Displ (in.)	t (sec)	Vel (in./sec)	t (sec)	Accl (in./sec^2)	t (sec)
DRAIN-2DX	Max	0.243	4.94	8.09	4.89	287.23	4.86
	Min	-0.205	4.85	-7.43	2.30	-291.61	4.94
NONLIN SDOF	Max	0.242	4.94	7.82	4.90	292.37	4.86
	Min	-0.195	4.84	-7.47	2.30	-290.89	4.94
NONLIN MDOF	Max	0.240	4.96	7.96	4.92	288.06	4.88
	Min	-0.198	4.86	-7.36	2.32	-288.35	4.96

Comment: The structure does not yield in this case.

Model 2. Simple Frame (P-Delta effects included)

Problem parameters

Weight = 15.0 k.

Initial Stiffness = 15.0 k/in.

Secondary Stiffness = 0.0 k/in.

Geometric Stiffness = 1.0 k/in.

Yield Strength = 5.0 k

Damping = 3.59 % of critical.

Ground Motion = Imperial Valley Earthquake (El Centro).

For this problem “Simple Frame” model is selected and P-Delta option is activated in *NONLIN*. The height of the frame is entered as 15 in. to produce a geometric stiffness of 1 k/in. The model is replicated in *DRAIN* as shown in Figure A.2 using a combination of truss and frame elements and rotational spring.

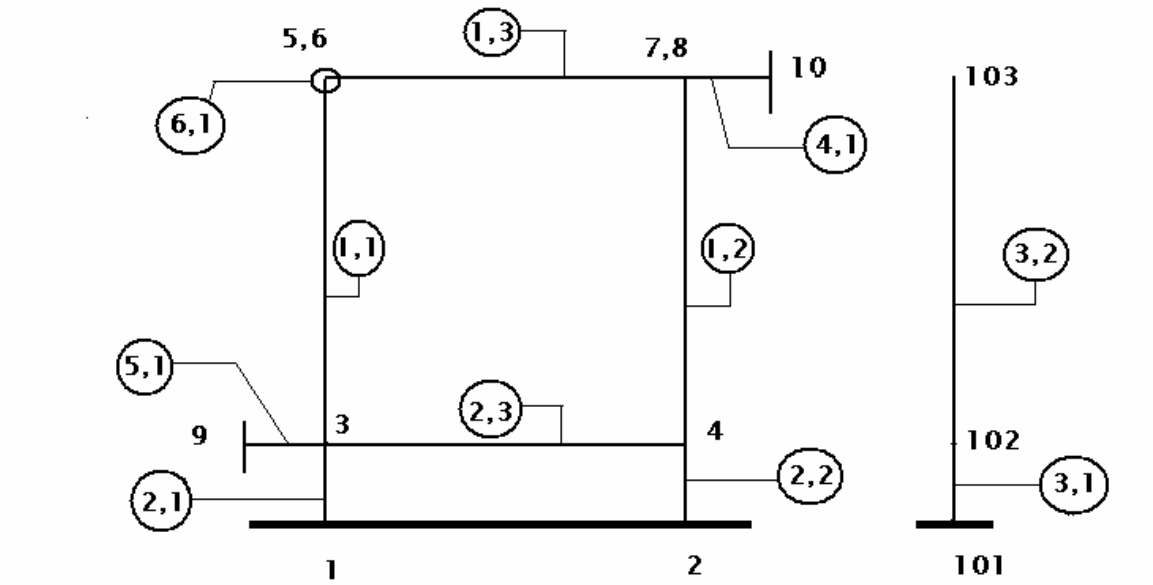

Fig A.2 "Simple Frame" with P-Delta effects created in *DRAIN 2-DX*

In this example three additional joints, 101, 102 and 103, have been added. 101 is a joint that is fixed to the ground. Joint 102 is restrained vertically and against rotation. Joint 103 is restrained only against rotation.

The horizontal degrees of freedom of joints 103 and 7 have been slaved. Members 3,1 and 3,2 are rigid elements that are added to take into account the P-Delta effect. The length of member 3,2 is 100 in., and a vertical downward load of 100 k is applied at joint 103 to result in a geometric stiffness of 1 k/in. The comparison of the results as obtained from *NONLIN* and *DRAIN* has been tabulated below in Table A.2.

Table A.2 Comparison of the results for the "Simple Frame" model with P-Delta Effects

Software	Timestep (sec)	Period of Vibration (sec)	Damping (% critical)
DRAIN-2DX	0.0005	0.331	3.176
NONLIN SDOF	0.0005	0.331	3.176
NONLIN MDOF	0.0005	0.330	3.176

		Displ (in.)	t (sec)	Vel (in./sec)	t (sec)	Accl (in./sec^2)	t (sec)
DRAIN-2DX	Max	2.020	14.00	9.31	2.25	188.36	2.20
	Min	-0.439	2.18	-8.14	2.42	-142.60	2.35
NONLIN SDOF	Max	2.780	26.40	9.30	2.26	189.46	2.20
	Min	-0.423	2.18	-8.17	2.42	-140.35	2.36
NONLIN MDOF	Max	1.850	26.40	9.16	2.28	188.96	2.22
	Min	-0.444	2.20	-8.20	2.44	-141.27	2.38

Comment: Due to the effect of geometric stiffness, the structure shows negative secondary stiffness after yielding.

Model 3. Braced Frame (Single degree of freedom problem)

Problem parameters

Weight = 15.0 k.

Initial Stiffness = 10.0 k/in.

Secondary Stiffness = 5.0 k/in.

Stiffness contributed by bracings = 5.0 k/in.

Yield Strength = 2.5 k.

Damping of frame = 5.00 % of critical.

Ground Motion = Imperial Valley Earthquake (El Centro).

For this problem “Braced Frame” model is selected from *NONLIN*. The model is replicated in *DRAIN* as in Figure A.3 using a combination of truss and frame elements and rotational spring. The structure has only one degree of freedom in the horizontal direction.

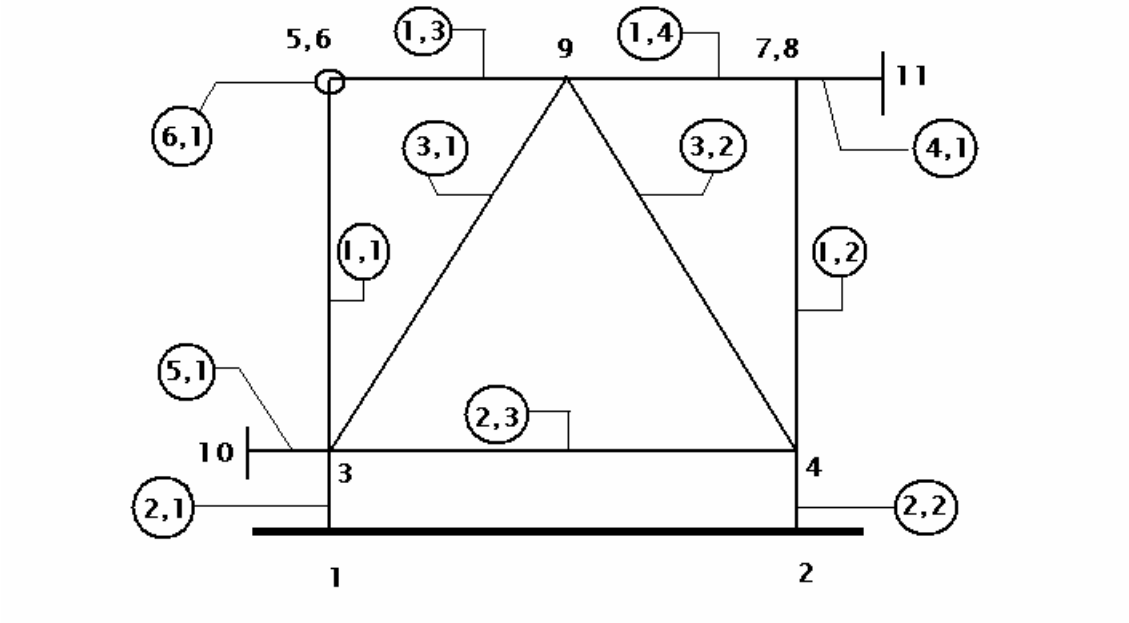

Fig A.3 "Braced Frame" created in *DRAIN 2-DX*

In the above model, the members marked 1,3 and 1,4 are frame elements connected between joints 6-9 and 9-7, respectively. Members 3,1 and 3,2 are truss bar elements; the combined stiffness in the horizontal direction is 5.0 k/in.

Combined stiffness is given by

$$\frac{2AE(\cos\theta)^2}{L} = \frac{2(141.4)(5)}{141.4}\left(\frac{1}{\sqrt{2}}\right)^2 = 5 \text{ k/in.} \qquad \text{A.7}$$

Apart from the bracing, the rest of the arrangement is the same as in the previous models. The bracing increases the stiffness of the model in the lateral direction.

The comparison of the results is presented in Table A.3.

Table A.3 Comparison of the results for the "Braced Frame" model

Software	Timestep (sec)	Period of Vibration (sec)	Damping (% critical)
DRAIN-2DX	0.0005	0.320	4.083
NONLIN MDOF	0.0005	0.319	4.082

		Displ (in.)	t (sec)	Vel (in./sec)	t (sec)	Accl (in./sec^2)	t (sec)
DRAIN-2DX	Max	0.639	4.55	10.38	2.25	213.97	2.44
	Min	-0.575	4.74	-11.21	2.41	-201.32	2.34
NONLIN MDOF	Max	0.628	4.56	10.19	2.26	215.33	2.46
	Min	-0.577	4.76	-11.06	2.44	-200.58	2.36

Comment: The structure yields with positive secondary stiffness

Model 4. Braced Frame (P-Delta effects included)

Problem parameters

Weight = 15.0 k.

Initial Stiffness = 10.0 k/in.

Secondary Stiffness = 5.0 k/in.

Stiffness contributed by bracings = 5.0 k/in.

Geometric Stiffness = 2.7272 k/in.

Yield Strength = 2.5 k.

Damping of frame = 5.00 % of critical.

Ground Motion = Imperial Valley Earthquake (El Centro).

For this problem “Braced Frame” model is used and P-Delta option is activated in *NONLIN*. The height of the frame is entered as 5.5 in. to produce a geometric stiffness of 2.72 k/in. The following illustration in Figure A.4 shows the *DRAIN* model.

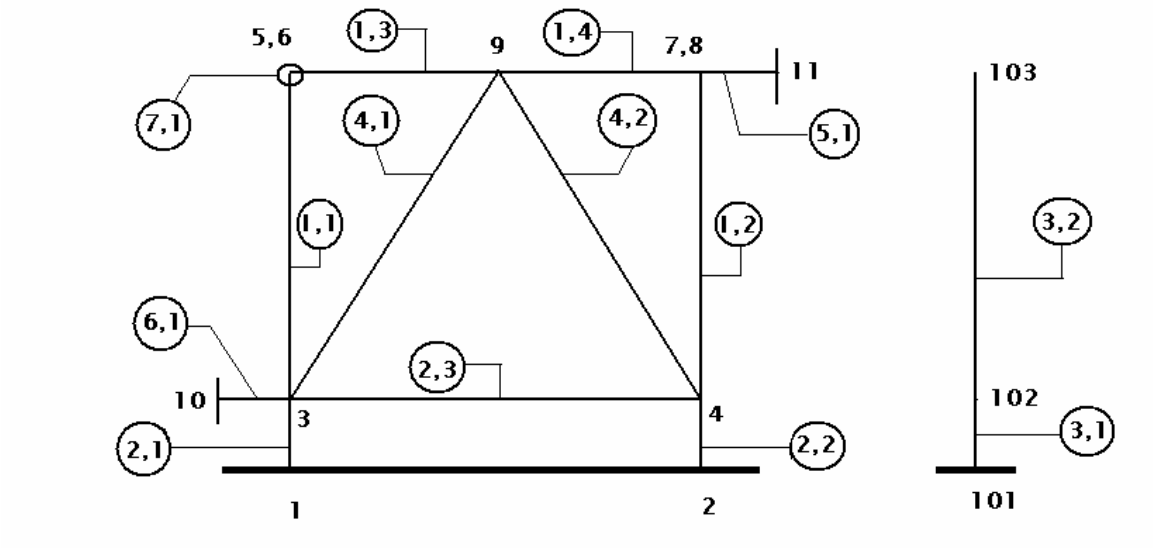

Fig A.4 "Braced Frame" with P-Delta effects created in *DRAIN 2-DX*

The height of member 3,2 is 100 in. and a vertical downward load of 272.72 k is applied at joint 103 in order to produce a geometric stiffness of 2.72 k/in. The analysis results are presented in Table A.4.

Table A.4 Comparison of the results for the "Braced Frame" model

Software	Timestep (sec)	Period of Vibration (sec)	Damping (% critical)
DRAIN-2DX	0.0005	0.3530	4.514
NONLIN MDOF	0.0005	0.3533	4.513

		Displ (in.)	t (sec)	Vel (in./sec)	t (sec)	Accl (in./sec^2)	t (sec)
DRAIN-2DX	Max	0.817	4.58	12.05	2.26	209.39	2.20
	Min	-0.707	4.80	-12.24	4.67	-202.30	2.36
NONLIN MDOF	Max	0.817	4.60	12.01	2.28	210.14	2.22
	Min	-0.707	482	-12.14	4.67	-202.30	2.36

Comment: Yielding occurs in the frame.

A.3 Verification of two degree of freedom systems

The three models having two degrees of freedom are “braced frame with device”, “isolated frame” and “isolated braced frame”. Each of these models has two mode shapes. Corresponding to each mode shape, the period of vibration and modal damping ratio are obtained. A comparison of these values is useful in establishing if the model is correctly set up. The maximum and minimum responses for each degree of freedom are also tabulated in order to complete the verification procedure.

Model 5. Braced Frame with device (Two degree of freedom problem)

Problem parameters

Properties of frame:

Weight = 15.0 k.

Initial Stiffness = 10.0 k/in.

Secondary Stiffness = 5.0 k/in.

Yield Strength = 2.5 k.

Damping of frame = 5.00 % of critical.

Properties of brace:

Stiffness contributed by bracings = 5.0 k/in.

Properties of device:

Weight = 1.0 k.

Initial Stiffness = 1.5 k/in.

Secondary stiffness = 0.78 k/in.

Yield Strength = 1.0 k.

Damping of device = 0.036

Ground Motion = Imperial Valley Earthquake (El Centro).

For this problem, “Braced Frame with device” model is selected.

The model is as shown in Figure A.5 replicated in *DRAIN* using a combination of truss and frame elements and rotational springs.

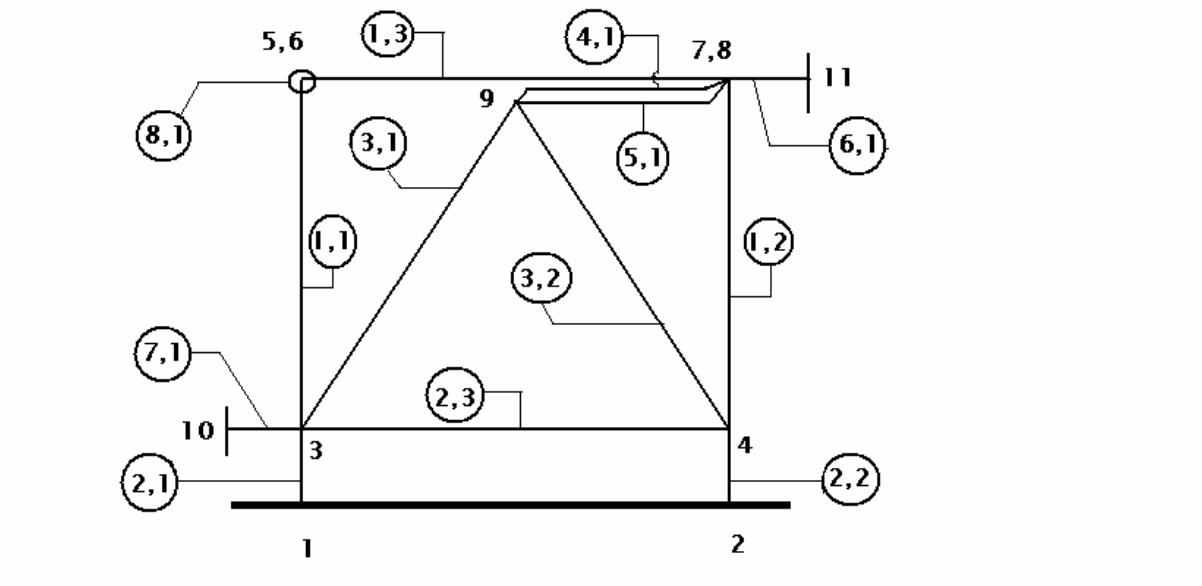

Fig A.5 “Braced Frame with device” created in *DRAIN 2-DX*

The "device" in the *NONLIN* model which accounts for internal passive damping is replaced in *DRAIN* by two members, 4-1 and 5-1, to take into account the stiffness and damping respectively. The mass of the device is applied at Joint 9, and it is restrained vertically and also against rotation.

For member 4-1, stiffness is calculated as in Equation A.8 where "A" is the cross sectional area, "E" is the modulus of elasticity and "L" is the length of the member:

$$\frac{A.E}{L} = \frac{100(1.5)}{100} = 1.5 \text{ k/in.} \qquad \text{A.8}$$

The damping of the device is contributed by member 5-1 and is given by Equation A.9. "β" is the multiplication factor to the stiffness term that results in the damping constant "c".

$$c = \frac{\beta.A.E}{L} = \frac{36(100)(0.001)}{100} = 0.036 \qquad \text{A.9}$$

The rest of the arrangement is the same as in previous models.

Table A.5 gives a comparison of the results as obtained in *DRAIN* and *NONLIN*.

Table A.5 Comparison of the results for the "Braced Frame with device" model

Software	Time-Step (sec)	Mode	System's Period of Vibration (sec)	Damping (% Critical)
DRAIN-2DX	0.0005	Mode No 1.	0.371	6.209
		Mode No 2.	0.125	14.301
NONLIN MDOF	0.0005	Mode No 1.	0.371	6.214
		Mode No 2.	0.125	14.300

Results for frame		Displ (in.)	t (sec)	Vel (in./sec)	t (sec)	Accl (in./sec^2)	t (sec)
DRAIN-2DX	Max	0.835	5.08	13.80	2.26	235.35	2.20
	Min	-0.941	2.17	-10.60	4.68	-203.84	2.37
NONLIN MDOF	Max	0.831	5.10	13.78	2.28	236.07	2.22
	Min	-0.936	2.18	-10.57	4.70	-201.91	2.40

Results for device		Displ (in.)	t (sec)	Vel (in./sec)	t (sec)	Accl (in./sec^2)	t (sec)
DRAIN-2DX	Max	0.248	5.05	5.21	2.21	149.32	2.44
	Min	-0.281	2.15	-3.70	4.67	-86.48	2.37
NONLIN MDOF	Max	0.245	5.06	5.01	2.24	150.29	2.46
	Min	-0.279	2.16	-3.59	4.68	-84.68	2.38

Comment: Yielding occurs in the frame. Device does not yield.

Model 6. Braced Frame with device (P-Delta effects included)

Problem parameters

Properties of frame:

Weight = 15.0 k.

Initial Stiffness = 10.0 k/in.

Secondary Stiffness = 5.0 k/in.

Geometric Stiffness = 1.0 k/in.

Yield Strength = 2.5 k.

Damping of frame = 5.00 % of critical.

Properties of brace:

Stiffness contributed by bracings = 5.0 k/in.

Properties of device:

Weight = 1.0 k.

Initial Stiffness = 1.5 k/in.

Secondary stiffness = 0.78 k/in.

Yield Strength = 1.0 k.

Damping of device = 0.036

Ground Motion = Imperial Valley Earthquake (El Centro).

For this problem, "Braced Frame with device" model is selected and P-Delta effects are included. The model in *DRAIN* is as shown in Figure A.6. All the properties are exactly the same as in Model 5, however the horizontal degree of freedom of joint 103 is slaved with joint 7. Members 3,1 and 3,2 are rigid bars. A load of 100 k is applied on joint 103 vertically downward to produce a geometric stiffness of 1.0 k/in. The vertical degree of freedom of joint 102 is restrained so that a contribution to P-Delta effects occurs only from member 3,2.

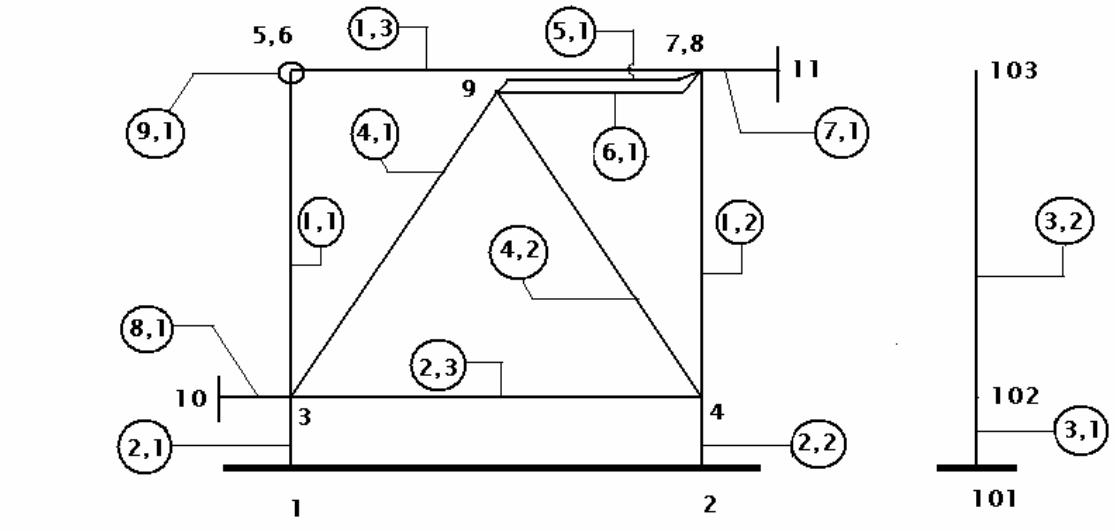

Fig A.6 "Braced Frame with device" having P-Delta effects created in *DRAIN 2-DX*

The results for the analysis are presented in Table A.6.

Table A.6 Comparison of the results for the "Braced Frame with device" model

Software	Time-Step (sec)	Mode	System's Period of Vibration (sec)	Damping (% Critical)
DRAIN-2DX	0.0005	Mode No 1.	0.389	6.526
		Mode No 2.	0.125	14.300
NONLIN MDOF	0.0005	Mode No 1.	0.389	6.522
		Mode No 2.	0.125	14.297

Results for frame		Displ (in.)	t (sec)	Vel (in./sec)	t (sec)	Accl (in./sec^2)	t (sec)
DRAIN-2DX	Max	0.911	5.11	15.16	2.28	266.12	2.20
	Min	-1.260	2.18	-9.72	4.68	-211.73	2.40
NONLIN MDOF	Max	0.894	5.12	15.14	2.30	266.97	2.22
	Min	-1.270	2.20	-9.73	4.70	-210.93	2.42

Results for device		Displ (in.)	t (sec)	Vel (in./sec)	t (sec)	Accl (in./sec^2)	t (sec)
DRAIN-2DX	Max	0.252	2.37	5.10	2.21	153.49	2.44
	Min	-0.347	2.15	-3.44	4.67	-111.03	2.37
NONLIN MDOF	Max	0.248	2.38	4.81	2.22	154.23	2.46
	Min	-0.346	2.16	-3.28	4.68	-107.56	2.38

Comment: Yielding occurs in the frame and the device.

Model 7. Isolated Frame (Two degree of freedom problem)

Problem parameters

Properties of frame:

Weight = 15.0 k.

Initial Stiffness = 10.0 k/in.

Secondary Stiffness = 5.0 k/in.

Yield Strength = 2.5 k.

Damping of frame = 5.00 % of critical.

Properties of isolator:

Weight = 5.0 k.

Initial Stiffness = 5.0 k/in.

Secondary stiffness = 2.5 k/in.

Yield Strength = 4.0 k.

Damping of isolator = 0.024

Ground Motion = Imperial Valley Earthquake – El Centro.

For this problem "Isolated Frame" model is selected from the various models available in *NONLIN*. The corresponding model in *DRAIN* is as shown in Figure A.7. The two degrees of freedom correspond to the frame and the isolator, respectively. In this model 4,1 and 5,1 represent the stiffness properties and damping of the isolator. Member 2,3 is a rigid bar as in the previous models. The mass of the isolator distributed to each of the two nodes 3 and 4 is given by the following expression:

$$m = \frac{5}{2.(386.4)} = 0.006469 \text{ k.sec}^2/\text{in.} \qquad \text{A.10}$$

The member 4,1 accounts for the stiffness of the isolator. This member is modeled with the help of a truss bar. The damping of the isolator is modeled with the help of member 5,1.

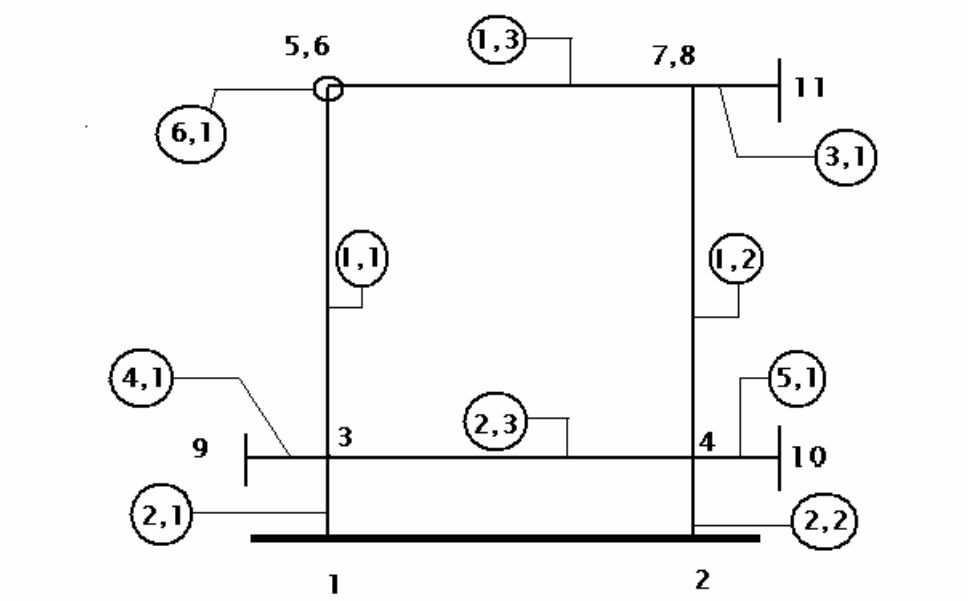

Fig A.7 "Isolated Frame" created in *DRAIN 2-DX*

The analysis results given by the two softwares are as shown in Table A.7.

Table A.7 Comparison of the results for the "Isolated Frame" model

Software	Time-Step (sec)	Mode	System's Period of Vibration (sec)	Damping (% Critical)
DRAIN-2DX	0.0005	Mode No 1.	0.730	9.528
		Mode No 2.	0.171	2.482
NONLIN MDOF	0.0005	Mode No 1.	0.729	9.530
		Mode No 2.	0.171	2.480

Results for frame		Displ (in.)	t (sec)	Vel (in./sec)	t (sec)	Accl (in./sec^2)	t (sec)
DRAIN-2DX	Max	2.060	2.78	15.42	2.52	222.52	2.24
	Min	-2.320	2.29	-23.36	2.16	-178.25	2.01
NONLIN MDOF	Max	2.040	2.80	15.42	2.54	223.37	2.26
	Min	-2.330	2.32	-23.38	2.18	-176.76	2.02

Results for isolator		Displ (in.)	t (sec)	Vel (in./sec)	t (sec)	Accl (in./sec^2)	t (sec)
DRAIN-2DX	Max	1.480	2.75	11.90	12.11	217.29	4.86
	Min	-1.470	2.33	-16.85	2.13	-177.72	5.37
NONLIN MDOF	Max	1.470	2.78	11.87	12.14	218.29	4.88
	Min	-1.480	2.36	-16.79	2.16	-173.41	5.40

Comment: Yielding occurs in the frame and the isolator.

Model 8. Isolated Frame (P-Delta effects included)

Problem parameters

Properties of frame:

Weight = 15.0 k.

Initial Stiffness = 8.0 k/in.

Secondary Stiffness = 1.0 k/in.

Yield Strength = 2.5 k.

Damping of frame = 5.00 % of critical.

Height of frame = 25 in.

Properties of isolator:

Weight = 5.0 k.

Initial Stiffness = 5.0 k/in.

Secondary stiffness = 2.5 k/in.

Yield Strength = 4.0 k.

Damping of device = 0.024

Height of isolator = 15 in.

Ground Motion = Imperial Valley Earthquake (El Centro).

For this problem, the P Delta option is activated in *NONLIN*. The height of frame and isolator are taken as 25 in. and 15 in., respectively in the *DRAIN* model in Figure A.8. In this model, joint 102 has a vertical degree of freedom to allow for P Delta effects in the isolator. The horizontal degrees of freedom of joints 7 and 103 are slaved, similarly, 4 and 102 have also been slaved.

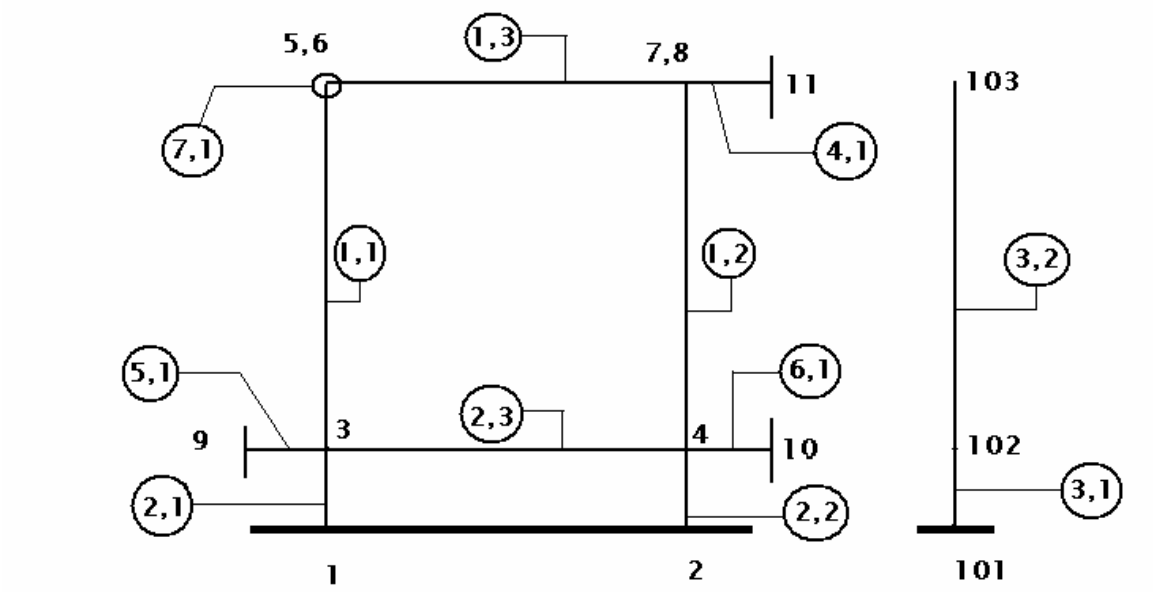

Fig A.8 "Isolated Frame" created in *DRAIN 2-DX*

The analysis results have been tabulated in Table A.8.

Table A.8 Comparison of the results for the "Isolated Frame" model

Software	Time-Step (sec)	Mode	System's Period of Vibration (sec)	Damping (% Critical)
DRAIN-2DX	0.0005	Mode No 1.	0.851	10.100
		Mode No 2.	0.200	2.849
NONLIN MDOF	0.0005	Mode No 1.	0.851	10.136
		Mode No 2.	0.199	2.847

Results for frame		Displ (in.)	t (sec)	Vel (in./sec)	t (sec)	Accl (in./sec^2)	t (sec)
DRAIN-2DX	Max	2.080	5.41	14.67	4.56	171.73	2.20
	Min	-2.360	12.00	-20.46	2.16	-170.12	2.08
NONLIN MDOF	Max	2.000	2.04	14.67	4.58	172.14	2.22
	Min	-2.490	12.02	-20.50	2.58	-169.58	2.10

Results for isolator		Displ (in.)	t (sec)	Vel (in./sec)	t (sec)	Accl (in./sec^2)	t (sec)
DRAIN-2DX	Max	1.330	2.78	10.57	12.22	152.05	2.44
	Min	-1.410	11.96	-11.48	2.17	-136.23	4.66
NONLIN MDOF	Max	1.320	2.00	10.59	12.24	149.64	2.46
	Min	-1.430	11.93	-11.24	2.18	-135.21	4.68

Comment: In this example yielding occurs in the frame as well as the isolator.

Model 9. Isolated Braced Frame (Two degree of freedom problem)

Problem parameters

Properties of frame:

Weight = 15.0 k.

Initial Stiffness = 8.0 k/in.

Secondary Stiffness = 1.0 k/in.

Yield Strength = 2.5 k.

Damping of frame = 5.00 % of critical.

Properties of brace:

Stiffness contributed by bracings = 50.0 k/in.

Properties of isolator:

Weight = 5.0 k.

Initial Stiffness = 5.0 k/in.

Secondary stiffness = 2.5 k/in.

Yield Strength = 4.0 k.

Damping of device = 0.024

Ground Motion = Imperial Valley Earthquake (El Centro).

For this problem, “Isolated Braced Frame” model has been selected from the various MDOF models available in *NONLIN*. This model is similar to the “Isolated Frame”; the bracing contributes to the horizontal stiffness of the frame. Figure A.9 illustrates the modeling of the system in *DRAIN-2DX*. Joint 9 at the top of the bracings has been restrained against vertical movement and rotation. Member 1,3 and 1,4 are rigid frame elements connected between joints 6 and 9 and joints 9 and 7, respectively.

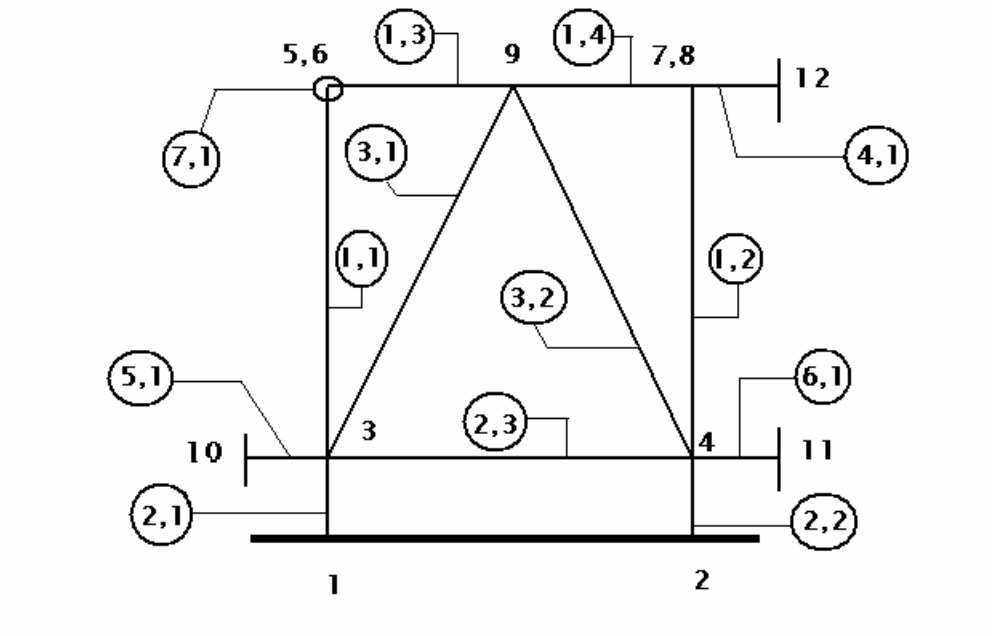

Fig A.9 "Isolated Braced Frame" created in *DRAIN 2-DX*

The comparison of the results between *DRAIN* and *NONLIN* is presented in Table A.9.

Table A.9 Comparison of the results for the "Isolated Braced Frame" model

Software	Time-Step (sec)	Mode	System's Period of Vibration (sec)	Damping (% Critical)
DRAIN-2DX	0.0005	Mode No 1.	0.6550	7.973
		Mode No 2.	0.0793	1.110
NONLIN MDOF	0.0005	Mode No 1.	0.6548	7.976
		Mode No 2.	0.0793	1.110

Results for frame		Displ (in.)	t (sec)	Vel (in./sec)	t (sec)	Accl (in./sec^2)	t (sec)
DRAIN-2DX	Max	1.880	1.96	14.05	2.28	254.29	2.20
	Min	-2.350	2.28	-22.25	2.14	-177.26	2.01
NONLIN MDOF	Max	1.870	1.98	14.03	2.50	255.31	2.22
	Min	-2.360	2.30	-22.25	2.16	-175.82	2.02

Results for isolator		Displ (in.)	t (sec)	Vel (in./sec)	t (sec)	Accl (in./sec^2)	t (sec)
DRAIN-2DX	Max	1.880	1.96	14.05	2.48	254.29	2.20
	Min	-2.350	2.28	-22.25	2.14	-177.26	2.01
NONLIN MDOF	Max	1.790	1.98	14.30	2.52	265.74	2.26
	Min	-2.250	2.30	-22.34	2.16	-175.11	2.00

Comment: Isolator yields, but no yielding takes place in the frame.

Model 10. Isolated Braced Frame (P-Delta effects included)

Problem parameters

Properties of frame:

Weight = 10.0 k.

Initial Stiffness = 6.0 k/in.

Secondary Stiffness = 0.0 k/in.

Yield Strength = 0.25 k.

Damping of frame = 5.00 % of critical.

Height of frame = 75 in.

Properties of brace:

Stiffness contributed by bracings = 50.0 k/in.

Properties of isolator:

Weight = 5.0 k.

Initial Stiffness = 5.0 k/in.

Secondary stiffness = 1.0 k/in.

Yield Strength = 4.0 k.

Damping of device = 0.024.

Height of isolator = 35 in.

Ground Motion = Imperial Valley Earthquake (El Centro).

For this example, P-Delta effects are included. The model in Figure A.10 is generated in *DRAIN* to compare the results obtained from *NONLIN*. This model is exactly similar to the "Isolated Frame" with P-Delta effects, but this has bracing which also contributes to the lateral stiffness of the frame.

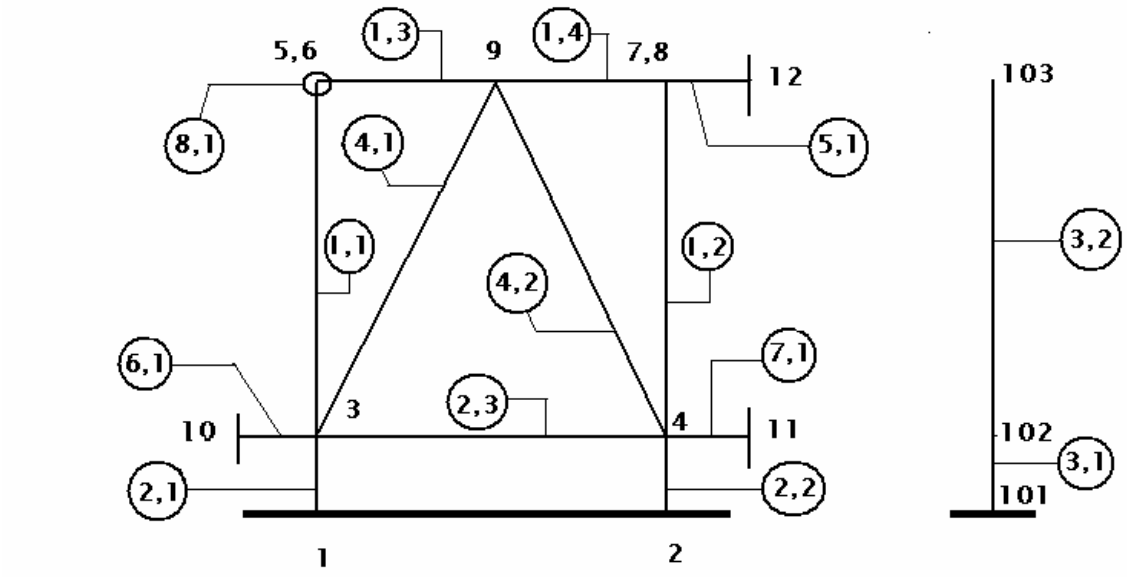

Fig A.10 "Isolated Braced Frame" with P Delta effects created in *DRAIN 2-DX*

After analysis, the results given by the two programs have been tabulated below in Table A.10.

Table A.10 Comparison of the results for the "Isolated Braced Frame" model

Software	Time-Step (sec)	Mode	System's Period of Vibration (sec)	Damping (% Critical)
DRAIN-2DX	0.0005	Mode No 1.	0.5900	7.630
		Mode No 2.	0.0784	1.085
NONLIN MDOF	0.0005	Mode No 1.	0.5890	7.626
		Mode No 2.	0.0767	1.069

Results for frame		Displ (in.)	t (sec)	Vel (in./sec)	t (sec)	Accl (in./sec^2)	t (sec)
DRAIN-2DX	Max	1.940	1.96	14.22	1.78	221.34	2.20
	Min	-1.610	2.27	-18.27	2.13	-165.79	4.66
NONLIN MDOF	Max	1.920	1.98	14.18	1.80	222.84	2.22
	Min	-1.640	2.28	-18.23	2.14	-165.15	4.68

Results for isolator		Displ (in.)	t (sec)	Vel (in./sec)	t (sec)	Accl (in./sec^2)	t (sec)
DRAIN-2DX	Max	1.900	1.95	13.49	1.78	201.04	2.24
	Min	-1.560	2.27	-18.43	2.14	-162.79	2.02
NONLIN MDOF	Max	1.870	1.98	13.42	1.80	203.02	2.26
	Min	-1.580	2.28	-18.44	2.16	-161.27	2.04

Comment: After incorporating the P-Delta effects, negative stiffness occurs in the frame.

A.4 Verification of three degree of freedom systems

"Isolated Braced Frame with Device" is the most general problem that can be solved using the MDOF model in *NONLIN*. This model has three degrees of freedom. There are three corresponding mode shapes, periods of vibration and modal damping ratios. A comparison of these values is useful in establishing if the model is correctly set up. The maximum and minimum responses for each degree of freedom are also tabulated in order to complete the verification procedure.

Model 11.

Isolated Braced Frame with Device (Three degree of freedom problem)

Problem parameters

Properties of frame:

Weight = 15.0 k.

Initial Stiffness = 4.5 k/in.

Secondary Stiffness = 1.0 k/in.

Yield Strength = 1.4 k.

Damping of frame = 3.59 % of critical.

Properties of brace:

Stiffness contributed by bracings = 50.0 k/in.

Properties of device:

Weight = 0.5 k.

Initial Stiffness = 3.0 k/in.

Secondary stiffness = 1.0 k/in.

Yield Strength = 0.75 k.

Damping of device = 0.025.

Properties of isolator:

Weight = 1.8 k.

Initial Stiffness = 3.0 k/in.

Secondary stiffness = 1.0 k/in.

Yield Strength = 1.8 k.

Damping of device = 0.025.

Ground Motion = Imperial Valley Earthquake (El Centro).

This is a three degree of freedom problem. The *DRAIN* model in the Figure A.11 example combines all the features that were used in all the previous models.

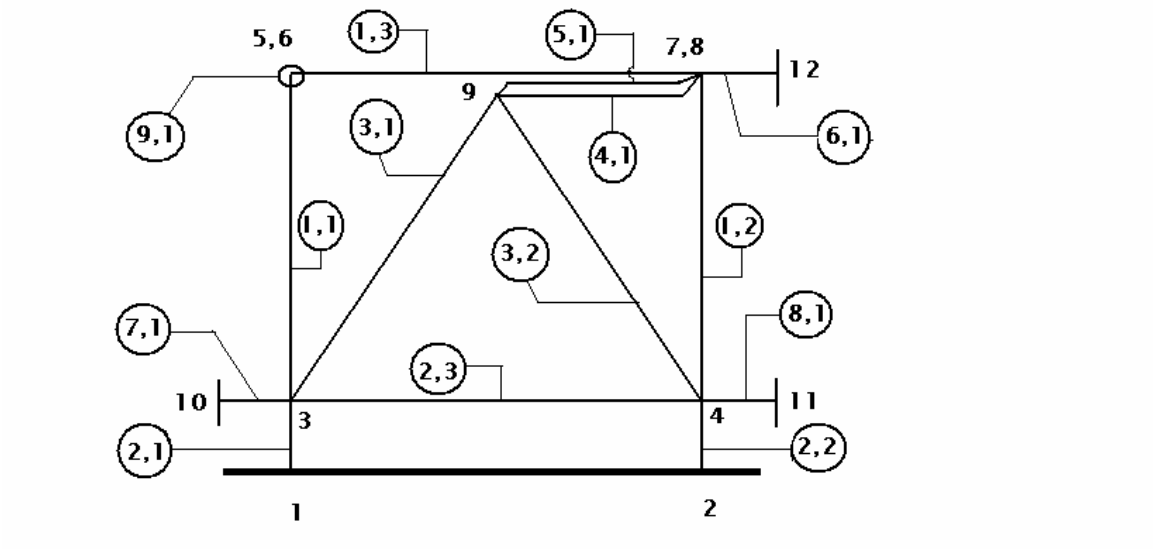

Fig A.11 "Isolated Braced Frame with Device" created in *DRAIN 2-DX*

The results obtained from *NONLIN* and *DRAIN* have been displayed below in Table A.11.

Table A.11 Comparison of the results for the "Isolated Braced Frame with Device" model

Software	Time-Step (sec)	Mode	System's Period of Vibration (sec)	Damping (% Critical)
DRAIN-2DX	0.0005	Mode No 1.	0.8820	7.379
		Mode No 2.	0.1440	9.913
		Mode No 3.	0.0280	3.608
NONLIN MDOF	0.0005	Mode No 1.	0.8820	7.381
		Mode No 2.	0.1440	9.914
		Mode No 3.	0.0277	3.606

Results for frame		Displ (in.)	t (sec)	Vel (in./sec)	t (sec)	Accl (in./sec^2)	t (sec)
DRAIN-2DX	Max	2.470	2.96	14.79	4.57	165.07	2.44
	Min	-2.070	4.41	-20.21	2.17	-166.85	2.07
NONLIN MDOF	Max	2.430	2.98	14.74	4.60	165.97	2.46
	Min	-2.110	4.42	-20.08	2.18	-165.69	2.10

Results for device		Displ (in.)	t (sec)	Vel (in./sec)	t (sec)	Accl (in./sec^2)	t (sec)
DRAIN-2DX	Max	1.850	2.96	12.43	2.72	137.08	2.44
	Min	-1.640	12.01	-15.24	2.17	-131.42	1.99
NONLIN MDOF	Max	1.830	2.98	12.42	2.74	137.96	2.46
	Min	-1.670	12.04	-15.06	2.18	-131.14	2.04

Results for isolator		Displ (in.)	t (sec)	Vel (in./sec)	t (sec)	Accl (in./sec^2)	t (sec)
DRAIN-2DX	Max	1.830	2.96	12.37	2.71	138.08	3.36
	Min	-1.620	12.01	-15.01	2.17	-129.03	2.01
NONLIN MDOF	Max	1.800	2.98	12.27	2.74	138.61	3.38
	Min	-1.650	12.04	-14.99	2.20	-127.21	2.02

Comment: Yielding occurs in the frame, device and the isolator.

Model 12.

Isolated Braced Frame with Device (P-Delta effects included)

Problem parameters

Properties of frame:

Weight = 8.5 k.

Initial Stiffness = 5.0 k/in.

Secondary Stiffness = 2.0 k/in.

Yield Strength = 2.5 k.

Damping of frame = 1.0 % of critical.

Height of frame = 100 in.

Properties of brace:

Stiffness contributed by bracings = 8.0 k/in.

Properties of device:

Weight = 0.05 k.

Initial Stiffness = 10.0 k/in.

Secondary stiffness = 2.0 k/in.

Yield Strength = 3.0 k.

Damping of device = 0.001.

Properties of isolator:

Weight = 3.0 k.

Initial Stiffness = 3.0 k/in.

Secondary stiffness = 1.0 k/in.

Yield Strength = 1.8 k.

Damping of device = 0.001.

Height of isolator = 15 in.

Ground Motion = Imperial Valley Earthquake (El Centro).

This is a typical three degree of freedom problem with P Delta effects included that can be solved using *NONLIN*. The model is illustrated below in Figure A.12.

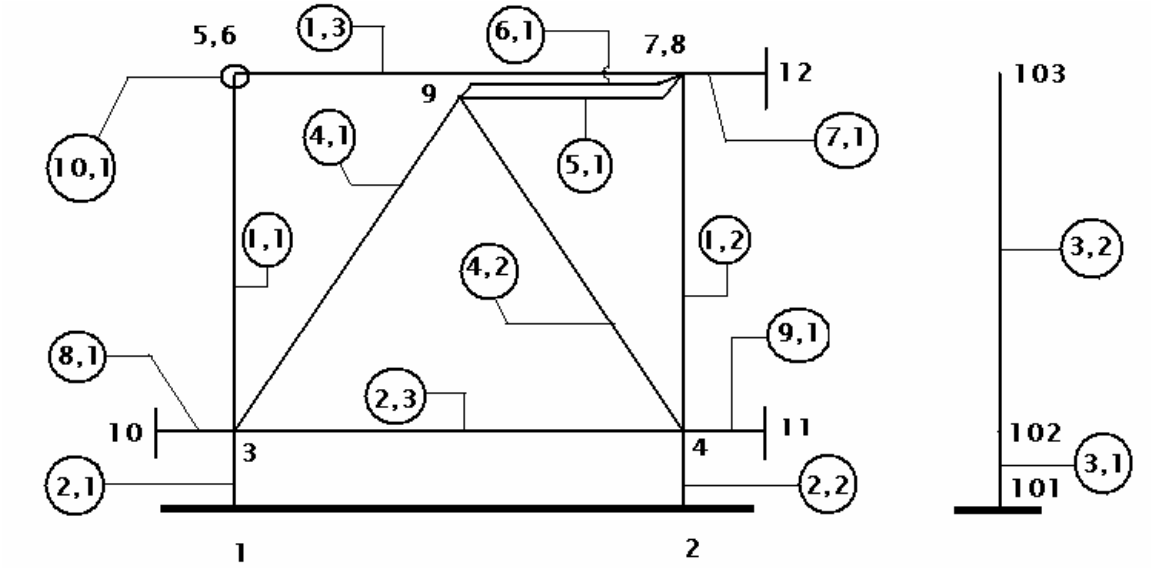

Fig A.12 "Isolated Braced Frame with Device" created in *DRAIN 2-DX* with P-Delta effects

The comparison of results from *NONLIN* and *DRAIN* are shown below in Table A.12.

Table A.12 Comparison of the results for the "Isolated Braced Frame with Device" model having P-Delta effects

Software	Time-Step (sec)	Mode	System's Period of Vibration (sec)	Damping (% Critical)
DRAIN-2DX	0.0005	Mode No 1.	0.7740	1.638
		Mode No 2.	0.1460	0.231
		Mode No 3.	0.0168	1.035
NONLIN MDOF	0.0005	Mode No 1.	0.7749	1.638
		Mode No 2.	0.1461	0.230
		Mode No 3.	0.0168	1.034

Results for device		Displ (in.)	t (sec)	Vel (in./sec)	t (sec)	Accl (in./sec^2)	t (sec)
DRAIN-2DX	Max	2.340	2.98	13.04	4.57	163.19	2.44
	Min	-2.140	12.01	-17.97	2.17	-171.27	2.10
NONLIN MDOF	Max	2.290	3.00	12.96	4.58	163.66	2.46
	Min	-2.200	12.04	-17.88	2.18	-167.16	2.12

Results for isolator		Displ (in.)	t (sec)	Vel (in./sec)	t (sec)	Accl (in./sec^2)	t (sec)
DRAIN-2DX	Max	2.270	2.97	13.42	1.91	191.17	2.44
	Min	-2.060	12.01	-17.17	2.16	-199.61	2.11
NONLIN MDOF	Max	2.220	3.00	13.18	1.94	189.23	2.46
	Min	-2.120	12.04	-17.24	2.18	-197.17	2.14

Comments: In this problem yielding occurs only in the isolator.

A.5 Conclusions

Based on the results from the above models, the validity of *NONLIN* for performing nonlinear response history analysis is established. In each of the models the results for each individual element such as damper, device, and isolator have been compared and tabulated. The effects of including P-Delta effects have also been considered, and in all the cases the solution converges to a reasonable degree of tolerance. The results from *NONLIN*'s single degree of freedom model also agree with those obtained from the multiple degree of freedom model and *DRAIN-2DX*. Hence *NONLIN*'s single degree of freedom is also accurate and is suitable for performing Incremental Dynamic Analysis, which is a procedure that involves the solution of a system subjected to earthquakes of monotonically increasing intensity levels.

VITA

(February 2004)

Samrat De was born on May 21, 1977 in Calcutta, India. After graduating from High School in 1994 he moved on to Regional Engineering College, Durgapur, India from where he got his Bachelor of Engineering (Honors) in Civil Engineering in 1999. Subsequently Samrat started working for Consulting Engineering Services (India) Limited as an Assistant Engineer posted at the Company's headquarters at New Delhi, India. He worked full time for three years. He arrived at Virginia Polytechnic Institute and State University, Blacksburg in the Fall of 2002 to pursue a Master of Science degree in Civil Engineering.